NONEQUILIBRIUM DYNAMICS IN LIVING CELLS AND SCALE-INVARIANT SUPERDIFFUSIVE PROCESSES

am Fachbereich Physik der Freien Universität Berlin eingereichte
Dissertation

zur Erlangung des Grades eines Doktors der Physik

vorgelegt von

ANDREAS DECHANT

Berlin, April 2014

Freie Universität Berlin

GUTACHTER:
Erstgutachter: Prof. Dr. Eric Lutz
Zweitgutachter: Prof. Dr. Roland Netz

Tag der Disputation: 04.06.2014

May you live in interesting times.

Dedicated to my parents.
Without your unwavering support, this would not have been possible.

ABSTRACT

A tracer bead attached to the cytoskeleton of a living cell shows two distinct types of anomalously diffusive behavior on different time scales: For times shorter that a few seconds, the motion is subdiffusive, with a diffusion exponent smaller than one, while on longer time scales, superdiffusive motion, with a diffusion exponent bigger than one, is prevalent. We introduce a stochastic model aimed at describing this transition, as well as the characteristic features of both the subdiffusive and superdiffusive motion. Our model is based on the fractional Langevin equation, which accurately reproduces the subdiffusive dynamics in a viscoelastic equilibrium environment. However, living cells are fundamentally out-of-equilibrium systems, and we accommodate this fact by including the motion of the cytoskeleton due to molecular motor activity as a nonequilibrium random process. In this way, our model accurately reproduces the transition from sub- to superdiffusion using a single stochastic equation of motion. It is also able to take into account the experimentally observed non-Gaussian behavior of the superdiffusive dynamics. As a direct consequence of our model, we obtain a generalized nonequilibrium Stokes-Einstein relation in terms of an effective temperature. This relation provides a connection between the diffusive dynamics and the mechanical response of the system, which is generally absent in nonequilibrium systems. Moreover, our model gives rise to an effective nonequilibrium noise force, which is nonstationary and possesses a time-dependent spectral density. This nonequilibrium noise can serve to classify the nonequilibrium dynamics in living cells.

The superdiffusive dynamics employed in our model, has the important properties of being asymptotically time-scale invariant. We present a general framework for treating such scale-invariant superdiffusive processes, based on a nonstationary scaling correlation function. Within this framework we develop generalizations for the Green-Kubo formula and for the Wiener-Khinchine theorem, both of which are, in their original formulation, only applicable to stationary systems. Our scaling Green-Kubo relation enables us to determine the anomalous diffusion coefficient for superdiffusive processes. It exposes an intricate dependence of this diffusion coefficient on the initial state of the system, as well as an intimate connection between stationarity and ergodicity. The corresponding scaling Wiener-Khinchine relation, on the other hand, allows us to determine the spectral density from the asymptotic scaling properties of the correlation function and relates the scale-invariant processes to $1/f$-noise.

ZUSAMMENFASSUNG

Eine Tracerpartikel, die an das Zytoskelett einer lebenden Zelle gebunden ist, zeigt, abhängig von der betrachteten Zeitskala, zwei unterschiedliche Formen von anomaler Diffusion: Für Beobachtungszeiten unterhalb von ein paar Sekunden ist die Bewegung des Teilchens subdiffusiv; hier ist der Diffusionsexponent kleiner als eins. Beobachtet man das Teilchen länger, stellt sich Superdiffusion mit einem Diffusionsexponenten größer als eins ein. Wir führen ein stochastisches Modell ein, das darauf abzielt, diesen Übergang und gleichsam das charakteristische Verhalten im sub- wie im superdiffusiven Bereich zu beschreiben. Unser Modell basiert auf der fraktionalen Langevin-Gleichung, die eine gute Beschreibung des subdiffusiven Verhaltens eines viskoelastischen Systems im Gleichgewicht liefert. Allerdings sind lebende Zellen ihrer Natur nach nicht im Gleichgewicht. Wir tragen dem Rechnung, indem wir die Bewegung des Zytoskeletts aufgrund der Aktivität molekularer Motoren als Zufallsprozess in unserem Modell berücksichtigen. Auf diese Weise ist unser Modell in der Lage, den Übergang zwischen Sub- und Superdiffusion mittels einer einzigen, stochastischen Bewegungsgleichung für den Tracer zu beschreiben. Eine direkte Konsequenz dieser Beschreibung ist eine Verallgemeinerung der Stokes-Einstein-Relation auf den Nichtgleichgewichtsfall mittels einer effektiven Temperatur. Diese stellt eine Verbindung zwischen dem diffusiven Verhalten und der mechanischen Antwort des Systems her, die für Systeme im Nichtgleichgewicht im Allgemeinen nicht besteht. Darüber hinaus ergibt sich aus unserem Modell ein effektives Nichtgleichgewichtsrauschen, das nichtstationär ist und eine zeitabhängige spektrale Dichte besitzt. Die Eigenschaften dieses Rauschens können zur Klassifikation der Nichtgleichgewichtsdynamik in lebenden Zellen dienen.

Die superdiffusive Dynamik, die in unserem Modell zum Einsatz kommt, besitzt zeitliche Skaleninvarianz. Für derartige skaleninvariante Prozesse erschließen wir einen allgemeinen Satz von Eigenschaften und Relationen, der auf der Definition einer nichtstationären skaleninvarianten Korrelationsfunktion aufbaut. Unter anderem erhalten wir Verallgemeinerungen der Green-Kubo-Formel und des Wiener-Khinchine-Theorems; beide sind in ihrer ursprünglichen Formulierung nur auf stationäre Prozesse anwendbar. Unsere skaleninvariante Green-Kubo-Relation ermöglicht es uns, den anormalen Diffusionskoeffizienten für superdiffusive Prozesse zu berechnen. Sie enthüllt außerdem eine komplizierte Abhängigkeit ebendieses Diffusionskoeffizienten vom Anfangszustand des Systems, sowie eine enge Verbindung zwischen Stationarität und Ergodizität. Die Verallgemeinerung des Wiener-Khinchine-Theorems dagegen erlaubt uns, die spektrale Dichte von skaleninvarianten Prozessen aus dem asymptotischen Verhalten ihrer Korrelationsfunktion zu bestimmen und bringt diese Prozesse dadurch mit $1/f$-Rauschen in Verbindung.

PUBLICATIONS

Some ideas and figures have appeared previously in the following publications:

A. Dechant and E. Lutz. "Connecting active and passive microrheology in living cells". *arXiv:1307.6466 [cond-mat]*, 2013. [Dech 13]

A. Dechant, E. Lutz, D. A. Kessler, and E. Barkai. "Scaling Green-Kubo relation and application to three aging systems". *Physical Review X*, Vol. 4, p. 011022, 2014. [Dech 14]

ACKNOWLEDGMENTS

This dissertation was supported by the Elsa-Neumann graduate funding and the Focus Area Nanoscale of the FU Berlin.

I want to express my sincerest gratitude to Prof. Dr. Eric Lutz for serving as my adviser. He left me the independence I wanted while offering me the guidance I needed and always knew to ask the right questions. Thank you Eric, it has been and still is a great pleasure working with you! I am very grateful to Prof. Dr. Piet Brouwer for accommodating me in his group at the FU during my time in Berlin. I really enjoyed working in this amiable and productive environment. A lot of thanks go to Prof. Dr. Eli Barkai for his repeated hospitality at Bar Ilan university and many insightful discussions. The same goes for Prof. Dr. David A. Kessler, whom I had the pleasure of cooperating with on several publications. I also thank the second referee for this thesis, Prof. Dr. Roland Netz, and all the other members of the committee for their time and efforts.

A great big thank you to all my colleagues from the Brouwer, von Oppen and Bergholtz groups at the FU Berlin. Though we did not have a lot of scientific overlap, I always enjoyed working alongside you. You really are a great team and I could not imagine any place where I would rather have spent the last two years.

A very personal thank you and a warm hug I want to give to Irina for ever so often brightening my mood during the last several months. To my close friends – you know who you are – I owe both an apology, for not being particularly socially minded during the final months of my thesis, and also a thank you, for taking my mind off work every now and then even so. I promise to make it up to you. You guys and girls rock!

CONTENTS

1 NONEQUILIBRIUM DYNAMICS IN LIVING CELLS 1
- 1.1 Particle tracking microrheology 4
  - 1.1.1 Experimental procedure and advantages 5
  - 1.1.2 Experimental results for equilibrium systems 6
  - 1.1.3 Ergodicity 9
- 1.2 Living cells as a nonequilibrium stochastic system 9
  - 1.2.1 Equilibrium and nonequilibrium dynamics 10
  - 1.2.2 Experimental observations in living cells 10

2 MOVING VISCOELASTIC MEDIUM MODEL 13
- 2.1 The fractional Langevin equation 15
  - 2.1.1 Langevin equation 15
  - 2.1.2 Fractional Langevin equation: Anticorrelated subdiffusion 17
- 2.2 Extension to superdiffusive nonequilibrium dynamics 21
  - 2.2.1 External nonequilibrium noise 22
  - 2.2.2 Active viscoelastic environment 23
  - 2.2.3 Properties of the nonequilibrium noise 29
- 2.3 Solution of the nonequilibrium fractional Langevin equation 36
  - 2.3.1 Frequency domain 36
  - 2.3.2 Time domain: Correlation functions and mean-square displacement 37
  - 2.3.3 Time domain: Linear response and creep function 42
  - 2.3.4 Equilibrium and stationarity 44

3 SCALE-INVARIANT SUPERDIFFUSIVE SYSTEMS 49
- 3.1 Scaling Green-Kubo relation 51
  - 3.1.1 Green-Kubo formula and range of validity 52
  - 3.1.2 Scaling correlation functions and scaling Green-Kubo relation 54
  - 3.1.3 Sensitivity to initial conditions 57
  - 3.1.4 Position correlation function 60
  - 3.1.5 Application to experimental data 61
  - 3.1.6 Deviations from scaling 63
- 3.2 Time averages and ergodicity 65
  - 3.2.1 Time-averaged square displacement 66
  - 3.2.2 Ergodicity and stationarity 69
- 3.3 Spectral properties 71
  - 3.3.1 Stationary processes and Wiener-Khinchine theorem 72
  - 3.3.2 Scaling in the frequency domain 73
  - 3.3.3 Spectral density for nonstationary scale-invariant systems 76
  - 3.3.4 Initial conditions in the frequency domain 80
- 3.4 Examples for scaling dynamics 82
  - 3.4.1 Fractional Gaussian noise 82
  - 3.4.2 Lévy walk 93
  - 3.4.3 Spectral density for nonequilibrium noise 98

4 APPLICATION TO DYNAMICS IN LIVING CELLS 101
4.1 Equilibrium and nonequilibrium dynamics 103
4.1.1 Transition from sub- to superdiffusion 103
4.1.2 Crossover time as a measure of active motion 108
4.2 Effective temperature and generalized Stokes-Einstein relation 109
4.2.1 Stokes-Einstein relation in time and frequency domain 109
4.2.2 Effective temperature and dynamics on different time scales 113
4.3 Spectral densities and nonequilibrium noise 114
4.4 Non-Gaussian statistics and confinement 119
4.5 Linear response 123
4.5.1 Creep function, initial conditions and diffusion 125
4.5.2 Aging and history dependence of the response 126
5 DISCUSSION AND OUTLOOK 131
A APPENDIX: MATHEMATICAL DETAILS 137
A.1 Mathematical identities 137
A.2 Asymptotic analysis of fractional integrals 140
A.3 Asymptotic behavior under Laplace inversion 151
B APPENDIX: NUMERICAL SIMULATIONS 155
B.1 Langevin trajectory simulations 155
B.2 Overview of simulation program 158

BIBLIOGRAPHY 161

1 NONEQUILIBRIUM DYNAMICS IN LIVING CELLS

In the eyes of a physicist, a living biological cell as a whole is almost hopelessly complex. A wealth of different constituents interact with each other through chemical and physical processes that take place on time and length scales spanning orders of magnitude - from the level of molecular dynamics at femtoseconds and nanometers up to hours and millimeters on the level of the entire cell. This makes the description of a living cell from first principles an impossible task. In order to obtain a meaningful physical model of the processes inside a cell, we need to focus on a specific set of time and length scales. Any dynamics that takes place outside this window of scales is only taken into account in an approximate manner or is even ignored outright. This is well justified if the respective processes happen on very different scales: Neither will the binding or unbinding of a single base pair of DNA have any measurable effect on the motion of the cell as a whole, nor will the center-of-mass motion of the cell change the DNA binding dynamics.

The main focus of this work is motion of and within an eukaryotic cell's cytoskeleton, more precisely the equilibrium and nonequilibrium dynamics of the network formed by the actin fibers. Specifically, we consider the results of so-called particle tracking microrheology experiments, where a tracer bead is bound to the actin network and the motion of the bead is then tracked. Here, the typical length scales on which the dynamics of the tracer are observed, range from one nanometer to several hundred nanometers [Burs 05, Trep 08, Gall 09]; time scales range from milliseconds to hundreds of seconds. Within these length scales fall the dimensions of the actin filaments (around 6 nm diameter [Albe 02]) and other constituents of the cytoskeleton and cytoplasm, as well as the typical step sizes of molecular motors (several tens of nanometers [Vale 00, Yild 03]). The dynamics of these objects thus need to be taken into account when studying the motion of the bead. At this point, we again encounter the problem of complexity. The cytoskeleton is composed of filaments of different sizes, which are cross-linked by and constantly subject to binding and unbinding of a multitude of proteins [Albe 02]. In addition to this, the filaments themselves and some of the proteins cause constant motion and rearrangement in the network [Albe 02]. All of these processes are highly nontrivial individually and their interplay in influencing the observable motion of the tracer bead is all but impossible to describe at this level of detail. However, the very same complexity, that impedes the microscopic description of the problem, also allows for a way out. Because the motion of the bead is caused by a multitude of interacting complex dynamical processes, it is essentially random on the experimentally observable level. We thus treat this motion as a random process, with stochastic forces arising both from the thermal motion of the cytoskeleton and its active motion due to the action of molecular motors.

The statistical description of complex physical systems has a long and extremely successful history. It is at the very heart of statistical mechanics, where the innumerable microscopic degrees of freedom are condensed into a handful of macroscopic quantities. Stochastic models have been successfully applied to describe a wide range of systems in physics and chemistry [Kamp 92], as well as other fields, such as finance [Hull 00], biology and medicine [Iosi 12]. The paradigmatic example for a stochastic process in physics is of course Brownian motion [Brow 28], which was described within a stochastic framework by Einstein [Eins 05], Smoluchowski [Smol 06] and Langevin [Lang 08]. Brownian motion describes the random fluctuations of the positions of particles suspended in a fluid due to collisions with the constituents of the fluid. The complexity in this case arises from the fluid itself, which at the microscopic level is an interacting many-particle system. Describing the motion of all the atoms and molecules of the fluid and their interactions among each other and the observed particles is near impossible, however, their combined effect on the particles' motion understood as a random process is captivatingly simple: In ideal Brownian motion, the motion of the observed particles is entirely uncorrelated, their velocity at each instant in time is random and independent of the velocity at earlier times. In this sense, Brownian motion is the "most random" stochastic process one can think of. This leads to what is called normal diffusion: The mean-square displacement, i.e. the statistical variance in the particles' positions, increases linearly with time, $\langle \Delta x^2(t) \rangle = 2D_1 t$. All the interactions within the fluid and between the fluid and the particle are encoded in the single macroscopically observable quantity of the diffusion coefficient D_1. Of course, if we want to resolve the motion of the probe particle down to the time and length scales where individual collision events play a role, this simplified stochastic picture breaks down and we actually have to consider the full microscopic dynamics. But as long as the experimentally relevant scales are sufficiently distinct from those of the microscopic processes, the stochastic description offers an excellent approximation.

As paradigmatic as Brownian motion and normal diffusion may be for stochastic processes in physics, even more interesting is the phenomenon referred to as anomalous diffusion. A diffusive process is called anomalous, if the mean-square displacement behaves as $\langle \Delta x^2(t) \rangle = 2D_\nu t^\nu$ with $\nu \neq 1$. This definition immediately implies that there are two sub-classes of anomalous diffusion [Klaf 87, Klaf 05]: Subdiffusion occurs for $0 < \nu < 1$, so that the variance of the particles' positions grows slower than linearly with time. For $\nu > 1$, on the other hand, the mean-square displacement grows faster than linearly in time and we speak of superdiffusion. Anomalous diffusion generally occurs when there is an additional long-ranged structure to the randomness of the stochastic process. Whereas normal diffusion corresponds to uncorrelated motion, subdiffusion may be caused by either long-ranged anticorrelations, meaning that the particle is more likely to be moving in the opposite direction at a later time, or stalling events, where the particle does not move at all for extended periods of time. An example for an anticorrelated subdiffusive process is fractional Brownian motion [Mand 68]; a subdiffusive process with stalling events is the continuous time random walk [Sche 73]. By contrast, superdiffusion may be due to positive long-range correlations, which cause the particle to be more likely to continue moving in the same direction, or due

to hopping events, where the particle suddenly jumps over a large distance. Fractional Brownian motion [Mand 68] or the Lévy walk [Shle 87] are possible examples for long-range correlated motion; the Lévy flight [Shle 86] describes hopping events. Both sub- and superdiffusion and the various underlying stochastic models have found numerous applications in physics and other fields of science. Subdiffusive dynamics occur in mathematics in the context of nonlinear maps [Bark 03], in currency exchange rates [Stal 03], in single proteins [Kou 04], biological cells [Toli 04, Gold 06], colloidal glasses [Indr 94, Week 02] and even for the propagation of cosmic rays in a background magnetic field [Shal 05]. Nonlinear maps [Zasl 08], financial data [Cohe 06] and biological cells [Burs 05, Trep 08, Gall 09, Gal 10] can also exhibit superdiffusive behavior, as can turbulent [Buda 06] and driven dissipative systems [Liu 08]. Superdiffusion can also be found in optical lattices [Sagi 12, Dech 12, Kess 12] and even in the foraging patterns of animals [Visw 08].

Note that in the above we quoted biological cells as an example for both sub- and superdiffusive dynamics. And indeed, sub- and superdiffusion not only both occur in living cells, but even within the same cell on different time scales. This behavior has been extensively confirmed in experiments [Burs 05, Trep 08, Gall 09, Brun 09]. While, when observed on short times (microseconds up to a few seconds), tracer bead bound to the cytoskeleton exhibits very slow subdiffusion with an exponent of $\nu \sim 0.2$, this behavior transitions into fast superdiffusion with an exponent of $\nu \sim 1.6$ at longer times up to several tens or hundreds of seconds. This transition already hints at the possibility that there may be multiple different physical processes responsible for the motion of the tracer bead. Understanding these processes, and providing a simple stochastic model for both sub- and superdiffusive behavior as well as the transition between them, is one of the main goals of the present work.

In the remainder of this Chapter we give a short overview of the experimental techniques used in particle tracking microrheology and the observables that can be thus obtained. This is followed by a short consideration of time versus ensemble averages and the notion of ergodicity as it pertains to experimental results. Further, we discuss what conclusions we can draw about the subdiffusive dynamics and possible stochastic models and how they are related to the equilibrium mechanical properties of the cell. The superdiffusive dynamics, on the other hand, are related to the active nonequilibrium forces originating from the action of molecular motors. How the motor activity translates into stochastic motion and what experiments can tell us about the properties of the latter concludes this chapter. In Chapter 2, we introduce and examine our main model for the description of sub- and superdiffusive dynamics in living cells, an extension of the equilibrium fractional Langevin equation to nonequilibrium dynamics via coupling to a moving medium. We find that sub- and superdiffusion correspond to the equilibrium and nonequilibrium properties of the system, respectively, and argue different stochastic models for the nonequilibrium dynamics. In Chapter 3, we take a step back from the actual physical system at hand, and discuss superdiffusive processes in a more general context. For the class of superdiffusive processes we consider, we develop a mathematical machinery, which is able to easily extract certain physical

quantities like the mean-square displacement, time averages and spectral densities from the processes' common scaling behavior. This machinery can be applied in a straightforward manner to superdiffusion in cells, but is also applicable to a wider range of superdiffusive systems. In particular it exposes an intricate dependence of the long-time dynamics on the initial preparation of the system, an effect which is absent for normal diffusive systems and which also has implications for ergodicity. Two central results of this formalism are generalizations of the Green-Kubo formula and the Wiener-Khinchine theorem, both important concepts in non-equilibrium statistical mechanics. Whereas their original formulations are limited to stationary processes, our results generalize them to a nonstationary context. The application of the model introduced in Chapter 2 to cellular dynamics is carried out in Chapter 4. There we discuss in more detail the transition from sub- to superdiffusion and introduce an effective temperature that describes the deviation from the equilibrium system in terms of the transition time. This effective temperature allows us to relate linear response and the nonequilibrium fluctuations in the system via a generalized nonequilibrium Stokes-Einstein relation. We compare the dynamics described by our stochastic model to experimental results and remark on which physical observables are suited to capture the essential properties of the system. Chapters 2 and 4 deal with the extension of equilibrium results to nonequilibrium systems – in our case living cells. Chapter 3, on the other hand, generalizes from stationary to nonstationary processes. While equilibrium necessarily implies stationarity, we show that nonequilibrium may also imply nonstationarity under certain conditions, thus providing a direct link between both concepts.

At this point, we shortly remark on the structure of this thesis. Many of the results require lengthy calculations, or are themselves of a rather technical nature. We thus decided to precede each Chapter by a thorough discussion of the main motivations and results, which also gives an overview over the chapter's contents. These discussions make no claim to being exhaustive in covering all the results of the main chapter, but aim to provide the reader with a good idea of what is to follow. In addition, each Section is preceded by a short summary of the main results and physical ideas contained therein. While this structure leads to some repetition, it is our sincere hope that it enables the reader to quickly grasp the physics and then, if desired, to descend into the mathematical details with a firm idea of what is going on.

1.1 PARTICLE TRACKING MICRORHEOLOGY

Since our theoretical considerations in the later Chapters focus on providing a model reproducing the results of particle tracking and microrheology experiments, we first familiarize ourselves with the experimental procedure and its results as pertaining to equilibrium systems. In Section 1.1.1 we discuss microrheological experiments in general and the particle tracking microrheology experiments whose results we use to justify our model in particular. We pay special attention to the distinction between the active and passive measurement scheme. In Section 1.1.2, we state some results for the equilibrium system, in particular, that the fluctuation-dissipation theorem, which connects the results of active and passive measure-

ments, is verified experimentally. Finally, in Section 1.1.3, we remark on how experimental data is analyzed and in particular on the concept of time and ensemble averages, which are generally taken to be interchangeable. We argue that this is not always the case and one needs to take care when comparing experimentally obtained time averages to the ensemble averages predicted by theory.

1.1.1 *Experimental procedure and advantages*

Rheology in general deals with the flow and deformation of matter. In a typical rheological experiment, one would apply an external stress to a sample and monitor how the sample reacts to it by either deforming elastically, flowing viscously or doing a combination of both [Find 13]. When it comes to cells, this approach can be used to probe the mechanical properties of the cell as a whole or of the cell's outer layer, the cell membrane. Even so, since cells are very small and very soft, delicate techniques able to measure forces in the pico-Newton and displacements in the nanometer range are required [Verd 09, Koll 11]. Such techniques include atomic force microscopy [Vian 99], magnetic [Baus 98] and optical [Ashk 97] tweezers, pipette suction [Evan 95] and micro-plate rheometry [Thou 97]. However, while these methods provide an increasingly consistent picture of the membrane and overall mechanical properties of the cell [Koll 11], they are not suited to probe specific regions in the interior of the cell in a non-intrusive manner [Weih 06].

This is where particle tracking microrheology [Maso 97, Wirt 09] comes into play. In this approach, the motion of tracer particles embedded within or bound to specific regions in the cell is observed via optical microscopy [Tsen 02, Croc 07, Lee 07] or laser tracking [Yama 00, Mass 07, Mizu 08]. These tracer particles may be endogenous to the cell [Yama 00, Toli 04] or artificial [Baus 99, Fene 01, Casp 02]. Compared to directly probing the cell mechanically, this method has several advantages [Weih 06]: Even when using artificial tracers, the measurement procedure is less disruptive to the cell as no mechanical fixtures are needed. This allows measurements to be performed on live cells and monitor active biological processes in the cell [Beil 03, Gira 04]. Furthermore, since the tracer particles may be inside the cell and bound to specific regions, the properties of these regions may be probed directly. For a statistical point of view, many cells and multiple tracer particles per cell may be analyzed at the same time [Burs 05, Gal 10], yielding better statistics than individually probing one cell at a time. Downsides of particle tracking microrheology are that, for endogenous tracers, there is generally some variation in their size and surface chemistry [Weih 06]. For artificial tracers on the other hand, one may not have complete control over the internalization of the tracers by the cell and there may be additional effects stemming from the binding dynamics themselves [Weih 06, Metz 10]. Due to its numerous advantages, particle tracking microrheology has been successfully employed in studying the properties of artificial equilibrium [Maso 97, Xu 98] and nonequilibrium [Mizu 08, Levi 09, Bert 12a, Stuh 12] systems designed to emulate cell behavior in a controlled way as well living cells themselves [Burs 05, Mass 07, Wilh 08, Gall 09, Bert 12b].

Generally, there are two distinct measurement schemes in particle tracking microrheology [Brau 07, Mizu 08, Lee 10]. In the passive scheme, the tracer particles are allowed to diffuse freely and their diffusive motion is observed. This yields information about both thermal and nonthermal fluctuations in the cell [Casp 02, Webe 12]. In the active scheme, an external force is applied to the tracer particles, e.g. via optical or magnetic tweezers, and the response of the tracers to the applied force is measured. This type of measurement directly probes the mechanical properties of the cell [Baus 99, Fabr 01, Chen 03]. In an equilibrium system, the results of both measurements are related and can be inferred from one another [Maso 97], see Section 1.1.2. As living cells are by definition not in equilibrium, both measurements are necessary to characterize their rheological properties [Gall 09, Robe 10, Bohe 13], see Section 1.2.2. In the experiments on which our theoretical model focuses, artificial tracer beads, a few micrometers in diameter, are coated in a peptide to specifically bind to the actin network through the cell membrane [Burs 05, Leno 07, Gall 09]. The dynamics of these beads are then recorded via optical microscopy, the external force on the beads is exerted either through a magnetic field [Burs 05, Leno 07] or via optical tweezers [Gall 09]. Figure 1.1 shows a typical time trace of one such bead obtained in the passive measurement scheme and a scanning electron microscope picture of beads on the cell membrane.

1.1.2 *Experimental results for equilibrium systems*

As remarked before, living biological cells are a fundamentally nonequilibrium system. Nevertheless, understanding their equilibrium behavior, i.e. in the absence of biological activity, is vital to, on the one hand, characterize their mechanical properties, and on the other hand understand precisely which observations are attributable to the biological activity. Several experiments also substitute artificial systems designed to emulate specific properties of cells [Ambl 96, Maso 97, Szym 09, Lee 10]. This allows to test specific hypotheses without having to deal with the complexity and inhomogeneity of actual cells. A common finding of experiments both on these artificial systems and on cells [Weis 04, Toli 04, Gold 06, Ball 06, Webe 10] is that, in the absence of active transport, the motion is subdiffusive, $\langle \Delta x^2(t) \rangle = 2D_\nu t^\nu$ with $\nu < 1$. Typical exponents range from $\nu \sim 0.2$ for the dynamics of the cytoskeleton [Ball 06, Trep 08, Gall 09] to $\nu \sim 0.8$ for small endogenous tracers in the interior of the cell [Weis 04, Toli 04, Gold 06]. The origin of this subdiffusive behavior is a phenomenon called crowding [Elli 03, Weis 04, Dix 08, Soko 12, Hofl 13]. In the cytoplasm inside the cell, the tracer cannot move freely due to the high volume fraction of space – up to 40 % – taken up by proteins and other macromolecules, but is confined to small volumes for extended periods of time. However, this confinement is not stationary, as the constituents of the cytoplasm themselves are constantly in motion, changing the geometry of the confinement and opening up pathways for the tracer to escape. Thus the motion of the tracer is somewhere between confined and freely diffusive, leading to a diffusion exponent < 1. On timescales beyond several seconds, the excursions between "traps" dominate the dynamics and diffusion returns to normal [Weis 13]. Several mathematical models for subdiffusion in crowded environments have been proposed [Soko 12, Hofl 13]. The three most widely discussed models are the con-

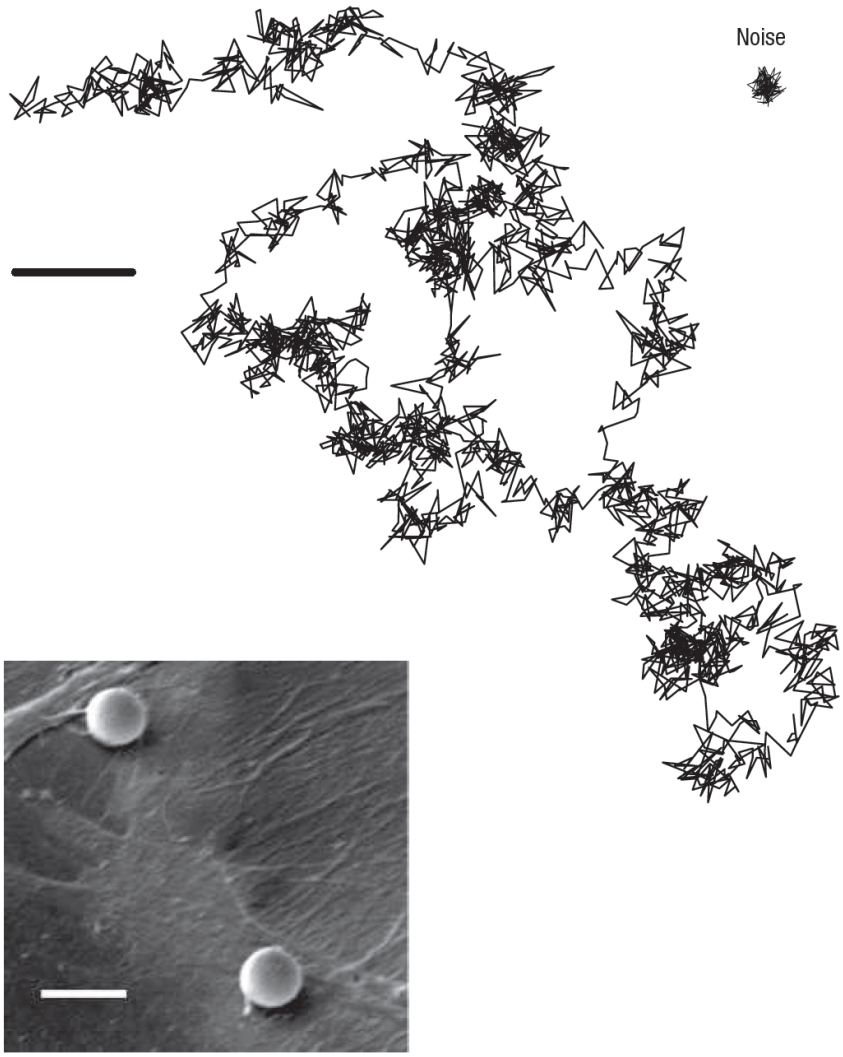

Figure 1.1: Typical trajectory of a tracer bead in the passive measurement scheme, the scale bar: 10 nm. Inset: Scanning electron microscope picture of two beads bound on a human airway smooth muscle cell. Image taken from Ref. [Burs 05].

tinuous time random walk, obstructed diffusion and fractional Brownian motion. In the continuous time random walk [Sche 73] the dynamics is described as an ordinary random walk, however, the particle has to wait for a random time t_w before taking the next step. If the distribution of the waiting times is such that the average waiting time is infinite, then longer and longer waiting times will occur and the mean-square displacement of the particle will increase sublinearly with time. Obstructed diffusion [Hofl 06], on the other hand, places the particle in a stationary array of obstacles. If the density of obstacles is precisely at a certain critical value, the so-called percolation threshold, then the particle is trapped in voids between obstacles most of the time, leading again to subdiffusion. In the third model, fractional Brownian motion [Mand 68], the cytoplasm is considered as a semi-viscous, semi-elastic medium. This interplay between viscous flow and elastic back-action leads to a long time memory, which induces the subdiffusive behavior and is discussed in more detail in Section 2.1.2. Each of these three models captures certain elements of the crowded cytoplasm: The continuous time random walk straightforwardly incorporates the idea of extended trapping times, obstructed diffusion captures the geometric picture of the particle being trapped and fractional Brownian motion takes into account the dynamic nature of the cytoplasm by allowing for elastic and viscous response. Which model in the end offers the most accurate description of subdiffusion in the cytoplasm is still debated [Soko 12, Hofl 13, Weis 13]. However, there is rather good evidence that, at least in artificial crowded systems, fractional Brownian motion may be the model of choice [Szym 09, Weis 13]. Some experimental and theoretical considerations also point to fractional Brownian motion for diffusion in cells on time scales of several milliseconds up to seconds [Magd 09, Webe 10], while for shorter time scales, the continuous time random walk has been suggested as a model for the dynamics [Jeon 11].

The second main result for the equilibrium dynamics is the mechanical response of the cell to external stress. In the context of microrheological measurements, applying a force to the tracer beads causes a time-dependent displacement of the beads. As with the diffusive motion, the time-dependence of the displacement is anomalous $\langle \Delta x(t) \rangle \sim t^{\nu'}$ [Maso 97, Xu 98, Desp 05, Ball 06, Gall 09] with an exponent ν' that is roughly the same as the subdiffusion exponent. This is not a coincidence, rather it is a consequence of the equilibrium dynamics of the system being probed. In equilibrium systems, thermal fluctuations lead to diffusion. However, these fluctuations act on the tracer particle through the same medium, in our case the cytoplasm and cytoskeleton, whose mechanical properties are responsible for the response to external forces. Thus diffusion and response in equilibrium systems are related via the so-called generalized Stokes-Einstein relation [Maso 97, Schn 97, Maso 00], which is a consequence of the fluctuation-dissipation theorem [Nyqu 28, Call 51, Reif 09]. This relation states that the response of the particle, called creep function or creep compliance [Xu 98, Wirt 09, Koll 11], is identical to the mean-square displacement up to a factor of temperature. A similar relation exists for the frequency dependent elastic modulus [Maso 95, Maso 97, Maso 00]. The Stokes-Einstein relation allows to infer the outcome of an active measurement, i.e. the response function, from a passive measurement of the mean-square dis-

placement or vice-versa and has been experimentally verified in various contexts [Maso 95, Khol 95, Banc 99]. For fractional Brownian motion, the Stokes-Einstein relation is a straightforward consequence from its mathematical description in terms of the fractional Langevin equation [Lutz 01], see Section 2.3.4.

1.1.3 *Ergodicity*

The theoretical results derived in the following sections will generally be stated in terms of ensemble averages. Such an ensemble average is understood to be over a number of realizations of the involved random processes large enough that the statistical error becomes negligible, ideally over infinitely many realizations. For typical single particle tracking experiments as in particle tracking microrheology, on the other hand, only a limited number of bead trajectories is available, usually on the order of several tens [Gall 09] to hundreds [Burs 05]. Each bead's trajectory can be monitored over extended periods of time on the order of several hours [Burs 05], so that for each single trajectory, ample data is available. For evaluating experimental data and in order to obtain statistically sound results, it is thus often indispensable to obtain quantities like the mean-square displacement and response functions from single trajectories via time averaging [Gall 09] or from a limited number of trajectories via a combination of time and ensemble averaging [Burs 05, Leno 07, Brun 09]. So how to compare the ensemble averages from theoretical considerations to time averages obtained from experiments? Most physical systems have the property of ergodicity [Papo 02], which guarantees that the time average of a quantity over a single realization will reproduce the ensemble average over all possible realizations, given that the averaging time is sufficiently long. This allows us to compute the time average for a small number of experimentally obtained trajectories and directly compare it to the ensemble average we obtained from our theory. However, this approach has to be taken with care, as there are some stochastic models that exhibit broken ergodicity [Bouc 92, Cugl 95], among them the continuous time random walk [Bel 05], which has been suggested as a model for the short-time diffusion in cells [Jeon 11]. In these models, the time averages over single trajectories display significant fluctuations even in the long-time limit and are not reproducible. We describe the intermediate-time dynamics using fractional Brownian motion, which is ergodic in principle [Deng 09], so that the fluctuations between individual time averages indeed vanish for long times. However, ergodicity by itself is only truly reached for infinite averaging times and the approach to ergodicity may be slow. So, even if the model is ergodic in principle and thus allows interchanging time and ensemble averages, we should still be aware that time averages may show sizable fluctuations for finite times [Deng 09, Froe 13].

1.2 LIVING CELLS AS A NONEQUILIBRIUM STOCHASTIC SYSTEM

While already the equilibrium mechanical properties of cells are rather complex, things get even more interesting once we take into account the nonequilibrium behavior. The motion of tracers in the cell crucially depends on the motion of the cell itself and its constituents. In particular, a bead bound to the cytoskeleton

will move according to the internal dynamics and structural reorganizations of the latter. In this way, microrheological experiments can yield valuable information about active biological processes in the cell.

1.2.1 *Equilibrium and nonequilibrium dynamics*

One important property that distinguishes nonequilibrium from equilibrium systems in general, is that their behaviors under active and passive measurement are no longer directly related by the Stokes-Einstein relation [Bonn 03, Chen 07, Mizu 07]. The fundamental reason for this is that the fluctuation-dissipation theorem does not hold for nonequilibrium systems, as their dynamics are not solely due to the coupling to a thermal bath. Instead, driving the system out of equilibrium may lead to additional fluctuations as well as changes in the mechanical properties. However, these changes depend on the precise type of nonequilibrium behavior and are not related in an universal manner. Living cells are driven out of equilibrium by the biological activity that distinguishes them from inanimate matter [Mizu 07, Kasz 07]. The mechanical activity of a cell is caused by certain proteins, called molecular motors [Schl 06, Kolo 07], which undergo periodic chemical reactions, changing their spatial conformation. These conformational changes effectively convert chemical energy (e.g. in the form of ATP) into mechanical motion [Vale 00, Yild 03]. That this molecular motor activity is indeed what causes the mechanical nonequilibrium behavior has been verified experimentally both in actual cells [Burs 05, Bran 08, Bran 09] and artificial model systems [MacK 08, Levi 09, Bert 12a]. The motor proteins form connections between actin fibers and generate relative motion between them, leading to active restructuring of the actin network [Mizu 07, MacK 08, Levi 09, Toyo 11]. Since typically many molecular motors act on an extended network of actin fibers [Levi 09], the impact of the cytoskeleton's active motion on a bead bound to it can be modeled as a stochastic process [Kuli 08, Brun 09].

1.2.2 *Experimental observations in living cells*

One of the key results of microrheological experiments in living cells is the occurrence of superdiffusion, $\langle \Delta x^2(t) \rangle = 2D_\nu t^\nu$ with $\nu > 1$ [Casp 02, Lau 03, Burs 05, Leno 07, Burs 07, Trep 08, Gall 09]. This superdiffusive motion is indicative of correlated motion and active transport in the cell and typically occurs on time scales longer than 1 s. For shorter time scales, thermal motion is dominant and the equilibrium subdiffusion prevails. Just as with the subdiffusion exponent $\nu \sim 0.2$, the superdiffusion exponent $\nu \sim 1.6$ is largely universal for experiments probing the cytoskeleton for various cell types [Trep 08], suggesting that both sub- and superdiffusion occur as a consequence of fundamental processes in the cytoskeleton and not due to specifics of individual cells. This makes modeling the dynamics as a stochastic system all the more promising, since in this approach, the microscopic details of the complex physical, chemical and biological processes occurring in the cell are subsumed in a small number of universal parameters. Figure 1.2 shows the typical mean-square displacement of a tracer bead obtained in a microrheological experiment [Gall 09]. Note the clear transition from subdiffusion to

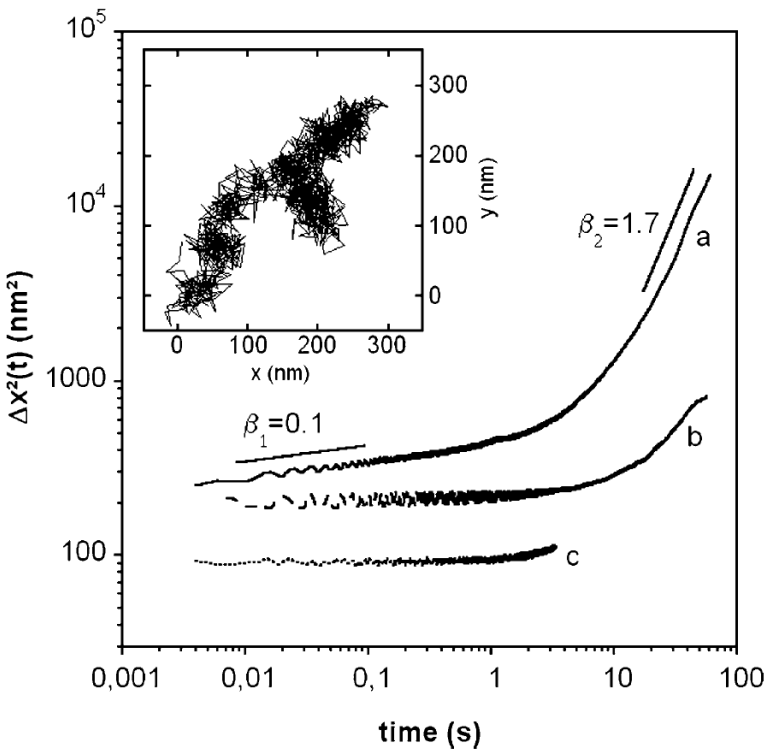

Figure 1.2: Left: Mean-square displacement of a tracer bead obtained in the passive measurement scheme. Control cell (a), ATP-depleted cell (b) and noise background (c). Right: Response of the tracer bead to an external force applied via optical tweezers. Images taken from Ref. [Gall 09].

superdiffusion with a transition time on the order of a few seconds. The superdiffusive motion has another characteristic feature, namely the underlying dynamics is non-Gaussian [Burs 05, Gal 10, Toyo 11, Gal 13]. Specifically, higher order moments of the particle displacement (e.g. $\langle \Delta x^4(t) \rangle$) are larger with respect to the second moment than expected be for Gaussian dynamics. The origin of these non-Gaussian effects are periods in which the tracer moves almost ballistically, i.e. in a straight line, which lead to unusually large displacements and contribute disproportionally to the higher-order moments. These periods of almost ballistic motion can be attributed to remodeling in the cytoskeleton as a result of motor activity [Burs 05, Toyo 11], see Section 1.2.1. Together with the equilibrium subdiffusion, this leads to intermittent dynamics [Burs 05], where periods of ballistic motion alternate with periods during which the tracer is almost immobile. On short timescales, where subdiffusion in prevalent, on the other hand, the dynamics is Gaussian, as expected from equilibrium dynamics. This supports the approach of characterizing sub- and superdiffusion as due to different stochastic processes, as we do in Section 2.2.

2 MOVING VISCOELASTIC MEDIUM MODEL

Rheological experiments on tracers bound to the cytoskeleton of living cells show a characteristic transition from subdiffusion on short time scales to superdiffusion on long time scales. In this Chapter, we develop a stochastic model, which is able to describe both this transition and the experimentally observed behavior in both the sub- and superdiffusive regime. The mathematical basis for our model is the fractional Langevin equation. The equilibrium fractional Langevin equation is an established model for anticorrelated subdiffusion and has been shown to reproduce many of the features of the equilibrium dynamics in cells and similar crowded environments. For this reason, we choose it as the foundation of our nonequilibrium model. In Section 2.1, we show how the fractional Langevin equation arises as a generalization of the Langevin equation and discuss its solution and the physical implications of the latter. The fractional Langevin equation describes the motion of a particle in a viscoelastic equilibrium environment. Mathematically, a long-ranged power-law memory kernel, which causes the evolution to depend on the entire history of the process, interpolates between viscous and elastic behavior. Since the memory kernel is a power-law, it has no characteristic time scale, and the process described by the fractional Langevin equation is asymptotically scale-invariant. The long-range memory induces negative, long-ranged correlations in the velocity. These long-range anticorrelations cause the particle to be more likely to reverse its velocity for long times and are responsible for the subdiffusive motion. Importantly, the fractional Langevin equation describes an equilibrium system, for which the fluctuation-dissipation theorem connects the thermal fluctuations with the dissipative mechanical properties.

In order to extend the fractional Langevin equation to nonequilibrium dynamics, we need to introduce a term which violates the fluctuation-dissipation theorem. We do this in Section 2.2 in two different but equivalent ways, both of which extend existing models. The first idea is based on Ref. [Brun 09]. There, an additional external noise term was introduced into the fractional Langevin equation. Since this noise is not related to the memory kernel via the fluctuation-dissipation theorem, it drives the system out of equilibrium and can indeed induce superdiffusion for long times. The external noise in Ref. [Brun 09] was assumed as stationary and good agreement between the model and the experimental system, which consisted of small endogenous particles in the cell's cytoplasm, was observed. For beads bound to the cytoskeleton, however, a careful analysis of the model's parameters reveals that it cannot possibly describe the experimental results. In particular, the external noise can no longer be stationary but its magnitude needs to increase with time. The first, heuristic, approach is thus to replace the stationary external noise of Ref. [Brun 09] with a nonstationary one. While this yields the desired sub- and superdiffusion, it does not reveal anything about the origin of the strange nonstationary behavior of the noise itself. This is where the second approach comes

into play. In Ref. [Metz 07], the tracer particle is treated as bound in a moving harmonic (i.e. elastic) trap moving at constant velocity. Here, both subdiffusion and superdiffusion emerge as a transient behaviors. The former between diffusion and confined motion within the trap, the latter between the confined motion and the ballistic motion of the trap itself. This approach, however, does not capture the viscoelastic properties of the medium and neither the subdiffusion nor superdiffusion exponent are related to the parameters of the model in a straightforward manner, as both are transient effects. While this model was able to reproduce the experimentally observed mean-square displacement rather well, it was found to exhibit too pronounced anticorrelations for short times and too pronounced correlations for long times when compared to the experimental data. We extend this model in two ways: Firstly, we do not treat the particle as bound elastically, but model its interaction with the medium (the cytoskeleton) with the viscoelastic fractional Langevin equation. This allows us to smoothly interpolate between viscous and elastic behavior and leads to reduced anticorrelations. Secondly, we do not model the motion of the cytoskeleton as purely ballistic but instead as a dedicated random process with reduced long-time correlations. With these two extensions in mind, we term our model "moving viscoelastic medium model".

More specifically, we introduce a random "medium velocity" process $v_m(t)$. For $v_m = 0$, our model corresponds to the fractional Langevin equation and thus reproduces the equilibrium subdiffusion. In contrast to a particle in a harmonic trap, subdiffusion not only occurs transiently, but as also as the asymptotic long-time behavior. For $v_m \neq 0$, on the other hand, the motion of the particle will asymptotically follow the motion of the medium and thus be governed by the properties of the process v_m. By choosing an appropriate stochastic process v_m, we thus realize superdiffusion for long times. We present three candidate processes that accomplish this superdiffusion: Stationary and nonstationary fractional Gaussian noise and the non-Gaussian Lévy walk. As with the subdiffusion, this superdiffusion does not only appear as a transient behavior but describes the long-time asymptotics as well. The viscoelastic moving medium model thus yields a smooth transition between short-time subdiffusion and long-time superdiffusion, cast into a stochastic Langevin-type equation of motion. The sub- and superdiffusion exponent are directly specified via the exponent $0 < \alpha < 1$ of the equilibrium fractional Langevin respectively the characteristic exponent $0 < \beta < 1$ of the process v_m. Since the nonequilibrium behavior is governed by a dedicated stochastic process, we can choose the latter to best match the experimental observations. Our model also allows identifying an effective external noise, which represents the force acting on the particle due to the motion of the cytoskeleton. As noted above, this external noise can be nonstationary in the sense that its magnitude increases with time. However, the nonstationarity can now be explained as the result of the combination of the viscoelastic medium and the motion of the latter, for details, we refer to Section 4.3 at this point. Note that our model incorporates both the one of Ref. [Brun 09] (for $2\alpha + \beta < 1$) and the one of Ref. [Metz 07] (for $\alpha = \beta = 1$) as special cases.

In Section 2.3 we explicitly solve the nonequilibrium fractional Langevin in terms of velocity and position correlation functions and discuss the asymptotic behavior of the latter. We show, that asymptotically, the solution exhibits a particular scaling behavior, which mirrors the asymptotic scale invariance of the involved stochastic processes. The mean-square displacement can be written as a sum of two terms, one that describes the contribution form the equilibrium subdiffusion with diffusion exponent $1-\alpha$, and one that corresponds to the superdiffusion introduced by the medium velocity process with diffusion exponent $1+\beta$. Since the former is the dominant contribution for short times and the latter for long times, our model reproduces the desired transition from sub- to superdiffusion. Further, it retains an important property of the equilibrium fractional Langevin equation: The anomalous response function or creep function, which describes the response of the particle to a constant external force. Since the fluctuation-dissipation theorem holds for the equilibrium component of the mean-square displacement, the creep function increases asymptotically with the same exponent $1-\alpha$. This relation between response and diffusion is called Stokes-Einstein relation. Finally, we discuss, in a more general context, the consequence of the presence of a nonequilibrium noise term in the Langevin equation. As it turns out, the resulting dynamics can be stationary for all times only if the system is in equilibrium and the fluctuation-dissipation theorem holds. For a nonequilibrium noise, there necessarily have to be finite-time deviations from the stationary behavior, even if the system does eventually become stationary for long times. This means that nonequilibrium and nonstationarity are intimately related and the study of more general, nonstationary correlation functions is necessary to understand the dynamics.

2.1 THE FRACTIONAL LANGEVIN EQUATION

In this Section, we set the stage for the following discussion and introduce our basic mathematical model, the fractional Langevin equation. We start out with a short review of stochastic Langevin dynamics in Section 2.1.1. Then in Section 2.1.2 we introduce the mathematical model proper, the generalized Langevin equation, of which the fractional Langevin equation is a particular case. Finally, we shortly outline the solution of the equilibrium fractional Langevin equation and discuss its most important properties.

2.1.1 *Langevin equation*

The Langevin equation [Lang 08, Coff 04] describes the motion of a probe particle of mass m in a thermal bath of temperature T,

$$\dot{v}(t) = -\gamma v(t) + \frac{1}{m}\eta(t). \tag{2.1}$$

Here γ is a relaxation rate describing the systematic dissipation of energy from the probe particle into the bath. $\eta(t)$ is a random force representing the fact that the thermal motion of the bath particles transfers momentum onto the probe via

collisions. Within the framework of the usual Langevin equation, this random force is unbiased and completely uncorrelated in time,

$$\langle \eta(t) \rangle = 0, \qquad \langle \eta(t_2)\eta(t_1) \rangle = 2m^2 D_v \delta(t_2 - t_1), \tag{2.2}$$

where D_v is the velocity diffusion coefficient and $\delta(t)$ is the Dirac delta function. It is furthermore Gaussian, meaning that all higher order correlations are either zero (for odd orders) or can be expressed as a sum of products of the second order correlator via the Gaussian moment theorem (for even orders). Since both the dissipation and the fluctuating force are due to the interaction of the probe particle with the bath, they are not independent of each other but are related via the temperature through the fluctuation-dissipation theorem [Coff 04, Reif 09] which links the velocity diffusion coefficient D_v and the relaxation rate γ,

$$D_v = \frac{\gamma k_B T}{m}, \tag{2.3}$$

where k_B is the Boltzmann constant. The fluctuation-dissipation theorem is a fundamental consequence of the equipartition theorem and applies to equilibrium systems only [Reif 09]. It expresses the fact that both the viscous friction and the kicks from the random force are due to interactions of the probe particle with the thermal bath. A direct consequence of Eq. (2.3) is the Stokes-Einstein relation (see Section 2.3.3) which relates the diffusive motion of the probe particle to its response to an external force. The Langevin equation (2.1) is Markovian [Doob 90], which means the evolution of the velocity only depends on its instantaneous value $v(t)$ at time t. Since Eq. (2.1) is linear in the velocity, we can immediately write down the formal solution,

$$\begin{aligned} v(t) &= v_0 e^{-\gamma t} + \frac{1}{m}\int_0^t dt'\, e^{-\gamma(t-t')}\eta(t'), \\ x(t) &= x_0 + \frac{v_0}{\gamma}\left(1 - e^{-\gamma t}\right) + \frac{1}{m}\int_0^t dt'' \int_0^{t''} dt' e^{-\gamma(t''-t')}\eta(t'), \end{aligned} \tag{2.4}$$

where $v_0 = v(0)$ and $x_0 = x(0)$ are the particle's initial velocity and position. Using the noise autocorrelation function Eq. (2.2), we obtain the results for the velocity and position autocorrelation,

$$\langle v(t_2)v(t_1) \rangle = \frac{k_B T}{m} e^{-\gamma(t_2-t_1)} + \left(\langle v_0^2 \rangle - \frac{k_B T}{m}\right) e^{-\gamma(t_2+t_1)}, \tag{2.5}$$

$$\begin{aligned} \langle x(t_2)x(t_1) \rangle = \langle x_0^2 \rangle &+ \frac{1}{\gamma}\langle v_0 x_0 \rangle \left(2 - e^{-\gamma t_2} - e^{-\gamma t_1}\right) \\ &+ \frac{1}{\gamma^2}\langle v_0^2 \rangle \left(1 - e^{-\gamma t_2} - e^{-\gamma t_1} + e^{-\gamma(t_2+t_1)}\right) \\ &+ \frac{2k_B T}{m\gamma} t_1 + \frac{k_B T}{m\gamma^2}\Big(2e^{-\gamma t_2} + 2e^{-\gamma t_1} \\ &- e^{-\gamma(t_2+t_1)} - e^{-\gamma(t_2-t_1)} - 2\Big), \end{aligned} \tag{2.6}$$

where we assumed that the initial values v_0 and x_0 are statistically independent of the random force, $\langle v_0\eta(t)\rangle = \langle x_0\eta(t)\rangle = 0$, as well as $t_2 > t_1$ without loss of generality. Equations (2.5) and (2.6) simplify in the limit of long times $t_2, t_1 \gg 1/\gamma$,

$$\langle v(t_2)v(t_1)\rangle \simeq \frac{k_B T}{m} e^{-\gamma(t_2-t_1)}, \tag{2.7}$$

$$\langle x(t_2)x(t_1)\rangle \simeq \left\langle \left(x_0 + \frac{v_0}{\gamma}\right)^2 \right\rangle + \frac{2k_B T}{m\gamma} t_1 + \frac{k_B T}{m\gamma^2} e^{-\gamma(t_2-t_1)}. \tag{2.8}$$

In particular, the velocity autocorrelation is stationary, it depends only on the time lag $t_2 - t_1$. The mean square velocity relaxes to its thermal value $\langle v^2\rangle_{th} = k_B T/m$ corresponding to the equipartition theorem in an exponential manner. For the mean square displacement $\langle \Delta x^2(t)\rangle$ with $\Delta x(t) = x(t) - x(0)$, we find normal diffusion,

$$\langle \Delta x^2(t)\rangle \simeq 2D_1 t \quad \text{with} \quad D_1 = \frac{k_B T}{m\gamma}. \tag{2.9}$$

The constant D_1 is called the spatial diffusion coefficient, the subscript 1 denoting that it refers to normal diffusion. The relation linking the spatial diffusion coefficient D_1 to the friction constant γ via the temperature is called Einstein relation [Eins 05]. The Markovian Langevin equation (2.1) describes the motion of the probe particle in an ideal viscous environment, which is unaffected by the particle's motion.

2.1.2 *Fractional Langevin equation: Anticorrelated subdiffusion*

In general, the equation describing the motion of the probe particle does not have to be Markovian. The more general case, which takes into account the existence of memory effects, is covered by the generalized Langevin equation [Mori 65, Kubo 65],

$$\dot{v}(t) = -\gamma \int_0^t dt'\, k(t-t')v(t') + \frac{1}{m}\eta(t). \tag{2.10}$$

The memory or friction kernel $k(t)$ takes into account the fact that the damping force acting on the particle may not only depend on its instantaneous velocity $v(t)$ but also on the velocity at earlier times $t' < t$. The value of the memory kernel function describes how the motion is affected by the velocity at earlier times. This retarded friction may be due to displacements of the surrounding medium caused by the motion of the particle or to an elastic-like behavior of the medium. Since the bath is assumed to be in thermal equilibrium, the fluctuation-dissipation theorem holds in its more general form [Kubo 66],

$$\langle \eta(t_2)\eta(t_1)\rangle = m\gamma k_B T\, k(|t_2 - t_1|). \tag{2.11}$$

The retardation in the memory kernel $k(t)$ thus is accompanied by correlations in the random force $\eta(t)$, which is still assumed as unbiased and Gaussian. The solution of Eq. (2.10) is most conveniently carried out in frequency space by introducing the Laplace transform $\tilde{f}(s)$ of a time-dependent function $f(t)$ [Doet 74],

$$\tilde{f}(s) \equiv \mathcal{L}[f(t)]_{t\to s} = \int_0^\infty dt\, e^{-st} f(t). \tag{2.12}$$

Under Laplace transform, the derivative and convolution in Eq. (2.10) are replaced by multiplications,

$$s\tilde{v}(s) - v_0 = -\gamma\tilde{k}(s)\tilde{v}(s) + \frac{1}{m}\tilde{\eta}(s). \tag{2.13}$$

The solution of Eq. (2.13) is then straightforward,

$$\begin{aligned}\tilde{v}(s) &= \frac{1}{s+\gamma\tilde{k}(s)}\left(v_0 + \frac{1}{m}\tilde{\eta}(s)\right),\\ \tilde{x}(s) &= \frac{x_0}{s} + \frac{1}{s^2+s\gamma\tilde{k}(s)}\left(v_0 + \frac{1}{m}\tilde{\eta}(s)\right).\end{aligned} \tag{2.14}$$

The generalized Langevin equation (2.10) reduces to the usual Langevin equation (2.1) if the friction kernel is infinitely short ranged, $k(t) = \delta(t)$, respectively $\tilde{k}(s) = 1$. A short ranged memory kernel with a finite memory time t_α, e.g. an exponential one $k(t) = e^{-t/t_\alpha}/t_\alpha$ or $\tilde{k}(s) = 1/(1+t_\alpha s)$, will lead to a non-Markovian dynamics on time scales shorter than the memory time $t \ll t_\alpha$. For long times $t \gg t_\alpha$ which according to the Tauberian theorems [Wien 32, Doet 74] corresponds to $t_\alpha s \ll 1$, the memory kernel is well approximated by a delta function $\tilde{k}(s) \simeq 1$ and the long-time dynamics becomes effectively Markovian.

The situation is markedly different when the memory kernel is a power law,

$$k(t) = \frac{1}{\Gamma(\alpha)t_\alpha}\left(\frac{t}{t_\alpha}\right)^{\alpha-1}, \qquad \tilde{k}(s) = (t_\alpha s)^{-\alpha}, \tag{2.15}$$

with $0 < \alpha < 1$ and the gamma function $\Gamma(a)$ [Abra 12]. For this form of the memory kernel, the generalized Langevin equation is called fractional Langevin equation [Lutz 01]. The name fractional originates form the definition of the Riemann-Liouville fractional integral operator J^α [Mill 93],

$$J^\alpha f(t) = \frac{1}{\Gamma(\alpha)}\int_0^t dt'\,(t-t')^{\alpha-1}f(t'), \tag{2.16}$$

in terms of which the fractional Langevin equation reads,

$$\begin{aligned}\dot{v}(t) &= -\frac{\gamma}{\Gamma(\alpha){t_\alpha}^\alpha}\int_0^t dt'\,(t-t')^{\alpha-1}v(t') + \frac{1}{m}\eta(t)\\ &= -\frac{\gamma}{{t_\alpha}^\alpha}J^\alpha v(t) + \frac{1}{m}\eta(t).\end{aligned} \tag{2.17}$$

Note that we keep the time scale t_α in Eq. (2.15) primarily to make clear the dimensionality of the respective quantities, from a practical point of view, we may also absorb it into the friction constant γ. This arbitrariness of the time scale t_α is not a coincidence: Due to the power-law form of Eq. (2.15), the memory is time-scale invariant, in that there exists no characteristic decay time after which memory effects can be truncated. Thus the memory kernel Eq. (2.15) does not reduce to a delta function for long times but is long ranged. Consequently, the non-Markovian effects persist even in the long time limit. The generalized Langevin equation Eq. (2.10) can be derived microscopically from a particle coupled to a

bath of oscillators [Zwan 80]. In terms of this derivation, the memory kernel $k(t)$ is related to the distribution of oscillator frequencies. Thus a long-ranged memory kernel indicates a broad distribution of relaxation times in the medium, as in the cellular cytoplasm due to presences of a multitude of different particle species [Ball 06]. Transforming Eq. (2.14) back to the time domain, we have with the definitions $\tilde{g}(s) = 1/(s + \gamma\tilde{k}(s))$ respectively $\tilde{h}(s) = \tilde{g}(s)/s$,

$$\begin{aligned} v(t) &= v_0 g(t) + \frac{1}{m}\int_0^t dt'\, g(t-t')\eta(t'), \\ x(t) &= x_0 + v_0 h(t) + \frac{1}{m}\int_0^t dt'\, h(t-t')\eta(t'). \end{aligned} \tag{2.18}$$

For the power law memory kernel Eq. (2.15), the kernel functions $g(t)$ and $h(t)$ are given by (generalized) Mittag-Leffler functions [Bate 55, Haub 11],

$$\begin{aligned} E_a(z) &= \sum_{n=0}^{\infty} \frac{1}{\Gamma(an+1)} z^n, \\ E_{a,b}(z) &= \sum_{n=0}^{\infty} \frac{1}{\Gamma(an+b)} z^n, \end{aligned} \tag{2.19}$$

which obey the following relation under Laplace transform [Haub 11],

$$\mathcal{L}\left[t^{b-1}E_{a,b}(-ct^a)\right]_{t\to s} = \frac{s^{-b}}{1+cs^{-a}}. \tag{2.20}$$

Comparing this to Eqs. (2.15) and (2.18), we find,

$$\begin{aligned} g(t) &= E_{\alpha+1}\left(-\gamma t_\alpha \left(\frac{t}{t_\alpha}\right)^{\alpha+1}\right), \\ h(t) &= tE_{\alpha+1,2}\left(-\gamma t_\alpha \left(\frac{t}{t_\alpha}\right)^{\alpha+1}\right). \end{aligned} \tag{2.21}$$

Using the fluctuation-dissipation theorem (2.11) to express the noise autocorrelation through the memory kernel, this allows computing the velocity autocorrelation function [Pott 03],

$$\begin{aligned} \langle v(t_2)v(t_1)\rangle = &\frac{k_B T}{m} E_{\alpha+1}\left(-\gamma t_\alpha \left(\frac{t_2-t_1}{t_\alpha}\right)^{\alpha+1}\right) \\ &+ \left(\langle v_0^2\rangle - \frac{k_B T}{m}\right) E_{\alpha+1}\left(-\gamma t_\alpha \left(\frac{t_2}{t_\alpha}\right)^{\alpha+1}\right) \\ &\times E_{\alpha+1}\left(-\gamma t_\alpha \left(\frac{t_1}{t_\alpha}\right)^{\alpha+1}\right). \end{aligned} \tag{2.22}$$

Similar to Eq. (2.5), the mean-square velocity relaxes to the thermal equilibrium value and the velocity autocorrelation becomes stationary in the long time limit. However, both the relaxation and the decay of the stationary autocorrelation are no

longer exponential but instead described by a Mittag-Leffler function. The asymptotic behavior of the latter for large respectively small negative arguments is given by [Haub 11],

$$\begin{aligned} E_{a,b}(-z) &\simeq \frac{1}{\Gamma(b-a)}z^{-1} - \frac{1}{\Gamma(b-2a)}z^{-2} + \mathcal{O}(z^{-3}) \text{ for } \quad z \gg 1 \\ E_{a,b}(-z) &\simeq \frac{1}{\Gamma(b)} - \frac{1}{\Gamma(a+b)}z + \mathcal{O}(z^2) \quad \text{for } z \ll 1, \end{aligned} \tag{2.23}$$

which means that the long time asymptotic velocity autocorrelation for $t_2, t_1 \gg t_\alpha(\gamma t_\alpha)^{-1/(\alpha+1)}$ is [Pott 03],

$$\begin{aligned} \langle v(t_2)v(t_1)\rangle \simeq \frac{k_B T}{m} E_{\alpha+1}\left(-\gamma t_\alpha \left(\frac{t_2-t_1}{t_\alpha}\right)^{\alpha+1}\right) \\ + \frac{1}{\Gamma^2(-\alpha)\gamma^2 {t_\alpha}^2}\left(\langle v_0^2\rangle - \frac{k_B T}{m}\right)\left(\frac{t_2}{t_\alpha}\frac{t_1}{t_\alpha}\right)^{-\alpha-1}. \end{aligned} \tag{2.24}$$

The relaxation into the equilibrium state now is algebraic instead of exponential, as is the asymptotic behavior of the stationary velocity autocorrelation for long time lags, $t_2 - t_1 \gg t_\alpha(\gamma t_\alpha)^{-1/(\alpha+1)}$,

$$\langle v(t_2)v(t_1)\rangle \simeq \frac{k_B T}{\Gamma(-\alpha) m \gamma t_\alpha}\left(\frac{t_2-t_1}{t_\alpha}\right)^{-\alpha-1}. \tag{2.25}$$

Since we have $0 < \alpha < 1$, the velocity autocorrelation function is asymptotically negative, implying that the velocity process is anticorrelated: At time t_2, it is more likely to find the particle moving in the opposite direction compared to its motion at time t_1 [Lutz 01]. Since the velocity correlation functions Eqs. (2.5) and (2.22) describe a particle in contact with an equilibrium environment, they both exhibit two characteristic properties: Firstly, for long times, the velocity of the particle will be distributed according to the thermal Maxwell-Boltzmann distribution, i.e. a Gaussian whose width is determined by the equipartition theorem. Secondly, if the particle starts out with a thermally distributed velocity, it will remain in this state for all time. The position autocorrelation function is obtained in a similar manner, a detailed discussion can be found in Ref. [Pott 03]. Here, we note that the mean square displacement is given by,

$$\begin{aligned} \langle \Delta x^2(t)\rangle &= \frac{2k_B T}{m} t^2 E_{\alpha+1,3}\left(-\gamma t_\alpha \left(\frac{t}{t_\alpha}\right)^{\alpha+1}\right) \\ &\simeq \frac{2k_B T}{\Gamma(2-\alpha)\gamma t_\alpha}\left(\frac{t}{t_\alpha}\right)^{1-\alpha}, \end{aligned} \tag{2.26}$$

where the second line is the asymptotic behavior for long times. Contrary to Eq. (2.9), we now have subdiffusion $\langle \Delta x^2(t)\rangle \sim 2D_\nu t^\nu$ with $\nu = 1-\alpha < 1$. This agrees with the anticorrelation found for the velocity (see Eq. (2.25), since if the particle is more likely to reverse its motion, we expect the spreading of a cloud of particles to slow down.

The power law memory kernel Eq. (2.15) was defined for values of the exponent $0 < \alpha < 1$. It is interesting to note what happens in the limits $\alpha \to 0$ respectively $\alpha \to 1$. For $\alpha \to 0$, we use the identity $E_1(z) = e^z$ in Eq. (2.22) and find that it reduces to Eq. (2.5), where the relaxation is exponential and we have normal diffusion. Thus $\alpha = 0$ corresponds to the case of a purely viscous thermal environment and thus normal diffusion. For $\alpha \to 1$, on the other hand, the memory kernel Eq. (2.15) is constant, $k(t) = 1/t_\alpha$. Equation (2.10) then reduces to an equation in $x(t)$,

$$\ddot{x}(t) = -\frac{\gamma}{t_\alpha}(x(t) - x(0)) + \frac{1}{m}\eta(t). \tag{2.27}$$

This is precisely the equation of motion of a noisy harmonic oscillator of frequency $\sqrt{\gamma/t_\alpha}$. Consequently, $\alpha = 1$ corresponds to a probe particle coupled to an elastic medium. Since the fractional Langevin equation for $0 < \alpha < 1$ interpolates between viscous and elastic behavior, the medium is in this regime referred to as viscoelastic [Koll 11]. In the context of a crowded medium, this can be imagined as its constituents being at the same time elastically deformed and viscously displaced by the motion of the probe particle.

2.2 EXTENSION TO SUPERDIFFUSIVE NONEQUILIBRIUM DYNAMICS

The fractional Langevin equation discussed in the previous section describes a subdiffusive equilibrium system. If we ultimately want to describe the dynamics in living cells, we need to extend this description to nonequilibrium and possibly superdiffusive systems. We want to retain the basic features of the equilibrium fractional Langevin equation, since, as discussed before, the latter accurately describes the equilibrium behavior and can thus be expected to serve as a useful starting point for discussing nonequilibrium systems. In this section we discuss two methods of accomplishing this extension: First, in Section 2.2.1, we model the nonequilibrium part in a heuristic way as an additional noise term and discuss the dynamics the qualitative dynamics subject to the properties of the nonequilibrium noise. Then, in Section 2.2.2 we present an alternative approach, where the nonequilibrium dynamics is induced by active motion of the environment and show how this relates to the heuristic nonequilibrium noise introduced before. To this end, we present three potential candidates for a stochastic process that describes the active motion of the environment. We also introduce the important concept of a scaling correlation function, which will be seen to describe most of the stochastic processes we are interested in and whose general properties will be exploited in the next chapter. Finally we discuss the resulting properties of this nonequilibrium noise for each of the three candidate choices in Section 2.2.3.

2.2.1 *External nonequilibrium noise*

A straightforward way to drive the system described by a generalized Langevin equation like Eq. (2.10) out of equilibrium is to introduce an additional force term $\xi(t)$ [Brun 09, Desp 11, Bohe 13],

$$\dot{v}(t) = -\gamma \int_0^t dt' k(t-t') v(t') + \frac{1}{m}\eta(t) + \frac{1}{m}\xi(t). \tag{2.28}$$

In general, $\xi(t)$ may contain both a deterministic and a stochastic part. We will discuss the effect of deterministic forces applied to the system in some detail in section 2.3.3. For now, we take $\xi(t)$ to be an unbiased stochastic force, $\langle \xi(t) \rangle = 0$. This form of $\xi(t)$ is a reasonable choice for the nonequilibrium forces due to the active motion in the cell, since these are mediated through molecular motors moving along the mostly randomly oriented actin network. As the nonequilibrium effects in living cells are generally observed on long time scales, the nonequilibrium noise correlations should decay more slowly than the thermal fluctuations. Since the latter are characterized by the exponent α via the fluctuation-dissipation theorem (2.11),

$$\langle \eta(t+\tau)\eta(t) \rangle = \frac{2m\gamma k_B T}{\Gamma(\alpha) t_\alpha} \left(\frac{\tau}{t_\alpha} \right)^{\alpha-1}, \tag{2.29}$$

a suitable choice for the nonequilibrium noise correlations might be [Brun 09],

$$\langle \xi(t+\tau)\xi(t) \rangle = \frac{a_\mu^2}{\Gamma(\mu)} \left(\frac{\tau}{t_\mu} \right)^{\mu-1}, \tag{2.30}$$

with $\alpha < \mu < 1$. Here t_μ is a time scale which governs the decay of the correlations. Due to the power-law nature of Eq. (2.30), however, the magnitude of this time scale is fundamentally inseparable from the constant a_μ which determines the magnitude of the noise. In this sense, we introduce t_μ only because it is convenient in order to check the dimensionality of the resulting expressions. This form of the nonequilibrium force was considered in Ref. [Brun 09] and shown to lead to enhanced diffusion compared to the equilibrium system. In principle, we may also consider $0 < \mu < \alpha$, however, as we will show in section 2.3, in this case the contribution of the nonequilibrium noise will be sub-dominant to the equilibrium noise in the long-time limit and thus asymptotically not lead to enhanced diffusion. The noise in Eq. (2.30) is explicitly stationary, i.e. its magnitude remains constant in time and the correlations depend only on the time lag τ. As we are considering nonequilibrium systems, there is however no reason to assume the noise as stationary. Moreover, we will see in Section 2.3.2 that a stationary noise cannot actually reproduce the experimental observations for a tracer bound to the cytoskeleton. A nonstationary generalization of Eq. (2.30) is given by,

$$\langle \xi(t+\tau)\xi(t) \rangle = \frac{2(-1)^{-\frac{\mu}{2}} c_\mu^2}{\Gamma^2\left(\frac{\mu}{2}\right)} \left(\frac{\tau}{t_\mu} \right)^{\mu-1} B\left(-\frac{t}{\tau}; \frac{\mu}{2}, \frac{\mu}{2} \right). \tag{2.31}$$

Here $B(x; a, b)$ is the incomplete beta function [Abra 12]. At first, this choice might appear somewhat random, but it is in fact a natural generalization of Eq. (2.30). To see this, we note that in the limit $t \gg \tau$,

$$\langle \xi(t+\tau)\xi(t)\rangle \simeq \begin{cases} \frac{c_\mu}{2\Gamma(\mu)\cos\left(\frac{\pi\mu}{2}\right)} \left(\frac{\tau}{t_\mu}\right)^{\mu-1} & \text{for} \quad \mu < 1 \\ \frac{1}{(\mu-1)\Gamma^2\left(\frac{\mu}{2}\right)} t^{\mu-1} & \text{for} \quad \mu > 1. \end{cases} \tag{2.32}$$

For $\mu < 1$, the nonstationary process defined by Eq. (2.31) reproduces the stationary one, Eq. (2.30) with $c_\mu = 2a_\mu \cos(\pi\mu/2)$, in the long-time limit. However, it describes a noise process that initially (at $t = 0$) has zero magnitude and thus is nonstationary for finite t. Equation (2.31) has the advantage that, contrary to the stationary expression Eq. (2.30), it also describes a valid stochastic process for $\mu > 1$, where there exists no stationary counterpart. In this regime, the magnitude of the noise Eq. (2.31) grows with time. Equation (2.31) reduces to a rather simple form in the frequency domain,

$$\langle \tilde{\xi}(s_2)\tilde{\xi}(s_1)\rangle = \frac{c_\mu^2}{{t_\mu}^{\mu-1}} \frac{(s_2 s_1)^{-\frac{\mu}{2}}}{s_2 + s_1}. \tag{2.33}$$

In the following, we will concentrate on the first and second moments of the respective quantities, for which it is sufficient to specify the two-time autocorrelation function of the nonequilibrium noise. If the noise is Gaussian, this also determines all higher order moments. In general, however, we may also consider non-Gaussian stochastic processes for the noise, which will require us to specify higher order correlation functions.

2.2.2 *Active viscoelastic environment*

In the preceding discussion, we introduced the nonequilibrium noise term into the fractional Langevin equation by hand. We now turn to a description of the nonequilibrium dynamics that is closer to the actual physical system of a tracer particle in the cytoskeleton of a living cell. In equilibrium, there is no active motion of the cell and the tracer diffuses in the viscoelastic environment of the cytoskeleton, described by the equilibrium fractional Langevin equation Eqs. (2.10) and (2.15). In living cells, however, the cytoskeleton will itself move due to the forces exerted by molecular motors along the actin filaments. We describe this motion as a stochastic process with a random velocity $v_m(t)$ of the viscoelastic medium. Assuming that the viscoelastic coupling between the tracer and the environment is unaffected by the motion of the latter, we can write down an equation of motion for the tracer based on Eq. (2.10),

$$\dot{v}(t) = -\gamma \int_0^t dt'\, k(t-t') \left(v(t') - v_m(t')\right) + \frac{1}{m}\eta(t). \tag{2.34}$$

In contrast to Eq. (2.10), the friction here does not depend on the absolute velocity of the particle but instead on its velocity relative to the surrounding medium, $v(t) - v_m(t)$. Note that the absolute velocity still appears in the inertial term on the left hand side of Eq. (2.34), since the particle does not follow the motion of the medium

instantly. This is similar to the approach taken in Ref. [Metz 07], where a tracer particle was considered to be trapped in a randomly moving potential. In contrast to the former approach, we allow for subdiffusive motion relative to the "trap" and consider the motion of the cytoskeleton as a dedicated random process.

The description of the nonequilibrium properties in terms of a moving environment is actually closely related to the heuristic description in terms of an additional nonequilibrium noise discussed previously. By identifying,

$$\xi(t) = m\gamma \int_0^t dt'\, k(t-t')v_m(t'), \tag{2.35}$$

Eq. (2.34) takes precisely the form of Eq. (2.28), relating the nonequilibrium noise and the motion of the surrounding medium. By specifying the properties of the process $v_m(t)$, we thus uniquely determine the nonequilibrium noise. Their autocorrelation functions are related in the time and frequency domain, respectively, via,

$$\begin{aligned}\langle \xi(t_2)\xi(t_1)\rangle &= m^2\gamma^2 \int_0^{t_2} dt'' \int_0^{t_1} dt'\, k(t_2-t'')k(t_1-t')\langle v_m(t'')v_m(t')\rangle,\\ \langle \tilde{\xi}(s_2)\tilde{\xi}(s_1)\rangle &= m^2\gamma^2 \tilde{k}(s_2)\tilde{k}(s_1)\langle \tilde{v}_m(s_2)\tilde{v}_m(s_1)\rangle.\end{aligned} \tag{2.36}$$

We will discuss the properties of the noise autocorrelation for different choices of the medium velocity autocorrelation in Section 2.2.3.

In the following, we will concentrate on three particular choices for the medium velocity $v_m(t)$. These three examples are fractional Gaussian noise of the Riemann-Liouville respectively Mandelbrot-van-Ness type and the Lévy walk. They all have in common that their autocorrelation functions behave as a power-law for long times.

Riemann-Liouville fractional Gaussian noise

Riemann-Liouville fractional Gaussian noise is a generalization of white noise to overdamped fractional Brownian motion [Lim 02]. The Langevin equation for Brownian motion of a particle in the overdamped limit (i.e. when inertial effects can be neglected) reads,

$$m\gamma v(t) = \xi(t), \tag{2.37}$$

where $\xi(t)$ is Gaussian white noise (see Eq. (2.2)). This means that the velocity itself is Gaussian white noise. By integrating both sides with respect to time, the can be written as,

$$m\gamma x(t) = \int_0^t dt'\xi(t'), \tag{2.38}$$

where we assume $x(0) = 0$ without loss of generality. The displacement $x(t)$ of the particle is thus given as an integral over white noise. This integral of course has to be evaluated according to the rules of stochastic calculus; we take all integrals

of this kind to be of the Stratonowich type [Kamp 81], although in our case this turns out to be irrelevant since we do not consider multiplicative noise. Equation (2.38) is equivalent to the long-time limit of Eq. (2.6) and leads to normal diffusion, Eq. (2.9). The generalization to fractional Brownian motion is done by replacing the integration in Eq. (2.38) by a fractional integral [Mill 93], see Eq. (2.16),

$$\begin{aligned} m\gamma x(t) &= \frac{1}{\Gamma\left(\frac{\beta}{2}+1\right)} \int_0^t dt' \left(\frac{t-t'}{t_\beta}\right)^{\frac{\beta}{2}} \xi(t') \\ &= t_\beta{}^{-\frac{\beta}{2}} J^{\frac{\beta}{2}+1} \xi(t), \end{aligned} \tag{2.39}$$

with $-1 < \beta < 1$. The resulting motion is subdiffusive for $\beta < 0$ and superdiffusive for $\beta > 0$. The exponent β is related to the Hurst exponent H which is often employed in the literature by $H = (\beta+1)/2$ [Hurs 51, Mand 68]. For $\beta > 0$, we can take the time-derivative of Eq. (2.39) and obtain for the velocity,

$$m\gamma v(t) = \frac{1}{\Gamma\left(\frac{\beta}{2}\right) t_\beta} \int_0^t dt' \left(\frac{t-t'}{t_\beta}\right)^{\frac{\beta}{2}-1} \xi(t'). \tag{2.40}$$

Since the process is scale-invariant, the time scale t_β is in principle arbitrary and is only kept for reasons of dimensionality. Since for usual Brownian motion, the velocity is described by white noise, Eq. (2.37), we call Eq. (2.40) fractional Gaussian noise, since it is the derivative of fractional Brownian motion. In this case, the initial velocity vanishes, $v(0) = 0$, which is referred to as Riemann-Liouville fractional Gaussian noise [Lim 02]. Note that in the subdiffusive case $\beta < 0$, Eq. (2.40) is not well-defined since the integral diverges at the upper boundary. This is an artifact of the overdamped description, taking into account inertial effects provides a short-time cutoff on the power-law kernel function and we end up with the fractional Langevin equation (2.17). We use Eq. (2.40) as one candidate for the medium velocity $v_m(t)$. In the Laplace domain, this then leads to the velocity autocorrelation function,

$$\langle \tilde{v}_m(s_2)\tilde{v}_m(s_1)\rangle = \frac{{v_{typ}}^2}{{t_\beta}^{\beta-1}} \frac{(s_2 s_1)^{-\frac{\beta}{2}}}{s_2+s_1}, \tag{2.41}$$

where we introduced the typical velocity scale $v_{typ} = \sqrt{2D_v t_\beta/\gamma^2}$. Using the identity Eq. (A.4), we find the corresponding expression in the time domain,

$$\langle v_m(t+\tau)v_m(t)\rangle = \frac{{v_{typ}}^2}{\Gamma^2\left(\frac{\beta}{2}\right){t_\beta}^{\beta-1}} \int_0^t dt' (t+\tau-t')^{\frac{\beta}{2}-1}(t-t')^{\frac{\beta}{2}-1}. \tag{2.42}$$

While the integral can be expressed in terms of a hypergeometric function, it is more interesting to note the scaling properties of this expression. By changing the variable of integration to $z = t'/t$, we have,

$$\langle v_m(t+\tau)v_m(t)\rangle = \frac{{v_{typ}}^2}{\Gamma^2\left(\frac{\beta}{2}\right)} \left(\frac{t}{t_\beta}\right)^{\beta-1} \int_0^1 dz \left(1+\frac{\tau}{t}-z\right)^{\frac{\beta}{2}-1} (1-z)^{\frac{\beta}{2}-1}. \tag{2.43}$$

The autocorrelation function of the nonequilibrium noise thus depends only on the initial time t and the ratio of the time lag τ and the initial time. We will encounter similar correlation functions for a number of different quantities, including the velocity and position. In Chapter 3 we will extensively discuss their origins and properties as well as their relation to superdiffusive dynamics. We term this type of correlation function "scaling correlation function" [Dech 14], since the dependence on the time lag τ scales with the initial time t, i.e. rescaling both τ and t by the same factor changes the overall value of the correlation function but not its qualitative behavior. We write the scaling correlation function in the following way,

$$\begin{aligned}
\langle v_m(t+\tau)v_m(t)\rangle &= \mathcal{C}\, t^{\beta-1}\phi\left(\frac{\tau}{t}\right),\\
\text{with}\quad \mathcal{C} &= \frac{{v_{typ}}^2}{\Gamma^2\left(\frac{\beta}{2}\right){t_\beta}^{\beta-1}},\\
\phi(y) &= \int_0^1 dz\,(1+y-z)^{\frac{\beta}{2}-1}(1-z)^{\frac{\beta}{2}-1}\\
&= (-1)^{\frac{-\beta}{2}}y^{\beta-1}B\left(-\frac{1}{y};\frac{\beta}{2},\frac{\beta}{2}\right).
\end{aligned} \tag{2.44}$$

We call $\phi(y)$ a scaling function. In this case, the integral defining $\phi_{m,RL}(y)$ can be expressed in terms of an incomplete beta function $B(x;a,b)$. The asymptotic behavior of integrals like the one in the definition of ϕ is examined in Appendix A.2. Using Eq. (A.44), we find to leading order,

$$\langle v_m(t+\tau)v_m(t)\rangle \simeq \frac{{v_{typ}}^2}{{t_\beta}^{\beta-1}}\begin{cases}\frac{\Gamma(1-\beta)\sin\left(\frac{\pi\beta}{2}\right)}{\pi}\tau^{\beta-1} & \text{for } t\gg\tau\\ \frac{1}{\Gamma\left(\frac{\beta}{2}+1\right)\Gamma\left(\frac{\beta}{2}\right)}\tau^{\frac{\beta}{2}-1}t^{\frac{\beta}{2}} & \text{for } \tau\gg t.\end{cases} \tag{2.45}$$

In the long-time limit $t\gg\tau$, the medium velocity process described by Riemann-Liouville fractional Gaussian noise thus tends to a stationary limit, while it is non-stationary for finite times, where its magnitude for any fixed $\tau\neq 0$ approaches the stationary value from below as a function of t. Equation (2.44) also describes a valid stochastic process for $\beta>1$. In this regime, there no longer is a stationary limit, instead, the magnitude of the process grows as $t^{\beta-1}$. Note that for $\beta<1$, the stationary correlation function Eq. (2.45) diverges in the limit $\tau\to 0$ and so the mean-square velocity $\langle {v_m}^2(t)\rangle$ is infinite. This divergence is due to the unphysical, infinitely short-ranged correlations of Gaussian white noise. Thus, the definition Eq. (2.40) generally needs to be supplemented by a short-time cutoff which describes the intrinsic time scales of the system and leads to a finite mean-square velocity. However, this short-time cutoff will be seen not to influence the asymptotic long-time dynamics described by Eq. (2.43) and we therefore do not need to take it into account explicitly.

Mandelbrot-van-Ness fractional Gaussian noise

Previously, we saw that Riemann-Liouville fractional Gaussian noise is asymptotically stationary in the long-time limit. This poses the question of whether it is possible to find a similar process with the same stationary correlation function,

which however is stationary for all times. From Eq. (2.45) we saw, that if we let the process described by Eq. (2.40) evolve for a long time, we get arbitrarily close to a stationary process. Thus, if the process starts out at $t = -\infty$, then, for any finite time, it will already have reached stationarity. This is precisely the definition of Mandelbrot-van-Ness fractional Gaussian noise [Mand 68],

$$m\gamma v(t) = \frac{1}{\Gamma\left(\frac{\beta}{2}\right) t_\beta} \int_{-\infty}^{t} dt' \left(\frac{t-t'}{t_\beta}\right)^{\frac{\beta}{2}-1} \xi(t'). \tag{2.46}$$

This expression does not have a straightforward representation in Laplace space, however, we can explicitly compute the autocorrelation function by using the fact that $\xi(t)$ is delta-correlated,

$$\begin{aligned}\langle v(t_2)v(t_1)\rangle = &\frac{2D_v}{\Gamma^2\left(\frac{\beta}{2}\right)\gamma^2 {t_\beta}^\beta} \\ &\times \int_{-\infty}^{t_2} dt'' \int_{-\infty}^{t_1} dt' \, [(t_2-t'')(t_1-t')]^{\frac{\beta}{2}-1} \delta(t''-t'). \end{aligned} \tag{2.47}$$

Assuming $t_2 = t+\tau > t_1 = t$ without loss of generality, we can evaluate the integral over t'',

$$\langle v(t+\tau)v(t)\rangle = \frac{2D_v}{\Gamma^2\left(\frac{\beta}{2}\right)\gamma^2 {t_\beta}^\beta} \int_{-\infty}^{t} dt' \, [(t+\tau-t')(t-t')]^{\frac{\beta}{2}-1}. \tag{2.48}$$

Changing the variable of integration to $z = (t'-t)/\tau$, we see that the correlation function is indeed stationary,

$$\langle v(t+\tau)v(t)\rangle = \frac{2D_v}{\Gamma^2\left(\frac{\beta}{2}\right)\gamma^2 {t_\beta}^\beta} \tau^{\beta-1} \int_0^\infty dz \, [(1+z)z]^{\frac{\beta}{2}-1}. \tag{2.49}$$

The remaining integral is just a constant, which evaluates to,

$$\int_0^\infty dz \, [(1+z)z]^{\frac{\beta}{2}-1} = \frac{2^{-\beta}}{\sqrt{\pi}} \Gamma\left(\frac{\beta}{2}\right) \Gamma\left(\frac{1}{2}-\frac{\beta}{2}\right). \tag{2.50}$$

Again we write this in terms of the velocity scale $v_{\text{typ}} = \sqrt{2D_v t_\beta/\gamma^2)}$ and have for the autocorrelation function of the medium velocity,

$$\langle v_m(t+\tau)v_m(t)\rangle = \frac{{v_{\text{typ}}}^2}{{t_\beta}^{\beta-1}} \frac{\Gamma(1-\beta)\sin\left(\frac{\pi\beta}{2}\right)}{\pi} \tau^{\beta-1}. \tag{2.51}$$

This is precisely the same as the stationary limit in Eq. (2.45). So, for long times, Riemann-Liouville and Mandelbrot-van-Ness fractional Gaussian noise indeed describe the same process, as they are both Gaussian and thus fully characterized by their autocorrelation function. Despite this asymptotic equality, we will see in Section 2.2.3 that the nonequilibrium noise induced by the respective medium ve-

locity is different even in the long-time limit. Note that Eq. (2.51) can in principle also be expressed in a scaling form similar to Eq. (2.44),

$$\begin{aligned}\langle v_m(t+\tau)v_m(t)\rangle &= \mathcal{C}\, t^{\beta-1}\phi\left(\frac{\tau}{t}\right),\\ \text{with}\quad \mathcal{C} &= \frac{{v_{typ}}^2}{{t_\beta}^{\beta-1}}\frac{\Gamma(1-\beta)\sin\left(\frac{\pi\beta}{2}\right)}{\pi},\\ \phi(y) &= y^{\beta-1}.\end{aligned} \tag{2.52}$$

While this seems to be an unnecessary complication, it actually shows that a stationary power-law correlation function is just a special case of the scaling form Eq. (2.44). As in the nonstationary case, we need to specify a short-time cutoff for Eq. (2.51) since it diverges as $\tau \to 0$.

Lévy walk

As our third example, we consider a non-Gaussian stochastic process, the Lévy walk [Shle 87, Klaf 90]. This process is a paradigm model for anomalous stochastic processes and has been thoroughly examined from a theoretical point of view and also successfully applied to a range of physical systems. Here we consider the simplest version of the Lévy walk, a system, which can have either velocity $+v_{typ}$ or $-v_{typ}$. At certain points in time, the system's velocity switches between these two values; the times between these switches are randomly drawn from a waiting time distribution $P_w(t_w)$. So the system starts out in one state, say $v(0) = +v_{typ}$, in which it stays for a random waiting time $t_{w,1}$. At $t = t_{w,1}$ the velocity changes to $v(t_{w,1}) = -v_{typ}$, remaining at this value for a new random waiting time $t_{w,2}$ until at $t = t_{w,1} + t_{w,2}$ it switches back to $+v_{typ}$ and so on. Since a new waiting time is drawn every time the process switches between states, this process is also called a renewal process [Godr 01]. The position dynamics of the system depend crucially on the waiting time distribution [Klaf 90, Godr 01]. If the latter is such that its second moment $\langle {t_w}^2\rangle$ is finite, then the displacement distribution is Gaussian by virtue of the central limit theorem and diffusion is normal. On the other hand, if $\langle {t_w}^2\rangle$ is infinite the system becomes superdiffusive in the long-time limit and the process is no longer Gaussian. In the following, we take the waiting time distribution to be asymptotically a power-law,

$$P_w(t_w) \sim \mathcal{N}\left(\frac{t_w}{t_\beta}\right)^{\beta-3} \qquad \text{for } t \gg t_\beta, \tag{2.53}$$

where $0 < \beta < 2$ and $\mathcal{N}$ is a normalization constant that depends on the precise behavior of the waiting time distribution for short times. $\beta < 0$ corresponds to the Gaussian case where the second moment is finite. For $0 < \beta 0$, the second moment is infinite, and for $1 < \beta < 2$, even the first moment ceases to exist. The Lévy walk has been extensively studied before and we make use of the known result for the asymptotic velocity autocorrelation function [Godr 01],

$$\langle v_m(t+\tau)v_m(t)\rangle \simeq \frac{{v_{typ}}^2}{(1-\beta){t_\beta}^{\beta-2}\langle t_w\rangle}t^{\beta-1}\left[\left(\frac{\tau}{t}\right)^{\beta-1} - \left(1+\frac{\tau}{t}\right)^{\beta-1}\right], \tag{2.54}$$

which is valid for $t, \tau \gg t_\beta$ and $0 < \beta < 1$. For later reference, the corresponding expression in Laplace space will also be useful. In terms of the variables t and τ, the latter is given by [Godr 01],

$$\mathcal{L}^2\left[\langle v_m(t+\tau)v_m(t)\rangle\right]_{t\to s}^{\tau\to u} \simeq \frac{\Gamma(\beta){v_{typ}}^2}{(1-\beta){t_\beta}^{\beta-2}\langle t_w\rangle}\frac{s^{1-\beta}-u^{1-\beta}}{s(s-u)}. \tag{2.55}$$

Using Eq. (A.21), we can write down the Laplace transform with respect to the time variables $t_1 = t$ and $t_2 = t+\tau$,

$$\langle \tilde{v}_m(s_2)\tilde{v}_m(s_1)\rangle \simeq \frac{\Gamma(\beta){v_{typ}}^2}{(1-\beta){t_\beta}^{\beta-2}\langle t_w\rangle}\frac{(s_2+s_1)^{2-\beta}-{s_2}^{2-\beta}-{s_1}^{2-\beta}}{s_2 s_1(s_2+s_1)}. \tag{2.56}$$

Equation (2.54) is the same type of scaling correlation function we found before,

$$\begin{aligned}\langle v_m(t+\tau)v_m(t)\rangle &= \mathcal{C}\, t^{\beta-1}\phi\left(\frac{\tau}{t}\right),\\ \text{with}\quad \mathcal{C} &= \frac{{v_{typ}}^2}{(1-\beta){t_\beta}^{\beta-2}\langle t_w\rangle},\\ \phi(y) &= y^{\beta-1}-(1+y)^{\beta-1}.\end{aligned} \tag{2.57}$$

The asymptotic behavior of this expression is straightforward,

$$\langle v_m(t+\tau)v_m(t)\rangle \simeq \frac{{v_{typ}}^2}{{t_\beta}^{\beta-2}\langle t_w\rangle}\begin{cases}\frac{1}{1-\beta}\tau^{\beta-1} & \text{for } t\gg\tau\\ \tau^{\beta-2}t & \text{for } \tau\gg t.\end{cases} \tag{2.58}$$

In the stationary limit $t \gg \tau$, the velocity autocorrelation of the Lévy walk is thus similar to the one obtained for fractional Gaussian noise, Eqs. (2.45) and (2.51). As before, Eq. (2.54) in principle has to be supplemented by a short-time cutoff to avoid the unphysical divergence as $\tau \to 0$. Since the Lévy walk is non-Gaussian, its properties are not uniquely determined by its two-time correlation function and consequently the process differs from the Gaussian processes discussed before. Indeed, higher order moments behave very differently for the two classes of processes.

All three processes we discussed share one important common property: They have positive, long-ranged, power-law correlations, which ultimately are responsible for the resulting superdiffusive behavior. Apart from this, there are some differences: Riemann-Liouville fractional noise is Gaussian and non-stationary. It tends to a stationary limit for long times, the limiting process is Mandelbrot-van-Ness fractional noise which is explicitly stationary. The Lévy walk, on the other hand is neither Gaussian nor stationary, though it too has a stationary long-time limit.

2.2.3 *Properties of the nonequilibrium noise*

While Eq. (2.36) provides a direct connection between the medium velocity and nonequilibrium noise autocorrelations, the actual properties of the latter are of

course highly dependent on the former. We thus examine the behavior of the nonequilibrium noise for the three choices of the process $v_m(t)$ introduced in Section 2.2.2. If the autocorrelation function of $v_m(t)$ is of the stationary power-law type obtained for Mandelbrot-van-Ness fractional Gaussian noise, Eq. (2.51), then using Eq. (A.24) this translates into the frequency domain as,

$$\langle \tilde{v}_m(s_2)\tilde{v}_m(s_1)\rangle = \frac{{v_{typ}}^2}{2\cos\left(\frac{\pi\beta}{2}\right){t_\beta}^{\beta-1}}\frac{{s_2}^{-\beta}+{s_1}^{-\beta}}{s_2+s_1}. \tag{2.59}$$

For the nonequilibrium noise we then have,

$$\langle \tilde{\xi}(s_2)\tilde{\xi}(s_1)\rangle = \frac{m^2\gamma^2{v_{typ}}^2}{2\cos\left(\frac{\pi\beta}{2}\right){t_\alpha}^{2\alpha}{t_\beta}^{\beta-1}}\frac{(s_2s_1)^{-\alpha}\left({s_2}^{-\beta}+{s_1}^{-\beta}\right)}{s_2+s_1}. \tag{2.60}$$

Applying the identity Eq. (A.4), we obtain the noise autocorrelation in the time domain, expressed in the scaling form used before,

$$\begin{aligned}
\langle \xi(t+\tau)\xi(t)\rangle &= \mathcal{C}_\xi\, t^{2\alpha+\beta-1}\phi_\xi\left(\frac{\tau}{t}\right),\\
\text{with}\quad \mathcal{C}_\xi &= \frac{m^2\gamma^2{v_{typ}}^2}{2\cos\left(\frac{\pi\beta}{2}\right)\Gamma(\alpha+\beta)\Gamma(\alpha){t_\alpha}^{2\alpha}{t_\beta}^{\beta-1}},\\
\phi_\xi(y) &= \int_0^1 dz\left[(1+y-z)^{\alpha+\beta-1}(1-z)^{\alpha-1}+(1+y-z)^{\alpha-1}(1-z)^{\alpha+\beta-1}\right],
\end{aligned} \tag{2.61}$$

With the help of Eq. (A.44), we can specify the asymptotic behavior of the nonequilibrium noise correlation function,

$$\begin{aligned}
\langle \xi(t+\tau)\xi(t)\rangle \simeq{}& \frac{m^2\gamma^2{v_{typ}}^2}{2\cos\left(\frac{\pi\beta}{2}\right){t_\alpha}^{2\alpha}{t_\beta}^{\beta-1}}\\
&\times\begin{cases}
\frac{\Gamma(1-2\alpha-\beta)[\sin(\pi\alpha)+\sin(\pi(\alpha+\beta))]}{\pi}\tau^{2\alpha+\beta-1} & \text{for } t\gg\tau,\ \beta<1-2\alpha\\[2ex]
\frac{2}{(2\alpha+\beta-1)\Gamma(\alpha+\beta)\Gamma(\alpha)}t^{2\alpha+\beta-1} & \text{for } t\gg\tau,\ \beta>1-2\alpha\\[2ex]
\frac{1}{\Gamma(\alpha+\beta)\Gamma(\alpha+1)}\tau^{\alpha+\beta-1}t^{\alpha}+\frac{1}{\Gamma(\alpha+\beta+1)\Gamma(\alpha)}\tau^{\alpha-1}t^{\alpha+\beta} & \text{for } \tau\gg t.
\end{cases}
\end{aligned} \tag{2.62}$$

If the medium velocity correlations and memory kernel are relatively short-ranged with $2\alpha+\beta<1$, the noise autocorrelation has a stationary limit for $t\gg\tau$ in which it only depends on the time lag τ. For longer-ranged correlations in $v_m(t)$ with $2\alpha+\beta>1$, the nonequilibrium noise is nonstationary and its magnitude increases with time. The existence of these two regimes will be seen to be a common property of correlation functions of the type Eq. (2.61). The combination $2\alpha+\beta$ measures the combined "range" of the memory and the medium velocity correlations, both a longer-range memory and longer-ranged medium velocity correlations increase

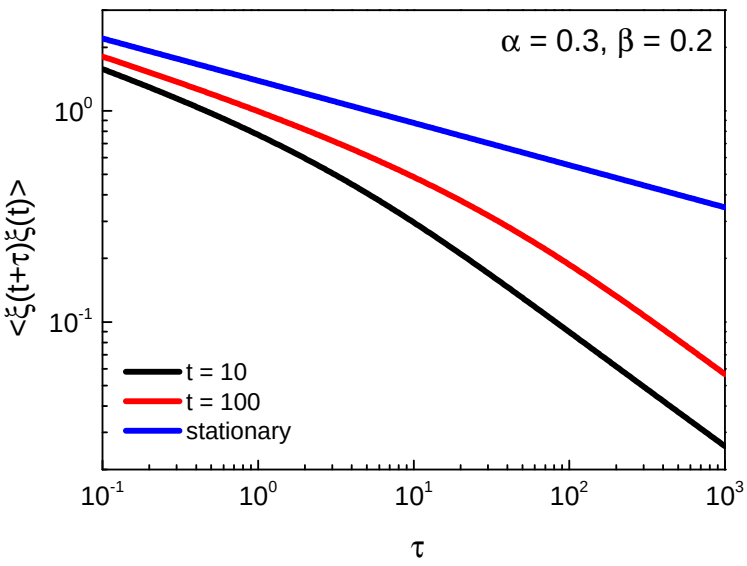

Figure 2.1: Nonequilibrium noise correlation function as a function of time lag for different overall times. In the regime $\beta < 2\alpha + 1$, the correlation function approaches a stationary limit as $t \to \infty$ (blue). For finite times, there is a transition between the stationary $\tau^{2\alpha+\beta-1}$ and the nonstationary behavior, the transition time is of the order of the overall time t.

its value and lead to enhanced correlations in the nonequilibrium noise. Figures 2.1, 2.2 and 2.3 show the behavior of the noise correlation function for three sets of parameters α and β at different times. In Fig. 2.1, we have $2\alpha + \beta < 1$ and the correlation function is asymptotically stationary; the approach to the stationary correlation function also follows a power law. Figures 2.2 and 2.3 show the correlation function in the nonstationary regime, where its magnitude increases with the overall time t as $t^{2\alpha+\beta-1}$. Though this is true in both cases, the behavior for large time lags can still be qualitatively different. For $\alpha + \beta < 1$ (Fig. 2.2), the correlations decay as a function of the time lag, indicating that the noise process will eventually become uncorrelated. For $\alpha + \beta > 1$ (Fig. 2.3), the correlations actually increase with the time lag, meaning that due to the increasing magnitude of the process, its current behavior will always be strongly dependent on its distant past. In all three cases, the overall time t also sets the time scale for the transition between short- and long-time behavior. This directly reflects the scale-invariant nature of the noise process which does not possess any intrinsic time scales.

A particularly simple relation between the two autocorrelation functions is obtained, if the medium velocity $v_m(t)$ is given by Riemann-Liouville fractional Gaussian noise, Eq. (2.41). The autocorrelation of the nonequilibrium noise is then of precisely the same type,

$$\langle \tilde{\xi}(s_2)\tilde{\xi}(s_1)\rangle = \frac{m^2\gamma^2 {v_{typ}}^2}{{t_\alpha}^{2\alpha}{t_\beta}^{\beta-1}} \frac{(s_2 s_1)^{-\frac{\beta}{2}-\alpha}}{s_2 + s_1}, \tag{2.63}$$

however, with the exponent β replaced by $\beta + 2\alpha$. This is also equivalent to the heuristic nonequilibrium noise Eq. (2.33) with noise exponent $\mu = 2\alpha + \beta$. For this reason, we will not consider the heuristic nonequilibrium noise separately, as the

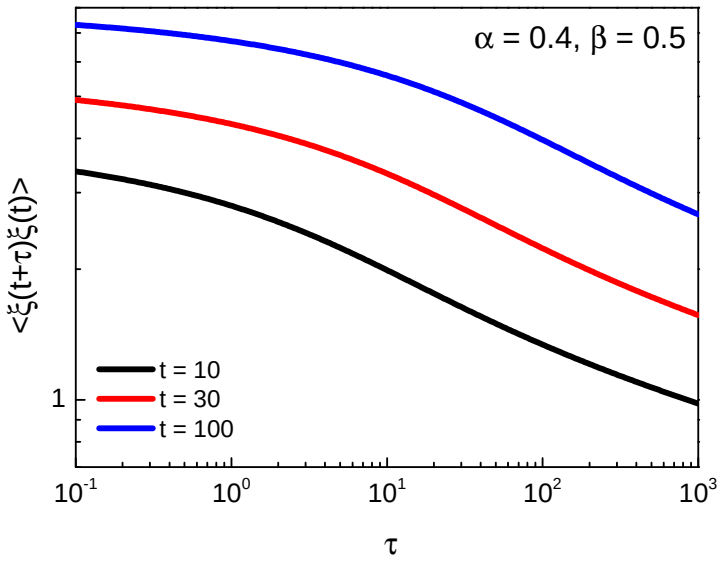

Figure 2.2: Nonequilibrium noise correlation function as a function of time lag for different overall times. In the regime $\alpha + \beta < 1 < 2\alpha + \beta$, the correlation function is nonstationary and its magnitude at $\tau = 0$ increases as $t^{2\alpha+\beta-1}$. In addition to the increasing overall magnitude of the correlation function, the transition time between the small-τ and large-τ behavior also increases linearly with the overall time t. For long time lags $\tau \gg t$, the correlation function decays as $\tau^{\alpha+\beta-1}$.

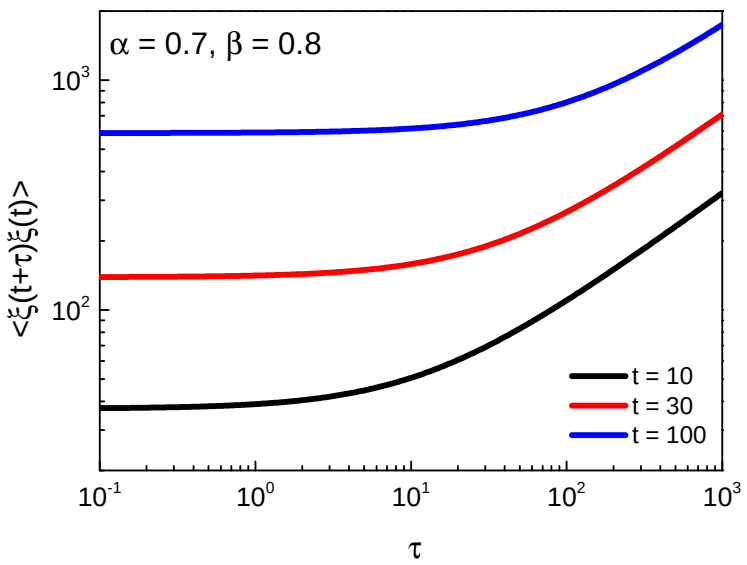

Figure 2.3: Nonequilibrium noise correlation function as a function of time lag for different overall times. In the regime $\alpha + \beta > 1$, the correlation function is nonstationary and its magnitude at $\tau = 0$ increases as $t^{2\alpha+\beta-1}$. In addition to the increasing overall magnitude of the correlation function, the transition time between the small-τ and large-τ behavior also increases linearly with the overall time t. For long time lags $\tau \gg t$, the correlation function increases as $\tau^{\alpha+\beta-1}$.

corresponding results can be obtained simply by changing β accordingly. Again using the identity (A.4) to transform this back to the time domain, we obtain a scaling form similar to Eq. (2.61),

$$\begin{aligned}
\langle \xi(t+\tau)\xi(t)\rangle &= \mathcal{C}_\xi \, t^{2\alpha+\beta-1} \phi_\xi\left(\frac{\tau}{t}\right), \\
\text{with} \quad \mathcal{C}_\xi &= \frac{m^2\gamma^2 {v_{\text{typ}}}^2}{\Gamma^2\left(\alpha+\frac{\beta}{2}\right) {t_\alpha}^{2\alpha} {t_\beta}^{\beta-1}}, \\
\phi_\xi(y) &= \int_0^1 dz \, (1+y-z)^{\alpha+\frac{\beta}{2}-1}(1-z)^{\alpha+\frac{\beta}{2}-1}.
\end{aligned} \tag{2.64}$$

The asymptotic behavior of this correlation function is rather similar to Eq. (2.62),

$$\langle \xi(t+\tau)\xi(t)\rangle \simeq \frac{m^2\gamma^2 {v_{\text{typ}}}^2}{{t_\alpha}^{2\alpha} {t_\beta}^{\beta-1}} \begin{cases} \frac{\Gamma(1-2\alpha-\beta)\sin\left(\pi\left(\alpha+\frac{\beta}{2}\right)\right)}{\pi} \tau^{2\alpha+\beta-1} \\ \qquad \text{for } t \gg \tau, \ \beta < 1-2\alpha \\ \frac{1}{(2\alpha+\beta-1)\Gamma^2\left(\alpha+\frac{\beta}{2}\right)} t^{2\alpha+\beta-1} \\ \qquad \text{for } t \gg \tau, \ \beta > 1-2\alpha \\ \frac{1}{\Gamma\left(\alpha+\frac{\beta}{2}+1\right)\Gamma\left(\alpha+\frac{\beta}{2}\right)} \tau^{\alpha+\frac{\beta}{2}-1} t^{\alpha+\frac{\beta}{2}} \\ \qquad \text{for } \tau \gg t. \end{cases} \tag{2.65}$$

In the long-time limit $t \gg \tau$, we again find a stationary regime for $2\alpha+\beta < 1$ and a nonstationary one with increasing variance for $2\alpha+\beta > 1$. In both cases functional dependence on the time lag τ respectively the overall time t is the same as the one in Eq. (2.62), however the the numerical prefactors of the nonstationary expressions ($2\alpha+\beta > 1$) differ. This is at odds with the fact that both Riemann-Liouville and Mandelbrot-van-Ness fractional Gaussian noise were seen to describe the same stochastic process in this limit, in the sense that the autocorrelation functions of $v_m(t)$ are identical (see Eqs. (2.45) and (2.51)). So even though both processes are asymptotically the same, the nonequilibrium noise induced by them is not, not even in the long time limit. This is due to the long-range power-law memory kernel linking the medium velocity and nonequilibrium noise, Eq. (2.36), which causes the noise process to be sensitive on the entire history of $v_m(t)$ even asymptotically. Only when the nonequilibrium noise itself is stationary, i.e. for $2\alpha+\beta < 1$, its long-time behavior is determined solely by the long-time stationary behavior of the velocity process. For long time lags $\tau \gg t$, the functional dependence on τ and t in Eqs. (2.65) an (2.62) is different. Here the nonstationary behavior of Riemann-Liouville fractional Gaussian noise leads to qualitative differences between the induced noise processes.

Finally, we want to derive the expression for the correlation function of the nonequilibrium noise for the Lévy walk medium velocity. To this end, we rewrite Eq. (2.36) so that the time-ordering of the correlation functions is explicit,

$$\begin{aligned}&\langle \xi(t+\tau)\xi(t)\rangle \\ &= m^2\gamma^2\left[\int_t^{t+\tau} dt'' \int_0^t dt' + \int_0^t dt'' \int_0^{t''} dt' + \int_0^t dt'' \int_{t''}^t dt'\right] \\ &\qquad \times k(t+\tau-t'')k(t-t')\langle v_m(t'')v_m(t')\rangle. \end{aligned} \tag{2.66}$$

In this way, we have $t'' > t'$ in the first and second integral and $t' > t''$ in the third one, allowing us to use Eq. (2.54) for the medium velocity correlation function. In the third integral, we interchange the order of integration and exchange the labels of the integration variables to obtain,

$$\begin{aligned}&\langle \xi(t+\tau)\xi(t)\rangle \\ &= m^2\gamma^2\Bigg[\int_t^{t+\tau} dt'' \int_0^t dt'\; k(t+\tau-t'')k(t-t')\langle v_m(t'')v_m(t')\rangle \\ &\quad + \int_0^t dt'' \int_0^{t''} dt'\; \Big[k(t+\tau-t'')k(t-t') + k(t-t'')k(t+\tau-t')\Big] \\ &\qquad \times \langle v_m(t'')v_m(t')\rangle\Bigg], \end{aligned} \tag{2.67}$$

where now $t'' > t'$ throughout the entire domain of integration. Using Eq. (2.57) for the medium velocity correlation, Eq. (2.15) for the kernel function and defining $z = t''/t$, $u = t'/t$, this can be rewritten as a scaling form,

$$\begin{aligned}&\langle \xi(t+\tau)\xi(t)\rangle \simeq \mathcal{C}_\xi\, t^{2\alpha+\beta-1}\phi_\xi\left(\frac{\tau}{t}\right), \\ &\quad \text{with} \quad \mathcal{C}_\xi = \frac{m^2\gamma^2 {v_{typ}}^2}{(1-\beta){t_\beta}^{\beta-2}{t_\alpha}^{2\alpha}\langle t_w\rangle}, \\ &\qquad \phi_\xi(y) = \int_0^1 dz \int_0^z du\, \Big[\big((1+y-z)(1-u)\big)^{\alpha-1} \\ &\qquad\qquad + \big((1-z)(1+y-u)\big)^{\alpha-1}\Big] u^{\beta-1}\phi_{m,LW}\left(\frac{z-u}{u}\right) \\ &\qquad\qquad + \int_1^{1+y} dz \int_0^1 du\, \big((1+y-z)(1-u)\big)^{\alpha-1} u^{\beta-1}\phi_{m,LW}\left(\frac{z-u}{u}\right). \end{aligned} \tag{2.68}$$

The integrals involved in the scaling function are discussed in Appendix A.2. Specifically, we obtain for the asymptotic behavior of the two-time correlation function to leading order, using Eqs. (A.57), (A.63) and (A.75),

$$\langle \xi(t+\tau)\xi(t)\rangle \simeq \frac{m^2\gamma^2 {v_{\text{typ}}}^2}{(1-\beta){t_\beta}^{\beta-2}\langle t_w\rangle} \begin{cases} c_{\xi,1}\tau^{2\alpha+\beta-1} \\ \qquad \text{for } t \gg \tau,\ \beta < 1-2\alpha \\ c_{\xi,2}t^{2\alpha+\beta-1} \\ \qquad \text{for } t \gg \tau,\ \beta > 1-2\alpha \\ c_{\xi,3}\tau^{\alpha-1}t^{\alpha+\beta} \\ \qquad \text{for } \tau \gg t, \end{cases} \tag{2.69}$$

where the coefficients are given by,

$$\begin{aligned} c_{\xi,1} &= -\frac{\pi\Gamma(\beta)\Gamma(1-2\alpha-\beta)}{\Gamma^2(1-\alpha)\sin(\pi(\alpha+\beta-1))} + \frac{\Gamma(\alpha)\Gamma(\beta)\Gamma(1-2\alpha-\beta)}{\Gamma(1-\alpha)} \\ &\quad + \frac{\Gamma^2(\alpha)\Gamma(\beta)\sin(\pi(2-\beta))}{\Gamma(2\alpha+\beta)\sin(\pi(\alpha+\beta-1)} \\ c_{\xi,2} &= 2\int_0^1 dz \int_0^1 dv\, z^{\alpha-1}(v+z-vz)^{\alpha-1}(1-z)^\beta(v^{\beta-1}-1) \\ c_{\xi,3} &= \int_0^1 dz \int_0^1 dv\, (v+z-vz)^{\alpha-1}(1-z)^\beta(v^{\beta-1}-1) \\ &\quad + \int_0^1 dz \int_0^1 dv\, z^{\alpha-1}(1-z)^\beta(v^{\beta-1}-1) \\ &\quad + \int_0^\infty dz \int_0^1 du\, u^{\alpha-1}\big((u+z)^{\beta-1}-(1+z)^{\beta-1}\big). \end{aligned} \tag{2.70}$$

The time-dependence of Eq. (2.69) in the long time limit $t \gg \tau$ is rather similar to the Gaussian cases Eqs. (2.62) and (2.65). This is not too surprising, since asymptotically, the two-time correlation function of $v_m(t)$ behaves in the same way as well. Note that Eq. (2.69) actually corresponds to Eq. (2.65), since it describes the nonstationary variant of the Lévy walk, where the first waiting time is selected at $t = 0$. We can also choose to use the stationary variant [Froe 13], where the process starts out during a waiting time. In this case, the stationary correlation function is the same as Eq. (2.51) apart from the prefactor, and we consequently arrive at the equivalent of Eq. (2.62). As with the two Gaussian processes, even though the stationary and nonstationary process are equivalent in the long-time limit, the respective induced nonequilibrium noise is not, but differs in magnitude. The preceding analysis only considers second order moments, i.e. two-time correlation functions. While these are sufficient to uniquely identify the process in the Gaussian cases, for the Lévy walk, higher order moments will generally behave differently. Thus, even though the stationary correlation functions for the Gaussian process and the Lévy walk coincide, the actual processes are still very different.

2.3 SOLUTION OF THE NONEQUILIBRIUM FRACTIONAL LANGEVIN EQUATION

Ultimately, we want to use our model, the fractional Langevin equation with nonequilibrium noise in the form of a moving medium, Eq. (2.34), to describe the diffusive dynamics in living cells. To this end we need to derive and understand the solution of Eq. (2.34), in particular in terms of the experimentally accessible quantities like the moments of the position of the particle. In Section 2.3.1, we give a formal solution to Eq. (2.34) in the Laplace (frequency) domain. Since the solution in the frequency domain is not very intuitive, we discuss the asymptotic properties of the solution in the time domain in the following two Sections. In Section 2.3.2, we focus on the two-time correlation functions and the mean-square displacement, which characterize the diffusive behavior of the system. We then move on to the mean displacement in the presence of an external force in Section 2.3.3 and introduce the notion of response and creep function. Finally, we discuss the fundamental difference between equilibrium and nonequilibrium for general Langevin dynamics in Section 2.3.4 and show that a nonequilibrium noise necessarily leads to nonstationarity.

2.3.1 *Frequency domain*

The formal solution of Eq. (2.34) is best obtained by switching to the frequency domain,

$$s\tilde{v}(s) - v_0 = -\gamma\tilde{k}(s)\big(\tilde{v}(s) - \tilde{v}_m(s)\big) + \frac{1}{m}\tilde{\eta}(s), \tag{2.71}$$

or in terms of the position $x(t) = \int_0^t dt'\, v(t') + x_0$,

$$s^2\tilde{x}(s) - sx_0 - v_0 = -\gamma\tilde{k}(s)\big(s\tilde{x}(s) - x_0 - \tilde{v}_m(s)\big) + \frac{1}{m}\tilde{\eta}(s). \tag{2.72}$$

The solution of Eqs. (2.71) and (2.72) is then a matter of simple algebra,

$$\begin{aligned}\tilde{v}(s) &= \frac{1}{s+\gamma\tilde{k}(s)}\left(\frac{1}{m}\tilde{\eta}(s) + v_0\right) + \frac{\gamma\tilde{k}(s)}{s+\gamma\tilde{k}(s)}\tilde{v}_m(s),\\ \tilde{x}(s) &= \frac{x_0}{s} + \frac{1}{s^2+s\gamma\tilde{k}(s)}\left(\frac{1}{m}\tilde{\eta}(s) + v_0\right) + \frac{\gamma\tilde{k}(s)}{s^2+s\gamma\tilde{k}(s)}\tilde{v}_m(s).\end{aligned} \tag{2.73}$$

We can use this formal solution to compute the moments of the velocity and position, provided that we know the corresponding moments of the noise $\eta(t)$ and the medium velocity $v_m(t)$. For the power-law memory kernel of the fractional Langevin equation, Eq. (2.15), we can immediately make a statement about the long-time behavior of the solution Eq. (2.73). For $t \gg t_\alpha(\gamma t_\alpha)^{-1/(\alpha+1)}$, which in the frequency domain corresponds to $s \ll (\gamma t_\alpha)^{1/(\alpha+1)}/t_\alpha$ [Doet 74], we have $s \ll \gamma\tilde{k}(s)$ and may thus neglect the inertial term. This approximation is called the overdamped limit and is generally a very good approximation for the experimentally relevant time scales, since the systems under consideration are heavily damped and have a large numerical value for γ. In the overdamped limit, Eq. (2.73) simplifies to,

$$\tilde{v}(s) \simeq \gamma^{-1}(t_\alpha s)^\alpha\left(\frac{1}{m}\tilde{\eta}(s) + v_0\right) + \tilde{v}_m(s). \tag{2.74}$$

In the absence of equilibrium noise $\eta(t) = 0$, this is precisely what we expect: Due to the coupling of the tracer particle to the moving environment, the motion of the former on long time scales follows the long-time motion of the latter. In the presence of equilibrium noise, the long-time behavior depends on behavior of $\eta(t)$ and $v_m(t)$, but in all cases of interest, the latter will be the dominant contribution for long times.

We will also be interested in the effect of an additional external probe force $F_p(t)$ applied to the tracer particle, this can be taken into account in a straightforward manner by including it as an additional term in the generalized Langevin equation (2.10) and leads to,

$$\tilde{x}(s) = \frac{x_0}{s} + \frac{1}{s^2 + \gamma s \tilde{k}(s)} \left(\frac{1}{m} \left(\tilde{\eta}(s) + \tilde{F}_p(s) \right) + v_0 \right) + \frac{\gamma \tilde{k}(s)}{s^2 + \gamma s \tilde{k}(s)} \tilde{v}_m(s), \quad (2.75)$$

and similarly for the velocity. Before we begin to study the explicit behavior of the solution Eq. (2.75) in the time domain, we remark that it is explicitly linear in the noise $\eta(t)$, the medium velocity $v_m(t)$ and the probe force $F_p(t)$. This linearity has two important consequences. Firstly, if $\eta(t)$ and $v_m(t)$ are Gaussian processes, then the motion of the tracer particle is a Gaussian process as well. Conversely, any non-Gaussian behavior of the tracer particle can be traced back to underlying stochastic processes. Secondly, any response to the probe force $F_p(t)$ will be linear in the latter, in that increasing the amplitude of the probe force will increase the amplitude of the response proportionally. This does of course not imply linearity in time, i.e. the response to a constant probe force can and will depend on time in a nonlinear manner. It does, however, restrict the validity of this approach to relatively small probe forces, as applying a large force will in general also impact the viscoelastic properties of the medium (i.e. γ or $k(t)$) and thus lead to a nonlinear dependence on the probe force [Fabr 01].

2.3.2 *Time domain: Correlation functions and mean-square displacement*

Using Eq. (2.73), the velocity autocorrelation function in frequency space is obtained as,

$$\begin{aligned}\langle \tilde{v}(s_2)\tilde{v}(s_1)\rangle = &\frac{\langle \tilde{\eta}(s_2)\tilde{\eta}(s_1)\rangle + m^2\langle {v_0}^2\rangle}{m^2\left(s_2 + \gamma\tilde{k}(s_2)\right)\left(s_1 + \gamma\tilde{k}(s_1)\right)} \\ &+ \frac{\gamma^2 \tilde{k}(s_2)\tilde{k}(s_1)\langle \tilde{v}_m(s_2)\tilde{v}_m(s_1)\rangle}{\left(s_2 + \gamma\tilde{k}(s_2)\right)\left(s_1 + \gamma\tilde{k}(s_1)\right)},\end{aligned} \quad (2.76)$$

where we assumed that the initial velocity v_0, the equilibrium noise $\eta(t)$ and the medium velocity $v_m(t)$ are stochastically independent of each other. Using the explicit form of the memory kernel Eq. (2.15), we can in principle transform this back into the time domain,

$$\begin{aligned}\langle v(t_2)v(t_1)\rangle = &\langle {v_0}^2\rangle f_{\alpha,0}(t_2) f_{\alpha,0}(t_1) \\ &+ \frac{1}{m^2}\int_0^{t_2} dt'' \int_0^{t_1} dt'\, f_{\alpha,0}(t_2 - t') f_{\alpha,0}(t_1 - t')\langle \eta(t'')\eta(t')\rangle \\ &+ \gamma^2 \int_0^{t_2} dt'' \int_0^{t_1} dt'\, f_{\alpha,\alpha}(t_2 - t') f_{\alpha,\alpha}(t_1 - t')\langle v_m(t'')v_m(t')\rangle,\end{aligned} \quad (2.77)$$

with the kernel function,

$$f_{a,b}(t) = t^b E_{a+1,b+1}\left(-\gamma t_\alpha \left(\frac{t}{t_\alpha}\right)^{a+1}\right), \tag{2.78}$$

where $E_{a,b}(x)$ is the generalized Mittag-Leffler function defined in Eq. (2.19). Except for numerical computation, Eq. (2.77) by itself is not particularly useful, since it does not provide any intuition about the fundamental behavior of the velocity autocorrelation. We may simplify it somewhat for the particular cases of the medium velocity correlations discussed in Section 2.2.2. For the stationary Gaussian medium velocity process, the velocity autocorrelation is given by Eq. (2.51) respectively Eq. (2.59) in Laplace space. Using this expression for the velocity correlations in Eq. (2.76) and dropping the equilibrium and initial velocity terms for now, we have,

$$\langle \tilde{v}(s_2)\tilde{v}(s_1)\rangle = \frac{\gamma^2 {v_{typ}}^2}{2\cos\left(\frac{\pi\beta}{2}\right) {t_\beta}^{\beta-1} {t_\alpha}^{2\alpha}} \frac{{s_2}^{-\alpha}{s_1}^{-\alpha}\frac{{s_2}^{-\beta}+{s_1}^{-\beta}}{s_2+s_1}}{\left(s_2+\gamma(t_\alpha s_2)^{-\alpha}\right)\left(s_1+\gamma(t_\alpha s_1)^{-\alpha}\right)}. \tag{2.79}$$

Using Eq. (A.4), we can write down the corresponding expression in the time-domain,

$$\begin{aligned}\langle v(t+\tau)v(t)\rangle = &\frac{\gamma^2 {v_{typ}}^2}{2\cos\left(\frac{\pi\beta}{2}\right) {t_\beta}^{\beta-1} {t_\alpha}^{2\alpha}} \\ &\times \int_0^t dt' \left[f_{\alpha,\alpha+\beta}(t'+\tau)f_{\alpha,\alpha}(t') + f_{\alpha,\alpha}(t'+\tau)f_{\alpha,\alpha+\beta}(t')\right].\end{aligned} \tag{2.80}$$

For the nonstationary Gaussian medium velocity, the corresponding velocity correlation is given by,

$$\langle v(t+\tau)v(t)\rangle = \frac{\gamma^2 {v_{typ}}^2}{{t_\beta}^{\beta-1} {t_\alpha}^{2\alpha}} \int_0^t dt'\, f_{\alpha,\alpha+\frac{\beta}{2}}(t'+\tau) f_{\alpha,\alpha+\frac{\beta}{2}}(t'), \tag{2.81}$$

while for the Lévy walk we have using Eq. (A.6),

$$\begin{aligned}\langle v(t+\tau)v(t)\rangle = &\frac{\gamma^2 {v_{typ}}^2}{(1-\beta){t_\beta}^{\beta-2}\langle t_w\rangle {t_\alpha}^{2\alpha}} \\ &\times \int_0^t dt' \Big[(t-t')^{\beta-1}\left[f_{\alpha,\alpha+1}(t'+\tau)f_{\alpha,\alpha}(t') + f_{\alpha,\alpha}(t'+\tau)f_{\alpha,\alpha+1}(t')\right] \\ &- \Gamma(\beta)\left[f_{\alpha,\alpha+\beta-1}(t'+\tau)f_{\alpha,\alpha+1}(t') + f_{\alpha,\alpha+1}(t'+\tau)f_{\alpha,\alpha+\beta-1}(t')\right]\Big].\end{aligned} \tag{2.82}$$

Again, these expressions as they are, are mostly useful for numerical computation. We can, however, draw some immediate conclusions from them. In Section 2.2.2, we saw that in all three instances the correlation function of the medium velocity has an unphysical divergence in the limit $\tau \to 0$. Even though the medium velocity correlations diverge and the mean-square medium velocity is thus not defined,

this still leads to a well defined mean-square velocity for the tracer particle, as Eqs. (2.80), (2.81) and (2.82) are finite for $\tau = 0$. We may thus ignore the short time cutoff on the medium velocity correlations for the purposes of our model. For $\beta < 1$, and since the kernel function behaves as $f_{a,b} \sim t^{b-a-1}$ for long times, all three expressions are finite in the limit $t \to \infty$, meaning that the mean-square velocity approaches a stationary limit $\langle v^2 \rangle_s$, as it should.

To gain some intuition about the behavior of Eq. (2.77) in certain limits, we examine its Laplace equivalent, Eq. (2.76) in more detail. In the long-time or overdamped limit, where both frequency variables are small, $s_2, s_1 \ll (\gamma t_\alpha)^{1/(\alpha+1)}/t_\alpha$, Eq. (2.76) simplifies to,

$$\langle \tilde{v}(s_2)\tilde{v}(s_1)\rangle \simeq \frac{1}{\gamma^2}\left({t_\alpha}^2 s_2 s_1\right)^\alpha \left(\frac{1}{m^2}\langle \tilde{\eta}(s_2)\tilde{\eta}(s_1)\rangle + \langle {v_0}^2\rangle\right) + \langle \tilde{v}_m(s_2)\tilde{v}_m(s_1)\rangle. \tag{2.83}$$

In order to identify the dominant contribution for long times, we consider the example of stationary Gaussian noise Eq. (2.30) respectively Eq. (2.59) for the medium velocity. We can write the latter as,

$$\langle \tilde{v}_m(s_2)\tilde{v}_m(s_1)\rangle = \frac{{v_{typ}}^2}{2\cos\left(\frac{\pi\beta}{2}\right){t_\beta}^{\beta-1}}\left[\frac{{s_2}^{-\beta-1}}{1+\frac{s_1}{s_2}} + \frac{{s_1}^{-\beta-1}}{1+\frac{s_2}{s_1}}\right]. \tag{2.84}$$

The advantage of this form is that we can immediately identify its scaling in the limit of small s_2 and s_1, which is given by the numerator, since the denominator only depends on the ratio of s_2 and s_1 and thus their relative magnitude. Using a similar argument for the equilibrium noise $\eta(t)$, we can write Eq. (2.76) as,

$$\begin{aligned}\langle \tilde{v}(s_2)\tilde{v}(s_1)\rangle \simeq{}& \frac{k_B T {t_\alpha}^\alpha}{m\gamma}\left[\frac{{s_2}^{\alpha-1}}{1+\frac{s_1}{s_2}} + \frac{{s_1}^{\alpha-1}}{1+\frac{s_2}{s_1}}\right] + \frac{\langle {v_0}^2\rangle {t_\alpha}^{2\alpha}}{\gamma^2}{s_2}^{2\alpha}\left(\frac{s_1}{s_2}\right)^\alpha \\ &+ \frac{{v_{typ}}^2}{2\cos\left(\frac{\pi\beta}{2}\right){t_\beta}^{\beta-1}}\left[\frac{{s_2}^{-\beta-1}}{1+\frac{s_1}{s_2}} + \frac{{s_1}^{-\beta-1}}{1+\frac{s_2}{s_1}}\right].\end{aligned} \tag{2.85}$$

As we will see later (see Section 3.3.2), this scaling form in the frequency domain is intimately related to the corresponding one in the time domain, Eq. (2.52). Since $0 < \alpha < 1$, the term contributed by the initial velocity is negligible for long times respectively small s_2 and s_1. The long-time velocity autocorrelation is thus independent of the initial velocity. For the two terms originating from the equilibrium respectively nonequilibrium noise, their relative size depends on the time scale. The equilibrium term scales as $s^{\alpha-1}$, while the nonequilibrium one scales as $s^{-\beta-1}$. For $\beta > 0$, the nonequilibrium term thus always gives the dominant contribution for long times. Similar arguments apply to the other two cases for the medium velocity, Eqs. (2.43) and (2.54), since the nonequilibrium term still scales as $s^{-\beta-1}$, as can be seen from the corresponding Laplace expressions Eqs. (2.41) and (2.56). Comparing Eq. (2.85) to the double Laplace transform of a stationary correlation function, Eq. (A.24), we see that for the stationary medium velocity process, also

the resulting velocity autocorrelation is stationary. It reads asymptotically in the time domain,

$$\langle v(t+\tau)v(t)\rangle \simeq \frac{k_B T}{\Gamma(-\alpha) m\gamma t_\alpha}\left(\frac{\tau}{t_\alpha}\right)^{-\alpha-1} + \frac{\Gamma(1-\beta)\sin\left(\frac{\pi\beta}{2}\right){v_{typ}}^2}{\pi}\left(\frac{\tau}{t_\beta}\right)^{\beta-1}. \tag{2.86}$$

As expected, the equilibrium part corresponds precisely to the asymptotic equilibrium result Eq. (2.24), but we have an additional nonequilibrium contribution due to the motion of the surrounding medium, given by Eq. (2.51). Similarly we find that, for the nonstationary Gaussian noise Eq. (2.43) and for the Lévy walk Eq. (2.54), the asymptotic velocity autocorrelation function is also given by the equilibrium contribution plus a nonequilibrium term representing the correlations of the medium velocity, Eqs. (2.41) and (2.56). Since the latter are nonstationary in the other two cases, so is the overall velocity autocorrelation.

For the position autocorrelation, we have from Eq. (2.73),

$$\langle \tilde{x}(s_2)\tilde{x}(s_1)\rangle = \frac{\langle {x_0}^2\rangle}{s_2 s_1} + \frac{\langle \tilde{\eta}(s_2)\tilde{\eta}(s_1)\rangle + m^2\langle {v_0}^2\rangle}{m^2\left({s_2}^2+\gamma s_2\tilde{k}(s_2)\right)\left({s_1}^2+\gamma s_1\tilde{k}(s_1)\right)} + \frac{\gamma^2\tilde{k}(s_2)\tilde{k}(s_1)\langle \tilde{v}_m(s_2)\tilde{v}_m(s_1)\rangle}{\left({s_2}^2+\gamma s_2\tilde{k}(s_2)\right)\left({s_1}^2+\gamma s_1\tilde{k}(s_1)\right)}, \tag{2.87}$$

where we assumed that the initial position x_0 is stochastically independent of the initial velocity v_0 and the stochastic processes $\eta(t)$ and $v_m(t)$. For the stationary Gaussian medium velocity, we can bring this into a form similar to Eq. (2.85),

$$\langle \tilde{x}(s_2)\tilde{x}(s_1)\rangle \simeq \frac{\langle {x_0}^2\rangle}{s_2 s_1} + \frac{\langle {v_0}^2\rangle {t_\alpha}^{2\alpha}}{\gamma^2}{s_2}^{2\alpha-2}\left(\frac{s_1}{s_2}\right)^{\alpha-1} + \frac{k_B T {t_\alpha}^\alpha}{m\gamma}\left[\frac{{s_2}^{\alpha-3}}{\frac{s_1}{s_2}\left(1+\frac{s_1}{s_2}\right)} + \frac{{s_1}^{\alpha-3}}{\frac{s_2}{s_1}\left(1+\frac{s_2}{s_1}\right)}\right] + \frac{{v_{typ}}^2}{2\cos\left(\frac{\pi\beta}{2}\right){t_\beta}^{\beta-1}}\left[\frac{{s_2}^{-\beta-3}}{\frac{s_1}{s_2}\left(1+\frac{s_1}{s_2}\right)} + \frac{{s_1}^{-\beta-3}}{\frac{s_2}{s_1}\left(1+\frac{s_2}{s_1}\right)}\right]. \tag{2.88}$$

With the exception of the first term due to the initial position, the relative scaling of the individual terms is the same as for the velocity autocorrelation Eq. (2.86). The term due to the initial velocity can be neglected for long times, while the equilibrium and nonequilibrium contributions scale as $s^{\alpha-3}$ and as $s^{-\beta-3}$ respectively. Thus, just as for the velocity, the long-time dynamics of the position are dominated

by the nonequilibrium term. However, the position autocorrelation is not stationary. Using Eq. (A.4), the Laplace inversion is straightforward,

$$\begin{aligned}
\langle x(t+\tau)x(t)\rangle &\simeq \langle {x_0}^2\rangle \\
&\quad + \frac{k_B T {t_\alpha}^\alpha}{\Gamma(1-\alpha)m\gamma}\int_0^t dt' \ \left[(t+\tau-t')^{-\alpha}+(t-t')^{-\alpha}\right] \\
&\quad + \frac{{v_{typ}}^2}{2\Gamma(\beta+1)\cos\left(\frac{\pi\beta}{2}\right){t_\beta}^{\beta-1}}\int_0^t dt' \ \left[(t+\tau-t')^{\beta}+(t-t')^{\beta}\right] \\
&= \langle {x_0}^2\rangle + \frac{k_B T {t_\alpha}^{2-\alpha}}{\Gamma(2-\alpha)m\gamma}\left[(t+\tau)^{1-\alpha}+t^{1-\alpha}-\tau^{1-\alpha}\right] \\
&\quad + \frac{{v_{typ}}^2 {t_\beta}^{1-\beta}}{2\Gamma(\beta+2)\cos\left(\frac{\pi\beta}{2}\right)}\left[(t+\tau)^{\beta+1}+t^{\beta+1}-\tau^{\beta+1}\right]. \qquad (2.89)
\end{aligned}$$

In particular, for $\tau = 0$, we find for the mean-square displacement,

$$\langle \Delta x^2(t)\rangle \simeq \frac{2k_B T t_\alpha}{\Gamma(2-\alpha)m\gamma}\left(\frac{t}{t_\alpha}\right)^{1-\alpha} + \frac{{v_{typ}}^2 {t_\beta}^2}{\Gamma(\beta+2)\cos\left(\frac{\pi\beta}{2}\right)}\left(\frac{t}{t_\beta}\right)^{\beta+1}. \qquad (2.90)$$

The first term describes the equilibrium subdiffusion Eq. (2.26), while the second term is superdiffusive since $\beta > 0$. Thus the fractional Langevin equation in a moving viscoelastic environment, Eq. (2.34), indeed describes a crossover from subdiffusion for short times to superdiffusion for long times. The same qualitative picture holds for the nonstationary Gaussian noise, Eq. (2.43), where we have for the asymptotic position autocorrelation,

$$\begin{aligned}
&\langle x(t+\tau)x(t)\rangle \\
&\simeq \langle {x_0}^2\rangle + \frac{2k_B T {t_\alpha}^{2-\alpha}}{\Gamma(2-\alpha)m\gamma}\left[(t+\tau)^{1-\alpha}+t^{1-\alpha}-\tau^{1-\alpha}\right] \\
&\quad + \frac{(-1)^{-\frac{\beta}{2}}{v_{typ}}^2 {t_\beta}^2}{\Gamma^2\left(\frac{\beta}{2}+1\right)}\left(\frac{\tau}{t_\beta}\right)^{\beta+1} B\left(-\frac{t}{\tau};\frac{\beta}{2}+1,\frac{\beta}{2}+1\right), \qquad (2.91)
\end{aligned}$$

and for the mean-square displacement,

$$\langle \Delta x^2(t)\rangle \simeq \frac{2k_B T t_\alpha}{\Gamma(2-\alpha)m\gamma}\left(\frac{t}{t_\alpha}\right)^{1-\alpha} + \frac{{v_{typ}}^2 {t_\beta}^2}{\Gamma^2\left(\frac{\beta}{2}+1\right)(\beta+1)}\left(\frac{t}{t_\beta}\right)^{\beta+1}. \qquad (2.92)$$

Similarly to what we saw in section 2.2.3, the expressions Eqs. (2.90) and (2.92) for the mean-square displacement for the stationary and nonstationary medium velocity process are different, even though the two medium velocity processes are asymptotically equivalent. This dependence of the long-time dynamics on the initial preparation of the system will be studied in more detail in Chapter 3. We already noted before that the nonstationary Gaussian case is mathematically equiv-

alent to the external noise Eq. (2.31) with noise exponent $\mu = 2\alpha + \beta$, so with this interpretation, we have,

$$\langle \Delta x^2(t) \rangle \simeq \frac{2k_B T t_\alpha}{\Gamma(2-\alpha) m\gamma} \left(\frac{t}{t_\alpha}\right)^{1-\alpha} + \frac{{c_\mu}^2 {t_\alpha}^{2\alpha}}{\Gamma^2\left(\frac{\mu}{2} - \alpha + 1\right)(\beta - 2\alpha + 1) m^2 \gamma^2 {t_\mu}^{2\alpha}} \left(\frac{t}{t_\mu}\right)^{\mu - 2\alpha + 1}, \tag{2.93}$$

with ${c_\mu}^2 = m^2\gamma^2 {v_{typ}}^2 {t_\beta}^{2\alpha-\mu-1}/({t_\alpha}^{2\alpha}{t_\mu}^{1-\mu})$. Note that an asymptotically stationary external noise for which $\mu < 1$, can only account for superdiffusion if $2\alpha < \mu$, i.e. relatively small values of α and thus rather viscous systems. This was in fact the situation in Ref. [Brun 09], where $\alpha \sim 0.03$, and thus a stationary noise was sufficient to describe the superdiffusive behavior. For typical experiments on the cytoskeleton, on the other hand we have $\alpha \sim 0.8$ and thus a nonstationary external noise is required to obtain superdiffusion – or in fact any dominant contribution from the nonequilibrium noise at all – for long times. A more thorough discussion and possible interpretation of this nonstationary noise can be found in Section 4.3. The corresponding expressions for the Lévy walk read,

$$\begin{aligned}
&\langle x(t+\tau)x(t)\rangle \\
&\simeq \langle {x_0}^2\rangle + \frac{2k_B T {t_\alpha}^{2-\alpha}}{\Gamma(2-\alpha)m\gamma}\left[(t+\tau)^{1-\alpha} + t^{1-\alpha} - \tau^{1-\alpha}\right] \\
&\quad + \frac{{v_{typ}}^2}{(1-\beta)\beta(\beta+1){t_\beta}^{\beta-2}\langle t_w\rangle}\Big[3t^{\beta+1} + (t+\tau)^{\beta+1} - \tau^{\beta+1} \\
&\quad + (\beta+1)\left(t^\beta\tau - t(t+\tau)^\beta - (t+\tau)t^\beta\right)\Big],
\end{aligned} \tag{2.94}$$

and,

$$\langle \Delta x^2(t)\rangle \simeq \frac{2k_B T t_\alpha}{\Gamma(2-\alpha)m\gamma}\left(\frac{t}{t_\alpha}\right)^{1-\alpha} + \frac{2{v_{typ}}^2 {t_\beta}^3}{\beta(\beta+1)\langle t_w\rangle}\left(\frac{t}{t_\beta}\right)^{\beta+1}. \tag{2.95}$$

In all three cases, the long-time dynamics is superdiffusive with a diffusion exponent $\beta + 1 > 1$. This is due to the long-time positively correlated motion of the surrounding medium, which the tracer particle asymptotically follows. Note that the equilibrium and nonequilibrium part of the asymptotic position autocorrelation function can individually be cast into a scaling form similar to Eq. (2.44). This is a consequence of the scaling form of the underlying velocity correlation function and will be examined in more detail in Section 3.1.

2.3.3 *Time domain: Linear response and creep function*

Up to now, we concentrated on the second moments of the solution Eq. (2.14), since the unbiased random forces due to the equilibrium and nonequilibrium noise do not affect the tracer particle's average position. This changes once we apply an external probe force. Taking the ensemble average of Eq. (2.75), we have,

$$\langle \tilde{x}(s)\rangle = \frac{\langle x_0\rangle}{s} + \frac{1}{s^2 + \gamma s\tilde{k}(s)}\left(\frac{1}{m}\tilde{F}_p(s) + \langle v_0\rangle\right), \tag{2.96}$$

or in the time domain,

$$\langle x(t)\rangle = \langle x_0\rangle + \frac{1}{m}\int_0^t dt'\, R(t-t')F_p(t') + \langle v_0\rangle R(t), \tag{2.97}$$

where we introduced the response function $R(t)$, which is defined by its Laplace transform,

$$\tilde{R}(s) = \frac{1}{s^2 + \gamma s\tilde{k}(s)}, \tag{2.98}$$

and for the power-law memory kernel Eq. (2.15) given in terms of a Mittag-Leffler function,

$$R(t) = tE_{\alpha+1,2}\left(-\gamma t_\alpha \left(\frac{t}{t_\alpha}\right)^{\alpha+1}\right). \tag{2.99}$$

Equation (2.97) makes the linearity of the response explicit, the motion of the tracer is linearly related to the applied force. Alternatively, we describe the response of the system by the creep function $J(t)$, which is defined as,

$$\tilde{J}(s) = \frac{1}{m}\frac{1}{s^3 + \gamma s^2\tilde{k}(s)} = \frac{1}{m}\frac{1}{s}\tilde{R}(s), \tag{2.100}$$

and for the case at hand given by,

$$J(t) = \frac{1}{m}t^2 E_{\alpha+1,3}\left(-\gamma t_\alpha \left(\frac{t}{t_\alpha}\right)^{\alpha+1}\right). \tag{2.101}$$

In terms of the creep function, Eq. (2.97) reads,

$$\langle x(t)\rangle = \langle x_0\rangle + \int_0^t dt'\, J(t-t')\frac{\partial F_p(t')}{\partial t'} + J(t)F_p(0) + m\langle v_0\rangle\frac{\partial J(t)}{\partial t}. \tag{2.102}$$

The advantage of expressing the response via the creep function is that, for a constant force $F_p(t) = F_0$ and a particle initially at rest, the response is precisely given by the creep function,

$$\langle x(t) - x_0\rangle = F_0 J(t). \tag{2.103}$$

Comparing the creep function Eq. (2.101) to the mean-square displacement in equilibrium, Eq. (2.26), we see that the two are closely related, namely,

$$\langle \Delta x^2(t)\rangle_{eq} = 2k_B T J(t). \tag{2.104}$$

This relation is a generalization of the Stokes-Einstein relation to the subdiffusive equilibrium dynamics [Lutz 01]. It is a direct consequence of the fluctuation-dissipation theorem Eq. (2.11) and thus only holds for equilibrium systems. The Stokes-Einstein relation has a profound consequence on the measurement of an equilibrium system: Since the response to an external force (active measurement) and the diffusive dynamics in the absence of an external force (passive measurement) are related by Eq. (2.104), it is possible to infer one from the measurement of

the other. Conversely, if the Stokes-Einstein relation is found to be violated, the system is out of equilibrium. Since the inclusion of the nonequilibrium noise has no impact on the response of the system but changes the diffusive dynamics dramatically, this obviously leads to a violation of the Stokes-Einstein relation, Eq. (2.104). Using the asymptotic properties of the Mittag-Leffler function, Eq. (2.23), we find the asymptotic behavior of the creep function,

$$J(t) \simeq \begin{cases} \frac{1}{2m} t^2 & \text{for } t \ll t_\alpha (\gamma t_\alpha)^{\frac{1}{\alpha+1}} \\ \frac{t_\alpha}{\Gamma(2-\alpha) m\gamma} \left(\frac{t}{t_\alpha}\right)^{1-\alpha} & \text{for } t \gg t_\alpha (\gamma t_\alpha)^{\frac{1}{\alpha+1}}. \end{cases} \tag{2.105}$$

The short time behavior corresponds to the acceleration of a free particle with a constant force, which for a particle at rest is precisely what we expect upon applying a force. For long times, on the other hand, the displacement of the particle increases sub-linearly with time, which is in contrast to the normal, purely viscous case $\alpha = 0$, where the displacement grows linearly. In terms of the velocity, this means that, even though a constant force is applied, the velocity decreases due to the elastic component of the medium, which leads to an increasing drag on the particle. However, the medium is still viscous enough that the displacement continues to grow, contrary to the purely elastic case $\alpha = 1$, where the particle displacement reaches a maximum value. The sub-linear time dependence of the response is a characteristic feature of a viscoelastic medium [Xu 98, Desp 05, Koll 11]. Note that Eq. (2.103) only relates the creep function to the particle displacement in such a simple manner for a constant force. If the applied force varies in time, its relation to the response is not so straightforward, as the latter will depend on the entire history of the applied force according to Eq. (2.102). This history dependence will be discussed in Section 4.5.

2.3.4 *Equilibrium and stationarity*

In the previous section, we saw that the equilibrium part of the mean-square displacement is in one-to-one correspondence with the response of the system to an external force via the Stokes-Einstein relation. This correspondence in fact holds for any equilibrium system described by a generalized Langevin equation (2.10). If the fluctuation-dissipation theorem Eq. (2.11) holds [Kubo 66] and the system is initially in thermal equilibrium, $\langle {v_0}^2 \rangle = k_B T/m$, then the position autocorrelation reads from Eq. (2.72),

$$\langle \tilde{x}(s_2)\tilde{x}(s_1)\rangle = \frac{\langle {x_0}^2\rangle}{s_2 s_1} + \frac{1}{m^2}\frac{\langle \tilde{\eta}(s_2)\tilde{\eta}(s_1)\rangle + m k_B T}{s_2 s_1 \left(s_2 + \gamma\tilde{k}(s_2)\right)\left(s_1 + \gamma\tilde{k}(s_1)\right)}. \tag{2.106}$$

Now we use Eq. (A.24) for the Laplace transform of the stationary noise autocorrelation,

$$\langle \tilde{\eta}(s_2)\tilde{\eta}(s_1)\rangle = m\gamma k_B T \frac{\tilde{k}(s_2) + \tilde{k}(s_1)}{s_2 + s_1}, \tag{2.107}$$

to obtain,

$$\begin{aligned}\langle\tilde{x}(s_2)\tilde{x}(s_1)\rangle &= \frac{\langle {x_0}^2\rangle}{s_2 s_1} + \frac{k_B T}{m}\frac{\gamma\tilde{k}(s_2)+s_2+\tilde{k}(s_1)+s_1}{s_2 s_1(s_2+s_1)\big(s_2+\gamma\tilde{k}(s_2)\big)\big(s_1+\gamma\tilde{k}(s_1)\big)} \\ &= \frac{\langle {x_0}^2\rangle}{s_2 s_1} + \frac{k_B T}{m}\frac{1}{s_2 s_1(s_2+s_1)}\left[\frac{1}{s_2+\gamma\tilde{k}(s_2)}+\frac{1}{s_1+\gamma\tilde{k}(s_1)}\right].\end{aligned} \tag{2.108}$$

We can transform this back to the time domain using Eq. (A.4),

$$\langle x(t+\tau)x(t)\rangle = \langle {x_0}^2\rangle + \frac{k_B T}{m}\int_0^t dt'\, h(t'+\tau)+h(t'), \tag{2.109}$$

where $h(t)$ is defined via its Laplace transform,

$$\tilde{h}(s) = \frac{1}{s^2+\gamma s\tilde{k}(s)}. \tag{2.110}$$

For $\tau = 0$, we then find for the mean-square displacement,

$$\langle \Delta x^2(t)\rangle = \frac{2k_B T}{m}\int_0^t dt' h(t'), \tag{2.111}$$

respectively for its Laplace transform,

$$\langle\widetilde{\Delta x^2}(s)\rangle = \frac{2k_B T}{m}\frac{1}{s}\tilde{h}(s) = \frac{2k_B T}{m}\frac{1}{s^3+\gamma s^2\tilde{k}(s)}. \tag{2.112}$$

Comparing this to the definition of the creep function, Eq. (2.100), we immediately obtain the Stokes-Einstein relation Eq. (2.104),

$$\langle\widetilde{\Delta x^2}(s)\rangle = 2k_B T\tilde{J}(s). \tag{2.113}$$

This is valid irrespective of the specific form of the memory kernel $k(t)$, the only requirement is the validity of the fluctuation-dissipation theorem Eq. (2.11). The equivalent of Eq. (2.108) for the velocity is,

$$\langle\tilde{v}(s_2)\tilde{v}(s_1)\rangle = \frac{k_B T}{m}\frac{1}{s_2+s_1}\left[\frac{1}{s_2+\gamma\tilde{k}(s_2)}+\frac{1}{s_1+\gamma\tilde{k}(s_1)}\right]. \tag{2.114}$$

This is precisely the Laplace transform of a stationary correlation function according to Eq. (A.24), and indeed we find,

$$\langle v(t+\tau)v(t)\rangle = \frac{k_B T}{m}g(\tau), \tag{2.115}$$

with

$$\tilde{g}(s) = \frac{1}{s+\gamma\tilde{k}(s)}. \tag{2.116}$$

Again, the stationarity of the velocity correlation function holds independent of the precise form of the memory kernel as long as the fluctuation-dissipation theorem is valid. This is not at all surprising, since equilibrium by definition implies stationarity. Note that the above considerations work if the system is initially in equilibrium. If the system starts out from a nonequilibrium initial condition $\langle {v_0}^2\rangle \neq k_B T/m$, then the relaxation process leads to deviations from the stationary velocity correlation function according to Eq. (2.22).

What now about the nonequilibrium situation? As we saw before, the inclusion of a nonequilibrium noise term, whether explicitly as in Section 2.2.1 or via a moving medium as in Section 2.2.2, leads to additional contributions to both the mean-square displacement and the velocity correlation function. The simplest nonequilibrium noise we might think of is one that resembles the equilibrium one in all respects but its magnitude. Such a noise, however, is within this framework indistinguishable from a temperature that corresponds to the magnitude of the thermal and nonequilibrium noise combined, and we thus ignore this possibility and only consider "strong" violations of the fluctuation-dissipation theorem, where the equality in Eq. (2.11) cannot be restored by rescaling the temperature. As an example, let us consider the stationary Gaussian medium velocity as a nonequilibrium noise and for now ignore the contribution from the thermal noise. We then have from Eq. (2.80),

$$\langle v(t+\tau)v(t)\rangle = \langle {v_0}^2\rangle f_{\alpha,0}(t+\tau)f_{\alpha,0}(t) + \frac{\gamma^2 {v_{\text{typ}}}^2}{2\cos\left(\frac{\pi\beta}{2}\right) {t_\beta}^{\beta-1}{t_\alpha}^{2\alpha}} \times \int_0^t dt' \left[f_{\alpha,\alpha+\beta}(t'+\tau)f_{\alpha,\alpha}(t') + f_{\alpha,\alpha}(t'+\tau)f_{\alpha,\alpha+\beta}(t')\right]. \tag{2.117}$$

In particular, we find for the mean-square velocity,

$$\langle v^2(t)\rangle = \langle {v_0}^2\rangle {f_{\alpha,0}}^2(t) + \frac{\gamma^2 {v_{\text{typ}}}^2}{\cos\left(\frac{\pi\beta}{2}\right) {t_\beta}^{\beta-1}{t_\alpha}^{2\alpha}} \int_0^t dt'\, f_{\alpha,\alpha+\beta}(t')f_{\alpha,\alpha}(t'), \tag{2.118}$$

which tends to a stationary limit as $t \to \infty$,

$$\langle v^2\rangle_s = \frac{\gamma^2 {v_{\text{typ}}}^2}{\cos\left(\frac{\pi\beta}{2}\right) {t_\beta}^{\beta-1}{t_\alpha}^{2\alpha}} \int_0^\infty dt'\, f_{\alpha,\alpha+\beta}(t')f_{\alpha,\alpha}(t'). \tag{2.119}$$

In the equilibrium case, if the system is initially in the stationary equilibrium state, it remains there for all time, in particular $\langle v^2(t)\rangle = k_B T/m$. Here however, if the system starts out with its stationary value for the mean-square velocity $\langle {v_0}^2\rangle = \langle v^2\rangle_s$, we find,

$$\langle v^2(t)\rangle = \langle v^2\rangle_s \left[1 + {f_{\alpha,0}}^2(t) - \frac{\int_t^\infty dt'\, f_{\alpha,\alpha+\beta}(t')f_{\alpha,\alpha}(t')}{\int_0^\infty dt'\, f_{\alpha,\alpha+\beta}(t')f_{\alpha,\alpha}(t')}\right]. \tag{2.120}$$

The expression in square brackets can only be evaluated numerically. While both the second and third term tend to zero as $t \to \infty$ (remember that $f_{a,b}(t) \sim t^{b-a-1}$ for long times), so that the mean-square velocity does approach its stationary value, this expression generally depends on time. This leads to the strange situation, where, even if the system initially has a mean-square velocity that corresponds to the stationary state, the mean-square velocity will still vary in time. The consequences of this are twofold: Firstly, the stationary state of the system is not uniquely described by its instantaneous stationary mean-square velocity. This is due to the long-time memory present in the system, which causes its evolution to

depend on its entire history and not only on its instantaneous state. Secondly, the system described by Eq. (2.34) is profoundly and for all times a nonequilibrium system, in contrast to the equilibrium system described by Eq. (2.10), which may start out in a nonequilibrium state but ultimately relaxes to equilibrium. In fact, the nonstationarity of the velocity dynamics is a fundamental feature of systems driven by nonequilibrium noise, as can be understood from the following argument. Assume that the velocity dynamics are described by a generalized Langevin type of equation,

$$\dot{v}(t) = -\gamma \int_0^t dt' \; k(t-t')v(t') + \frac{1}{m}\xi(t), \tag{2.121}$$

where $\xi(t)$ is a nonequilibrium noise which is not related to $k(t)$ by a fluctuation-dissipation relation. The formal solution to this equation is given by,

$$v(t) = \frac{1}{m}\int_0^t dt' \; g(t-t')\xi(t') + g(t)v_0, \tag{2.122}$$

where $g(t)$ is defined by Eq. (2.116). Now suppose the velocity correlation function is stationary for all times. Then we can write,

$$\langle v(t+\tau)v(t)\rangle = \langle v(\tau)v_0\rangle = \frac{1}{m}\int_0^\tau dt' \; g(\tau-t')\langle \xi(t')v_0\rangle + g(\tau)\langle {v_0}^2\rangle. \tag{2.123}$$

The noise at some later time $t > 0$ has to be independent of the initial velocity $\langle \xi(t)v_0\rangle = 0$ due to causality – after all, the force causes the motion of the particle and not the other way round. This means that if the velocity correlation function is stationary for all times, then it is inescapably given by,

$$\langle v(t+\tau)v(t)\rangle = \langle {v_0}^2\rangle g(\tau). \tag{2.124}$$

This is, however, entirely independent of the nonequilibrium noise, which we know not to be true. Since the only assumption aside from causality was the stationarity of the velocity correlation function, this only leaves one conclusion: The velocity correlation function for a Langevin system driven by nonequilibrium noise cannot be stationary for all times, no matter what the initial condition is. This does not prevent the velocity correlation function from being asymptotically stationary, but for finite times, deviations from stationarity necessarily occur. Using Eq. (2.118) and the equivalent expression for the nonstationary Gaussian medium velocity process, we find that the mean-square velocity asymptotically approaches its stationary value as,

$$\begin{aligned}\langle v^2(t)\rangle - \langle v^2\rangle_s \simeq \frac{\langle {v_0}^2\rangle {t_\alpha}^{2\alpha}}{\gamma^2} t^{-2\alpha-2} \\ - \begin{cases} \frac{{v_{\text{typ}}}^2 {t_\alpha}^\alpha}{\cos\left(\frac{\pi\beta}{2}\right)\Gamma(\beta)\Gamma(-\alpha-1)(\beta-\alpha-2)\gamma {t_\beta}^{\beta-1}} t^{\beta-\alpha-2} \\ \frac{{v_{\text{typ}}}^2}{\Gamma^2\left(\frac{\beta}{2}\right)(1-\beta){t_\beta}^{\beta-1}} t^{\beta-1}, \end{cases}\end{aligned} \tag{2.125}$$

where the first line corresponds to the stationary and the second line to the nonstationary process. In the latter case, the nonstationarity of the medium velocity process itself yields the dominant nonstationary correction as expected. However, even if the medium velocity process is initially stationary, there are finite-time nonstationary corrections due to the nonequilibrium nature of the system, which dominate the contributions from the initial condition for long times.

3 SCALE-INVARIANT SUPERDIFFUSIVE SYSTEMS

Note: Parts of this Chapter are based on Ref. [Dech 14].

In the previous Chapter, we studied the properties of the fractional Langevin equation and its extension to superdiffusive nonequilibrium dynamics. We found that the correlation functions for the medium velocity, as well as the resulting ones for the nonequilibrium noise and for the position could be cast in a particular scaling form. Moreover, the velocity correlation function was seen to be nonstationary for a nonequilibrium system. While the scaling forms obtained in the previous Chapter are motivation enough to study their properties and consequences on other physical quantities, the contents of this section also apply to a more general class of stochastic processes. We therefore omit the discussion of the respective results in the context of nonequilibrium dynamics in cells in this Chapter and rather employ the results derived here in the next Chapter where appropriate. In Section 3.1, we formalize the idea of a scaling correlation function. The scale invariance of the dynamics is expressed by the fact that a rescaling of time only changes the correlation function algebraically. Moreover, the age of the system, instead of some intrinsic characteristic time scale, determines the rate at which the system decorrelates. The scaling correlation function is thus generally an aging correlation function, meaning that it not only depends on the time lag τ but also on the overall time t, called the age of the system. This is equivalent to the nonstationarity of the correlation function, although the term aging is mostly used to describe long-time nonstationarity. This includes systems, where the relaxation into a stationary state takes place on time scales longer than or comparable to the measurement time, and systems where no stationary state exists. Besides aging correlation functions, our general scaling form also includes stationary power-law correlation functions as a particular case.

One of the central consequences of such a scaling correlation function is that it leads to a generalization of the Green-Kubo formula, which relates the diffusion coefficient and the velocity correlations. The traditional Green-Kubo formula invariably leads to normal diffusion, $\langle \Delta x^2(t) \rangle = 2D_1 t$, but applies only to systems whose velocity correlations are stationary and relatively short ranged and thus breaks down for the scale invariant aging systems we consider. Our generalization, which we call scaling Green-Kubo relation, is able to treat these cases and leads to superdiffusion, $\langle \Delta x^2(t) \rangle = 2D_\nu t^\nu$ with $\nu > 1$. Both relations express the diffusion coefficient as an integral over a function that characterizes the velocity dynamics. For the Green-Kubo formula, this is the stationary velocity correlation function itself, for the scaling Green-Kubo relation, it is the scaling function which depends on the ratio of the time lag τ and the age t. Our scaling Green-Kubo relation leads to a novel effect, which does not occur for normal diffusion, namely that the diffusive properties of the system depend strongly on its initial prepara-

tion and the involved time scales. This dependence can persist for arbitrarily long times, which is in stark contrast to systems with exponential relaxation, where the intrinsic characteristic time scale sets the time scale for any deviations from the unique long-time behavior. This means that, in particular, the diffusion coefficient is not unique for superdiffusive systems, but can take different values depending on the initial state of the system.

The existence of a scaling correlation function for the velocity translates into a scaling correlation function for the position. A striking consequence of this scaling position correlation is that the system is nonergodic if it is not initially in a stationary state, as we show in Section 3.2. Ergodicity, in the sense we discuss it here, means that the time-average of a quantity – in this case the square of the particle displacement – is equal to the ensemble average for sufficiently long averaging times. If a system is ergodic, we may thus use a single realization or measurement of a time-dependent stochastic quantity to infer its average value. For the scaling systems we discuss here, this is only true, if the system is initially in the stationary state. If the system is not stationary at the start of the measurement, then the slow relaxation towards the stationary state will lead to a discrepancy between the time and ensemble-averaged square displacements that persists for arbitrarily long times. Of particular importance is the dependence of these findings on the respective time scales: If the system starts out in a nonstationary initial state, then the relaxation time that needs to pass, before the system can be considered as stationary in terms of ergodic behavior, has to be much longer than the desired measurement time. Again, due to scale invariance, it is not some intrinsic time scale of the system that dictates the length of the relaxation time, but the actual measurement time.

In Section 3.3 we turn from time-dependent to frequency dependent quantities. The scaling velocity correlation function leads to a similar scaling form both for its Laplace transform and for the power spectral density. The former is useful, because the analytic calculation of the correlation functions is often easier in the Laplace domain, in particular for non-Markovian systems. The relation between the scaling velocity correlation function and the velocity spectral density, on the other hand, generalizes another central result of statistical mechanics, the Wiener-Khinchine theorem. In its original form, it expresses the spectral density as the Fourier transform of the stationary autocorrelation function. As with the Green-Kubo formula, the scaling function takes the place of the stationary velocity correlation function. There is, however, one crucial difference between the original Wiener-Khinchine theorem and our scaling generalization: In our case, the spectral density generally depends on time as well as frequency. Where in the scaling correlation function, the age of the system set the time scale for the decay of the correlations, it now sets the frequency scale. This directly mirrors the scale-invariance of the system: Whether a frequency is high or low is not determined in comparison to some intrinsic frequency scale but in comparison to the measurement time. In the limit where the measurement time is much longer than the inverse frequency, the velocity spectral density becomes time-independent in most cases and decays as a function of frequency as $\omega^{1-\nu}$, where $\nu > 1$ is the diffusion exponent. This means that a process

described by a scaling velocity correlation function is a realization of $1/f$-noise. In the opposite limit, where the frequency is much smaller than the inverse measurement time, the scaling form of the spectral density yields a time-dependent low-frequency cutoff, so the total power, while possibly time-dependent, is finite for finite times. For the position spectral density, we find that it is time-dependent, its overall value increasing with time, and depends on frequency as ω^{-2}, independent of the diffusion exponent ν. In contrast to the velocity spectral density, the frequency-dependence of the position spectral density does not allow to deduce the scaling behavior and the diffusion exponent; these are encoded in the time-dependence of the position spectral density.

Finally in Section 3.4, we apply these results to the stochastic processes we are going to used to model nonequilibrium superdiffusion in cells, fractional Gaussian noise and the Lévy walk. All three velocity processes we consider are all characterized by a single parameter β. In the regime $0 < \beta < 1$, which is relevant for superdiffusion in cells, all three processes lead to superdiffusion, $\langle \Delta x^2(t) \rangle \sim D_\nu t^\nu$ with $\nu = \beta + 1$. In this regime, the velocity correlation functions are asymptotically stationary. However, as discussed before, deviations from the the stationary behavior lead to changes in the anomalous diffusion coefficient D_ν, which persist for arbitrarily long times. For this reason, we find different results for the stationary Gaussian process, Mandelbrot-van-Ness fractional Gaussian noise, and for the nonstationary Gaussian process, Riemann-Liouville fractional Gaussian noise, even though both processes are asymptotically equivalent. For the non-Gaussian Lévy walk, we similarly find a stationary and a nonstationary value for the diffusion coefficient. Depending on the process and the exponent β, these two values can differ substantially and only coincide in the limit $\beta \to 0$, which corresponds to normal diffusion. By contrast, the velocity spectral density is, apart from the low-frequency cutoff, insensitive to the distinction between stationary and nonstationary processes. For $1 < \beta < 2$, both the fractional Gaussian process and the Lévy walk are only defined in their nonstationary variants and no longer have a well-defined stationary limit. While for the Lévy walk, diffusion is quasi-ballistic with diffusion exponent $\nu = 2$ in this regime, the fractional Gaussian velocity process, which now corresponds to Riemann-Liouville fractional Brownian motion, leads to faster-than-ballistic expansion with $\nu = \beta + 1$. In the latter case, the occurrence of superballistic diffusion depends on the initial condition: It can only be observed on time scales longer than an initial relaxation time, for shorter times, the motion is ballistic as well.

3.1 SCALING GREEN-KUBO RELATION

The Taylor-Green-Kubo (or Green-Kubo for short) formula is an important tool in relating the diffusive properties of a system to the underlying velocity dynamics. While it is conceptually very simple, expressing the diffusion constant as an integral over the stationary velocity autocorrelation function, it nevertheless has some rather profound consequences. It asserts, that for a wide class of possible velocity processes, diffusion will always be normal, $\langle \Delta x^2(t) \rangle \simeq 2D_1 t$, i.e. the mean-square displacement of the particle increases linearly with time. The only influence of the

specific details of the process on the dynamics is through the numerical value of the diffusion coefficient D_1. In Section 3.1.1, we shortly review the Green-Kubo formula as it applies to normal diffusion and outline the limits of its validity; in particular the Green-Kubo formula cannot be applied to nonstationary processes. We then introduce a class of correlation functions in Section 3.1.2, for which the Green-Kubo formula does not work, since they decay slowly with time or are nonstationary. For this class of what we call scaling correlation functions, we provide a generalization of the Green-Kubo formula, termed scaling Green-Kubo relation, and show that it leads to superdiffusion, relating the diffusion exponent and diffusion coefficient to the scaling of the velocity correlation function. In Section 3.1.3, we discuss the effect of initial conditions on the diffusive dynamics and show that the initial state of the system may have a persistent effect on the diffusion coefficient. The robustness of the scaling correlation function becomes apparent in Section 3.1.4, where we show how scaling in the velocity correlation function in a natural way leads to scaling in the position correlation function, extending the scaling Green-Kubo relation from the one-time moments (i.e. the mean-square displacement) to two-time moments. Moreover, apart from being an analytical tool to determine the superdiffusive behavior from a known velocity autocorrelation function, the scaling Green-Kubo relation can also be used as a tool for data analysis. In Section 3.1.5 we employ it in this manner and show how a proper rescaling of data can be used to identify the diffusion exponent and coefficient. Since the scaling Green-Kubo formula relies on the asymptotic long-time scaling of the velocity correlations, it is important to quantify how possible short-time deviations from the scaling behavior impact the results and we do so in Section 3.1.6.

3.1.1 *Green-Kubo formula and range of validity*

For many systems, among them the paradigmatic example for diffusion, Brownian motion (see Eq. (2.1) and the following discussion), the relaxation of the velocity into the stationary state is exponential. In this case, on time scales that are long compared to the typical intrinsic characteristic time scales, the system's velocity correlation function,

$$C_v(t+\tau, t) = \langle v(t+\tau)v(t)\rangle - \langle v(t+\tau)\rangle\langle v(t)\rangle, \tag{3.1}$$

can be assumed to be stationary for all practical purposes,

$$C_v(t+\tau, t) = C_{v,s}(\tau), \tag{3.2}$$

where the subscript s denotes stationarity, i.e. that the correlation function is independent of t. Since the displacement $x(t)$ of a particle relative to its initial position $x(0) = x_0$ is related to its velocity by $x(t) = \int_0^t dt'\, v(t')$, the mean-square displacement,

$$\langle \Delta x^2(t)\rangle = \langle x^2(t)\rangle - \langle x(t)\rangle^2, \tag{3.3}$$

is related to the velocity autocorrelation by,

$$\langle \Delta x^2(t)\rangle = \int_0^t dt'' \int_0^t dt'\, C_v(t'', t'). \tag{3.4}$$

Since the velocity correlation function is by definition invariant under exchanging its arguments, we may equivalently write this as,

$$\langle \Delta x^2(t) \rangle = 2 \int_0^t dt'' \int_0^{t''} dt' \; C_v(t'', t'). \tag{3.5}$$

If the velocity correlation function is stationary, then we can change variables from t' to $\tau = t'' - t'$,

$$\langle \Delta x^2(t) \rangle = 2 \int_0^t dt'' \int_0^{t''} d\tau \; C_{v,s}(\tau). \tag{3.6}$$

Taking the derivative with respect to t, we find,

$$\frac{d}{dt} \langle \Delta x^2(t) \rangle = 2 \int_0^t d\tau \; C_{v,s}(\tau). \tag{3.7}$$

In principle, the derivative of the mean-square displacement can be positive or negative, indicating either diffusion or concentration of tracer particles. We are interested in the long-time dynamics of diffusive systems, where the mean-square displacement increases as a function of time. Then there are three possibilities for the expression on the right hand side of Eq. (3.7). If it tends to a constant, then we define this constant as the diffusion coefficient,

$$D_1 = \lim_{t \to \infty} \int_0^t d\tau \; C_{v,s}(\tau). \tag{3.8}$$

In this situation, the mean-square displacement increases linearly with time and we have normal diffusion asymptotically,

$$\langle \Delta x^2(t) \rangle \simeq 2t \int_0^\infty d\tau \; C_{v,s}(\tau) = 2D_1 t. \tag{3.9}$$

Equation (3.9) is the Green-Kubo formula [Tayl 21, Gree 53, Kubo 57]. It ascertains that for normal diffusion, the diffusion coefficient is given by the integral over the stationary velocity correlation function. There are two conditions for it to be valid: The correlation function has to be stationary and this stationary correlation function has to be such that the integral in Eq. (3.9) is finite. Both conditions are satisfied for systems with an exponential correlation function like Eq. (2.7),

$$C_{v,s}(\tau) = \frac{k_B T}{m} e^{-\gamma \tau}, \tag{3.10}$$

where the Green-Kubo formula immediately gives us the Einstein relation [Eins 05],

$$D_1 = \frac{k_B T}{m\gamma}, \tag{3.11}$$

in agreement with Eq. (2.9). However, exponential relaxation is not a requirement for the validity of the Green-Kubo formula, as long as the stationary correlation function decays faster than τ^{-1} for long times, the integral and thus the normal diffusion coefficient D_1 will be finite. Normal diffusion is thus the expected behavior for systems with sufficiently short-ranged correlations.

The other two possibilities for Eq. (3.7) both lead to anomalous diffusion. If the expression on the right hand side of Eq. (3.7) tends to zero for long times, then the normal diffusion coefficient D_1 vanishes. This can then lead to subdiffusion, $\langle \Delta x^2(t) \rangle \simeq 2D_\nu t^\nu$ with $0 < \nu < 1$, if the integral in Eq. (3.7) behaves as $t^{\nu-1}$ for long times. Or, if the integral goes to zero even faster, then we will have no diffusion at all and a constant mean-square displacement $\langle \Delta x^2(t) \rangle \simeq 2D_0$ in the long-time limit. Both of these possibilities require that the stationary velocity correlation function $C_{v,s}(\tau)$ changes sign as a function of τ, i.e. that the velocity dynamics becomes anticorrelated. An example for this kind of behavior is the equilibrium fractional Langevin equation, where we found the Mittag-Leffler type behavior Eq. (2.25) which has a negative long-time tail. On the other hand, if the correlations are positive but long-ranged, the integral in Eq. (3.7) will increase as a function of time. Then the dynamics are superdiffusive, as we saw for the three examples of the nonequilibrium moving medium in Section 2.3. This last case is the one on which we will focus on below, including the possibility of a nonstationary velocity correlation function. To summarize, the mean-square displacement behaves as,

$$\langle \Delta x^2(t) \rangle \simeq 2D_\nu t^\nu. \tag{3.12}$$

Subdiffusion $0 < \nu < 1$ requires anticorrelations in the velocity, whereas superdiffusion $\nu > 1$ arises for long-ranged positive correlations [Morg 02]. For general short-ranged correlations, we have normal diffusion $\nu = 1$ with the corresponding diffusion coefficient D_1 given by the Green-Kubo formula Eq. (3.9).

3.1.2 *Scaling correlation functions and scaling Green-Kubo relation*

We now introduce a general class of velocity correlation functions, for which the Green-Kubo formula Eq. (3.8) fails. We call them scaling correlation functions and they are of the form [Dech 14],

$$C_\nu(t+\tau, t) \simeq \mathcal{C} t^{\nu-2} \phi\left(\frac{\tau}{t}\right), \tag{3.13}$$

with $\mathcal{C} > 0$. This form generally only holds asymptotically, i.e. when both t and τ are large compared to some intrinsic time scale t_c of the system. In the following, we consider the case $\nu > 1$, which leads to superdiffusion. Obviously, Eq. (3.13) generally describes a nonstationary correlation function, since it depends on the age t of the system as well as on the time lag τ. This, the Green-Kubo formula Eq. (3.9) is not applicable. While a similar scaling function with $\nu < 1$ can be found for subdiffusive dynamics (see e.g. Eq. (2.25)), the asymptotic scaling properties alone are not sufficient to characterize the diffusive behavior in this case. The asymptotic behavior of the positive-valued function $\phi(y)$, which we term scaling function, has to lie within the following limits,

$$\phi(y) \lesssim \begin{cases} a_l y^{\delta_l} & \text{with } -1 < \delta_l \quad \text{for } y \ll 1 \\ b_u y^{\delta_u} & \text{with } \delta_u < \nu - 1 \quad \text{for } y \gg 1, \end{cases} \tag{3.14}$$

with positive constants a_l and b_u. We then use Eq. (3.5) to find the mean-square displacement,

$$\langle \Delta x^2(t) \rangle \simeq 2\mathcal{C} \int_0^t dt'' \int_0^{t''} dt' \, t'^{\nu-2} \phi\left(\frac{t''-t'}{t'}\right). \tag{3.15}$$

Obviously, this can only hold asymptotically, since we used the asymptotic form of the correlation function and also extended the lower limits of the integrals to zero. For now, we just assume this is permissible and postpone the discussion of possible contributions from the short-time behavior to Section 3.1.6. We introduce the variable $y = (t''-t')/t'$ in the t'-integral,

$$\langle \Delta x^2(t) \rangle \simeq 2\mathcal{C} \int_0^t dt'' \, t''^{\nu-1} \int_0^\infty dy \, (1+y)^{-\nu} \phi(y). \tag{3.16}$$

The integral over t'' is now straightforward and we arrive at,

$$\langle \Delta x^2(t) \rangle \simeq 2\frac{\mathcal{C}}{\nu} t^\nu \int_0^\infty dy \, (1+y)^{-\nu} \phi(y). \tag{3.17}$$

This relation is very similar to the Green-Kubo formula, Eq. (3.9), and we call it scaling Green-Kubo relation, since it relies on the scaling form of the asymptotic velocity correlation function. Comparing Eq. (3.17) with the general form of the mean-square displacement, Eq. (3.12), we can identify the anomalous diffusion coefficient,

$$D_\nu = \frac{\mathcal{C}}{\nu} \int_0^\infty dy \, (1+y)^{-\nu} \phi(y). \tag{3.18}$$

The scaling Green-Kubo relation Eq. (3.17) is the complement to the Green-Kubo formula Eq. (3.9) for superdiffusive dynamics. The Green-Kubo formula describes normal diffusion under the condition that the velocity correlation function is stationary and integrable, the precise details of the correlation function only influence the diffusion coefficient D_1. Similarly, the scaling Green-Kubo relation results in superdiffusion, provided the velocity correlation function is of the scaling form Eq. (3.13). The important ingredient is the scaling exponent $\nu - 2$ which results in the diffusion exponent ν. As with the Green-Kubo formula, the particular shape of the scaling function $\phi(y)$ only influences the anomalous diffusion coefficient D_ν, but not the qualitative dynamics. Let us note that this formalism is not restricted to velocity and position. The only requirement is that one variable is given by the time-integral over the other, which is in turn described by a scaling correlation function. The above can then be applied in a straightforward manner to e.g. time averages, $\bar{x}(t) = \int_0^t dt' x(t')/t$. Three examples for the applicability of the scaling Green-Kubo relation to different physical systems are discussed in Ref. [Dech 14].

The scaling correlation function Eq. (3.13) is generally nonstationary, since it depends on both the overall time t and the time lag τ. However, for the particular choice of the scaling function $\phi(y) \propto y^{\nu-2}$ with $\nu < 2$, it also includes the special case of stationary power-law correlation functions,

$$C_{\nu,s}(\tau) \simeq \mathcal{C}_s \tau^{\nu-2}, \tag{3.19}$$

with $\mathcal{C}_s > 0$. For $\nu > 1$, these correlation functions, though stationary, are not covered by the Green-Kubo formula Eq. (3.9), since the integral in Eq. (3.7) increases with time. In this case, the scaling Green-Kubo relation Eq. (3.17) gives us,

$$\langle \Delta x^2(t) \rangle \simeq 2D_{\nu,s} t^{\nu} \quad \text{with} \quad D_{\nu,s} = \frac{\mathcal{C}_s}{\nu(\nu-1)}. \tag{3.20}$$

While the velocity correlation function may not be explicitly stationary, it may approach the stationary behavior Eq. (3.19) in the limit of long overall time $t \gg \tau$ (see e.g. Eq. (2.44)). In this case, an obvious question is whether the actual nonstationary correlation function and its long-time stationary limit describe the same diffusive dynamics. For the paradigmatic example for normal diffusion, Brownian motion (see Eq. (2.6)), this is in fact the case. Here the nonstationary and stationary velocity correlation functions yield the same mean-square displacement apart from short time corrections. Whether this is also true in the superdiffusive case will be discussed in Section 3.1.3. Another special case of Eq. (3.13) is that of a pure aging correlation function for $\nu = 2$,

$$C_{\nu,a}\left(\frac{\tau}{t}\right) \simeq \mathcal{C}_a \phi\left(\frac{\tau}{t}\right). \tag{3.21}$$

Such a correlation function is known from a variety of systems [Bouc 92, Cugl 94], including the Lévy walk (see Section 2.2.2) for $1 < \beta < 2$ [Godr 01]. For these kinds of systems, the scaling Green-Kubo relation Eq. (3.17) gives us quasi-ballistic superdiffusion,

$$\langle \Delta x^2(t) \rangle \simeq 2D_2 t^2 \quad \text{with} \quad D_2 = \frac{\mathcal{C}_a}{2} \int_0^{\infty} dy\, (1+y)^{-2} \phi(y). \tag{3.22}$$

For the Lévy walk, this kind of behavior corresponds to the regime where the average waiting time is infinite and particles thus tend to spend a significant amount of the observation time traveling in the same direction, causing ballistic-like motion [Godr 01, Jung 02, Froe 13]. While the term aging describes any kind of dynamics which depends on the overall age t, it is particularly fitting here, since the existence of a scaling function implies that the correlation time increases linearly with the age of the system, in contrast to the normal case, where the correlation time is set by the intrinsic characteristic time scale. The third important example of Eq. (3.13) we want to highlight is $\nu > 2$ and $\phi(y) \simeq a_0$ for $y \ll 1$. Here we have for long overall times $t \gg \tau$,

$$C_{\nu}(t+\tau, t) \simeq a_0 \mathcal{C} t^{\nu-2}, \tag{3.23}$$

which is independent of τ. Because the correlation function has to be continuous, this implies that the mean-square velocity $\langle \Delta v^2(t) \rangle = \langle v^2(t) \rangle - \langle v(t) \rangle^2 = C_{\nu}(t,t)$ increases with time,

$$\langle \Delta v^2(t) \rangle \simeq a_0 \mathcal{C} t^{\nu-2}. \tag{3.24}$$

This corresponds to an overall acceleration of the particles and leads to faster than ballistic superdiffusion. We refer to this situation as superaging, as in addition to usual aging, the magnitude of the velocity correlation function increases with time. While we do not encounter this situation for the velocity correlation function for

superdiffusion in cells, which is subballistic and possesses a stationary limit for the velocity, this form of the correlation function is precisely the one that does occur for the position and thus can be used to apply some of the following results to the position dynamics.

3.1.3 *Sensitivity to initial conditions*

We now want to consider a slightly different situation. So far, we defined the displacement $x(t)$ of a particle relative to its initial position at time $t = 0$. Instead, we now want to examine the relative displacement with respect to some large initial time t_0, $x_{t_0}(t) = x(t + t_0) - x(t_0)$, so that $x_{t_0=0} = x(t)$. Physically, this corresponds to letting the system evolve for some time t_0 from its initial state and then measuring the displacement starting at t_0. For this reason we call t_0 the relaxation time and t the measurement time. The relative displacement is related to the velocity of the particle by $x_{t_0}(t) = \int_{t_0}^{t+t_0} dt'\, v(t')$ and we thus have for the corresponding relative mean-square displacement,

$$\langle \Delta {x_{t_0}}^2(t)\rangle = \langle {x_{t_0}}^2(t)\rangle - \langle x_{t_0}(t)\rangle^2 = \int_{t_0}^{t+t_0} dt'' \int_{t_0}^{t+t_0} dt'\, C_v(t'', t'). \tag{3.25}$$

We shift both integration variables by t_0,

$$\begin{aligned}\langle \Delta {x_{t_0}}^2(t)\rangle &= \int_0^t dt'' \int_0^t dt'\, C_v(t'' + t_0, t' + t_0) \\ &= 2\int_0^t dt'' \int_0^{t''} dt'\, C_v(t'' + t_0, t' + t_0).\end{aligned} \tag{3.26}$$

If the velocity correlation function is of the scaling form Eq. (3.13), then we have,

$$\begin{aligned}\langle \Delta {x_{t_0}}^2(t)\rangle &\simeq 2\mathcal{C} \int_0^t dt'' \int_0^{t''} dt'\, (t' + t_0)^{\nu-2} \phi\left(\frac{t'' - t'}{t' + t_0}\right) \\ &= 2D_\nu^{\frac{t}{t_0}} t^\nu,\end{aligned} \tag{3.27}$$

with the formally time-dependent anomalous diffusion coefficient,

$$D_\nu^{\frac{t}{t_0}} = \mathcal{C} \int_0^1 dz \left(z + \frac{t_0}{t}\right)^{\nu-1} \int_0^{z\frac{t}{t_0}} dy\, (1 + y)^{-\nu} \phi(y). \tag{3.28}$$

Here we introduced the variables $y = (t'' - t')/(t' + t_0)$ and $z = t''/t$. In the limit $t \gg t_0$ we can neglect the second term in parentheses and this reduces to Eq. (3.18),

$$D_\nu^\infty = D_\nu = \frac{\mathcal{C}}{\nu} \int_0^\infty dy\, (1 + y)^{-\nu} \phi(y). \tag{3.29}$$

The expression given by the scaling Green-Kubo relation Eq. (3.17) thus corresponds to the actual long-time limit, when the measurement time is much longer than all involved time scales including the relaxation time. In the opposite limit $t_0 \gg t$, on the other hand, we can neglect the first term in parentheses,

$$D_\nu^{\frac{t}{t_0}} \simeq \mathcal{C} \left(\frac{t}{t_0}\right)^{1-\nu} \int_0^1 dz \int_0^{z\frac{t}{t_0}} dy\, (1 + y)^{-\nu} \phi(y). \tag{3.30}$$

The upper boundary of the inner integral is very small and the asymptotic behavior thus depends only on the behavior of the scaling function for small arguments, $\phi(y) \simeq a_1 y^{\delta_1}$,

$$D_\nu^{\frac{t}{t_0}} \simeq \frac{a_1 \mathcal{C}}{(\delta_1+1)(\delta_1+2)} \left(\frac{t}{t_0}\right)^{\delta_1-\nu+2}. \tag{3.31}$$

If the velocity correlations have a stationary limit, then, as we saw before, this means $\phi(y) \simeq a_{\nu-2} y^{\nu-2}$ for small y (corresponding to $t \gg \tau$) with a positive constant $a_{\nu-2}$. Consequently, the diffusion coefficient in this limit is given by the same expression as if we had used the stationary correlation function in the first place,

$$D_\nu^0 = D_{\nu,s} = \frac{\mathcal{C}_s}{\nu(\nu-1)}, \tag{3.32}$$

with $\mathcal{C}_s = a_{\nu-2}\mathcal{C}$. In the case where the velocity correlations are asymptotically stationary, both the full nonstationary and the stationary correlation function yield the same diffusion exponent, however, the corresponding anomalous diffusion coefficient is different. We found the same behavior for the asymptotic mean-square displacement in Section 2.3.2, where we saw that nonstationary and stationary fractional Gaussian noise yield different results for the diffusion coefficient, even though the two processes are asymptotically equivalent. The diffusion coefficient is thus not unique but instead, even for long times, sensitive to whether the system was initially in the stationary state (i.e. infinite relaxation time) or not. For a finite relaxation time, the measured diffusion coefficient exhibits a crossover from the stationary value Eq. (3.32) on time scales shorter that t_0 to the nonstationary one Eq. (3.29) on time scales longer than t_0. Note, however, that both limiting values for the diffusion coefficient are themselves independent of t_0. This is in contrast to the normal diffusive case, where, as long as either the relaxation time or the measurement time are large compared to the intrinsic relaxation time, both the stationary and the nonstationary velocity correlation function yield the same diffusion coefficient. Such a persistent dependence of the long-time dynamics on the initial state of the system is known from a certain class of dynamical systems [Zumo 93] and single file diffusion [Leib 13].

This discrepancy is even more pronounced in the superaging case, where we have $\nu > 2$ and $\phi(y) \simeq a_0$, and thus,

$$D_\nu^{\frac{t}{t_0}} \simeq \frac{a_0 \mathcal{C}}{2} \left(\frac{t}{t_0}\right)^{2-\nu}. \tag{3.33}$$

For the mean-square displacement this results in,

$$\langle \Delta x_{t_0}{}^2(t) \rangle \simeq a_0 \mathcal{C}\, t_0^{\nu-2} t^2 = \langle \Delta v^2(t_0) \rangle\, t^2, \tag{3.34}$$

where we used Eq. (3.24) for the mean-square velocity. Here the dynamics are qualitatively different depending on the relative size of the measurement time and relaxation time. If $t_0 \gg t$, the mean-square velocity, which grows with time, is large but more or less constant on the time scale of the measurement, leading to ballistic

spreading. As the measurement time becomes comparable to the relaxation time, the increase of the mean-square velocity makes itself felt, until at long measurement times $t \gg t_0$, the acceleration of the particles dominates the dynamics and leads to faster that ballistic diffusion.

Finally, there is the borderline case $\nu = 2$, with a logarithmic behavior of the scaling function, $\phi(y) \simeq -a^* \ln(y)$ with $a^* > 0$ for $y \ll 1$. This case corresponds to pure aging, Eq. (3.21), and leads to,

$$D_\nu^{\frac{t}{t_0}} \simeq -\frac{a^* \mathcal{C}}{2} \ln\left(\frac{t}{t_0}\right), \tag{3.35}$$

and thus ballistic expansion with a diffusion coefficient increasing logarithmically with t_0,

$$\langle \Delta x_{t_0}{}^2(t) \rangle \simeq -a^* \mathcal{C} \ln\left(\frac{t}{t_0}\right) t^2. \tag{3.36}$$

The logarithmic increase of the diffusion coefficient with the relaxation time reflects a logarithmic growth of the mean-square velocity, $\langle \Delta v^2(t) \rangle \simeq a^* \mathcal{C} \ln(t)$. Interestingly, this logarithmic growth is not sufficient to enhance diffusion beyond the quasi-ballistic behavior for $t \gg t_0$, see Eq. (3.22).

An important observation is that, as a direct consequence of the scaling form Eq. (3.13) for the velocity correlation, the time-dependent diffusion coefficient depends on the ratio of the measurement time t and the relaxation time t_0. Thus, due to the absence of any intrinsic time scales, the relevant time scale for the dynamics is set by the relaxation time t_0, which is not intrinsic to the system but rather set by its history and initial preparation and thus in principle an experimentally controllable parameter. The above behavior is in stark contrast to normal diffusion and also the subdiffusive equilibrium motion described by the fractional Langevin equation Eq. (2.17). For normal diffusion, we find from Eq. (2.5),

$$\begin{aligned}\langle \Delta x^2(t) \rangle_{t_0} = &\frac{2k_B T}{m\gamma} t \\ &+ \frac{k_B T}{m\gamma^2}\left(2e^{-\gamma t} + e^{-\gamma(t+2t_0)} - 2e^{-2\gamma t_0} - e^{-2\gamma(t+t_0)} - 2\right),\end{aligned} \tag{3.37}$$

and for the equilibrium fractional Langevin equation, we find from Eq. (2.22),

$$\begin{aligned}\langle \Delta x^2(t) \rangle_{t_0} \simeq &\frac{2k_B T}{\Gamma(2-\alpha) m\gamma t_\alpha}\left(\frac{t}{t_\alpha}\right)^{1-\alpha} \\ &+ \frac{2k_B T}{\Gamma^2(1-\alpha) m\gamma^2 t_\alpha{}^2}\left[\left(\frac{t+t_0}{t_\alpha}\right)^{-2\alpha} - \left(\frac{(t+t_0)t_0}{t_\alpha{}^2}\right)^{-\alpha}\right].\end{aligned} \tag{3.38}$$

While in both cases, there are t_0-dependent corrections to the mean-square displacement, the important difference is that these become negligible for long times. Independent of t_0, the mean-square displacement and thus the (anomalous) diffusion coefficient are unique in the long-time limit. This underlines a fundamental difference between the sub- or normal diffusive equilibrium dynamics and the superdiffusive dynamics described by the scaling correlation function Eq. (3.13).

3.1.4 *Position correlation function*

So far, we focused on the mean-square displacement and how it is related to the scaling velocity autocorrelation function. If we instead consider the position autocorrelation function,

$$C_x(t+\tau,t) = \langle x(t+\tau)x(t)\rangle - \langle x(t+\tau)\rangle\langle x(t)\rangle, \tag{3.39}$$

we can relate it to the velocity correlation function by,

$$C_x(t+\tau,t) = \int_0^{t+\tau} dt'' \int_0^t dt'\, C_v(t'',t'). \tag{3.40}$$

Since the scaling correlation function Eq. (3.13) requires explicit time ordering of its arguments, we divide the above integral accordingly,

$$C_x(t+\tau,t) = 2\int_0^t dt'' \int_0^{t''} dt'\, C_v(t'',t') + \int_t^{t+\tau} dt'' \int_0^t dt'\, C_v(t'',t'), \tag{3.41}$$

where we used the symmetry of the correlation function under exchanging its arguments. The first term is precisely the mean square displacement at time t and thus given by Eq. (3.17). In the second term, we use the scaling form Eq. (3.13) for the velocity correlation function and change variables to $u = (t''-t')/t'$ and $w = t''/t - 1$ to obtain,

$$\begin{aligned} C_x(t+\tau,t) &\simeq 2D_v t^\nu + \mathcal{C} t^\nu \int_0^{\frac{\tau}{t}} dw\, w^{\nu-1} \int_w^\infty du\, (1+u)^{-\nu}\phi(u) \\ &= t^\nu \left[2D_v + \mathcal{C}\psi\left(\frac{\tau}{t}\right)\right], \end{aligned} \tag{3.42}$$

which is again of a scaling form similar to Eq. (3.42) with a new scaling function $\psi(y)$,

$$\begin{aligned} \psi(y) &= \int_0^y dw\, (1+w)^{\nu-1} \int_w^\infty du\, (1+u)^{-\nu}\phi(u) \\ &= \frac{1}{\nu}((1+y)^\nu - 1)\int_0^\infty du\, (1+u)^{-\nu}\phi(u) \\ &\quad - \int_0^y dw\, (1+w)^{\nu-1}\int_0^w du\, (1+u)^{-\nu}\phi(u). \end{aligned} \tag{3.43}$$

The scaling velocity autocorrelation function thus directly results in a scaling position autocorrelation function. This emphasizes the fact that the scaling behavior is a fundamental property of the system.

Moreover, the asymptotic behavior of the scaling function $\phi(y)$ determines the one of the derived scaling function $\psi(y)$. For small y, assuming that $\phi(y) \simeq a_1 y^{\delta_1}$, we have,

$$\begin{aligned} \psi(y) &\simeq \left(y + \frac{\nu-1}{2}y^2\right)\int_0^\infty du\, (1+u)^{-\nu}\phi(u) \\ &\quad - \frac{a_1}{(\delta_1+1)(\delta_1+2)} y^{\delta_1+2} + \mathcal{O}(y^{\delta_1+3}). \end{aligned} \tag{3.44}$$

For the particular case of an asymptotically stationary velocity correlation, $\phi(y) \simeq a_{\nu-2} y^{\nu-2}$, this gives us,

$$\psi(y) \simeq \left(y + \frac{\nu-1}{2} y^2\right) \int_0^\infty du\, (1+u)^{-\nu} \phi(u) - \frac{a_{\nu-2}}{\nu(\nu-1)} y^\nu + \mathcal{O}(y^{\nu+1}), \tag{3.45}$$

whereas for the superaging type, $\phi(y) \simeq a_0$, we have,

$$\psi(y) \simeq y \int_0^\infty du\, (1+u)^{-\nu} \phi(u) + \left(\frac{\nu-1}{2} - \frac{a_0}{2}\right) y^2 + \mathcal{O}(y^3). \tag{3.46}$$

Since we have $\delta_l > -1$ (see Eq. (3.14)), the leading order of $\psi(y)$ is linear in y independent of the small-y behavior of $\phi(y)$,

$$\psi(y) \simeq \nu D_\nu y. \tag{3.47}$$

This is in agreement with $C_x(t,t) = \langle \Delta x^2(t) \rangle \simeq 2D_\nu t^\nu$. For large y and for $\phi(y) \simeq b_u y^{\delta_u}$, we get,

$$\psi(y) \simeq \frac{1}{\nu} y^\nu \int_0^\infty du\, (1+u)^{-\nu} \phi(u) - \frac{b_u}{(\delta_u+1)(\nu-1-\delta_u)} y^{\delta_u+1} + \mathcal{O}(y^{\nu-1}). \tag{3.48}$$

Since we have $\delta_u + 1 < \nu$ (see Eq. (3.14)), the leading order is now proportional to y^ν, which gives us for the position correlation function in the limit $\tau \gg t$,

$$C_x(t+\tau, t) \simeq D_\nu \tau^\nu. \tag{3.49}$$

The leading order asymptotic behavior of the position correlation function thus, just like the mean-square displacement, depends on the detailed shape of the correlation function only through the diffusion coefficient D_ν. Once again, special care needs to be given to the case where $\nu = 2$ and the leading order behavior of the velocity scaling function is logarithmic, $\phi(y) \simeq -a^* \ln(y)$ for $y \ll 1$, where we have for small y instead of Eq. (3.44),

$$\psi(y) \simeq \left(y + \left(\frac{1}{2} - \frac{3a^*}{4}\right) y^2\right) \int_0^\infty du\, (1+u)^{-\nu} \phi(u) + \frac{c^*}{2} y^2 \ln(y). \tag{3.50}$$

3.1.5 *Application to experimental data*

Note: This section is derived from and closely follows Ref. [Dech 14].

The scaling Green-Kubo relation Eq. (3.17) cannot only be used to calculate the diffusion coefficient from an analytically known velocity correlation function, but also serves as a data analysis method for a generic velocity correlation function that has been obtained experimentally or numerically. To this end, we use the velocity correlation function generated by performing numerical Langevin simulations of free diffusion under the influence of a friction force that is inversely proportional to the velocity. Such a Langevin dynamics describes, for example, the diffusion of

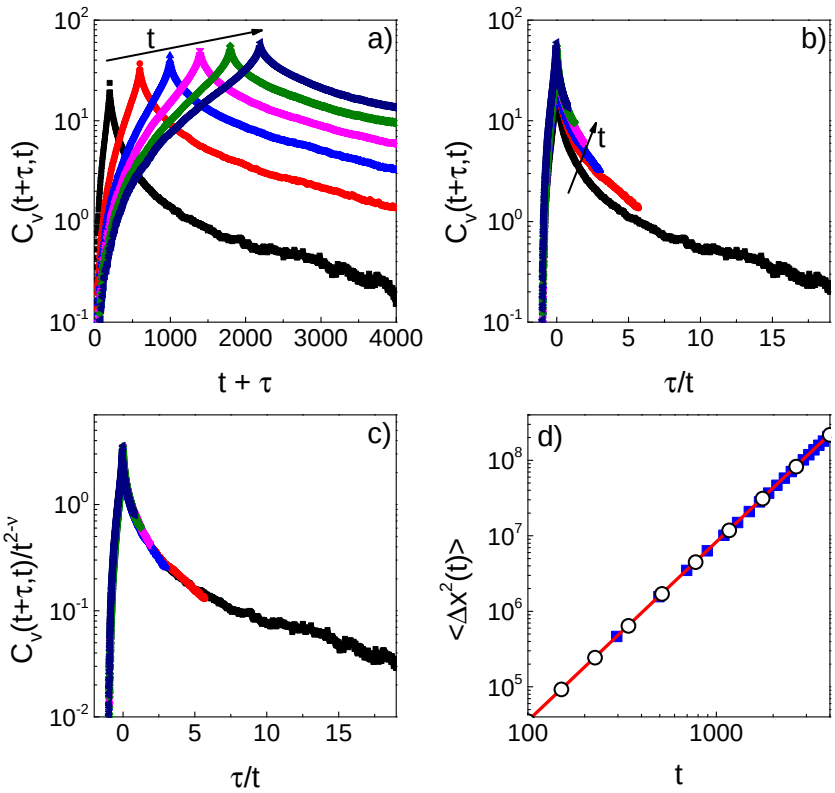

Figure 3.1: Computation of the diffusion exponent and coefficient for cold atoms in optical lattices from the correlation function using the scaling Green-Kubo formula Eq. (3.17). a) Correlation function as a function of the total time $t+\tau$ for different values of t. b) Correlation function plotted as a function of τ/t. c) After rescaling by $t^{\nu-2}$ with $\nu = 2.37$. d) Mean square displacement obtained by integrating over the rescaled correlation function $\phi(s)$ (empty circles) compared to the analytical result (red line) and the mean square displacement obtained directly from the Langevin simulation (blue squares). From the rescaling and integration procedure, we obtain $\nu \simeq 2.37$ and $D_\nu \simeq 0.321$, which agrees well with the asymptotic analytical results $\nu = 2.37$ and $D_\nu = 0.323$.

cold atoms in a shallow optical lattice [Cast 91] or the dynamics of bubbles in DNA [Foge 07]. While this system will not be discussed in this work, it is a further example for the occurrence of a scaling correlation function of the type Eq. (3.13). Here, we use it as a black box to generate data for the correlation function to which we apply the scaling Green-Kubo relation. Applying Eq. (3.17) to the measured correlation function requires identifying the scaling behavior of the latter. This is done in the following way, as illustrated in Fig. 3.1. First, we obtain the correlation function as a function of the time lag τ for different times t and plot it as a function of τ/t (Fig. 3.1a) and b)). Then we rescale the resulting curves by $t^{\nu-2}$, the correct value of ν being obtained when the data collapses onto a single curve (Fig. 3.1c)). This determines the diffusion exponent ν. The single rescaled curve is then the function $\phi(s)$ in Eq. (3.17). Multiplying $\phi(s)$ by $(1+s)^{-\nu}$ and numerically integrating the resulting curve, we obtain the generalized diffusion coefficient D_ν. In Fig. 3.1d), we compare the results obtained in this way to the mean square displacement obtained directly from the numerical simulations by integrating the velocity process and also to the asymptotic analytical one and find good agreement within the accuracy of the numerical simulations. Compared to determining the diffusion exponent and coefficient directly from the data for the mean square displacement, this rescaling method has the advantage that it does not require any fitting of power-laws to the data and is thus potentially more accurate.

3.1.6 *Deviations from scaling*

The scaling form of the velocity autocorrelation function, Eq. (3.13) will generally only be valid asymptotically, that is, when both the overall time t and the time lag τ are large. Nevertheless, in Eq. (3.15), we assumed the scaling form to hold for all times and to give the dominant contribution to the mean-square displacement. We now want to assess when this approximation is valid and how short-time deviations from the scaling behavior impact the result. For an arbitrary velocity autocorrelation, we have,

$$\langle \Delta x^2(t) \rangle = 2 \int_0^t dt'' \int_0^{t''} dt' \; C(t'', t'). \tag{3.51}$$

We assume that the scaling form Eq. (3.13) holds for $t' > t_c$ and $t'' - t' > t_c$, with some characteristic time t_c. While the short-time cutoff to the scaling behavior t_c

might in principle be different for t' and $t''-t'$, we can ignore this complication by choosing t_c as the larger of the two. Splitting the integral accordingly,

$$\begin{aligned}\langle \Delta x^2(t)\rangle = 2\Bigg[&\underbrace{\int_{2t_c}^{t} dt'' \int_{t_c}^{t''-t_c} dt'}_{I_1} \\ &+ \underbrace{\int_{t_c}^{t} dt'' \int_{t''-t_c}^{t''} dt'}_{I_2} + \underbrace{\int_{2t_c}^{t} dt'' \int_{0}^{t_c} dt'}_{I_3} \\ &+ \underbrace{\int_{0}^{t_c} dt'' \int_{0}^{t''} dt'}_{I_4} + \underbrace{\int_{t_c}^{2t_c} dt'' \int_{0}^{t''-t_c} dt'}_{I_5}\Bigg] C(t'',t'). \end{aligned} \tag{3.52}$$

In I_1, we can now use the scaling form Eq. (3.13) to find,

$$I_1 \simeq \mathcal{C} t_c^{\nu} \int_1^{\frac{t}{t_c}-1} dz\, z^{\nu-1} \int_{\frac{1}{z}}^{z} dy\, (1+y)^{-\nu}\phi(y), \tag{3.53}$$

where we introduced the variables $y = (t''-t')/t'$ and $z = t'/t_c - 1$. Since we are interested in the long-time asymptotic behavior of the mean-square displacement, we consider the limit $t \gg t_c$. If $\nu > 1$ and $\phi(y)$ satisfies the bounds Eq. (3.14) the main contribution to the integral stems from large values of z and we may write,

$$\begin{aligned}\int_{\frac{1}{z}}^{z} dy\, (1+y)^{-\nu}\phi(y) = &\int_0^{\infty} dy\, (1+y)^{-\nu}\phi(y) \\ &- \int_0^{\frac{1}{z}} dy\, (1+y)^{-\nu}\phi(y) - \int_z^{\infty} dy\, (1+y)^{-\nu}\phi(y). \end{aligned} \tag{3.54}$$

Using the small- respectively large-argument behavior of $\phi(y)$, Eq. (3.14), we then have for I_1,

$$\begin{aligned} I_1 \simeq \mathcal{C}\Bigg[&\frac{1}{\nu} t^{\nu} \int_0^{\infty} dy\, (1+y)^{-\nu}\phi(y) \\ &- a_1 t_c^{\nu} \int_1^{\frac{t}{t_c}} dz\, z^{\nu-1} \int_0^{\frac{1}{z}} dy\, y^{\delta_l} - b_u t_c^{\nu} \int_1^{\frac{t}{t_c}} dz\, z^{\nu-1} \int_z^{\infty} dy\, y^{\delta_u-\nu}\Bigg]. \end{aligned} \tag{3.55}$$

The first term is just our previous result Eq. (3.17), which corresponds to $t_c = 0$, while the other two terms give sub-leading corrections,

$$\begin{aligned} I_1 \simeq t^{\nu}\Bigg[&D_{\nu} - \frac{a_l \mathcal{C}}{(\delta_l+1)(\nu-\delta_l-1)} \left(\frac{t}{t_c}\right)^{-\delta_l-1} \\ &- \frac{b_u \mathcal{C}}{(\delta_u+1)(\nu-\delta_u-1)} \left(\frac{t}{t_c}\right)^{\delta_l+1-\nu} + \mathcal{O}(1)\Bigg]. \end{aligned} \tag{3.56}$$

In order to evaluate the remaining contributions in Eq. (3.52), we need to specify the short-time behavior of the velocity correlation function. However, it is immediately apparent that the terms I_4 and I_5 are independent of t and thus just give a

constant contribution. The two terms I_2 and I_3 can be estimated, if we assume that the velocity correlations decay as a function of the time lag, $C_v(t+\tau, t) \leqslant C_v(t,t) = \langle \Delta v^2(t) \rangle$. If we further assume that the velocity mean-square displacement is constant $\langle \Delta v^2(t) \rangle = {v_0}^2$ or at most exhibits a power-law increase $\langle \Delta v^2(t) \rangle = a_0 \mathcal{C} t^{\nu-2}$ for $\nu > 2$ (see Eq. (3.24)), then we can estimate,

$$I_2 + I_3 \leqslant \left[\int_{t_c}^{t} dt'' \int_{t''-t_c}^{t''} dt' + \int_{2t_c}^{t} dt'' \int_{0}^{t_c} dt' \right] \langle \Delta v^2(t') \rangle. \tag{3.57}$$

For the case of a constant velocity mean-square displacement, we find,

$$I_2 + I_3 \leqslant 2 t_c t {v_0}^2 - 3 {t_c}^2 {v_0}^2, \tag{3.58}$$

and thus at most a linear contribution, which is sub-dominant to I_1 since we have $\nu > 1$. For the velocity mean-square displacement increasing as a power-law, we find,

$$\begin{aligned} I_2 + I_3 &\leqslant a_0 \mathcal{C} \Bigg[\frac{1}{\nu(\nu-1)} \left[t^\nu - {t_c}^\nu - (t-t_c)^\nu \right] + \frac{1}{\nu-1} {t_c}^{\nu-1} t \\ &\simeq \frac{1}{(\nu-1)} \left[t_c t^{\nu-1} + {t_c}^{\nu-1} t \right] \Bigg], \end{aligned} \tag{3.59}$$

where we expanded for $t \gg t_c$ in the last step. Since this contribution is at most of order $t^{\nu-1}$, it is also sub-dominant to the one stemming from I_1. Summarizing, we indeed find that the scaling part of the correlation function gives the dominant contribution to the mean-square displacement and we can thus neglect the short-time deviations from the scaling behavior in the superdiffusive case. This also allows us to forgo explicitly specifying a short-time cutoff on the correlation function, even if it diverges in the limit $\tau \to 0$, as is the case for the processes discussed in Section 2.2.2, as long as this divergence is integrable.

3.2 TIME AVERAGES AND ERGODICITY

In the previous Section, we derived a number of relations for ensemble-averaged quantities like the mean-square displacement and correlation functions. By definition, an ensemble average requires a large number of realizations – ideally infinitely many – to be accurately reproducible. In practice, this means repeating an experiment many times in a reproducible manner or measuring a quantity that is itself the average of many individual stochastic systems. In many experiments, however, only a small or moderate number of realizations is available for data analysis. This is particularly true for single particle tracking and microrheology experiments, where typically a small number of trajectories, each consisting of a large number of data points, is available [Burs 05, Gall 09]. For this reason, time averages over a single trajectory are often performed instead of or in addition to the ensemble averaging over the available trajectories. In this Section, we discuss how a specific time-averaged quantity, the time-averaged square displacement is related to the mean-square displacement. To this end, we define the time-averaged square displacement in Section 3.2.1 and compute its ensemble average in terms of the scaling position correlation function. For a large class of systems, which are

called mean-square ergodic, this time-averaged square displacement is for long times equivalent to the ensemble-averaged mean square displacement, allowing to substitute time-averaging for ensemble-averaging and vice versa [Papo 02]. For the superdiffusive systems we consider, we show in Section 3.2.2, that mean-square ergodicity is not a given and generally depends on the initial state of the system. In particular, we relate the mean-square ergodicity to whether or not the system was in a stationary state at the start of the measurement.

3.2.1 *Time-averaged square displacement*

The time-averaged square displacement is defined as,

$$\overline{\Delta x^2(t,\delta)} = \frac{1}{t-\delta}\int_0^{t-\delta} dt'[x(t'+\delta)-x(t')]^2, \tag{3.60}$$

so it is the running time average over the square of the relative displacement between two times separated by a time lag δ. Obviously, we have to demand $\delta < t$. The interesting case is actually $\delta \ll t$, since only then will the time average extend over a significant part of the trajectory and will yield statistically significant information. Since the time average is performed over a single trajectory, the time-averaged square displacement is a random variable for finite averaging time t. The statistical properties of this random variable are related to those of the process $x(t)$. Since two processes, e.g. stationary fractional Gaussian noise and the stationary Lévy walk may have the same two-time correlation function but result in ergodic respectively nonergodic behavior, i.e. different statistics for the time-averaged square displacement, the correlation function is obviously not sufficient to specify the asymptotic behavior of Eq. (3.60). However, we can use the scaling forms Eqs. (3.13) or rather (3.42) to make statements about the ensemble average of the time-averaged square displacement,

$$\begin{aligned}\left\langle\overline{\Delta x^2(t,\delta)}\right\rangle &= \frac{1}{t-\delta}\int_0^{t-\delta} dt'\ \left\langle[x(t'+\delta)-x(t')]^2\right\rangle \\ &= \frac{1}{t-\delta}\int_0^{t-\delta} dt'\ \left[\langle\Delta x^2(t'+\delta)\rangle + \langle\Delta x^2(t')\rangle - 2C_x(t'+\delta,t')\right] \\ &\quad + \frac{1}{t-\delta}\int_0^{t-\delta} dt'\ \left[\langle x(t'+\delta)\rangle^2 + \langle x(t')\rangle^2 - 2\langle x(t'+\delta)\rangle\langle x(t')\rangle\right].\end{aligned} \tag{3.61}$$

If there is no average drift of the tracer particle, $\langle x(t)\rangle = 0$, then the second integral vanishes, which we will assume in the following. Using the scaling form Eq. (3.42) for the position autocorrelation, we then find,

$$\begin{aligned}\left\langle\overline{\Delta x^2(t,\delta)}\right\rangle \simeq \frac{1}{t-\delta}\int_0^{t-\delta} dt'\ &\left[\langle\Delta x^2(t'+\delta)\rangle - \langle\Delta x^2(t')\rangle\right] \\ &- 2\mathcal{C}\frac{1}{t-\delta}\int_0^{t-\delta} dt'\ t'^{\nu}\psi\left(\frac{\delta}{t'}\right),\end{aligned} \tag{3.62}$$

with the scaling function Eq. (3.43). The first two terms are trivial to evaluate assuming that $\langle \Delta x^2(t)\rangle \simeq 2D_\nu t^\nu$,

$$\left\langle \overline{\Delta x^2(t,\delta)} \right\rangle \simeq \frac{2D_\nu}{\nu+1}\frac{1}{t-\delta}\left[t^{\nu+1}-\delta^{\nu+1}-(t-\delta)^{\nu+1}\right] - 2\mathcal{C}\frac{\delta^{\nu+1}}{t-\delta}\int_{\frac{\delta}{t-\delta}}^{\infty} dy\, y^{-\nu-2}\psi(y), \tag{3.63}$$

where we introduced $y = \delta/t'$ in the last term. To find the asymptotic behavior of the remaining integral for $t \gg \delta$, we note that in this limit, the lower boundary of the integral is small. Since $\psi(y)$ increases as y^ν for large arguments (see Eq. (3.48)), the entire integrand vanishes as y^{-2} for large y. We may thus focus on the small-argument expansion of $\psi(y)$, Eq. (3.44), the error being at most a constant contribution from the integral. We then have,

$$\begin{aligned}\left\langle \overline{\Delta x^2(t,\delta)} \right\rangle \simeq{}& \frac{2D_\nu}{\nu+1}\frac{1}{t-\delta}\left[t^{\nu+1}-\delta^{\nu+1}-(t-\delta)^{\nu+1}\right] \\ &- 2\frac{\delta^{\nu+1}}{t-\delta}\Bigg[D_\nu\left(\frac{\delta}{t-\delta}\right)^{-\nu} \\ &- \frac{a_1\mathcal{C}}{(\delta_1+1)(\delta_1+2)(\nu-\delta_1-1)}\left(\frac{\delta}{t-\delta}\right)^{\delta_1-\nu+1} \\ &+ \frac{\nu D_\nu}{2}\left(\frac{\delta}{t-\delta}\right)^{1-\nu} + \mathcal{O}(1)\Bigg],\end{aligned} \tag{3.64}$$

where we used Eq. (3.18) for D_ν. Expanding for $t \gg \delta$ we find,

$$\begin{aligned}\left\langle \overline{\Delta x^2(t,\delta)} \right\rangle \simeq{}& \frac{1}{t-\delta}\left[2D_\nu\delta t^\nu - \nu D_\nu\delta^2 t^{\nu-1} - \delta^{\nu+1} + t^{\nu+1}\mathcal{O}((\delta/t)^3)\right] \\ &- \frac{1}{t-\delta}\Bigg[2D_\nu\delta t^\nu - \nu D_\nu\delta^2 t^{\nu-1} \\ &- \frac{2a_1\mathcal{C}}{(\delta_1+1)(\delta_1+2)(\nu-\delta_1-1)}\delta^{\delta_1+2}t^{\nu-\delta_1-1} \\ &+ t^{\nu+1}\mathcal{O}((\delta/t)^3) + \mathcal{O}(1)\delta^{\nu+1}\Bigg] \\ \simeq{}& t^\nu\left[\frac{2a_1\mathcal{C}}{(\delta_1+1)(\delta_1+2)(\nu-\delta_1-1)}\left(\frac{\delta}{t}\right)^{\delta_1+2} + \mathcal{O}\left(\left(\frac{\delta}{t}\right)^{\nu+1}\right)\right].\end{aligned} \tag{3.65}$$

Both for an asymptotically stationary correlation function, $\nu < 2$, $\delta_1 = \nu - 2$, and the superaging case $\nu > 2$, $\delta_1 = 0$, the leading order is given by the first term. Comparing the result to Eqs. (3.32) respectively (3.33), we can write this as,

$$\left\langle \overline{\Delta x^2(t,\delta)} \right\rangle \simeq \begin{cases} 2D_{\nu,s}\delta^\nu & \text{for } \nu < 2,\ \phi(y) \simeq c_{\nu-2}y^{\nu-2} \\ -a^*\mathcal{C}\delta^2\ln\left(\frac{\delta}{t}\right) & \text{for } \nu = 2,\ \phi(y) \simeq c^*\ln(y) \\ \frac{1}{\nu-1}\langle \Delta v^2(t)\rangle\delta^2 & \text{for } \nu > 2,\ \phi(y) \simeq c_0. \end{cases} \tag{3.66}$$

Before we discuss these results in detail, we want to examine a slightly different situation, similar to Section 3.1.3. If we let the system relax for a time t_0 before starting to measure the time-averaged square displacement, the latter is given by,

$$\overline{\Delta x_{t_0}{}^2(t,\delta)} = \frac{1}{t-\delta}\int_{t_0}^{t_0+t-\delta} dt'[x(t'+\delta)-x(t')]^2. \tag{3.67}$$

With the same arguments as above, we can express the ensemble mean of the time-averaged square displacement as,

$$\begin{aligned}\left\langle\overline{\Delta x_{t_0}{}^2(t,\delta)}\right\rangle \simeq \frac{2D_\nu}{\nu+1}\frac{1}{t-\delta}&\left[(t+t_0)^{\nu+1}-(t_0+\delta)^{\nu+1}\right.\\ &\left.-(t+t_0-\delta)^{\nu+1}+t_0{}^{\nu+1}\right]\\ -2\mathcal{C}\frac{\delta^{\nu+1}}{t-\delta}&\int_{\frac{\delta}{t_0+t-\delta}}^{\frac{\delta}{t_0}} dy\, y^{-\nu-2}\psi(y),\end{aligned} \tag{3.68}$$

where, as before, we assumed that there is no average drift. For this expression, there are in three limits that are of interest, since we still want to maintain $t \gg \delta$. For $t \gg \delta t_0$, we can just take the limit $t_0 \to 0$ and end up with Eq. (3.66) to leading order. If, on the other hand $t_0 \gg \delta$, then both the lower and upper limit of the integral are small and we may replace $\psi(y)$ by its small argument expansion, Eq. (3.44), to find,

$$\begin{aligned}\left\langle\overline{\Delta x_{t_0}{}^2(t,\delta)}\right\rangle \simeq \frac{2D_\nu}{\nu+1}\frac{1}{t-\delta}&\left[(t+t_0)^{\nu+1}-(t_0+\delta)^{\nu+1}\right.\\ &\left.-(t+t_0-\delta)^{\nu+1}+t_0{}^{\nu+1}\right]\\ -\frac{1}{t-\delta}&\Big[2D_\nu\delta\big((t+t_0-\delta)^\nu-t_0{}^\nu\big)\\ &+\nu D_\nu\delta^2\big((t+t_0-\delta)^{\nu-1}-t_0{}^{\nu-1}\big)\\ &-\frac{2a_1\mathcal{C}}{(\delta_1+1)(\delta_1+2)(\nu-\delta_1-1)}\delta^{\delta_1+2}\\ &\times\big((t+t_0-\delta)^{\nu-\delta_1-1}-t_0{}^{\nu-\delta_1-1}\big)\Big].\end{aligned} \tag{3.69}$$

Expanding for $\delta \ll t_0$ and $\delta \ll t+t_0$, we see that the terms of first and second order in δ cancel and we are left with,

$$\begin{aligned}\left\langle\overline{\Delta x_{t_0}{}^2(t,\delta)}\right\rangle \simeq \frac{1}{t}&\frac{2a_1\mathcal{C}}{(\delta_1+1)(\delta_1+2)(\nu-\delta_1-1)}\delta^{\delta_1+2}\\ &\times\big((t+t_0)^{\nu-\delta_1-1}-t_0{}^{\nu-\delta_1-1}-(\nu-\delta_1-1)(t+t_0)^{\nu-\delta_1-2}\delta\big).\end{aligned} \tag{3.70}$$

Now we still have to distinguish between the two cases $t \gg t_0$ and $t_0 \gg t$, where we find,

$$\left\langle\overline{\Delta x_{t_0}{}^2(t,\delta)}\right\rangle \simeq \begin{cases}\frac{2a_1\mathcal{C}}{(\delta_1+1)(\delta_1+2)(\nu-\delta_1-1)}t^\nu\left(\frac{\delta}{t}\right)^{\delta_1+2} & \text{for } t \gg t_0\\ \frac{2a_1\mathcal{C}}{(\delta_1+1)(\delta_1+2)}t_0^\nu\left(\frac{\delta}{t_0}\right)^{\delta_1+2} & \text{for } t_0 \gg t.\end{cases} \tag{3.71}$$

The result for $t \gg t_0$ is the same one we had for $t_0 = 0$, whereas in the case $t_0 \gg t$, we now have for the stationary and superaging case respectively,

$$\left\langle \overline{\Delta x^2(t,\delta)} \right\rangle \simeq \begin{cases} 2D_{\nu,s}\delta^\nu & \text{for } \nu < 2,\ \phi(y) \simeq c_{\nu-2} y^{\nu-2} \\ -a^* \mathcal{C} \delta^2 \ln\left(\frac{\delta}{t_0}\right) & \text{for } \nu = 2,\ \phi(y) \simeq c^* \ln(y) \\ \langle \Delta v^2(t_0) \rangle \delta^2 & \text{for } \nu > 2,\ \phi(y) \simeq c_0. \end{cases} \tag{3.72}$$

3.2.2 *Ergodicity and stationarity*

Now that we know how the ensemble mean of the time-averaged square displacement behaves in the limits of interest, we discuss how this relates ergodicity and stationarity. A stochastic process is ergodic, if it allows to infer the behavior of the entire ensemble of possible realizations from a single realization [Papo 02, Soko 08]. In the context of the trajectory of a tracer particle, this means that by observing and averaging a single trajectory for a sufficiently long time, we may reconstruct ensemble averages. For the diffusive behavior, the observable of interest is the mean-square displacement [Saxt 97]. We thus refer to a process as mean-square ergodic, if the time-averaged square displacement coincides with the ensemble-averaged mean square displacement in the limit of long times,

$$\lim_{t\to\infty} \overline{\Delta x^2(t,\delta)} = \langle \Delta x^2(\delta) \rangle. \tag{3.73}$$

This means that for every single trajectory, averaging the square displacement for a long enough time will reproduce the mean-square displacement with arbitrary accuracy. The above condition can be broken down into two more tangible ones. Firstly, the ensemble average of the time-averaged square displacement has to coincide with the mean-square displacement,

$$\lim_{t\to\infty} \left\langle \overline{\Delta x^2(t,\delta)} \right\rangle = \langle \Delta x^2(\delta) \rangle. \tag{3.74}$$

This guarantees that at least on average, we will get the right result by performing the time average. However, this alone is not sufficient, since, for finite times, the time-averaged square displacement itself is random, and will have a finite variance. Only if, in addition to Eq. (3.74), this variance tends to zero, we are guaranteed to get the same result for the time-averaged square displacement in the long time limit for every realization. This can be quantified in terms of the so-called ergodicity breaking parameter [Deng 09],

$$\mathrm{EB}(t,\delta) = \frac{\left\langle \overline{\Delta x^2(t,\delta)}^2 \right\rangle - \left\langle \overline{\Delta x^2(t,\delta)} \right\rangle^2}{\left\langle \overline{\Delta x^2(t,\delta)} \right\rangle^2}. \tag{3.75}$$

This quantity measures the variance of the time-averaged square displacement, normalized to its mean value. If the ergodicity breaking parameter tends to zero for long times, while the time-averaged square displacement may still deviate from

the mean value, the deviation relative to this mean value gets arbitrarily small. Thus, the second condition for mean-square-ergodicity is,

$$\lim_{t\to\infty} EB(t,\delta) = 0. \tag{3.76}$$

If either of the two conditions Eqs. (3.74) and (3.76) is violated, the system is not ergodic with respect to the mean-square displacement. However, the violations of the two conditions are of a different quality. If Eq. (3.74) holds but Eq. (3.76) does not, then this means that the time-averaging reproduces the ensemble average on average, but the variance between trajectories is so large that every single trajectory strongly deviates from the mean. In the opposite case, the time-averaging procedure leads to the same result for every trajectory, but this result is not the same as the ensemble mean.

Since Eq. (3.75) involves fourth order moments of $x(t)$, we cannot make any statement about the validity of Eq. (3.76) by specifying just the two-time correlation function Eq. (3.13), unless we assume the process to be Gaussian. Nevertheless, the analysis in the previous section allows us to specify when the condition Eq. (3.74) holds for the general type of system we consider here. For $t_0 \gg t$, i.e. when the system can be assumed to be stationary on the time scale of the measurement, then the mean time-averaged square displacement is given by Eq. (3.72). Comparing this to the corresponding mean-square displacement Eqs. (3.32) respectively (3.33), we see that both coincide:

$$\left\langle \overline{\Delta x_{t_0}{}^2(t,\delta)} \right\rangle \simeq \langle \Delta x_{t_0}{}^2(\delta)\rangle. \tag{3.77}$$

Both square displacements scale ballistically with a diffusion coefficient that depends on the relaxation time t_0 for $\nu > 2$ and sub-ballistic with the stationary diffusion coefficient $D_{\nu,s}$ for $\nu < 2$. So, in the limit $t_0 \gg t$, the system might be ergodic, provided that the second condition Eq. (3.76) holds. However, for $\nu > 2$, even without knowing the precise form of the ergodicity breaking parameter, we can conclude from a simple physical argument that the system will be nonergodic. The condition $t_0 \gg t$ corresponds to the situation where the mean-square velocity $\langle \Delta v^2(t_0)\rangle$ of the particles is initially large. Each trajectory will on average have a large initial velocity $v(t_0)$, which does not change appreciably on the time scale t of the measurement. Thus, while the time-averaged square displacement for each trajectory will indeed show ballistic growth, the prefactor, which is given by this initial velocity will be different for every realization. The ergodicity breaking parameter for $t_0 \gg t$ will thus be substantial and the system will not be ergodic on these time scales. This agrees with the observation of broken ergodicity for ballistic transport [Lapa 07, Deng 09]. For $\nu < 2$, on the other hand, the mean-square velocity reaches a stationary limit, and the system will be ergodic if Eq. (3.76) holds. The same is true for an explicitly stationary correlation function, corresponding to $t_0 = \infty$.

If, on the other hand, the system is explicitly nonstationary on the time scale of the measurement, i.e. $t \gg t_0$, the time-averaged square displacement and the mean-square displacement are not equivalent,

$$\left\langle \overline{\Delta x_{t_0}{}^2(t,\delta)} \right\rangle \neq \langle \Delta x_{t_0}{}^2(\delta) \rangle. \tag{3.78}$$

In the case $\nu < 2$, where a stationary correlation function exists, the time-averaged square displacement is given by the stationary result $D_{\nu,s}$, Eq. (3.32), while the mean-square displacement has the same diffusion exponent but the numerically different nonstationary diffusion coefficient D_ν, Eq. (3.29). For $\nu > 2$, where the mean-square velocity increases with time, even the diffusion exponent is different. While the mean-square displacement grows faster than ballistic with an exponent ν and a time-independent diffusion coefficient Eq. (3.29), the time-averaged square displacement grows ballistic with an exponent 2 and a diffusion coefficient that increases with the overall measurement time t, see Eq. (3.66). The diffusion coefficient is given by the time average of the mean square velocity, $(1/t)\int_0^t dt' \langle \Delta v^2(t') \rangle$. Both for $\nu < 2$ and $\nu > 2$, the result for the time-averaged square displacement Eq. (3.66) resembles the corresponding stationary one, Eqs. (3.32) and (3.33), even if the process is nonstationary. This is not a coincidence, since, in order to get a statistically meaningful result from the time-averaged square displacement, we have to take the limit of long averaging time $t \gg \delta$. This however means, that only time lags which are short compared to the measurement time are considered in the averaging procedure. For these time lags, the system is well described by a stationary approximation and thus the time-averaged square displacement fails to capture the nonstationary behavior. In summary, superdiffusive systems described by the scaling velocity correlation function Eq. (3.13) are nonergodic if they are nonstationary, in the sense that the time-averaged square displacement does not reproduce the ensemble averaged one. Only if the system is initially stationary, will the time-averaged square displacement correspond to the ensemble-averaged one and the system may be ergodic. In particular, a ballistic scaling of the time-averaged square displacement does not imply ballistic scaling for the mean-square displacement.

We can also turn this statement around in order to obtain a criterion for stationarity: If the mean of the time-averaged square displacement and the mean-square displacement coincide, the system is in a stationary state, at least on the time scale of the measurement. If, on the other hand, they differ, this means that the system is nonstationary on the time scale of the measurement. Note that this kind of statement requires studying the ensemble mean of the time-averaged square displacement, since the result for a single trajectory may still differ from the ensemble average if the system is stationary but nonergodic.

3.3 SPECTRAL PROPERTIES

So far, we have considered the implications of the scaling velocity correlation function Eq. (3.13) for time-dependent quantities, like the mean-square displacement and the position autocorrelation. However, the existence of an asymptotic scaling correlation function also has important implications for frequency-dependent

quantities. In Section 3.3.1, we introduce the notion of a spectral density and in a handwaving way argue an important relation with numerous applications in statistical mechanics and signal analysis, the Wiener-Khinchine theorem. As useful and widely applicable as the Wiener-Khinchine theorem is, like the Green-Kubo formula, there are certain cases where it is not applicable. We show that our previously introduced scaling correlation functions are precisely one of this cases and in Section 3.3.2 obtain a scaling relation, which generalizes the Wiener-Khinchine theorem to nonstationary scaling processes and yields a scaling form for the spectral density. Yet another scaling form can be obtained in Laplace space. Due to the added complexity of nonstationary dynamics, the interpretation of the scaling spectral density is not as straightforward as for the Wiener-Khinchine theorem. Nevertheless, we can extract its asymptotic properties, provided we know the asymptotic properties of the original scaling correlation function, as we show in Section 3.3.3. Finally, since, as we saw in Section 3.1.3, the initial preparation plays an important role in the diffusive long-time properties of the system, it is natural to ask whether this is also true for the long-time spectral properties. In Section 3.3.4 we show that, for a rather wide class of systems, this is not the case and the spectral density is independent of the initial state of the system.

3.3.1 *Stationary processes and Wiener-Khinchine theorem*

Instead of examining a time-resolved signal, e.g. the velocity $v(t)$, it is often useful to instead consider the Fourier-transform of the signal, as the latter yields information about periodicity and typical time scales in the signal. Since a random process $v(t)$ is not square-integrable, we consider its so-called windowed Fourier transform $\hat{v}(\omega, t)$ [Mill 04],

$$\hat{v}(\omega, t) = \frac{1}{\sqrt{t}} \int_0^t dt' \, e^{-i\omega t} v(t'). \tag{3.79}$$

This quantity, like $v(t)$ itself, is of course a random variable, so in order to examine its properties, we need to consider ensemble averages. In particular, we will be interested in the spectral density, which is the second moment of $\hat{v}(\omega, t)$,

$$S_v(\omega, t) = \langle \hat{v}^*(\omega, t)\hat{v}(\omega, t)\rangle - \langle \hat{v}^*(\omega, t)\rangle\langle \hat{v}(\omega, t)\rangle, \tag{3.80}$$

where $\hat{v}^*(\omega, t)$ denotes the complex conjugate of the windowed Fourier transform. From the definition of the velocity correlation function Eq. (3.1) we can deduce a relation between the latter and the spectral density,

$$\begin{aligned} S_v(\omega, t) &= \frac{1}{t} \int_0^t dt'' \int_0^t dt' \, e^{-i\omega(t''-t')} C_v(t'', t') \\ &= \frac{2}{t} \int_0^t dt'' \int_0^{t''} dt' \, \cos(\omega(t''-t')) C_v(t'', t'). \end{aligned} \tag{3.81}$$

Generally, the spectral density will depend on both time t and frequency ω, however, in a number of important cases it becomes time-independent in the long time limit. The total power $\mathcal{P}_v(t)$, defined as the integral of the spectral density over all

frequencies, is by virtue of Eq. (3.81) related to the time average of the mean-square velocity by,

$$\begin{aligned}\mathcal{P}_v(t) &= \int_0^\infty d\omega\ S_v(\omega, t) \\ &= \frac{2\pi}{t}\int_0^t dt''\int_0^t dt'\ \delta(t''-t')C_v(t'',t') \\ &= \frac{2\pi}{t}\int_0^t dt'\langle\Delta v^2(t')\rangle. \end{aligned} \tag{3.82}$$

Thus, if the mean-square velocity tends to a constant value for long times, the total power is finite, whereas if the mean-square velocity increases with time, the total power increases as well.

In particular, if the velocity correlation function is stationary, $C_v(t+\tau, t) = C_{v,s}(\tau)$, Eq. (3.81) can be further simplified,

$$\begin{aligned}S_v(\omega, t) &= \frac{2}{t}\int_0^t dt''\int_0^{t''} dt'\ \cos(\omega(t''-t'))C_{v,s}(t''-t') \\ &= \frac{2}{t}\int_0^t dt''\int_0^{t''} d\tau\ \cos(\omega\tau)C_{v,s}(\tau). \end{aligned} \tag{3.83}$$

If the Fourier-cosine transform of the stationary correlation function exists,

$$\hat{C}_{v,s}(\omega) = 2\int_0^\infty d\tau\ \cos(\omega\tau)C_{v,s}(\tau), \tag{3.84}$$

then we can write the spectral density as,

$$S_v(\omega, t) = \hat{C}_{v,s}(\omega) - \frac{2}{t}\int_0^t dt''\int_{t''}^\infty d\tau\ \cos(\omega\tau)C_{v,s}(\tau). \tag{3.85}$$

The Wiener-Khinchine theorem [Wien 30, Mill 04] asserts that, if the stationary velocity correlation function is integrable, i.e. $\int_0^\infty d\tau\ C_{v,s}(\tau)$ is finite, then the second term will tend to zero in the long-time limit and we have,

$$\lim_{t\to\infty} S_v(\omega, t) = S_{v,s}(\omega) = \hat{C}_{v,s}(\omega). \tag{3.86}$$

The spectral density of a stationary process that has an integrable correlation function is thus time-independent and given by the Fourier-cosine transform of the correlation function. Since the velocity correlation function is integrable, so is the spectral density and the total power Eq. (3.82) of the process is finite. Similar to the Green-Kubo formula, Eq. (3.9), we want to derive a generalization of the Wiener-Khinchine theorem Eq. (3.86) that is able to treat both stationary processes whose correlation function is not integrable and nonstationary processes.

3.3.2 *Scaling in the frequency domain*

In order to study the frequency-dependent properties of a system described by the scaling velocity correlation Eq. (3.13), it is useful to see how these scaling properties

translate into the frequency domain. Starting from Eq. (3.81) and introducing the scaling correlation function, we have,

$$S_\nu(\omega, t) \simeq \frac{2\mathcal{C}}{t} \int_0^t dt'' \int_0^{t''} dt' \, \cos(\omega(t''-t'))t'^{\nu-2}\phi\left(\frac{t''-t'}{t'}\right). \tag{3.87}$$

Introducing the variables $y = (t''-t')/t'$ and $z = t''/t$, this gives us,

$$\begin{aligned} &S_\nu(\omega, t) \\ &\quad \simeq 2\mathcal{C}t^{\nu-1} \int_0^1 dz \, z^{\nu-1} \int_0^\infty dy \, (1+y)^{-\nu} \cos\left(\omega t z \frac{y}{y+1}\right) \phi(y) \\ &\quad = 2\mathcal{C}t^{\nu-1}\zeta(\omega t). \end{aligned} \tag{3.88}$$

We thus find a scaling form for the spectral density with a spectral scaling function $\zeta(x)$ defined in terms of the original scaling function $\phi(x)$,

$$\zeta(x) = \int_0^1 dz \, z^{\nu-1} \int_0^\infty dy \, (1+y)^{-\nu} \cos\left(xz\frac{y}{1+y}\right) \phi(y). \tag{3.89}$$

Here, the scaling variable is ωt instead of τ/t. In this sense, this is similar to the Wiener-Khinchine theorem Eq. (3.86) in that in both cases the time lag τ corresponds to the frequency ω. We stress, however, that in the nonstationary case, the spectral density is not the Fourier transform of the autocorrelation function with respect to τ. We will use this scaling form to discuss the asymptotic properties of the spectral density in Section 3.3.3.

Another scaling relation in frequency space can be found for the Laplace transform of the velocity correlation function. First of all, we consider the velocity correlation function $C_\nu(t+\tau, t)$ as a function of the overall time t and the time lag τ. We call this correlation function the time-ordered correlation function $\vec{C}_\nu(t, \tau)$, since it implies a time ordering:

$$\vec{C}_\nu(t, \tau) = C_\nu(t+\tau, t) = C_\nu(t, t+\tau). \tag{3.90}$$

Taking the double Laplace transform with respect to t and τ,

$$\tilde{\vec{C}}_\nu(s, u) = \mathcal{L}^2\left[\vec{C}_\nu(t, \tau)\right]_{t\to s}^{\tau\to u}, \tag{3.91}$$

we have, using the scaling form Eq. (3.13),

$$\tilde{\vec{C}}_\nu(s, u) \simeq \mathcal{C} \int_0^\infty dt \int_0^\infty d\tau \, e^{-st-u\tau} t^{\nu-2} \phi\left(\frac{\tau}{t}\right). \tag{3.92}$$

Introducing the variable $y = \tau/t$, we get,

$$\tilde{\vec{C}}_\nu(s, u) \simeq \mathcal{C} \int_0^\infty dt \int_0^\infty dy \, e^{-(s+uy)t} t^{\nu-1} \phi(y). \tag{3.93}$$

Now the integration over t is just the Laplace transform of a power-law,

$$\tilde{\vec{C}}_\nu(s, u) \simeq \mathcal{C}\Gamma(\nu) \int_0^\infty dy \, (s+uy)^{-\nu} \phi(y). \tag{3.94}$$

We thus have a scaling form also in the frequency domain,

$$\begin{aligned}
&\tilde{\tilde{C}}_\nu(s,u) \simeq \mathcal{C} u^{-\nu} \chi\left(\frac{s}{u}\right) \\
&\text{with} \quad \chi(z) = \Gamma(\nu) \int_0^\infty dy\ (z+y)^{-\nu} \phi(y),
\end{aligned} \tag{3.95}$$

with a frequency scaling function $\chi(z)$ directly related to the time scaling function $\phi(y)$. In Appendix A.1, we derive a relation between the Laplace transforms of the time-ordered and the regular symmetric two-time correlation functions, Eq. (A.21). Using this relation, we find,

$$\begin{aligned}
\tilde{C}_\nu(s_2,s_1) &\simeq \mathcal{C}\left({s_2}^{-\nu} \chi\left(1+\frac{s_1}{s_2}\right) + {s_1}^{-\nu} \chi\left(1+\frac{s_2}{s_1}\right)\right) \\
&= \mathcal{C}(s_2 s_1)^{-\frac{\nu}{2}} \left(\left(\frac{s_1}{s_2}\right)^{\frac{\nu}{2}} \chi\left(1+\frac{s_1}{s_2}\right) + \left(\frac{s_2}{s_1}\right)^{\frac{\nu}{2}} \chi\left(1+\frac{s_2}{s_1}\right)\right).
\end{aligned} \tag{3.96}$$

The asymptotic behavior of the frequency scaling function $\chi(z)$ is determined by the one of $\phi(y)$. If the latter is given by Eq. (3.14) with $-1 < \delta_l < \nu - 1$ and $-1 < \delta_u < \nu - 1$, we find using Eq. (A.88),

$$\tilde{\tilde{C}}_\nu(s,u) \simeq \mathcal{C} \begin{cases} a_l \Gamma(\delta_l+1)\Gamma(\nu-\delta_l-1) s^{\delta_l-\nu+1} u^{-\delta_l-1} \text{ for } s \ll u \\ b_u \Gamma(\delta_u+1)\Gamma(\nu-\delta_u-1) s^{\delta_u-\nu+1} u^{-\delta_u-1} \text{ for } u \ll s. \end{cases} \tag{3.97}$$

In particular, the limit $s \ll u$ corresponds to the long-time limit $t \gg \tau$, and the above corresponds directly to the Laplace transform of the stationary velocity autocorrelation function Eq. (3.19) for $\nu < 2$, $\delta_l = \nu - 2$, respectively to the Laplace transform of the increasing mean-square velocity Eq. (3.24) for $\nu > 2$, $\delta_l = 0$.

The relation between the time- and frequency scaling functions, Eq. (3.95) can also be inverted. To this end, we start from Eq. (3.93) but now perform the y-integration first,

$$\begin{aligned}
\tilde{\tilde{C}}_\nu(s,u) &\simeq \mathcal{C} \int_0^\infty dt\ e^{-st} t^{\nu-1} \tilde{\phi}(ut) \\
&= \mathcal{C} u^{-\nu} \int_0^\infty dx\ e^{-\frac{s}{u}x} x^{\nu-1} \tilde{\phi}(x),
\end{aligned} \tag{3.98}$$

where $\tilde{\phi}(x)$ is the Laplace transform of $\phi(y)$. Comparing this to Eq. (3.95), we identify,

$$\begin{aligned}
&\chi(z) = \mathcal{L}\left[x^{\nu-1} \mathcal{L}\left[\phi(y)\right]_{y\to x}\right]_{x\to z} \\
&\Rightarrow \phi(y) = \mathcal{L}^{-1}\left[x^{1-\nu} \mathcal{L}^{-1}\left[\chi(z)\right]_{z\to x}\right]_{x\to y},
\end{aligned} \tag{3.99}$$

thus relating $\phi(y)$ to $\chi(z)$ via a double inverse Laplace transform. We now use the explicit inversion formula for the Laplace transform,

$$\mathcal{L}^{-1}\left[\tilde{f}(s)\right]_{s\to t} = \frac{1}{2\pi i} \int_{-i\infty+\epsilon}^{i\infty+\epsilon} ds\ e^{st} \tilde{f}(s), \tag{3.100}$$

where ϵ is a some real number chosen such that all nonanalytic points s_0 of $\tilde{f}(s)$ have $\Re(s_0) < \epsilon$. Applying this, we find for $\phi(y)$,

$$\phi(y) = \frac{1}{2\pi i \Gamma(\nu - 1)} \int_{-i\infty+\epsilon}^{i\infty+\epsilon} dz\, (y+z)^{\nu-2} \chi(z), \tag{3.101}$$

where $\epsilon > 0$ is now a positive infinitesimal.

3.3.3 *Spectral density for nonstationary scale-invariant systems*

In the previous Section, we derived the scaling form Eq. (3.88) for the spectral density. Together with the known asymptotic behavior of the time-scaling function, we can use this scaling form to extract the asymptotic behavior of the spectral density. Since the relevant scaling variable is ωt, we will discuss the limits $\omega t \ll 1$ and $\omega t \gg 1$. For $\omega t \ll 1$, the asymptotic behavior of the expression Eq. (3.88) is straightforward, since we can just replace the cosine by 1 and find,

$$\mathcal{C}\zeta(0) = D_\nu, \tag{3.102}$$

with the anomalous diffusion coefficient D_ν given by Eq. (3.18). Thus in the low-frequency limit $\omega t \ll 1$, the spectral density is independent of ω and given by the mean-square displacement divided by time,

$$S_\nu(\omega, t) \simeq \frac{1}{t} \langle \Delta x^2(t) \rangle. \tag{3.103}$$

There is thus a low frequency cutoff on the spectral density, which is of the order of the inverse measurement time $\omega \simeq t^{-1}$, and below which the spectral density is just given by the time integral over the square of the signal. This represents the fact that in any measurement it is not possible to resolve frequencies that are well below the inverse measurement time.

More interesting is the opposite, long-time limit $\omega t \gg 1$, which corresponds to the situation described by the Wiener-Khinchine theorem Eq. (3.86). Instead of directly using the definition of the scaling function Eq. (3.88) to find its asymptotic behavior, we will instead employ Eq. (3.95). To do so, we need to link the spectral density to the Laplace transform of the correlation function. We can write the time ordered correlation function in terms of its Laplace transform as,

$$\vec{C}_\nu(t, \tau) = -\frac{1}{4\pi^2} \int_{-i\infty+\epsilon}^{i\infty+\epsilon} ds \int_{-i\infty+\epsilon'}^{i\infty+\epsilon'} du\, e^{st} e^{u\tau} \tilde{\vec{C}}_\nu(s, u). \tag{3.104}$$

Plugging this into Eq. (3.81), we find by carrying out the integrals over t' and t'',

$$\begin{aligned} S_\nu(\omega, t) = -\frac{1}{4\pi^2 t} \int_{-i\infty+\epsilon}^{i\infty+\epsilon} ds \int_{-i\infty+\epsilon'}^{i\infty+\epsilon'} du\, \tilde{\vec{C}}_\nu(s, u) \Bigg[\frac{1}{s(s-u-i\omega)} e^{st} \\ - \frac{1}{(u+i\omega)(s-u-i\omega)} e^{(i\omega+u)t} + \frac{1}{s(u+i\omega)} + [\omega \to -\omega] \Bigg], \end{aligned} \tag{3.105}$$

where $\omega \to -\omega$ denotes terms with ω replaced by $-\omega$. We now use the results obtained in Appendix A.3, in particular Eq. (A.101) to find the asymptotic behavior

of this expression. We cannot apply the latter result right away, since the above expression has poles in the positive half-plane. However, if we change variables from s to $s+u$, we have instead,

$$\begin{aligned} S_\nu(\omega,t) = &-\frac{1}{4\pi^2 t}\int_{-i\infty+\epsilon}^{i\infty+\epsilon} ds \int_{-i\infty+\epsilon'}^{i\infty+\epsilon'} du\, \tilde{\tilde{C}}_\nu(s+u,u) \\ &\times\Bigg[\frac{1}{(s+u)(s-i\omega)}e^{(s+u)t} - \frac{1}{(u+i\omega)(s-i\omega)}e^{(i\omega+u)t} \\ &+\frac{1}{(s+u)(u+i\omega)} + [\omega\to-\omega]\Bigg]. \end{aligned} \tag{3.106}$$

Here ϵ and ϵ' can now be chosen as positive infinitesimals and we can apply Eq. (A.101). We note that the third term in square brackets is independent of t and thus gives at most a constant contribution. We start out with the s-integral in the first term. Since the leading order asymptotic behavior is given by the behavior of the integrand function near its nonanalytic points, we focus on the latter. We have a branch point at $s=-u$ and a simple pole at $s=i\omega$. Since $\Re(u)>0$, the latter one gives the dominant contribution for long times and we have, using Eq. (A.101),

$$\frac{1}{2\pi i}\int_{-i\infty+\epsilon}^{i\infty+\epsilon} ds\, e^{(s+u)t}\frac{\tilde{\tilde{C}}_\nu(s+u,u)}{(s+u)(s-i\omega)} \simeq e^{(u+i\omega)t}\frac{\tilde{\tilde{C}}_\nu(u+i\omega,u)}{u+i\omega}. \tag{3.107}$$

In the ensuing u-integral, we have branch points at $u=-i\omega$ and $u=0$, which both have the same real part and thus both have to be taken into account. We expand the integrand function around these points,

$$\begin{aligned} \frac{1}{u+i\omega}\tilde{\tilde{C}}_\nu(u+i\omega,u)\Big|_{u=0} &\simeq b_u\Gamma(\delta_u+1)\Gamma(\nu-\delta_u-1)(i\omega)^{\delta_u-\nu}u^{-\delta_u-1} \\ \frac{1}{u+i\omega}\tilde{\tilde{C}}_\nu(u+i\omega,u)\Big|_{u=-i\omega} &\simeq a_l\Gamma(\delta_l+1)\Gamma(\nu-\delta_l-1)(u+i\omega)^{\delta_l-\nu} \\ &\quad\times\left[(-i\omega)^{-\delta_l-1}-(\delta_l+1)(-i\omega)^{-\delta_l-2}(u+i\omega)\right], \end{aligned} \tag{3.108}$$

where we also included the sub-leading order contribution in the expansion at $u=-i\omega$ for reasons that will become apparent later. For the first term in the spectral density, we then find using Eq. (A.101),

$$\begin{aligned} &-\frac{1}{4\pi^2 t}\int_{-i\infty+\epsilon}^{i\infty+\epsilon} ds \int_{-i\infty+\epsilon'}^{i\infty+\epsilon'} du\, \frac{\tilde{\tilde{C}}_\nu(s+u,u)}{(s+u)(s-i\omega)}e^{(s+u)t} \\ &\simeq b_u\Gamma(\nu-\delta_u-1)e^{i\omega t}t^{\delta_u-1}(i\omega)^{\delta_u-\nu} \\ &\quad+\frac{a_l\Gamma(\delta_l+1)}{\nu-\delta_l-1}t^{\nu-\delta_l-2}(-i\omega)^{-\delta_l-1} - a_l\Gamma(\delta_l+2)t^{\nu-\delta_l-3}(-i\omega)^{-\delta_l-2}. \end{aligned} \tag{3.109}$$

For the second term, we compute the u-integration first, where we have a branch point at $u=-s$ and at $u=0$ and a simple pole at $u=-i\omega$, the latter two of which dominate since $\Re(s)>0$. Consequently,

$$\begin{aligned} &-\frac{1}{2\pi i}\int_{-i\infty+\epsilon'}^{i\infty+\epsilon'} du\, e^{(i\omega+u)t}\frac{\tilde{\tilde{C}}_\nu(s+u,u)}{(u+i\omega)(s-i\omega)} \\ &\simeq -\frac{\tilde{\tilde{C}}_\nu(s-i\omega,-i\omega)}{s-i\omega} - b_u\Gamma(\nu-\delta_u-1)e^{i\omega t}t^{\delta_u-1}s^{\delta_u-\nu}(i\omega)^{-1}. \end{aligned} \tag{3.110}$$

The first term is independent of time, while for the second one, we have,

$$\frac{1}{2\pi i}\int_{-i\infty+\epsilon}^{i\infty+\epsilon} ds\, s^{\delta_u-\nu}. \tag{3.111}$$

This expression is straightforward to evaluate and is zero since $\delta_u < \nu - 1$ (see Eq. (3.14)). Summing up, we find for the asymptotic spectral density in the long time limit,

$$\begin{aligned}
S_\nu(\omega,t) \simeq \mathcal{C}\Big[&b_u\Gamma(\nu-\delta_u-1)e^{i\omega t}t^{\delta_u-1}(i\omega)^{\delta_u-\nu} \\
&+\frac{a_1\Gamma(\delta_1+1)}{\nu-\delta_1-1}t^{\nu-\delta_1-2}(-i\omega)^{-\delta_1-1} \\
&-a_1\Gamma(\delta_1+2)t^{\nu-\delta_1-3}(-i\omega)^{-\delta_1-2}+[\omega\to-\omega]\Big] \\
=2\mathcal{C}\Big[&b_u\Gamma(\nu-\delta_u-1)t^{\delta_u-1}\omega^{\delta_u-\nu}\cos\left(\omega t+\frac{\pi(\delta_u-\nu)}{2}\right) \\
&-\frac{a_1\Gamma(\delta_1+1)\sin\left(\frac{\pi\delta_1}{2}\right)}{\nu-\delta_1-1}t^{\nu-\delta_1-2}\omega^{-\delta_1-1} \\
&+a_1\Gamma(\delta_1+2)\cos\left(\frac{\pi\delta_1}{2}\right)t^{\nu-\delta_1-3}\omega^{-\delta_1-2}\Big]+\mathcal{O}(t^{-1}).
\end{aligned} \tag{3.112}$$

Let us make some general remarks about this expression. The very first term oscillates as a function of time. Since the spectral density is by definition positive, this implies that $\delta_u < \nu - \delta_1 - 1$, since otherwise, the oscillating term would dominate in the long-time limit. This provides a physical constraint on the behavior of the scaling function $\phi(y)$ for large, respectively small arguments. If this constraint holds, then the asymptotic behavior of the spectral density is given solely by the small-argument expansion of the scaling function and thus the long-time behavior $t \gg \tau$ of the velocity correlation function,

$$\begin{aligned}
S_\nu(\omega,t) \simeq 2\mathcal{C}\Big[&-\frac{a_1\Gamma(\delta_1+1)\sin\left(\frac{\pi\delta_1}{2}\right)}{\nu-\delta_1-1}t^{\nu-\delta_1-2}\omega^{-\delta_1-1} \\
&+a_1\Gamma(\delta_1+2)\cos\left(\frac{\pi\delta_1}{2}\right)t^{\nu-\delta_1-3}\omega^{-\delta_1-2}\Big]+\mathcal{O}(t^{-1}).
\end{aligned} \tag{3.113}$$

This is remarkable, since, as we saw earlier, other quantities like the diffusion coefficient do depend on the entire scaling function even in the long-time limit, see the discussion in Section 3.1.3. As a consequence, there is generally no straightforward relation between the diffusive dynamics and the long-time spectral density. We will elaborate some more on the consequences of this in Section 4.2.1.

Since knowing the small-argument expansion of the scaling function is sufficient to deduce the spectral density, we now consider a particular case of the former, which holds for most of the cases we consider. We assume,

$$\phi(y) \simeq a_{\nu-2}y^{\nu-2} + a_0 + a_1 y + \mathcal{O}(y^2). \tag{3.114}$$

Note that for the constant term a_0, the leading order contribution in Eq. (3.113) vanishes. We thus have,

$$S_\nu(\omega, t) \simeq 2\mathcal{C}\Big[a_{\nu-2}\Gamma(\nu-1)\sin\left(\frac{\pi\nu}{2}\right)\omega^{1-\nu} + \left(a_0 - \frac{a_1}{\nu-2}\right)t^{\nu-3}\omega^{-2}\Big]. \tag{3.115}$$

For the case of an asymptotically stationary correlation function, we have $\nu < 2$, and the leading order is given by the first term,

$$S_\nu(\omega, t) \simeq 2a_{\nu-2}\mathcal{C}\Gamma(\nu-1)\sin\left(\frac{\pi\nu}{2}\right)\omega^{1-\nu}. \tag{3.116}$$

The spectral density is thus independent of time and is equal to the Fourier-cosine transform of the stationary velocity autocorrelation function, reproducing the Wiener-Khinchine theorem Eq. (3.86). This result is interesting in its own right, since we did not assume the correlation function to be stationary in the first place. However, the leading order contribution to the spectral density in the long-time limit $\omega t \gg 1$ is indeed given by the stationary long-time limit of the velocity correlation function. Any deviations from the stationary correlation function thus only enter as sub-leading corrections to the spectral density. This is in contrast to the mean-square displacement, where we found different results depending on whether the system is initially stationary or not even in the long-time limit, see Eqs. (3.29) and (3.32). The reason for this discrepancy between mean-square displacement and spectral density is best understood by looking at Eq. (3.88). For $\omega t \gg 1$, the integrand will oscillate rapidly except for very small values of y. These rapid oscillations cause any deviations from the stationary small-y behavior to average to zero and the result thus depends only on the long-time stationary limit. In other words, the frequency variable ω corresponds to the time-lag τ rather than the overall time t, so $\omega t \gg 1$ corresponds to $t \gg \tau$ and thus the stationary limit. In the superaging case, we have $\nu > 2$ and the leading order now depends on the value of ν. For $\nu < 3$, the first term in Eq. (3.113) is the leading one, which is again independent of time and equal to the stationary result Eq. (3.116). Even though for $2 < \nu < 3$, the velocity increases subdiffusively with time and the velocity correlation function thus has no stationary limit, the corresponding spectral density is time-independent and the same as for the stationary case. This changes for $\nu > 3$, where the velocity increases superdiffusively and the second term in Eq. (3.113) is the leading one. The spectral density is then time-dependent and increases as $t^{\nu-3}$,

$$S_\nu(\omega, t) \simeq 2\mathcal{C}\left(a_0 - \frac{a_1}{\nu-2}\right)t^{\nu-3}\omega^{-2}. \tag{3.117}$$

Its frequency dependence is the same as for a normal diffusive process, i.e. proportional to ω^{-2}. As the spectral density has to be positive, this provides yet another physical constraint on the small-argument behavior of the scaling function, $a_1 < (\nu-2)a_0$. This result also applies to the position spectral density. In Section 3.1.4, we saw that the position correlation function also follows a scaling

form Eq. (3.42). Using the corresponding small argument expansion of the scaling function, we find,

$$S_x(\omega, t) \simeq D_\nu t^{\nu-1}\omega^{-2} = \frac{\langle \Delta x^2(t)\rangle}{2t}\omega^{-2}. \tag{3.118}$$

For a superdiffusive system, the position spectral density thus is always time-dependent and depends on frequency as ω^{-2}.

As long as the variance of the velocity increases at most subdiffusively ($1 < \nu < 3$), the velocity spectral density is asymptotically time-independent,

$$S_v(\omega, t) \simeq S_{v,s}(\omega) = 2a_{\nu-2}\mathcal{C}\Gamma(\nu-1)\sin\left(\frac{\pi\nu}{2}\right)\omega^{1-\nu}. \tag{3.119}$$

Thus, a velocity process with a correlation function of the scaling type Eq. (3.13) and $\phi(y) \simeq a_0 + a_{\nu-2}y^{\nu-2} + \mathcal{O}(y)$ for small y describes a variant of 1/f-noise [Milo 02] in the long-time limit. The term 1/f-noise refers to any kind of random process whose power spectral density behaves as $S(\omega) \sim \omega^{-\alpha}$ with $0 < \alpha < 2$. In our case, we have $\alpha = \nu - 1$. The measurement time dependent low-frequency cutoff Eq. (3.103) is also observed for general 1/f-noise [Milo 02, Niem 13].

3.3.4 *Initial conditions in the frequency domain*

Finally, we want to consider a situation similar to Section 3.1.3. We let the system evolve for a relaxation time t_0 and then measure the spectral density for a time t. Modifying Eq. (3.87) accordingly is straightforward,

$$S_v(\omega, t, t_0) \simeq \frac{2\mathcal{C}}{t}\int_0^t dt'' \int_0^{t''} dt' \cos(\omega(t''-t'))(t'+t_0)^{\nu-2}\phi\left(\frac{t''-t'}{t'+t_0}\right). \tag{3.120}$$

We introduce the variables $y = (t''-t')/(t'+t_0)$ and $z = t''/t$,

$$S_v(\omega, t, t_0) \simeq 2\mathcal{C}t^{\nu-1}\int_0^1 dz \left(z+\frac{t_0}{t}\right)^{\nu-1} \times \int_0^{z\frac{t}{t_0}} dy\,(1+y)^{-\nu}\cos\left(\omega t\left(z+\frac{t_0}{t}\right)\frac{y}{y+1}\right)\phi(y). \tag{3.121}$$

For $t \gg t_0$, we can take the limit $t_0 \to 0$ and obtain Eq. (3.88). For $t_0 \gg t$, we can approximate $z + t_0/t \simeq t_0/t$ and find,

$$S_v(\omega, t, t_0) \simeq 2\mathcal{C}{t_0}^{\nu-1}\int_0^1 dz \int_0^{z\frac{t}{t_0}} dy\,(1+y)^{-\nu}\cos\left(\omega t_0\frac{y}{y+1}\right)\phi(y). \tag{3.122}$$

Since $zt/t_0 \ll 1$, we can expand the integrand for small y,

$$S_v(\omega, t, t_0) \simeq 2a_1\mathcal{C}{t_0}^{\nu-1}\int_0^1 dz \int_0^{z\frac{t}{t_0}} dy\,\cos(\omega t_0 y)y^{\delta_1}. \tag{3.123}$$

The relevant scaling variable is now ωt_0. For $\omega t_0 \ll 1$, we can approximate the cosine by 1 and get,

$$S_v(\omega, t, t_0) \simeq \frac{2a_1\mathcal{C}}{(\delta_1+1)(\delta_1+2)} t^{\delta_1+1} {t_0}^{\nu-\delta_1-2}. \tag{3.124}$$

Comparing this to Eq. (3.31), we see that this is precisely the mean-square displacement for $t_0 \gg t$ divided by time,

$$S_v(\omega, t, t_0) \simeq \frac{1}{t}\langle \Delta {x_{t_0}}^2(t)\rangle, \tag{3.125}$$

similar to what we found in Eq. (3.103). Since $\omega t_0 \ll 1$ and $t_0 \gg t$ also imply $\omega t \ll 1$, this again states that frequencies below the inverse measurement time cannot be resolved and the spectral density is just the time integral of the signal. The same result holds if we have $\omega t_0 \gg 1$ but $\omega t \ll 1$, since then the argument of the cosine in Eq. (3.123) is also small. If we have both $\omega t_0 \gg 1$ and $\omega t \gg 1$, on the other hand, we have to explicitly evaluate the integral in Eq. (3.123). This yields a Hypergeometric function, or upon expansion for large ωt,

$$\begin{aligned} S_v(\omega, t, t_0) \simeq 2a_1\mathcal{C}t_0^{\nu-\delta_1-2}t^{\delta_1+1}\Bigg[&-\Gamma(\delta_1+1)\sin\left(\frac{\pi\delta_1}{2}\right)(\omega t)^{-\delta_1-1} \\ &+\Gamma(\delta_1+2)\cos\left(\frac{\pi\delta_1}{2}\right)(\omega t)^{-\delta_1-2} - (\omega t)^{-2}\cos(\omega t)\Bigg]. \end{aligned} \tag{3.126}$$

As before, we consider this expression both for an asymptotically stationary correlation function and for the superaging case, with the small argument expansion of $\phi(y)$ given by Eq. (3.114). For $\nu < 2$, the first term is the leading order one,

$$S_v(\omega, t, t_0) \simeq 2a_{\nu-2}\mathcal{C}\Gamma(\nu-1)\sin\left(\frac{\pi\nu}{2}\right)\omega^{1-\nu}. \tag{3.127}$$

This is precisely the same result as Eq. (3.116). Since the spectral density only depends on the stationary long-time limit of the correlation function, the relaxation time t_0 does influence the result. The same is true for the superaging case and $2 < \nu < 3$. For $\nu > 3$, on the other hand, the leading order contribution to the spectral density according to Eq. (3.126) is given by,

$$S_v(\omega, t, t_0) \simeq 2\mathcal{C}{t_0}^{\nu-3}\omega^{-2}\left[a_0\left(\frac{t_0}{t}\right)(1-\cos(\omega t)) - a_1\right]. \tag{3.128}$$

Since $t_0 \gg t$ and $\langle \Delta v^2(t_0)\rangle \simeq 2\mathcal{C}a_0{t_0}^{\nu-2}$ (see Eq. (3.24)), we can write this as,

$$S_v(\omega, t, t_0) \simeq \frac{1}{t}\langle \Delta v^2(t_0)\rangle\omega^{-2}(1-\cos(\omega t)). \tag{3.129}$$

In the – somewhat artificial – case that the mean-square velocity increases faster than linear with time, a long relaxation time thus leads to an oscillating spectral density.

3.4 EXAMPLES FOR SCALING DYNAMICS

In the previous Sections, we have derived several relations for processes that exhibit a particular asymptotic scaling behavior Eq. (3.13) in their velocity correlations. We now want to apply these results to two systems that fall into this category: Fractional Gaussian noise in Section 3.4.1 and the Lévy walk in Section 3.4.2, both of which were introduced in Section 2.2. For both systems, we will review their velocity correlation functions and apply the results of the preceding discussions to extract a number of quantities. Finally, in Section 3.4.3, we apply the same machinery to obtain the spectral density of the nonequilibrium noise which was introduced the previous chapter in Section 2.2.3.

3.4.1 *Fractional Gaussian noise*

Fractional Gaussian noise was introduced in Section 2.2.2 as the derivative of fractional Brownian motion. We consider the nonstationary Riemann-Liouville variant with the velocity correlation function Eq. (2.44),

$$\begin{aligned} &C_v(t+\tau,t) \simeq \mathcal{C}\, t^{\beta-1}\phi\left(\frac{\tau}{t}\right), \\ &\quad \text{with} \quad \mathcal{C} = \frac{{v_{\text{typ}}}^2}{{t_\beta}^{\beta-1}}, \quad \phi(y) = \frac{1}{\Gamma^2\left(\frac{\beta}{2}\right)}\int_0^1 dz\,(y+z)^{\frac{\beta}{2}-1} z^{\frac{\beta}{2}-1}, \end{aligned} \tag{3.130}$$

and $0 < \beta < 2$, as well as the stationary Mandelbrot-van-Ness one, Eq. (2.52),

$$\begin{aligned} &C_v(t+\tau,t) \simeq \mathcal{C}_s\, \tau^{\beta-1}, \\ &\quad \text{with} \quad \mathcal{C}_s = \frac{{v_{\text{typ}}}^2}{{t_\beta}^{\beta-1}}\frac{\Gamma(1-\beta)\sin\left(\frac{\pi\beta}{2}\right)}{\pi}, \end{aligned} \tag{3.131}$$

and $0 < \beta < 1$. As discussed before, the nonstationary variant reduces to the stationary one for $t \gg \tau$ and $\beta < 1$. From the above, we can immediately identify the diffusion exponent, $\nu = \beta + 1$. For the nonstationary variant, we further require the small- and large-argument expansion of the scaling function, which can be obtained using Eq. (A.44),

$$\phi(y) \simeq \begin{cases} \frac{\Gamma(1-\beta)\sin\left(\frac{\pi\beta}{2}\right)}{\pi} y^{\beta-1} + \frac{1}{(\beta-1)\Gamma^2\left(\frac{\beta}{2}\right)} + \frac{1}{2\Gamma^2\left(\frac{\beta}{2}\right)} y + \mathcal{O}(y^2) \\ \qquad\qquad \text{for } y \ll 1,\ \beta \neq 1 \\ \frac{2}{\beta\Gamma^2\left(\frac{\beta}{2}\right)} y^{\frac{\beta}{2}-1} + \frac{\beta-2}{(\beta+2)\Gamma^2\left(\frac{\beta}{2}\right)} y^{\frac{\beta}{2}-2} + \mathcal{O}(y^{\frac{\beta}{2}-3}) \\ \qquad\qquad \text{for } y \gg 1. \end{cases} \tag{3.132}$$

Mean-square displacement

The anomalous diffusion coefficient D_v is given by Eq. (3.18),

$$\begin{aligned} D_v &= \frac{\mathcal{C}}{(\beta+1)\Gamma^2\left(\frac{\beta}{2}\right)} \int_0^\infty dy\ (1+y)^{-\beta-1} \int_0^1 dz\ (y+z)^{\frac{\beta}{2}-1} z^{\frac{\beta}{2}-1} \\ &= \frac{\mathcal{C}}{2(\beta+1)\Gamma^2\left(\frac{\beta}{2}+1\right)}, \end{aligned} \tag{3.133}$$

which coincides with Eq. (2.92),

$$\langle \Delta x^2(t) \rangle \simeq 2D_v t^{\beta+1}. \tag{3.134}$$

The stationary counterpart is given by,

$$D_{v,s} = \frac{\mathcal{C}_s}{\beta(\beta+1)}, \tag{3.135}$$

which can easily be seen to agree with Eq. (2.90). For $\beta > 1$ and a long relaxation time before the measurement of the mean-square displacement, we find by virtue of Eq. (3.33),

$$D_v^{\frac{t}{t_0}} = \frac{\mathcal{C}}{2(\beta-1)\Gamma^2\left(\frac{\beta}{2}\right)} \left(\frac{t}{t_0}\right)^{1-\beta}, \tag{3.136}$$

respectively ballistic expansion,

$$\langle \Delta {x_{t_0}}^2(t) \rangle \simeq \frac{\mathcal{C}}{(\beta-1)\Gamma^2\left(\frac{\beta}{2}\right)} {t_0}^{\beta-1} t^2. \tag{3.137}$$

The two values for the diffusion coefficient Eqs. (3.133) and (3.135) are shown in Fig. 3.2 as a function of the diffusion exponent. Note that both agree for normal diffusion, and are different for superdiffusion. This indicates that the persistence of the initial condition, leading to different values for the anomalous diffusion coefficient, is indeed particular to anomalous diffusion. The corresponding mean-square displacement is shown in Figs. 3.3 and 3.4: If the velocity dynamics have a stationary limit (Fig. 3.3), the stationary diffusion coefficient Eq. (3.135) correctly describes the mean-square displacement for times much shorter than the relaxation time t_0. On longer time scales, where the deviations of the system from the stationary state become noticeable, we observe a transition to the nonstationary diffusion coefficient. The diffusion exponent is the same in both limits. The nonstationary variant of fractional Gaussian noise Eq. (3.130) corresponds to a process that at $t = 0$ starts with zero velocity, $\langle v^2(0) \rangle = 0$. Relaxation into the stationary state means that the mean-square velocity increases to its stationary value. For the stationary variant, on the other hand, the mean-square velocity already starts out with its stationary value, which remains constant in time. Since the relaxation towards the stationary state follows a slow power-law, the mean-square velocity for nonstationary initial conditions will be reduced compared to the stationary one even for long times. Consequently, the mean-square displacement, which is the integral over the velocity correlation function, will also be reduced in the long-time

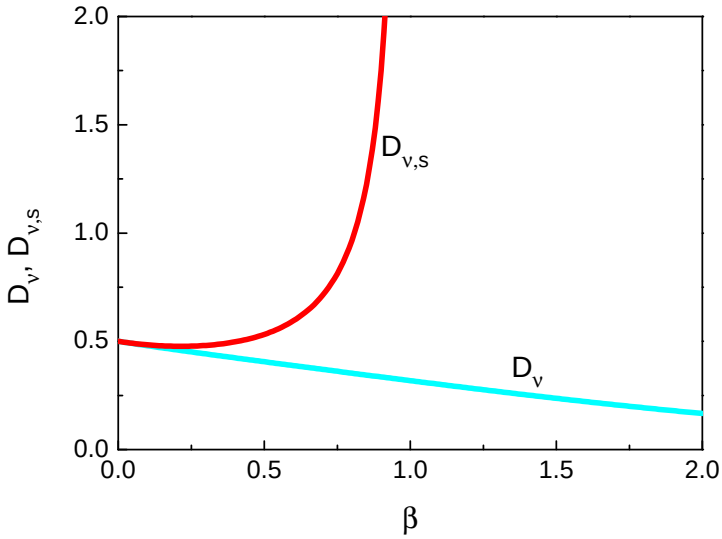

Figure 3.2: Anomalous diffusion coefficient D_v in units of $\mathcal{C}$ for fractional Brownian motion as a function of the exponent β. The cyan line is the nonstationary result Eq. (3.133), the red line the stationary one Eq. (3.135). Both results coincide in the limit of normal diffusion $\beta \to 0$, but differ for superdiffusion. For $\beta > 1$, there is no stationary diffusion coefficient, the stationary result diverges as $\beta \to 1$.

limit and thus the stationary diffusion coefficient will always be larger than the nonstationary one. For the particular value of $\beta = 0.7$ shown in Fig. 3.3, we have $D_v = 0.37\mathcal{C}$ and $D_{v,s} = 0.71\mathcal{C}$, which makes for a quite pronounced difference between the nonstationary and stationary result. If the velocity itself is nonstationary, i.e. the mean-square velocity increases with time (Fig. 3.4), then also the diffusion exponent is different, as we find ballistic motion with a diffusion coefficient that depends on the relaxation time t_0 for times shorter than t_0 and a crossover to superballistic motion for longer times. For $t_0 = 0$, the initial velocity is zero and the particles immediately feel the overall acceleration as the mean-square velocity increases, leading to superballistic accelerated expansion. By contrast, if $t_0 \gg t$, then the initial mean-square velocity is large and the already fast particles move ballistically until their velocities change significantly, which will only happen for times long compared to t_0, where the mean-square velocity will again increase, explaining the crossover to superballistic behavior.

Time-averaged square displacement and ergodicty

In Section 3.2, we found that if the system is initially in the stationary state, the mean-square displacement and the mean time-averaged square displacement coincide, both being given by the stationary result Eq. (3.72). For a nonstationary system, by contrast, the mean-square displacement and the mean time-averaged square displacement were found to differ, preventing the system from being ergodic in the mean-square sense. Even if the mean of the time-averaged square displacement is identical to the mean-square displacement, we still require the ergodicity breaking parameter Eq. (3.75) to vanish in the long-time limit, so that the time average actually reproduces the ensemble average for each trajectory. The er-

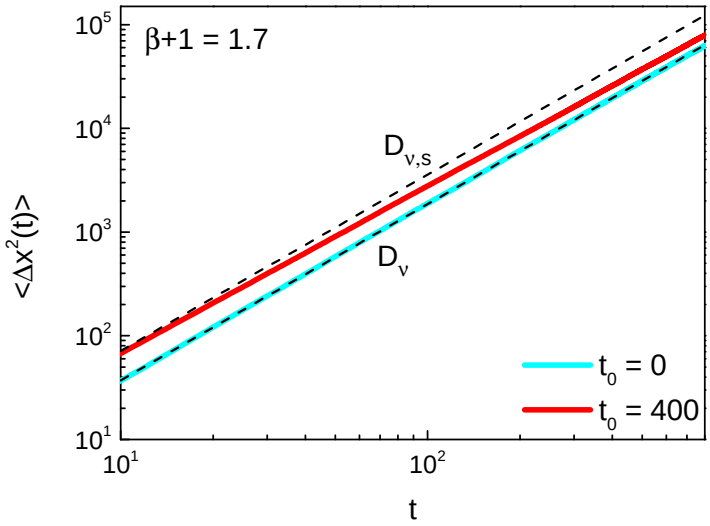

Figure 3.3: Mean-square displacement for fractional Brownian motion for subballistic superdiffusion, $\beta = 0.7$. Colored lines: numerical Langevin simulations; dashed lines: analytic asymptotic results. We have two results for the diffusion coefficient (dashed lines). If the system is initially nonstationary, the diffusion coefficient is given by D_ν, Eq. (3.133) (cyan line). For a finite relaxation time t_0, on the other hand, we have the stationary result $D_{\nu,s}$, Eq. (3.135) for short times $t \ll t_0$. For longer times, we see a transition to the nonstationary result (red line).

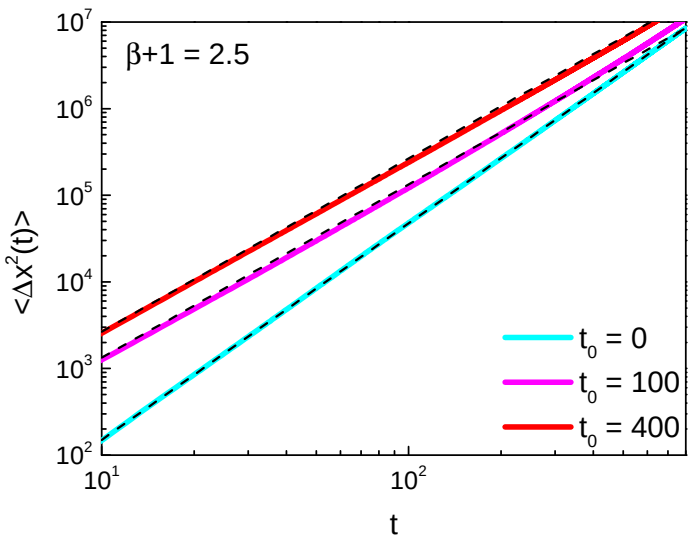

Figure 3.4: Mean-square displacement for fractional Brownian motion for superballistic superdiffusion, $\beta = 1.5$. Colored lines: numerical Langevin simulations; dashed lines: analytic asymptotic results. If the initial velocity is zero, the growth of the mean-square velocity Eq. (3.24) leads to an overall acceleration of the particles and to faster-than-ballistic expansion (cyan line), Eq. (3.134). For longer relaxation times t_0, we observe ballistic expansion for short times $t \ll t_0$ (red and magenta lines), and the diffusion coefficient depends on the relaxation time t_0, Eq. (3.137). For longer times, the ongoing increase of the mean square velocity leads to superballistic diffusion (magenta line).

godicity breaking parameter is related to the variance of the time-averaged square displacement,

$$\left\langle \overline{\Delta x^2(t,\delta)}^2 \right\rangle - \left\langle \overline{\Delta x^2(t,\delta)} \right\rangle^2, \tag{3.138}$$

which requires four-time moments of $x(t)$. Since the system is Gaussian, these can in principle be reduced to products of two-time moments via the Gaussian moment theorem (also known as Isserlis' theorem [Isse 16]),

$$\begin{aligned}\langle x(t_4)x(t_3)x(t_2)x(t_1)\rangle = &\langle x(t_4)x(t_3)\rangle\langle x(t_2)x(t_1)\rangle \\ &+ \langle x(t_4)x(t_2)\rangle\langle x(t_3)x(t_1)\rangle \\ &+ \langle x(t_4)x(t_1)\rangle\langle x(t_3)x(t_2)\rangle.\end{aligned} \tag{3.139}$$

For the case of a stationary velocity autocorrelation function $\beta < 1$ and thus sub-ballistic superdiffusion, the ergodicity breaking parameter has been calculated in Ref. [Deng 09] and has been shown to vanish for long times as $EB(t,\delta) \sim (t/\delta)^{2\beta-2}$. The ergodicity breaking parameter for both stationary and nonstationary initial conditions is show in Fig. 3.5 for $\beta = 0.7$. As predicted, the ergodicity breaking parameter tends to zero and the time-averaged square displacement reproduces the same result for each trajectory. This is shown in Figs. 3.6 and 3.7, where the time averages of the individual trajectories are plotted alongside the mean of the time-averaged square displacement and the mean-square displacement. Both for stationary and nonstationary initial conditions, the individual time averages follow the mean time average, deviating for long δ where the condition of long averaging time $t \gg \delta$ is no longer fulfilled. For an almost stationary initial condition ($t_0 \gg t$, Fig. 3.6), the ensemble average also coincides with the mean time average and the system is thus mean-square ergodic if it is initially stationary. On the other hand, if the system is initially nonstationary ($t_0 = 0$, Fig. 3.7), the mean-square displacement is different form the time-averaged square displacement and is not reproduced by the individual time averages. For the superballistic case $\beta > 1$, the explicit calculation of the ergodicity breaking parameter is more involved and we restrict ourselves to extracting the ergodicity breaking parameter from our Langevin simulations. We can, however, make a statement for the case where the relaxation time is long compared to the averaging time $t_0 \gg t \gg \delta$. Since then the particle ensemble starts out with a large mean square velocity $\langle \Delta v^2(t_0)\rangle$ and spreads ballistically, each trajectory will on average have a large initial velocity $v(t_0)$, which does not change appreciably on the time scale t of the measurement. Thus, while the time-averaged square displacement for each trajectory will indeed show ballistic growth, the prefactor, which is given by this initial velocity will be different for every realization. The ergodicity breaking parameter for $t_0 \gg t$ will thus be substantial and the system will not be ergodic on these time scales. As we see in Fig. 3.7 the ergodicty breaking parameter, does not approach zero on the observed time scales and there is thus significant variation in the individual realizations, all of which scale ballistically, see Fig. 3.9. Finally, note that the ergodicity breaking parameter approaches 2 in the limit of vanishing averaging time $t \to \delta$. This is not a coincidence, but a signature of the Gaussian nature of the process. For zero averaging time, the time-averaged square displacement is equal to $x^2(\delta)$. Since for a Gaussian process, we have $\langle x^4(t)\rangle = 3\langle x^2(t)\rangle$ as a consequence of the Gaussian

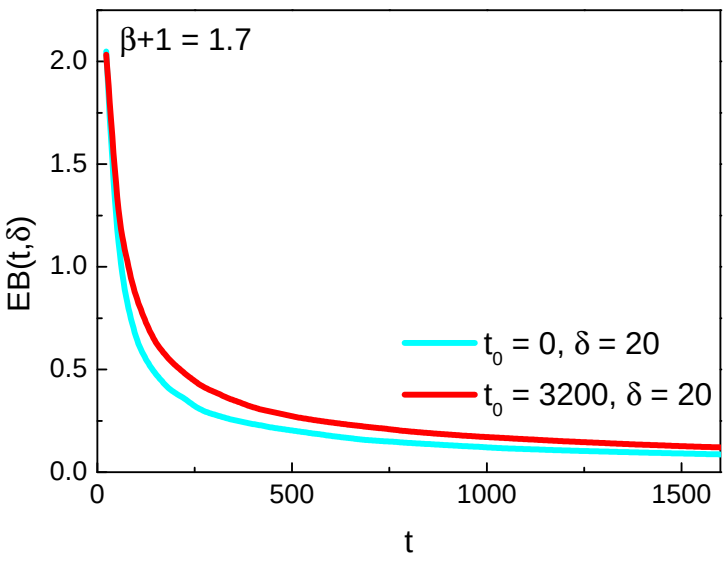

Figure 3.5: Ergodicity breaking parameter for fractional Brownian motion as a function of averaging time, Lagevin simulations for the subballistic case. Both for an almost stationary (red line) and nonstationary (cyan line) initial condition, the ergodicity breaking parameter tends to zero and individual time averages will follow the mean time average. Since the initial velocity is larger in the stationary case, the ergodicity breaking parameter is enhanced in comparison to the nonstationary case with $v_0 = 0$.

moment theorem Eq. (3.139), we have $EB(t,\delta) \simeq (\langle x^4(t)\rangle - \langle x^2(t)\rangle)/\langle x^2(t)\rangle = 2$ in this limit. To summarize, the process fractional Gaussian noise velocity process only leads to ergodic dynamics for a stationary initial condition in the subballistic case $\beta < 1$.

Spectral density

Building on the results of Section 3.3, it is straightforward to derive the spectral density for both velocity and position. For the velocity spectral density, we have from Eqs. (3.103), (3.113) and (3.132),

$$S_v(\omega,t) \simeq \begin{cases} \mathcal{C}\omega^{-\beta} & \text{for } \omega t \gg 1 \\ \frac{1}{t}\langle \Delta x_{t_0}{}^2(t)\rangle & \text{for } \omega t \ll 1, \end{cases} \tag{3.140}$$

where the mean-square displacement is given by either Eq. (3.134) with diffusion coefficient Eq. (3.135) or Eq. (3.133), or Eq. (3.137), depending on the relative size of t and t_0 and whether $\beta < 1$ or $\beta > 1$. The velocity spectral density thus scales as $\omega^{-\beta}$ in the long-time limit, which is characteristic for fractional Gaussian noise [Flan 89]. For $\beta \to 0$, the spectral density is independent of frequency, in this limit the velocity corresponds to white noise. For $\beta \to 2$, on the other hand, the spectral density is proportional to ω^{-2}, as is typical for Brownian motion. In addition, there is a time-dependent low-frequency cutoff for frequencies much lower than the inverse measurement time. For frequencies below the cutoff, the value of the

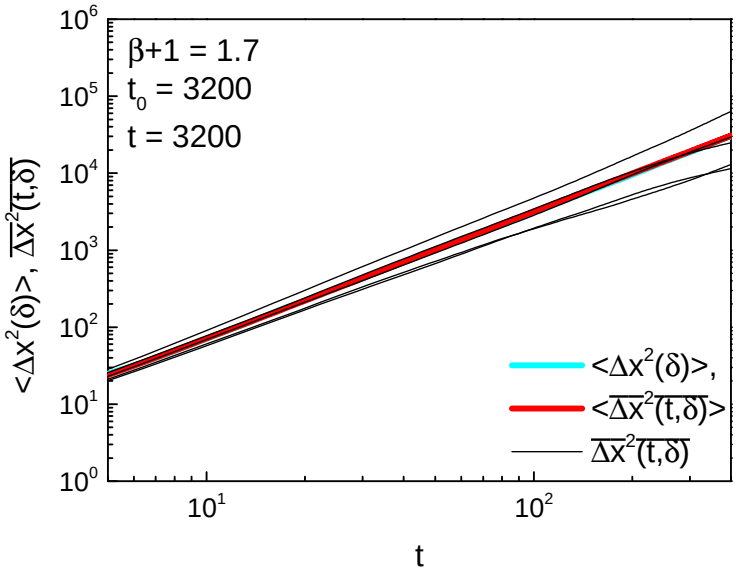

Figure 3.6: Mean-square displacement and time-averaged square displacement for fractional Brownian motion as a function of time lag, Langevin simulations with an almost stationary initial condition. If the system is initially stationary (i.e. $t_0 \gg \delta$), the mean-square displacement (cyan line) and the ensemble averaged square displacement (red line) coincide. Both are described by the stationary diffusion coefficient Eq. (3.135). Since the ergodicity breaking parameter tends to zero in subballistic regime, single realizations (thin black lines) of the time-averaged square displacement also follow the ensemble average for sufficiently long averaging time, $\delta \ll t$.

spectral density is essentially given by the mean-square displacement. This behavior is confirmed by Langevin simulations, Fig. 3.10 for $\beta < 1$, respectively Fig. 3.11 for $\beta > 1$. For $\beta > 1$ and finite times, respectively intermediate frequencies, it may be necessary to include the sub-leading order contribution from Eq. (3.113),

$$S_v(\omega, t) \simeq \mathcal{C}\omega^{-\beta} + \frac{\mathcal{C}}{(\beta-1)\Gamma^2\left(\frac{\beta}{2}\right)} t^{\beta-2}\omega^{-2}, \tag{3.141}$$

which corresponds to the dotted lines in Fig. 3.11. Both figures are for the case $t_0 = 0$, since here, the value of t_0 essentially only changes the value of the spectral density below the low-frequency cutoff and the sub-leading order correction. The frequency dependence of the velocity spectral density, $S_v(\omega) \sim \omega^{-\beta}$, directly relates to the diffusion exponent $\nu = \beta + 1$. Compared to the velocity autocorrelation function, which can asymptotically be either stationary for $\beta < 1$ or nonstationary for $\beta > 1$, the velocity spectral density has the advantage of encoding the dynamics in a single exponent and thus providing a straightforward characterization of the system. The relation between the velocity dynamics in the time domain and the corresponding spectral density, becomes clear when considering the total power,

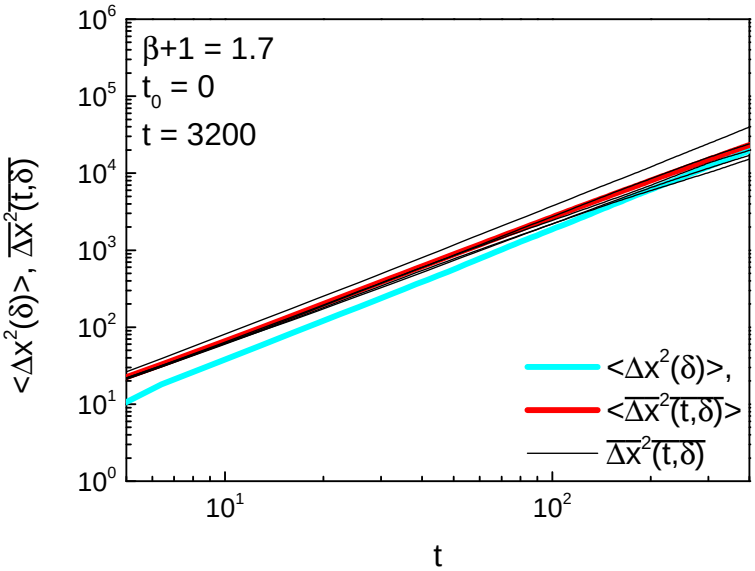

Figure 3.7: Mean-square displacement and time-averaged square displacement for fractional Brownian motion as a function of time lag, Lagevin simulations for the nonstationary case. If the system is initially nonstationary, then the mean-square displacement (cyan line) is described by the nonstationary diffusion coefficient Eq. (3.133), while the mean time-averaged square displacement (red line) follows the stationary behavior Eq. (3.135). While the ergodicity breaking parameter tends to zero, meaning that the time-averaged square displacement for a single trajectory (thin black lines) follows its ensemble mean, the system is not ergodic in the sense that it does not reproduce the mean-square displacement.

Eq. (3.82). As the behavior of the spectral density is different for $\omega t \ll 1$ and $\omega t \gg 1$, we consider as a crude approximation,

$$\begin{aligned} P_\nu(t) &\sim \int_0^{\frac{1}{t}} d\omega\, S_\nu(\omega,t) + \int_{\frac{1}{t}}^{\infty} d\omega\, S_\nu(\omega,t) \\ &\sim \frac{1}{t^2}\langle \Delta x^2(t)\rangle + \mathcal{C}\int_{\frac{1}{t}}^{\infty} d\omega\, \omega^{-\beta}. \end{aligned} \tag{3.142}$$

For $\beta < 1$, the second term diverges as $\omega \to \infty$, so the total power appears to be infinite. This unphysical behavior has its origin in the divergence of the correlation function Eq. (3.130) as $\tau \to 0$. If, as discussed briefly in Section 2.2.2, we specify a short-time cutoff, say t_c, for the correlation function, then this results in a high-frequency cutoff ω_c for the spectral density and thus,

$$P_\nu(t) \sim 2D_\nu t^{\beta-1} + \frac{\mathcal{C}}{1-\beta}\left({\omega_c}^{1-\beta} - t^{\beta-1}\right). \tag{3.143}$$

For $\beta < 1$, the first and third term vanishes for long times, and the total power is a constant given by the high-frequency respectively short-time cutoff, which is also responsible for a finite mean-square velocity, in agreement with Eq. (3.82). For $\beta > 1$, on the other hand, both the first and third term increase with time and so the total power, like the mean-square velocity, grows as $t^{\beta-1}$, also in agreement with Eq. (3.82). Physically, this increasing total power is due to the ongoing acceleration

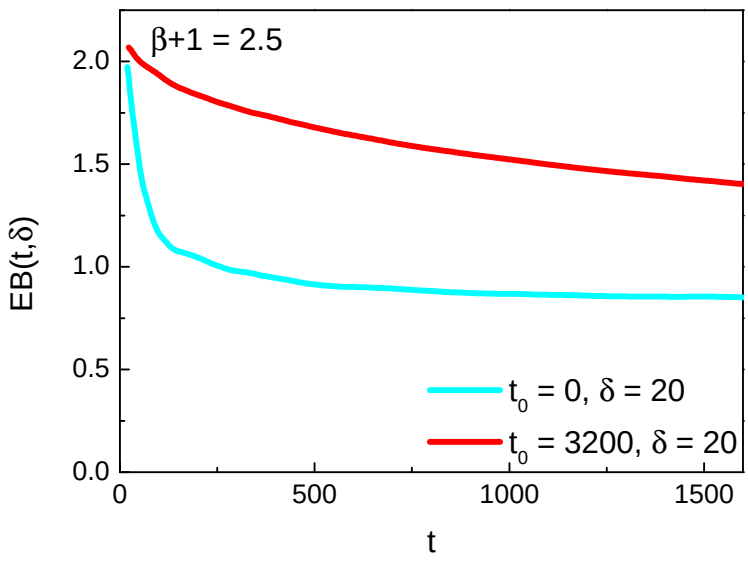

Figure 3.8: Ergodicity breaking parameter for fractional Brownian motion as a function of averaging time, Lagevin simulations for the superballisitc case. Even for zero intial velocity (cyan line), the ergodicity breaking parameter does not tend to zero, indicating that there is significant variaton in the behavior of individual trajectories. For a long relaxation time t_0 and thus large variation in the intial velocity $\langle \Delta v^2(t_0)\rangle$, this variation is even more pronounced (red line).

of particles in the superballistic regime. Finally, we note that the velocity process defined by fractional Gaussian noise, Eqs. (3.130) and (3.131), is Gaussian $1/f$-noise with exponent β.

The position spectral density can be obtained in the same way by taking into account that the position correlation function also has a scaling form, Eq. (3.42), with a different scaling function and an exponent that is increased by 2 with respect to the scaling exponent of the velocity correlation function, so that the corresponding scaling exponent is now $\nu = \beta + 3$. Writing the position correlation function as,

$$C_x(t+\tau, t) \simeq \mathcal{C} t^{\beta+1} \psi^* \left(\frac{\tau}{t}\right), \tag{3.144}$$

we have from Eq. (3.44),

$$\psi^*(y) \simeq \frac{1}{\mathcal{C}} \left(2D_\nu + (\beta+1) D_\nu y\right). \tag{3.145}$$

The corresponding expressions for $t_0 \gg t$ are obtained in the same manner,

$$C_x(t+\tau, t) \simeq \mathcal{C} \begin{cases} t^{\beta+1} \psi_s^* \left(\frac{\tau}{t}\right) & \text{for } \beta < 1 \\ {t_0}^{\nu-2} t^2 \psi_{\text{ball}}^* \left(\frac{\tau}{t}\right) & \text{for } \beta > 2, \end{cases} \tag{3.146}$$

with

$$\begin{aligned} \psi_s^*(y) &\simeq \frac{1}{\mathcal{C}} \left(2D_{\nu,s} + (\beta+1) D_{\nu,s} y\right) \\ \psi_{\text{ball}}^*(y) &\simeq 2a_0 + a_0 y. \end{aligned} \tag{3.147}$$

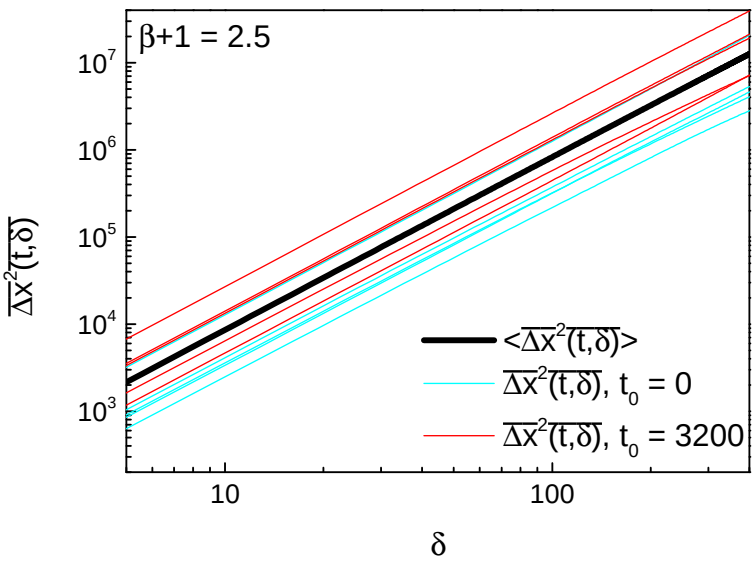

Figure 3.9: Time-averaged square displacement for frational Brownian motion as a function of time lag, Lagevin simulations for the superballisitc case. Both for zero intial velocity (thin cyan lines) and large initial velocity $\langle \Delta v^2(t_0)\rangle$ (thin red lines) individual realizations, while all exhibiting ballistic behavior, differ significantly form the mean time-averaged square displacement (black line).

The position spectral density then always behaves as ω^{-2} in the long-time limit $\omega t \gg 1$ according to Eq. (3.113),

$$S_x(\omega,t) \simeq \begin{cases} D_v t^\beta \omega^{-2} & \text{for } t \gg t_0 \\ D_{v,s} t^\beta \omega^{-2} & \text{for } t_0 \gg t,\ \beta < 1 \\ \frac{3a_0\mathcal{C}}{2(\beta-1)\Gamma^2\left(\frac{\beta}{2}\right)} {t_0}^{\beta-1} t\, \omega^{-2} & \text{for } t_0 \gg t,\ \beta > 1. \end{cases} \tag{3.148}$$

Depending on the relative size of t and t_0 and the value of β, the prefactor of this ω^{-2} frequency dependence increases with time as t^β or linearly, as is shown in Fig. 3.12 Note that it is Eq. (3.113) and not Eq. (3.129) that describes the long-time behavior of the position spectral density for $t_0 \gg t$. The reason for this is that the relaxation time in Eq. (3.129) applies to the velocity process, i.e. the velocity starts out with a large variance $\langle \Delta v^2(t_0)\rangle$. The measurement of the position process, by contrast, starts at $t = 0$, i.e. $\langle \Delta {x_{t_0}}^2(0)\rangle = 0$. So, while the mean-square displacement depends on t_0, the relaxation time for the position process is actually zero. As with the velocity spectral density, there is a low-frequency cutoff for $\omega t \ll 1$. The value of the spectral density below the cutoff is given by the integral over the position scaling function $\psi(y)$, Eq. (3.43),

$$S_x(\omega,t) \simeq t^{v+1} \frac{1}{v+2} \int_0^\infty dy\ (1+y)^{-v-2} \left[2D_v + \mathcal{C}\psi(y)\right], \tag{3.149}$$

which is the analog of Eq. (3.103) and in this case increases with time as $t^{\beta+3}$. Since the long-time position spectral density always behaves as ω^{-2} for superdiffusion

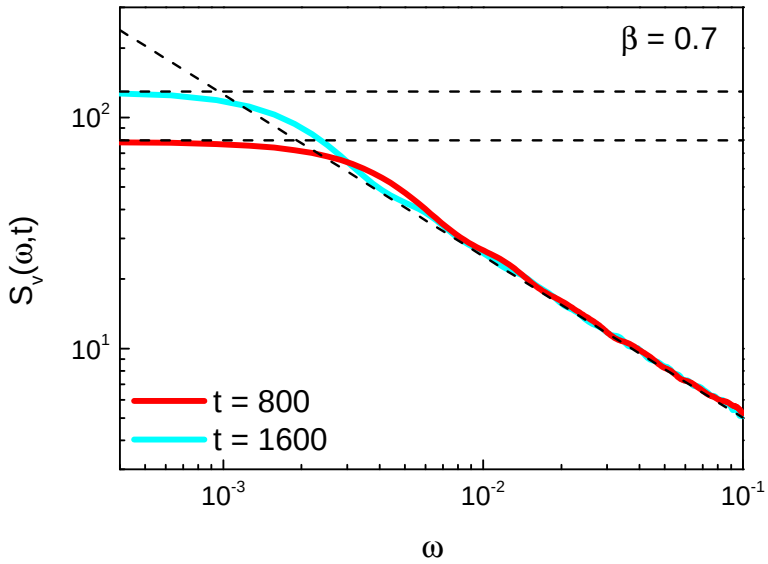

Figure 3.10: Velocity spectral density as a function of frequency in the subballistic regime $\beta < 1$ for different measurement times. The colored lines are the results of Langevin simulations, the black dashed lines are the corresponding asymptotic analytic result Eq. (3.140). For $\omega t \gg 1$, the spectral density is well-described by the $\omega^{-\beta}$ behavior, independent of the measurement time t. For low frequencies, there is a cutoff, which is shifted to lower frequencies for longer measurement times.

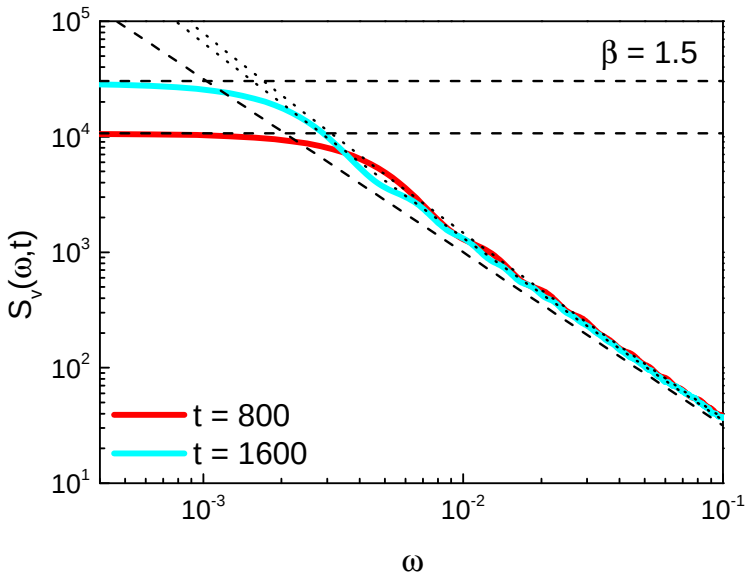

Figure 3.11: Velocity spectral density as a function of frequency in the superballistic regime $\beta > 1$ for different measurement times. The colored lines are the results of Langevin simulations, the black dashed lines are the corresponding asymptotic analytic result Eq. (3.140). Even though the velocity correlation function is nonstationary, the spectral density asymptotically follows a time-independent $\omega^{-\beta}$ behavior. For intermediate frequencies, however, the agreement is not very good, and can be improved by including the sub-leading order correction Eq. (3.141) (dotted lines). As in the subballistic regime there is a low-frequency cutoff, which is shifted to lower frequencies for longer measurement times.

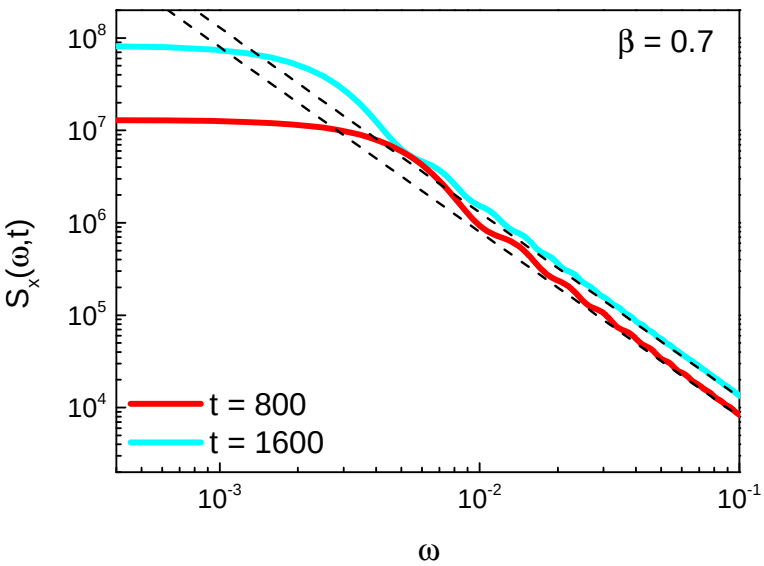

Figure 3.12: Position spectral density as a function of frequency in the subballistic regime $\beta < 1$ for different measurement times and $t_0 = 0$. The colored lines are the results of Langevin simulations, the black dashed lines are the corresponding asymptotic analytic result Eq. (3.148). For $\omega t \gg 1$, the position spectral density behaves as ω^{-2}, however, its magnitude increases with measurement time as t^β.

$\beta > 0$, its frequency dependence cannot characterize the diffusive dynamics of the system, in contrast to the velocity spectral density, Eq. (3.140). The position spectral density is thus less suited as a simple quantity to characterize the scaling of the system, since this requires identifying the dependence on the measurement time. Note that the often used relation $S_v(\omega) = \omega^{-2} S_x(\omega)$, which holds for subdiffusion and normal diffusion, cannot be applied to superdiffusion.

3.4.2 *Lévy walk*

The Lévy walk as introduced in Section 2.2.2 has the velocity correlation function Eq. (2.57),

$$\begin{aligned} C_v(t+\tau,t) &\simeq \mathcal{C}\, t^{\beta-1} \phi\left(\frac{\tau}{t}\right), \\ \text{with} \quad \mathcal{C} &= \frac{{v_{\text{typ}}}^2}{{t_\beta}^{\beta-2}\langle t_w\rangle}, \\ \phi(y) &= \frac{1}{1-\beta}\left(y^{\beta-1} - (1+y)^{\beta-1}\right), \\ 0 &< \beta < 1, \end{aligned} \tag{3.150}$$

where $\langle t_w \rangle$ is the average waiting time between switches in the velocity. As with fractional Gaussian noise, this correlation function has a stationary limit for $t \gg \tau$,

which is the same as the above but with $\phi(y) = y^{\beta-1}$ and $\mathcal{C}_s = \mathcal{C}/(1-\beta)$. The small- and large-argument expansion of the scaling function is straightforward,

$$\phi(y) \simeq \begin{cases} \frac{1}{1-\beta} y^{\beta-1} - \frac{1}{1-\beta} + y + \mathcal{O}(y^2) & \text{for } y \ll 1 \\ y^{\beta-2} + \frac{\beta-2}{2} y^{\beta-3} + \mathcal{O}(y^{\beta-4}) & \text{for } y \gg 1. \end{cases} \tag{3.151}$$

The average waiting time is infinite for $1 < \beta < 2$, where the velocity correlation function is given by [Godr 01, Froe 13],

$$\begin{aligned} C_v(t+\tau, t) &\simeq \mathcal{C}_a \phi_a\left(\frac{\tau}{t}\right), \\ \text{with} \quad \mathcal{C}_a &= {v_{\text{typ}}}^2 \\ \phi_a(y) &= -\frac{\sin(\pi\beta)}{\pi} B\left(\frac{1}{1+y}; 2-\beta, \beta-1\right), \\ 1 &< \beta < 2. \end{aligned} \tag{3.152}$$

In this regime, the correlation function is of the pure aging type, Eq. (3.21) with $\nu = 2$. The expansion of the scaling function is,

$$\phi_a(y) \simeq \begin{cases} 1 + \frac{\sin(\pi\beta)}{\pi(\beta-1)} y^{\beta-1} - \frac{\sin(\pi\beta)}{\beta} y^{\beta} + \mathcal{O}(y^{\beta+1}) & \text{for } y \ll 1 \\ -\frac{\sin(\pi\beta)}{\pi(2-\beta)} y^{\beta-2} + \frac{\sin(\pi\beta)}{\pi(3-\beta)} y^{\beta-3} + \mathcal{O}(y^{\beta-4}) & \text{for } y \gg 1. \end{cases} \tag{3.153}$$

Mean-square displacement

For $\beta < 1$, the diffusive properties of the Lévy walk are very similar to those of fractional Brownian motion, Eq. (3.134). The anomalous diffusion coefficient is given by,

$$\begin{aligned} D_\nu &= \frac{\mathcal{C}}{\beta(\beta+1)} \\ D_{\nu,s} &= \frac{\mathcal{C}}{(1-\beta)\beta(\beta+1)}, \end{aligned} \tag{3.154}$$

with a diffusion exponent $\nu = \beta + 1$,

$$\langle \Delta x^2(t) \rangle \simeq 2 D_\nu t^{\beta+1}. \tag{3.155}$$

For $1 < \beta < 2$, while the correlation function is aging, we can nevertheless take the limit $t_0 \gg t$, in which the diffusion coefficient is still independent of t_0 and determined by the leading order of the expansion Eq. (3.153). We have,

$$\begin{aligned} D_\nu &= \frac{\mathcal{C}_a(\beta-1)}{2} \\ D_{\nu,s} &= \frac{\mathcal{C}_a}{2}, \end{aligned} \tag{3.156}$$

with a diffusion exponent $\nu = 2$ and thus ballistic motion,

$$\langle \Delta x^2(t) \rangle \simeq 2 D_\nu t^2. \tag{3.157}$$

This is different from fractional Brownian motion, where we found a superballistic phase for $\beta > 1$ due to the increasing mean-square velocity. For the Lévy walk, the mean-square velocity is asymptotically constant for all values of β, and the diffusion is thus at most ballistic. Note that for $\beta < 1$, the mean waiting time enters the constant $\mathcal{C}$. Since the waiting time diverges as $\beta \to 1$, this changes the dependence of Eq. (3.154) on β. For the simple choice of the waiting time distribution,

$$P_w(t_w) = \begin{cases} 0 & \text{for } t_w \leqslant t_\beta \\ \frac{2-\beta}{t_0}\left(\frac{t_w}{t_\beta}\right)^{\beta-3} & \text{for } t_w > t_\beta, \end{cases} \tag{3.158}$$

which we also use in our Langevin simulations, the mean waiting time is given by,

$$\langle t_w \rangle = \frac{2-\beta}{1-\beta} t_\beta. \tag{3.159}$$

For this choice of the waiting time distribution the anomalous diffusion coefficient is plotted in Fig. 3.13. For the Lévy walk, the notion of stationarity and relaxation into the stationary state is different than for fractional Brownian motion. Whereas in the former case, the relaxation of the mean-square velocity towards its stationary value was responsible for the discrepancy between stationary and nonstationary diffusion coefficient, the velocity for the Lévy walk is constant. Here, the nonstationary initial condition corresponds to having the first switch in the velocity at $t = 0$ for every trajectory. In the subballistic regime $\beta < 1$, while the mean waiting time is finite, the variance of the waiting time is infinite, meaning that vastly different waiting times will occur. In particular, once a long waiting time occurs, the corresponding particle will get stuck at its current velocity for a long time. As we let the process evolve for a time t_0, the portion of particles that a currently stuck at one velocity increases, leading to more correlated motion and thus a larger diffusion coefficient in the stationary state, where the portion of stuck particles saturates. This effect is even more pronounced in the ballistic regime $\beta > 1$. Here the mean waiting time is infinite, meaning that at some point for every trajectory a waiting time will occur that will last for the rest of the entire evolution, leading to ballistic motion. For $t_0 \gg t$, this means that this will have occurred for almost every trajectory and thus the diffusion coefficient corresponds to deterministic ballistic motion, as every particle just moves at a constant velocity.

Time-averaged square displacement and ergodicty

For the mean of the time-averaged square displacement, similar arguments as for the fractional Brownian motion case hold, with the exception of the absence of the superballistic phase. The mean of the time-averaged square displacement will be equal to the mean-square displacement it the system starts out in a stationary state, see Eq. (3.72). If the system is not initially stationary, then the mean of the time-averaged square displacement will still follow the stationary behavior Eq. (3.66), which, however, is now different from the mean-square displacement. Since the Lévy walk, in contrast to fractional Brownian motion, is non-Gaussian, its higher order moments cannot be expressed in terms of its second order moments by the

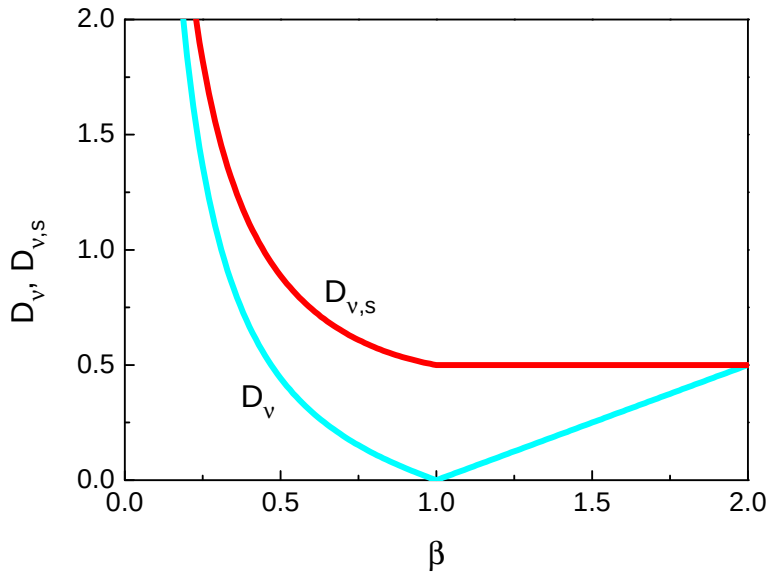

Figure 3.13: Anomalous diffusion coefficient D_v for the Lévy walk as a function of the exponent β. The cyan line is the nonstationary result and the red line the stationary one (see Eqs. (3.154) and (3.156)). In the limit of normal diffusion $\beta \to 0$, both results diverge, indicating a qualitative change in the dynamics. For superdiffusion $0 < \beta < 1$ and ballistic expansion $1 < \beta < 2$, the two results for the diffusion coefficient differ. As $\beta \to 2$, velocity does not change at all and the dynamics resembles purely ballistic motion with a constant velocity $\pm v_{typ}$.

Gaussian moment theorem Eq. (3.139). Indeed, the ergodicity breaking parameter Eq. (3.75), which was calculated for the Lévy walk in Ref. [Froe 13], is seen to be non-zero in the ballistic regime $\beta > 1$ in the long time limit. Since the mean waiting time is infinite, even for long measurement times, there will frequently occur events where the particle has the same velocity for a substantial amount of the measurement time. A typical trajectory will thus not reproduce the ensemble average and the system is nonergodic. In the subballistic regime, the ergodicity breaking parameter does tend to zero for long averaging times and the system is ergodic [Froe 13], provided it starts out in the stationary state. The ergodicity breaking parameter for the Lévywalk as a function of averaging time is shown in Fig. 3.14. Note that, although the ergodicity breaking parameter tends to zero in the subballistic regime, it is overall much larger than for fractional Brownian motion with the same diffusive behavior. Thus, even though the system is ergodic in this regime, variations between individual trajectories can be substantial for finite times and the subballistic Lévy walk may in practice behave in a nonergodic manner. This is due to the Lévy walk being non-Gaussian, which also manifests itself in the fact that the ergodicity breaking parameter is larger than 2 for zero averaging time, indicating that higher order moments are enhanced compared to the Gaussian case.

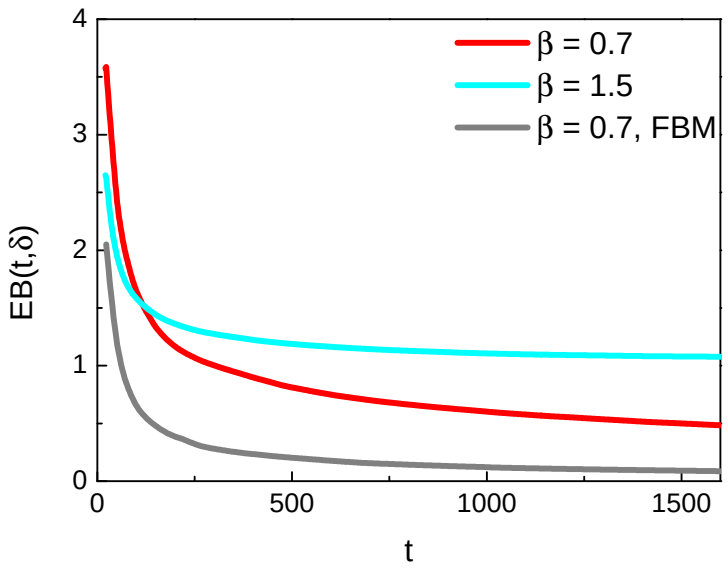

Figure 3.14: Ergodicity breaking parameter for the Lévy walk as a function of averaging time for a time lag $\delta = 20$. The red curve shows the result for the subballistic phase $\beta < 1$, the gray curve is the corresponding result for fractional Brownian motion with the same value of β. While in both cases, the ergodicity breaking parameter tends to zero for long averaging times, it is significantly larger for the Lévy walk, mirroring the non-Gaussian nature of the process. In the ballistic phase $\beta > 1$, the ergodicity breaking parameter does not tend to zero but is finite for long times (cyan curve).

Spectral density

In the subballistic regime $\beta < 1$, the velocity and position spectral density for the Lévy walk behave in exactly the same was as for fractional Brownian motion, Eqs. (3.140) and (3.148), since its stationary velocity correlation function, respectively the mean-square displacement, are identical apart from prefactors. Specifically, the spectral densities for $\beta < 1$ in the long-time limit $\omega t \gg 1$ behave as,

$$\begin{aligned} S_v(\omega, t) &\simeq \frac{2\mathcal{C}\Gamma(\beta)\cos\left(\frac{\pi\beta}{2}\right)}{1-\beta}\omega^{-\beta} \\ S_x(\omega, t) &\simeq \frac{1}{t}\langle \Delta x_{t_0}{}^2(t)\rangle \omega^{-2}. \end{aligned} \tag{3.160}$$

Note, however, that the sub-leading order for the velocity spectral density vanishes for the Lévy walk due to the coefficients in Eq. (3.151), i.e. there is no correction proportional to ω^{-2}. In the ballistic regime $\beta > 1$, the situation is different. While the position spectral density is given by the same expression as before with the appropriate mean-square displacement, the velocity spectral density is qualitatively different than for fractional Gaussian noise,

$$S_v(\omega, t) \simeq \begin{cases} \frac{2\mathcal{C}\Gamma(\beta)\cos\left(\frac{\pi(2-\beta)}{2}\right)}{(\beta-1)(2-\beta)} t^{1-\beta}\omega^{-\beta} & \text{for } \omega t \gg 1 \\ \frac{1}{t}\langle \Delta x_{t_0}{}^2(t)\rangle & \text{for } \omega t \ll 1. \end{cases} \tag{3.161}$$

While the frequency dependence of the velocity spectral density is the same as in the subballistic regime, it is now explicitly time-dependent, its magnitude decreases as $t^{1-\beta}$. Comparing this to Eq. (3.143), we find an asymptotically constant total power also in the ballistic regime $\beta > 1$. The time-dependent spectral density for the Lévy walk in relation to $1/f$-noise was also discussed in Ref. [Niem 13, Sade 13].

3.4.3 *Spectral density for nonequilibrium noise*

The final scaling system we want to examine is the nonequilibrium noise discussed in Section 2.2.3. In contrast to the previous two cases, the scaling correlation function here does not describe a velocity but rather a random force. In the context of the active viscoelastic medium (see Section 2.2.2) this is an effective force due to the combination of the random motion of the medium and the particle's viscoelastic coupling to the latter. Thus the time integral of this force does not describe the particle's actual momentum and the quantities corresponding to the mean-square and time-average square displacement are not meaningful. Because of this, we here concentrate on the spectral properties of the nonequilibrium noise. The noise correlation function is of the same scaling form as Eq. (3.13) and given by Eqs. (2.61), (2.64) and (2.68) for the stationary and nonstationary Gaussian respectively Lévy walk case,

$$C_\xi(t+\tau,t) = \mathcal{C} t^{2\alpha+\beta-1} \phi\left(\frac{\tau}{t}\right). \tag{3.162}$$

The scaling exponent is now $\nu = 2\alpha+\beta+1$ and the constant $\mathcal{C}$ is given in the equations quoted above. We remind ourselves that the exponent α controls the decay of the memory kernel in the fractional Langevin equation (i.e. larger values of α correspond to longer-ranged memory) and β describes the correlations of the medium velocity (i.e. larger values of β correspond to more correlated motion). Of particular importance are the small-argument expansions of the respective scaling functions, which can be found using the expressions in the former equations and the asymptotic expansions of certain integrals given in Appendix A.2. We find,

$$\phi(y) \simeq a_{2\alpha+\beta-1} y^{2\alpha+\beta-1} + a_0 + a_1 y + \mathcal{O}(y^2). \tag{3.163}$$

For the stationary Gaussian case, the coefficients are given by,

$$\begin{aligned} a_{2\alpha+\beta-1} &= \frac{\Gamma(\alpha)\Gamma(\alpha+\beta)\big(\sin(\pi\alpha)+\sin(\pi(\alpha+\beta))\big)}{\Gamma(2\alpha+\beta)\sin(\pi(2\alpha+\beta))}, \\ a_0 &= \frac{2}{2\alpha+\beta-1}, \quad a_1 = 1, \\ \mathcal{C} &= \frac{m^2\gamma^2 {v_{\text{typ}}}^2}{2\cos\left(\frac{\pi\beta}{2}\right)\Gamma(\alpha)\Gamma(\alpha+\beta){t_\alpha}^{2\alpha}{t_\beta}^{\beta-1}}, \end{aligned} \tag{3.164}$$

for the nonstationary Gaussian case, we instead have,

$$\begin{aligned} a_{2\alpha+\beta-1} &= \frac{\Gamma^2\left(\alpha+\frac{\beta}{2}\right)\sin\left(\pi\left(\alpha+\frac{\beta}{2}\right)\right)}{\Gamma(2\alpha+\beta)\sin(\pi(2\alpha+\beta))}, \\ a_0 &= \frac{1}{2\alpha+\beta-1}, \quad a_1 = \frac{1}{2}, \\ \mathcal{C} &= \frac{m^2\gamma^2 {v_{\text{typ}}}^2}{\Gamma^2\left(\alpha+\frac{\beta}{2}\right){t_\alpha}^{2\alpha}{t_\beta}^{\beta-1}}, \end{aligned} \tag{3.165}$$

and, finally, for the Lévy walk,

$$\begin{aligned} a_{2\alpha+\beta-1} &= \frac{\Gamma(\beta)\cos\left(\frac{\pi\beta}{2}\right)}{\Gamma(2\alpha+\beta)\cos\left(\pi\left(\alpha+\frac{\beta}{2}\right)\right)} \\ a_0 &= 2\int_0^1 dz \int_0^1 du\, z^{\alpha-1}(u+z-uz)^{\alpha-1}(1-z)^\beta(u^{\beta-1}-1) \\ a_1 &= (\alpha-1)\int_0^1 dz \int_0^1 du\, z^{\alpha-1}(u+z-uz)^{\alpha-2}(1-z)^\beta(u^{\beta-1}-1), \\ \mathcal{C} &= \frac{m^2\gamma^2 {v_{\text{typ}}}^2}{(1-\beta)\langle t_w\rangle {t_\alpha}^{2\alpha}{t_\beta}^{\beta-2}}. \end{aligned} \tag{3.166}$$

We first focus on $\alpha < 1/2$ and $2\alpha+\beta < 1$ corresponding to relatively short-ranged memory and weakly correlated medium velocity. Here, the nonequilibrium noise correlation function is stationary, $C_{\xi,s}(\tau) \sim \tau^{2\alpha+\beta-1}$ and the noise spectral density in the long-time limit $\omega t \gg 1$ is given by,

$$S_\xi(\omega,t) \simeq 2\mathcal{C}a_{2\alpha+\beta-1}\Gamma(2\alpha+\beta)\cos\left(\pi\left(\alpha+\frac{\beta}{2}\right)\right)\omega^{-2\alpha-\beta}. \tag{3.167}$$

Using the parameters listed above, we find for both the stationary and nonstationary Gaussian velocity process,

$$S_\xi(\omega,t) \simeq \frac{m^2\gamma^2 {v_{\text{typ}}}^2}{{t_\alpha}^{2\alpha}{t_\beta}^{\beta-1}}\omega^{-2\alpha-\beta} = m^2\gamma^2(\omega t_\alpha)^{-2\alpha}S_{v_m}(\omega,t). \tag{3.168}$$

Since the stationary autocorrelation function of the nonequilibrium noise depends only on the asymptotically stationary medium velocity correlation function (see Section 2.2.3), so does the spectral density. It is thus the same for both the stationary and nonstationary medium velocity process. For the Lévy walk, we have,

$$\begin{aligned} S_\xi(\omega,t) &\simeq \frac{\Gamma(\beta)\cos\left(\frac{\pi\beta}{2}\right)m^2\gamma^2 {v_{\text{typ}}}^2}{(1-\beta){t_\alpha}^{2\alpha}\langle t_w\rangle {t_\beta}^{\beta-2}}\omega^{-2\alpha-\beta} \\ &= m^2\gamma^2(\omega t_\alpha)^{-2\alpha}S_{v_m}(\omega,t). \end{aligned} \tag{3.169}$$

As long as the nonequilibrium noise is stationary, its spectral density is thus simply related to the one of the medium velocity (see Eqs. (3.140) and (3.160)) by a factor of $m^2\gamma^2(\omega t_\alpha)^{-2\alpha}$. This is not unexpected, as the respective Laplace transforms are related by $\tilde{\xi}(s) = m\gamma(st_\alpha)^{-\alpha}\tilde{v}_m(s)$. For $1 < 2\alpha+\beta < 2$, the leading order

of the noise spectral density is still given by Eq. (3.167). As was the case with the velocity spectral density, we may need to take into account the sub-leading order to accurately capture its frequency dependence. The noise spectral density, including the time-dependent sub-leading order, is then,

$$S_\xi(\omega,t) \simeq 2\mathcal{C}a_{2\alpha+\beta-1}\Gamma(2\alpha+\beta)\cos\left(\pi\left(\alpha+\frac{\beta}{2}\right)\right)\omega^{-2\alpha-\beta} + 2\mathcal{C}\left(a_0-\frac{a_1}{2\alpha+\beta-1}\right)t^{2\alpha+\beta-2}\omega^{-2}. \tag{3.170}$$

Note that the coefficients a_0 and a_1 are different depending on whether the medium velocity process was initially stationary or nonstationary. The simple relation between the nonequilibrium noise and the medium velocity spectral densities stated above thus fails for the sub-leading order. This failure is even more pronounced in the regime of very long-ranged memory or highly correlated motion of the medium $2 < 2\alpha+\beta < 3$. Here the sub-leading order in Eq. (3.170) is now the leading order contribution. The leading order term is then proportional to ω^{-2} and grows with the magnitude of the noise,

$$S_\xi(\omega,t) \simeq 2\mathcal{C}\left(a_0-\frac{a_1}{2\alpha+\beta-1}\right)t^{2\alpha+\beta-2}\omega^{-2} = \frac{1}{t}\langle\xi^2(t)\rangle\omega^{-2}. \tag{3.171}$$

Thus, if the magnitude of the nonequilibrium noise increases superdiffusively, then its spectral density will depend on time even in the long-time limit. A possible interpretation of this superdiffusive nonequilibrium noise in the context of the dynamics in cells is discussed in Section 4.3. Note that here, the time-dependent spectral density is indeed different, depending on whether the medium velocity process was initially stationary or not. Specifically, we have for the stationary Gaussian case,

$$S_\xi(\omega,t) \simeq \frac{m^2\gamma^2{v_{\text{typ}}}^2}{\cos\left(\frac{\pi\beta}{2}\right)\Gamma(\alpha)\Gamma(\alpha+\beta)(2\alpha+\beta-1){t_\alpha}^{2\alpha}{t_\beta}^{\beta-1}}t^{2\alpha+\beta-2}\omega^{-2}, \tag{3.172}$$

while the corresponding expression for the nonstationary Gaussian case reads,

$$S_\xi(\omega,t) \simeq \frac{m^2\gamma^2{v_{\text{typ}}}^2}{\Gamma^2\left(\alpha+\frac{\beta}{2}\right)(2\alpha+\beta-1){t_\alpha}^{2\alpha}{t_\beta}^{\beta-1}}t^{2\alpha+\beta-2}\omega^{-2}. \tag{3.173}$$

These two expressions coincide only for $\beta \to 0$, where the medium velocity corresponds to Gaussian white noise. In particular, the coefficient of expression Eq. (3.172) diverges as $\beta \to 1$, where the medium velocity process ceases to have a well-defined stationary limit. In the nonstationary case, Eq. (3.173), by contrast the coefficient is finite as $\beta \to 1$.

4 APPLICATION TO DYNAMICS IN LIVING CELLS

Note: Parts of this Chapter are based on Ref. [Dech 13].

Nonequilibrium dynamics in living cells depends strongly on the observed time scales. For tracers bound to the cytoskeleton, there is a characteristic transition between a very slow subdiffusive motion for short times and relatively fast superdiffusion for longer times, with a transition time on the order of a few seconds. Interestingly, both the respective diffusion exponents and the transition time are largely universal for a wide range of cell types [Trep 08]. Our model of a tracer particle coupled viscoelastically to an actively moving environment, which we introduced in Section 2.2.2, describes a smooth transition between the subdiffusive short-time and superdiffusive long-time behavior within the Langevin formalism. The subdiffusive behavior is due to the motion of the tracer particle in a viscoelastic equilibrium environment, while the nonequilibrium motion of the environment itself leads to superdiffusion. In particular, the exponent α, that describes the decay of the memory kernel and thus the mechanical properties of the equilibrium medium, also determines the subdiffusion exponent $1-\alpha$. The superdiffusion exponent $\beta+1$, on the other hand, is solely determined by the correlations of the medium velocity $v_m(t)$ and thus the active motion of the medium. The moving viscoelastic medium model disentangles the equilibrium and nonequilibrium behavior and allows to quantify them individually by observing the short-time subdiffusion, respectively long-time superdiffusion. In Section 4.1, we compare our model to experimental data of superdiffusion in living cells and extract the respective exponents. The transition from equilibrium subdiffusion to nonequilibrium superdiffusion can be characterized by a crossover time t_c, which relates the magnitude of the active motion to the temperature.

The short-time subdiffusion exponent also appears in another context: Since the subdiffusive motion is indicative of the equilibrium mechanical properties of the cell, it is related to the linear response of the tracer to an externally applied force via the Stokes-Einstein relation, see Section 2.3.3. The response thus follows a power-law with the same exponent as the subdiffusive mean-square displacement. The Stokes-Einstein relation also has an important experimental implication: It allows to predict the diffusive motion due to thermal fluctuations by measuring the response in an active microrheological experiment. Conversely, the response can be inferred from passively measuring the mean-square displacement. For longer times, the Stokes-Einstein relation breaks down, as the diffusive motion is now dominated by the nonequilibrium behavior of the cell. Here, both active and passive measurements are required to determine the response respectively mean-square displacement. However, we can reconnect diffusion and response by introducing a time-dependent effective temperature in Section 4.2. This effective temperature quantifies how far the system, when viewed on a certain time scale, is from equilibrium. We thus obtain a generalized Stokes-Einstein relation which is

valid for all time scales. Moreover, the same effective temperature also relates the subdiffusive short-time and superdiffusive long-time behavior of the mean-square displacement. Aside from the sub- and superdiffusion exponents, the effective temperature only depends on the transition time t_c. Within the framework of the generalized Stokes-Einstein relation and the effective temperature, we thus connect the results of active and passive measurement for living cells. It allows to either predict the mechanical response by comparing the short- and long-time diffusive behavior observed in the passive measurement or to predict the short-time subdiffusion and the transition time from long-time active and passive measurements. Applying the effective temperature to an experiment where both active and passive measurements were performed on the same cells [Gall 09], we find $T_{\text{eff}}(t) \sim t^{\lambda}$ with $\lambda = 1.37 \pm 0.07$ from comparing the short- and long-time passive measurement and $\lambda = 1.31 \pm 0.08$ from comparing the active and passive measurement. Within experimental errors, the time-dependence of the effective temperature is thus indeed the same for both situations and our generalized Stokes-Einstein relation holds. This lends strong support to our nonequilibrium model, of which the generalized Stokes-Einstein relation is a direct result.

Another central concept of our moving viscoelastic medium model is the nonequilibrium noise, which arises as an effective force from the viscoelastic mechanical properties and the motion of the cytoskeleton. In Section 4.3, we argue that, in order to realize both slow subdiffusion for short times and fast superdiffusion for long times, this nonequilibrium noise necessarily has to be a nonstationary stochastic process, whose magnitude increases with time. As a measurable consequence of this, we calculate the power spectral density of this effective noise force using the results of Sections 3.3 and 3.4.3. We predict that for the sub- and superdiffusion exponents observed in experiments, the power spectral density depends on frequency as ω^{-2}, a behavior which was suggested in Ref. [Lau 03]. Moreover, we find that the power spectral density is time-dependent and its overall magnitude increases with time. This is a signature of the strongly nonstationary behavior of the external noise. More generally, we classify the nature of the nonequilibrium dynamics as either force-like, where the active motion can be modeled through a stationary external noise, or velocity-like, where the noise is nonstationary and has to be interpreted in the context of our moving medium model.

While the mean-square displacement is a useful quantity to characterize the spreading of particles due to the combination of thermal and active fluctuations in the cell, it does not yield any detailed information about the stochastic properties of the associated random processes. A quantity that goes a step beyond the mean-square displacement is the so-called non-Gaussian parameter, which characterizes the relative size of fourth and second moments of the displacement compared to a Gaussian distribution. It vanishes for a Gaussian distribution, and is positive respectively negative if the displacement distribution has more respectively less weight on its tails than a Gaussian distribution. The non-Gaussian parameter was measured in several experiments [Burs 05, Toyo 11, Gal 12, Gal 13] on cells and artificial models of the cytoskeleton. While for short times, it is close to zero, indicating that the equilibrium dynamics is Gaussian, it is clearly positive for longer

times. The long-time nonequilibrium dynamics are thus non-Gaussian, with a high prevalence of larger than average displacements. Our model allows to reproduce this non-Gaussian behavior by using a non-Gaussian process for the medium velocity $v_m(t)$. Specifically, we model the motion of the cytoskeleton using the Lévy walk, which we introduced in Section 2.2.2. On even longer time scales the experimentally observed non-Gaussian parameter decreases again. We emulate this behavior in our model by placing the particle in a confining potential and examine the effect of the latter on the mean-square displacement and the non-Gaussian parameter. The results are discussed and compared with the experimental findings in Section 4.4.

In the final Section of this chapter, Section 4.5, we focus on the linear response of a viscoelastic system and its peculiar properties. Due to the presence of the superdiffusive nonequilibrium fluctuations in living cells there exists a lower threshold for the magnitude of the external force necessary in order to distinguish the response from the noise background. Contrary to equilibrium systems, this threshold increases with the desired measurement time, i.e. longer times require larger forces to accurately determine the response of a single particle. Even more curious is the response in the presence of prestress. Due to the long-range viscoelastic memory, the response depends in a detailed manner on the history of the system, in particular whether a force has been applied in the past. In this case, the response to an applied force may be in the opposite direction or even change direction as a function of time. These results are distinct from the prestress and rejuvenation effects observed experimentally so far, and could provide a further experimental confirmation for the viscoelastic nature of the cytosekeleton.

4.1 EQUILIBRIUM AND NONEQUILIBRIUM DYNAMICS

4.1.1 *Transition from sub- to superdiffusion*

The dynamics described by the fractional Langevin equation with coupling to an active environment Eq. (2.34) depends strongly on the time scales under consideration. The shortest time scale is the transition time from underdamped to overdamped motion, $t_{over} = t_\alpha(\gamma t_\alpha)^{-1/(\alpha+1)}$. For times shorter than this transition time, the overdamped approximation used to derive the asymptotic results in Section 2.3.2 is not valid. On these time scales, the fractional Langevin equation describes ballistic dynamics and oscillations in the mean-square displacement. Since the friction constant γ of the cytoplasm is very large, the transition time is typically far below any time scales accessible in experiment (Ref. [Brun 09] estimates $t_{over} \sim 10^{-12}$ s). Thus, we can safely assume the overdamped approximation to be valid. If this is the case, then, according to Eqs. (2.90), (2.92) respectively (2.95), the mean-square displacement has two contributions,

$$\langle \Delta x^2(t) \rangle \simeq \frac{2k_B T t_\alpha}{\Gamma(2-\alpha) m\gamma} \left(\frac{t}{t_\alpha}\right)^{1-\alpha} + 2D_v t^{\beta+1}, \tag{4.1}$$

where the diffusion coefficient D_v is different, depending on which model we assume for the autocorrelations of the medium velocity (see Eqs. (3.134) and (3.154)).

The first term describes the equilibrium subdiffusion, while the second one is the superdiffusive contribution due to the nonequilibrium active motion. Due to the different time-dependencies of the two terms, the first one will give the dominant contribution for short times, while the second one is responsible for the long-time dynamics. This transition between the subdiffusive equilibrium dynamics and the superdiffusive nonequilibrium one is precisely what is observed in a large number of experiments [Burs 05, Leno 07, Trep 08, Gall 09], where the motion of a microscopic bead attached to the cytoskeleton is tracked.

Typical values for the equilibrium and nonequilibrium exponents found in experiments [Burs 05, Leno 07, Trep 08, Gall 09] are $\alpha \sim 0.8$ and $\beta \sim 0.6$. The rather large value of α means that the mechanical properties of the cytoskeleton are more elastic than viscous, leading to slow subdiffusion in equilibrium $\langle \Delta x^2(t) \rangle_{eq} \sim t^{0.2}$. We can thus imagine the cytoskeleton as a network of elastic fibers, which are however, not rigidly bound together but can move with respect to each other, leading to a small degree of viscosity. The exponent α also determines the response of a tracer embedded in the cytoskeleton to an external force, see Sections 2.3.3 and 4.5. This allows to determine α both from passive measurements of the diffusive behavior and from actively probing the mechanical properties of the cell and both values generally agree very well [Gall 09]. The nonequilibrium motion of the cytoskeleton with exponent $\beta \sim 0.6$ is significantly more correlated than completely random Brownian motion, which corresponds to $\beta = 0$. This leads to substantially enhanced diffusion $\langle \Delta x^2(t) \rangle \sim t^{1.6}$ for long times. The sub- and superdiffusive dynamics are captured by the exponents α and β in Eq. (4.1). Within our simple stochastic model, these exponents are independent of each other. Whereas α accounts for the viscoelastic mechanical properties of the cytoskeleton, β characterizes the motion of the latter due to the activity of molecular motors. In reality, the motion of the cytoskeleton depends on its mechanical properties and altering the latter will impact the former. Thus, the exponents α and β are generally not independent of each other in the actual physical system. Nevertheless, as our description in terms of the moving viscoelastic medium model accounts for the subdiffusive equilibrium and superdiffusive nonequilibrium motion with independent stochastic processes, it allows to study the impact of changes in the cells' properties on both independently. For example, weakening crosslinks in the actin network is expected to soften the cytoskeleton and thus reduce α, leading to less elastic and more viscous motion. At the same time, since these crosslinks are responsible for mediating the active forces in the cytoskeleton, we also expect the motion of the latter to be less correlated, leading to a reduction in β [Fabr 11]. By measuring the changes in the sub- and superdiffusion exponent, we can thus directly infer how the mechanical and active properties of the cell change. Another example often employed in experiments is depletion of ATP [Burs 05, Leno 07, Gall 09], impairing molecular motor activity and thus reducing the active motion of the cytoskeleton and possibly the exponent β. This procedure should not change the cytoskeleton's mechanical properties and thus have no impact on the exponent α.

In Section 2.2.2 we presented three candidate processes for the medium velocity process $v_m(t)$, whose properties we subsequently examined in Section 3.4. This

poses the question of which of these stochastic processes is best suited to describe the nonequilibrium superdiffusion. First of all, all three processes lead to the same diffusion exponent $\nu = \beta + 1$ for the same value of the parameter β, the only difference being the diffusion coefficient. Since the parameters that enter the anomalous diffusion coefficient are within our model not related to any microscopic parameters, we have no way of telling which process is the most favorable one by way of the mean-square displacement. Let us first address the question of stationarity: We saw in Sections 3.1.3 and 3.2.2 that the initial stationarity of the process has an measurable influence on the long-time dynamics. In principle, we could decide whether the sought process is stationary or not by comparing the mean-square displacement to the time-averaged square displacement, see Section 3.2.2. Unfortunately, we do not have any experimental data available to perform this comparison. However, in order to be able to distinguish between the nonstationary and stationary processes in experiment, we need to measure for times t that are much longer than the time that has elapsed since the initialization of the nonstationary process. In living cells, this is almost impossible even under the most ideal conditions. Microrheological experiments are typically performed on time scales of up to several hundreds of seconds, whereas before the measurement, the incubation and preparation of the cells usually takes several hours [Gall 09]. Furthermore, living cells are not ideal realizations of a stochastic process. Cell-to-cell variation and changes within the individual cells are most certainly going to influence the measurement result much more than any possible deviations from stationary behavior detectable on these time scales. Consequently, we may restrict ourselves to the stationary variants of the respective processes for this purpose. This still leaves the stationary fractional Gaussian process and the stationary Lévy walk as possible choices. On the level of second moments, i.e. the mean-square displacement and spectral densities, these two processes are indistinguishable. However, several experiments have shown that the nonequilibrium dynamics in living cells and comparable model systems are indeed non-Gaussian, suggesting that the stationary Lévy walk may be the best choice among our candidate processes. We discuss these non-Gaussian effects in more detail in Section 4.4; for now, we will use the stationary Lévy walk for further comparisons with experiments.

An example for the result of a microrheological experiment [Gall 09] is shown in Fig. 4.1. There, the time-average square displacement of a silica bead bound to the actin cortex of a mouse muscle cell was measured, the data in the figure are the time average over a single trajectory. As a function of time the square displacement exhibits the characteristic crossover from subdiffusion with exponent $1 - \alpha \sim 0.1$ to superdiffusion with exponent $1 + \beta \sim 1.7$, the crossover time being on the order of several seconds. We used our moving viscoelastic medium model Eq. (2.34) to reproduce these results numerically, see Fig. 4.2. We choose this particular experiment, because to our knowledge, it is the only one where both active and passive measurements were performed on the same sample, allowing to test our model's predictions on both. In the passive measurement, a short-time subdiffusion exponent of $1 - \alpha = 0.12 \pm 0.01$ and a long-time superdiffusion exponent of $\beta + 1 = 1.49 \pm 0.06$ was obtained. The creep function, on the other hand, was found to increase with an exponent $1 - \alpha^* = 0.18 \pm 0.02$. While α and α^* do not agree

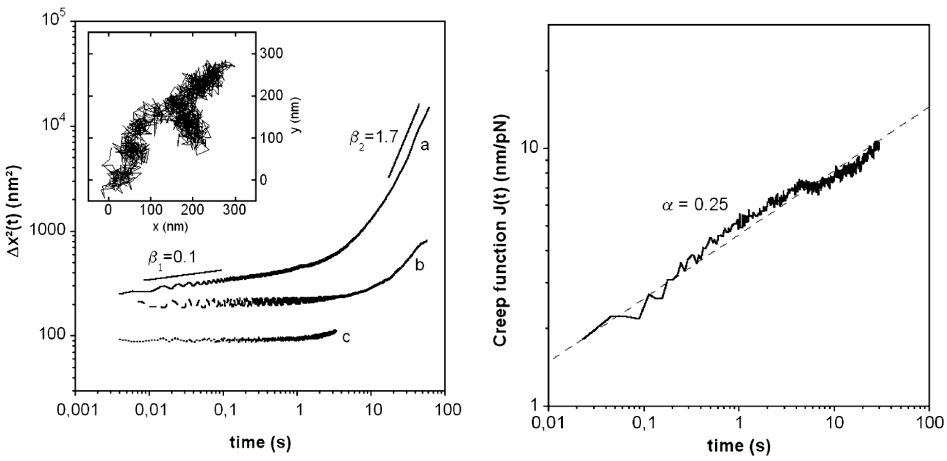

Figure 4.1: Left: Experimentally obtained mean-square displacement for a tracer bead bound to the actin cortex of a mouse muscle cell. Curve a is a control cell, b is an actin depleted cell with significantly reduced diffusion and c is the noise background. The inset shows the trajectory corresponding to a. Note the transition from short-time subdiffusion to long-time superdiffusion. Right: Displacement of the bead in response to a constant external force on the order of several pico-Newtons. The displacement increases with time in a nonlinear manner, with an exponent that is roughly on the order of the subdiffusion exponent. Image taken from Ref. [Gall 09].

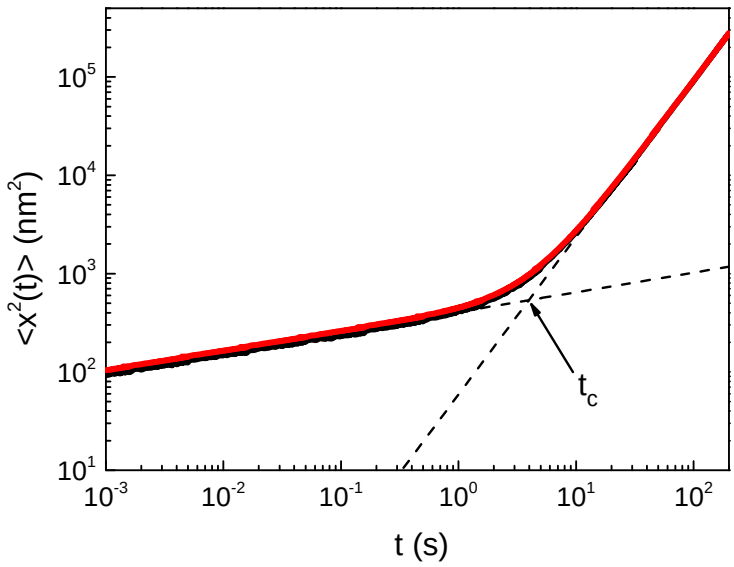

Figure 4.2: Mean-square displacement (black line) and ensemble mean of the time-averaged square displacement (red line) for $\alpha = 0.8$ and $\beta = 0.6$ obtained from numerical Langevin simulations using the stationary Lévy walk for the nonequilibrium motion. The parameters were chosen to mimic the experimental results depicted in Fig. 4.1. The asymptotic behavior of the mean-square displacement is very well described by the analytic expression Eq. (4.1) (dashed lines), the crossing point between the short- and long-time asymptote determines the crossover time $t_c \sim 4.0$ s. As both the equilibrium noise and the nonequilibrium moving medium are described by stationary processes, the mean-square displacement is almost indistinguishable from the mean of the time-averaged square displacement.

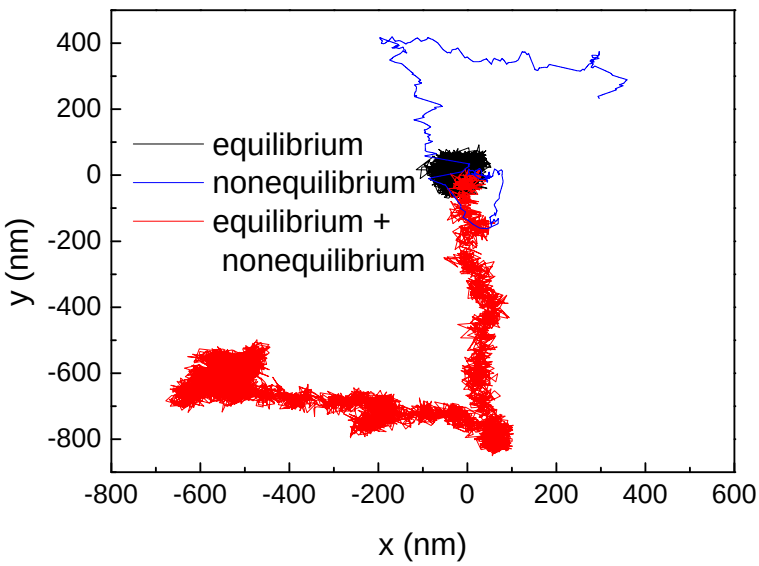

Figure 4.3: Typical trajectory for $\alpha = 0.8$ and $\beta = 0.6$ obtained from numerical Langevin simulations using the stationary Lévy walk for the nonequilibrium motion. The parameters were chosen to mimic the experimental results depicted in Fig. 4.1. All trajectories start at the origin. The motion of the simulated tracer including both equilibrium and nonequilibrium noise qualitatively reproduces the trajectories observed in experiment (red). For comparison trajectories under the influence of only equilibrium (black) respectively nonequilibrium (blue) noise are shown.

perfectly with one another, they are close enough to conjecture that the short-time mean square displacement indeed corresponds to equilibrium motion. The numerical simulation presented in Fig. 4.2 is in excellent agreement with the asymptotic expression Eq. (4.1) and in good agreement with the experimental result, though the parameters were estimated rather than fitted. In the simulation, we used a stationary Lévy walk for the medium velocity $v_m(t)$, see Section 3.4.2 for details. The parameters used in the simulation are,

$$\begin{aligned} &\alpha = 0.8, \quad \beta = 0.6, \quad t_\alpha = t_\beta = 1\ \mathrm{s} \\ &m = 9.21 \cdot 10^{-15}\mathrm{kg}, \quad \gamma = 2.4 \cdot 10^9 \frac{1}{\mathrm{s}}, \quad T = 300\mathrm{K}, \quad v_{\mathrm{typ}} = 6.3 \frac{\mathrm{nm}}{\mathrm{s}}. \end{aligned} \tag{4.2}$$

The choice of the time scales t_α and t_β is arbitrary, as we noted in Sections 2.1.2 and 2.2.2, since we only consider the scale-invariant asymptotic behavior; for this reason we may set them to 1 s for convenience. The above parameters also allowed us to get a good qualitative reproduction of individual trajectories, Fig. 4.3, indicating that the model is qualitatively well-suited to describing the experimental results. Our numerical simulations allow us to go beyond the experiment and to turn off the active motion of the medium respectively the equilibrium noise. If the particle is only affected by the equilibrium noise, the anticorrelated subdiffusive motion causes it to fluctuate around its initial position but prevents it from moving very far. On the other hand, a particle influenced only by the long-range correlated nonequilibrium Lévy walk motion of the medium moves around almost ballistically, causing it to travel large distances but only covering a small area while doing

so. Only with the combination of equilibrium and nonequilibrium motion is the particle transported effectively through the cell while also covering a large area. We speculate that this combination of short-time subdiffusion and long-time superdiffusion might be advantageous to the cell. Subdiffusion is known to enhance the reaction probability at nearby target sites [Guig 08, Sere 12], allowing ample time for chemical reactions to take place. The superdiffusive motion complements this by transporting particles through the cell at an enhanced rate, giving them the chance to come into contact with target sites at very different locations.

4.1.2 *Crossover time as a measure of active motion*

Both the subdiffusive equilibrium and the superdiffusive nonequilibrium motion are characterized not only by the respective exponents α, β but also by their respective diffusion coefficients. For the subdiffusive motion, we have,

$$\begin{aligned} &\langle \Delta x^2(t)\rangle_{eq} \simeq 2D_{eq}t^{1-\alpha} \\ &\text{with} \quad D_{eq} = \frac{k_B T t_\alpha{}^\alpha}{\Gamma(2-\alpha)m\gamma}, \end{aligned} \tag{4.3}$$

so that the diffusion coefficient is proportional to the temperature of the system. For the long-time superdiffusive motion, on the other hand,

$$\langle \Delta x^2(t)\rangle \simeq 2D_\nu t^{\beta+1}, \tag{4.4}$$

with a diffusion coefficient D_ν that is specific to the model used for the motion of the cytoplasm. The two diffusion coefficients can be related to each other by introducing a crossover time t_c, at which the two contributions to the mean-square displacement are equal,

$$\langle \Delta x^2(t_c)\rangle_{eq} = \langle \Delta x^2(t_c)\rangle_{noneq}, \tag{4.5}$$

where the subscripts eq and noneq denote the equilibrium respectively nonequilibrium contribution to the mean square displacement. The crossover time is then given by,

$$t_c = \left(\frac{D_\nu}{D_{eq}}\right)^{-\frac{1}{\alpha+\beta}}. \tag{4.6}$$

For fixed exponents α, β, an increase in the nonequilibrium diffusion coefficient D_ν leads to a decreasing crossover time, as the superdiffusive motion sets in earlier. The crossover time t_c measures the relative amplitude of the equilibrium and nonequilibrium motion and is thus a useful quantity to characterize the physical system. An increase in temperature, for example, is expected to enhance the equilibrium diffusion coefficient via Eq. (4.3). However, it might also lead to increased molecular motor activity and thus enhance the nonequilibrium diffusion coefficient. In this scenario, the crossover time quantifies how much the equilibrium respectively nonequilibrium properties of the cell are affected by the temperature change: If the crossover time increases, then the enhanced thermal equilibrium fluctuations are the dominant effect, if it decreases, the rise in molecular

motor activity is prevalent. Experimental data indeed shows that the crossover time decreases with increasing temperature [Leno 07], suggesting that motor activity increases disproportionately with respect to thermal fluctuations. Typical values for the crossover time observed in experiments are on the order of $t_c \sim 1$ s [Burs 05, Leno 07, Trep 08, Gall 09].

4.2 EFFECTIVE TEMPERATURE AND GENERALIZED STOKES-EINSTEIN RELATION

In microrheological experiments, there are two qualitatively different measurement schemes, see Section 1.1. In the passive scheme, a bead is embedded into the cytoplasm and its random motion within the cell is observed without exerting any external force on it. This type of measurement probes the diffusive properties of the cell. In the active scheme, a probe force is applied to the tracer particle and its response, i.e. its motion in reaction to the external force, is observed. This measurement scheme probes the mechanical properties of the cell, rather than the inherent random motion. For an equilibrium system, these two measurement schemes are related, the response to the external force follows the same time-dependence as the mean-square displacement. In Section 4.2.1, we discuss the Stokes-Einstein relation, and show how it can be generalized to the nonequilibrium case via a time-dependent effective temperature, which depends on the crossover time between sub- and superdiffusion. A similar relation with a frequency-dependent effective temperature is derived as well. Section 4.2.2 is dedicated to the interpretation of these effective temperatures in terms of the nonequilibrium dynamics of the system. In particular we see when and how the time-dependent and frequency-dependent effective temperature are related.

4.2.1 *Stokes-Einstein relation in time and frequency domain*

In the equilibrium system described by the fractional Langevin equation (2.10), we saw in Section 2.3.3 that the diffusion of the tracer particle in the absence of an external force and its response to a probe force are intimately related by the Stokes-Einstein relation Eq. (2.104) [Lutz 01],

$$\langle \Delta x^2(t) \rangle_{eq} = 2k_B T J(t). \tag{4.7}$$

It relates the mean-square displacement, which quantifies the random motion of the particle due to thermal fluctuations, to the creep function, which is the response of the particle to a constant external force, via the temperature. In equilibrium, both increase as $t^{1-\alpha}$ due to the viscoelastic properties of the thermal environment. This changes if we take into account the active motion of the cytoskeleton. While Eq. (4.7) is expected to remain valid in the short-time subdiffusive regime, for long times, the mean-square displacement behaves superdiffusively. Since we assumed the motion of the viscoelastic medium to be random in the sense that it does not have any favored direction, $\langle v_m(t) \rangle = 0$, it will have no impact on the response of the particle to an external force. Thus the behavior of the mean-square displacement is changed, while the creep function remains the same and

the Stokes-Einstein relation Eq. (4.7) is thus no longer valid. This is not surprising, as the latter is a direct consequence of the fluctuation-dissipation theorem Eq. (2.11), which only holds for equilibrium systems. We may impose a relation similar to Eq. (4.7),

$$\langle \Delta x^2(t) \rangle \simeq 2k_B T_{\text{eff}}(t) J(t), \tag{4.8}$$

valid for both the equilibrium and nonequilibrium situation, however, this necessitates a time-dependent effective temperature $T_{\text{eff}}(t)$. Comparing the generalized Stokes-Einstein relation Eq. (4.8) to the asymptotic mean-square displacement Eq. (4.1) and creep function Eq. (2.105), we find the expression for this effective temperature,

$$\frac{T_{\text{eff}}(t)}{T} \simeq 1 + \frac{D_v}{D_{\text{eq}}} t^{\alpha+\beta} = 1 + \left(\frac{t}{t_c}\right)^{\alpha+\beta}. \tag{4.9}$$

Here t_c is the crossover time between sub- and superdiffusion introduced in Eq. (4.6). For short times $t \ll t_c$, the effective temperature is equal to the physical one and the original Stokes-Einstein relation holds. This relates the result of the active measurement to the one of the passive measurement and allows to infer the result of one from the other. For long times $t \gg t_c$, on the other hand, the effective temperature increases with time and is larger than the physical temperature. For the experiment discussed in Section 4.1.1, we find from comparing the results of the active and passive measurement that $T_{\text{eff}} \sim t^{\lambda}$ with $\lambda = 1.31 \pm 0.08$. The effective temperature thus increases strongly for long times, indicating the strong effect of the active motion of the cytoskeleton on the tracer.

An equivalent to the Stokes-Einstein relation Eq. (4.7) exists in the frequency domain. We examine the velocity spectral density for the equilibrium system, which is related to the Laplace transform of the velocity autocorrelation by,

$$S_v(\omega, t) = \frac{1}{t}\mathcal{L}^{-2}\left[\frac{\tilde{C}_v(s_2, s_1)}{(s_2 + i\omega)(s_1 - i\omega)}\right]_{s_2 \to t}^{s_1 \to t}. \tag{4.10}$$

This relation can easily be verified by noting that the laplace transform of the windowed Fourier transform Eq. (3.79) is given by,

$$\mathcal{L}\left[\sqrt{t}\hat{v}(\omega, t)\right]_{t \to s} = \frac{1}{s}\tilde{v}(s - i\omega). \tag{4.11}$$

Equation (4.10) then follows from the definition of the spectral density. Using the equilibrium part of Eq. (2.76) with a thermal initial condition $\langle v_0 \rangle^2 = k_B T/m$, we see that the velocity correlation function can be written as,

$$\tilde{C}_v(s_2, s_1) = \frac{k_B T}{m(s_2 + s_1)}\left[\frac{1}{s_2 + \gamma\tilde{k}(s_2)} + \frac{1}{s_1 + \gamma\tilde{k}(s_1)}\right], \tag{4.12}$$

where we used the fluctuation-dissipation theorem Eq. (2.11) for the equilibrium noise. As discussed in the derivation of Eq. (3.113), the long-time $\omega t \gg 1$ behavior of the spectral is given by the behavior of the term in square brackets in Eq. (4.10)

at its nonanalytic points. Here, the dominant contribution comes from $s_2 = -i\omega$, $s_1 = i\omega$ and we approximate,

$$\begin{aligned} S_v(\omega, t) &\simeq \frac{k_B T}{mt} \mathcal{L}^{-2} \left[\frac{1}{(s_2 + s_1)(s_2 + i\omega)(s_1 - i\omega)} \right]_{s_2 \to t}^{s_1 \to t} \\ &\quad \times \left[\frac{1}{i\omega + \gamma \tilde{k}(i\omega)} + \frac{1}{-i\omega + \gamma \tilde{k}(-i\omega)} \right] \\ &= \frac{2k_B T}{m} \Re \left[\frac{1}{i\omega + \gamma \tilde{k}(i\omega)} \right] \\ &= S_{v,eq}(\omega), \end{aligned} \tag{4.13}$$

where $\Re[z]$ denotes the real part. The equivalent of the response or creep function in frequency space is the complex elastic modulus. Consider applying a oscillating probe force $F_p(t) = F_0 e^{i\omega t}$, where for now we allow complex values and take the real or imaginary part afterwards. The response in Laplace space is then given by Eq. (2.96),

$$\langle \tilde{x}(s) \rangle = \frac{F_0}{m} \frac{1}{s^2 + \gamma s \tilde{k}(s)} \frac{1}{s - i\omega}, \tag{4.14}$$

for a particle initially at rest at the origin. For long times $\omega t \gg 1$, we then have in the time domain,

$$\langle x(t) \rangle \simeq F_0 e^{i\omega t} \frac{1}{(i\omega)^2 + \gamma i\omega \tilde{k}(i\omega)}. \tag{4.15}$$

The complex shear modulus $G(\omega)$ is defined as the ratio of the applied force and the response,

$$G(\omega) = \frac{F_p(t)}{\langle x(t) \rangle} = m\big((i\omega^2 + \gamma i\omega \tilde{k}(i\omega)\big). \tag{4.16}$$

Comparing this to Eq. (4.13), we find,

$$S_{v,eq}(\omega) = -2k_B T \omega \Im[G^{-1}(\omega)] = 2k_B T \omega \frac{\Im[G(\omega)]}{|G(\omega)|^2}. \tag{4.17}$$

This is the equivalent of the Stokes-Einstein relation in frequency space [Reif 09]. Where the time space Stokes-Einstein relation Eq. (4.7) links the mean-square displacement to the response to a constant probe force, the frequency space version links the velocity spectral density to the response to an oscillating probe force. The imaginary part $\Im[G(\omega)]$ of the complex modulus is also referred to as the loss modulus (the real part as the storage modulus), since it describes the component of the response that is out of phase with the applied force and thus dissipation into the medium. Hence, the relation between the velocity spectral density and the loss modulus is not surprising as a consequence of the fluctuation-dissipation theorem. For low frequencies $\omega \ll 1/t_{over}$, where t_{over} is the transition time from underdamped to overdamped regime, the complex modulus is asymptotically given by,

$$\begin{aligned} G(\omega) &\simeq m\gamma t_\alpha^{-\alpha} (i\omega)^{1-\alpha} \\ \Re[G(\omega)] &\simeq m\gamma t_\alpha^{-\alpha} \sin\left(\frac{\pi\alpha}{2}\right) \omega^{1-\alpha} \\ \Im[G(\omega)] &\simeq m\gamma t_\alpha^{-\alpha} \cos\left(\frac{\pi\alpha}{2}\right) \omega^{1-\alpha}. \end{aligned} \tag{4.18}$$

These results confirm the physical picture of a viscoelastic medium: In the viscous limit $\alpha \to 0$, the storage modulus is zero and the system is purely dissipative. As the system becomes more and more elastic, the storage modulus increases, while the loss modulus decreases, until for a fully elastic system $\alpha \to 1$, the system is no longer dissipative at all. Both the loss and storage modulus increase with frequency as $\omega^{1-\alpha}$ [Fabr 01, Ball 06, Hoff 09, Bert 12b], so the system at the same time gets more dissipative and rigid as the frequency increases. The increased dissipation is due to the larger velocity of the particle as it is driven with a higher frequency, which leads to a larger viscous friction. At the same time this means that to maintain a certain amplitude of the response at high frequencies a stronger external force is required to counteract the friction, leading to increased rigidity. For the nonequilibrium system, we saw that the velocity spectral density is given by Eq. (3.119),

$$S_v(\omega) \simeq 2a_{\beta-1}\mathcal{C}\Gamma(\beta)\cos\left(\frac{\pi\beta}{2}\right)\omega^{-\beta}. \tag{4.19}$$

Then, imposing a condition similar to the frequency space Stokes-Einstein relation Eq. (4.17), we find a frequency dependent effective temperature,

$$\frac{\mathcal{T}_{\text{eff}}(\omega)}{T} \simeq 1 + \left(\frac{\omega}{\omega_c}\right)^{-\alpha-\beta}$$
$$\text{with} \quad \omega_c = \left(\frac{k_B T t_\alpha{}^\alpha \cos\left(\frac{\pi\alpha}{2}\right)}{a_{\beta-1}\mathcal{C}m\gamma\Gamma(\beta)\cos\left(\frac{\pi\beta}{2}\right)}\right)^{-\frac{1}{\alpha+\beta}}. \tag{4.20}$$

This effective temperature is the frequency space equivalent of Eq. (4.9). Qualitatively, it describes the same behavior with a crossover frequency ω_c: For high frequencies $\omega \gg \omega_c$ (corresponding to short times) the effective temperature is equal to the physical one and the system shows equilibrium behavior. For low frequencies $\omega \ll \omega_c$ (corresponding to long times), on the other hand, the effective temperature in increased with respect to the physical one.

Comparing Eqs. (4.9) and (4.20) immediately poses the question of how the time- and frequency dependent effective temperature are related, or rather, whether there exists a direct relation between the crossover time t_c and the crossover frequency ω_c. Generally, the answer is no, as can be understood from the following argument. The crossover time depends on the ratio between the superdiffusion coefficient D_v and the equilibrium diffusion coefficient D_{eq}. As we saw in Section 3.1.3, the diffusion coefficient D_v is sensitive to whether the medium velocity $v_m(t)$ was initially stationary or not. On the other hand, the velocity spectral density only depends on the small-argument expansion of the velocity scaling function Eq. (3.13), and thus on the stationary velocity correlation function. Consequently, the long-time behavior of the velocity spectral density is independent of whether the system was initially stationary or not. For this reason, the time dependent effective temperature $T_{\text{eff}}(t)$ is sensitive to the initial state of the system, whereas the frequency dependent one $\mathcal{T}_{\text{eff}}(\omega)$ is not, and hence there exists no general relation

between them. If the system is assumed to be initially stationary, however, then the stationary diffusion coefficient is given by Eq. (3.32),

$$D_{v,s} = \frac{a_{\beta-1}\mathcal{C}}{\beta(\beta+1)}. \tag{4.21}$$

In this case, comparing Eqs. (4.6) and (4.20) yields a relation between crossover time and frequency,

$$\omega_c = \frac{1}{t_c}\left(\frac{\Gamma(\beta+2)\cos\left(\frac{\pi\beta}{2}\right)}{\Gamma(2-\alpha)\cos\left(\frac{\pi\alpha}{2}\right)}\right)^{\frac{1}{\alpha+\beta}}, \tag{4.22}$$

which depends only on the exponents α and β. So as a rule of thumb we have $\omega_c \sim 1/t_c$, as expected. For the typical experimental values $\alpha \sim 0.8$ and $\beta \sim 0.6$ the precise relation is $\omega_c \simeq 2.17/t_c$ and should be taken into account when comparing results as a function of time respectively frequency. Since the stationary case is the typical situation for microrheological experiments (see the discussion in Section 4.1.1), we can use Eq. (4.22) to relate the crossover time and frequency and can thus determine either one from the measurement of the mean-square displacement or the spectral density.

4.2.2 *Effective temperature and dynamics on different time scales*

Now that we have defined the effective temperatures Eqs. (4.9) and (4.20), we want to elucidate their physical meaning. For the frequency dependent effective temperature Eq. (4.20), the interpretation is relatively straightforward: The measured velocity spectral density at low frequencies is enhanced by a factor $\mathcal{T}_{\text{eff}}(\omega)/T$ compared to the equilibrium system. In this sense, $\mathcal{T}_{\text{eff}}(\omega)$ is not an actual (thermal or kinetic) temperature but should be interpreted as a measure of how far the system, when considered at a certain frequency, is from its equilibrium state. Similar definitions of an effective temperature have been employed to characterize the out-of-equilibrium behavior of different systems [Cugl 97, Pott 05, Wilh 08, Cugl 11]. In the same way, the time dependent effective temperature should be understood as a statement about time scales rather than a dynamic quantity that increases with time. When observed on short time scales, the system behaves as if in equilibrium, whereas on long time scales the nonequilibrium contribution to the dynamics is dominant. This interpretation is supported by the fact that $T_{\text{eff}}(t)$ not only relates the long-time superdiffusive mean-square displacement to the response to an external force via the generalized Stokes-Einstein relation Eq. (4.8), but also to the short-time equilibrium mean-square displacement,

$$\langle \Delta x^2(t)\rangle \simeq \frac{T_{\text{eff}}(t)}{T}\langle \Delta x^2(t)\rangle_{\text{eq}}. \tag{4.23}$$

The time dependent effective temperature $T_{\text{eff}}(t)$ measures by how much the diffusive dynamics on a certain time scale is enhanced compared to the equilibrium system. The effective temperature can thus also be determined from a solely passive measurement by comparing the short-time subdiffusive and long-time superdiffu-

sive behavior. Similarly, the frequency dependent effective temperature provides a relation between the total spectral density and the equilibrium one,

$$S_v(\omega) \simeq \frac{\mathcal{T}_{\text{eff}}(\omega)}{T} S_{v,\text{eq}}(\omega). \tag{4.24}$$

In the experiment discussed in Section 4.1.1 [Gall 09], the result of comparing the short- and long-time diffusive behavior obtained by passive measurement is $T_{\text{eff}} \sim t^{\lambda}$ with $\lambda = 1.37 \pm 0.07$. This agrees with the value of $\lambda = 1.31 \pm 0.08$ found by comparing the active and passive measurement in Section 4.2.1 within experimental errors.

4.3 SPECTRAL DENSITIES AND NONEQUILIBRIUM NOISE

In the previous section, we obtained the velocity spectral density for $\omega t \gg 1$, Eqs. (4.13) and (4.24),

$$S_v(\omega) = \frac{2k_B T}{m}\left(1 + \left(\frac{\omega}{\omega_c}\right)^{-\alpha-\beta}\right) \Re\left[\frac{1}{i\omega + \gamma(i\omega t_\alpha)^{-\alpha}}\right]. \tag{4.25}$$

The behavior of this expression depends in an intricate manner on the frequency scale. For low frequencies $\omega \ll \omega_c$, while still $\omega t \gg 1$, we can neglect the contribution from the equilibrium spectral density (the 1 in the parentheses) and obtain the nonequilibrium result, Eq. (4.19). If $\omega \gg \omega_c$, the equilibrium contribution Eq. (4.13) to the spectral density dominates. For the equilibrium velocity spectral density, we again find different asymptotic behaviors. For $\omega \ll 1/t_{\text{over}}$, which corresponds to the overdamped dynamics, the second term in the denominator is dominant and we find,

$$S_{v,\text{eq}}(\omega) \simeq \frac{2k_B T {t_\alpha}^\alpha}{m\gamma} \cos\left(\frac{\pi\alpha}{2}\right) \omega^{\alpha}. \tag{4.26}$$

In this regime, the spectral density increases with ω. For $\omega \ll 1/t_{\text{over}}$, on the other hand,

$$S_{v,\text{eq}}(\omega) \simeq \frac{2k_B T\gamma}{m {t_\alpha}^\alpha} \cos\left(\frac{\pi\alpha}{2}\right) \omega^{-\alpha-2}, \tag{4.27}$$

which decreases with ω, indicating a maximum for frequencies $\omega \sim 1/t_{\text{over}}$. In addition to the long-time behavior, we saw in Section 3.3.3 that there is a time-dependent low-frequency cutoff for $\omega t \ll 1$. Summarizing these results, the velocity spectral density behaves as,

$$S_v(\omega, t) \simeq \begin{cases} 2D_v t^{\beta} & \text{for } \omega \ll 1/t \\ 2a_{\beta-1}\mathcal{C}\Gamma(\beta)\cos\left(\frac{\pi\beta}{2}\right)\omega^{-\beta} & \text{for } 1/t \ll \omega \ll \omega_c \\ \frac{2k_B T {t_\alpha}^\alpha}{m\gamma}\cos\left(\frac{\pi\alpha}{2}\right)\omega^{\alpha} & \text{for } \omega_c \ll \omega \ll 1/t_{\text{over}} \\ \frac{2k_B T\gamma}{m {t_\alpha}^\alpha}\cos\left(\frac{\pi\alpha}{2}\right)\omega^{-\alpha-2} & \text{for } \omega \gg 1/t_{\text{over}}. \end{cases} \tag{4.28}$$

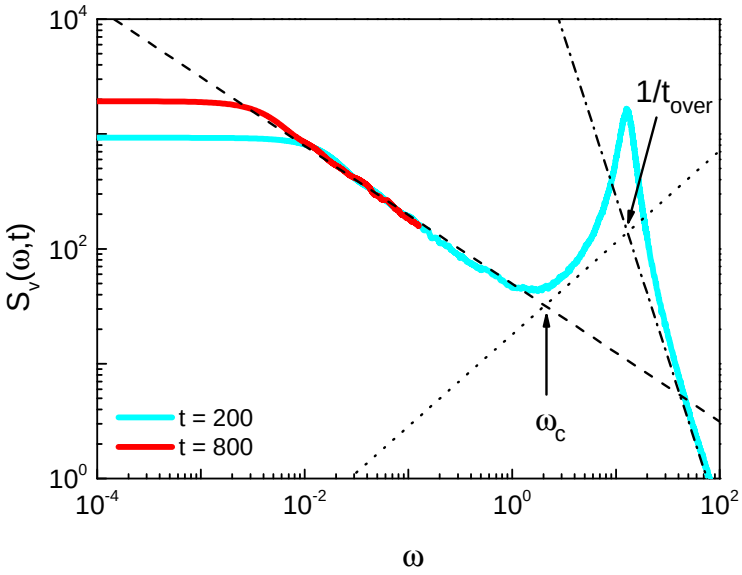

Figure 4.4: Velocity spectral density for $\alpha = 0.8$ and $\beta = 0.6$ as a function of frequency obtained from Langevin simulations (cyan line). The model used for the nonequlibrium motion is the stationary Lévy walk. The asymptotic behavior Eq. (4.28) is indicated by the dashed ($1/t \ll \omega \ll \omega_c$), dotted ($\omega_c \ll \omega \ll 1/t_{over}$) and dash-dotted ($1/t_{over} \ll \omega$) lines. The crossing points between the asymptotes are the corresponding crossover frequencies. Apart from the low-frequency cutoff, the spectral density is time-independent (red line).

The nonmonotonous behavior of the velocity spectral density as a function of frequency, which is shown in Fig. 4.4, yields a wealth of information about the system. The decay for $1/t \ll \omega \ll \omega_c$ and can be used to determine the nonequilibrium exponent β. If the spectral density is evaluated for different measurement times, then this information can be compared with the increase of the value below the cutoff, which also yields information about the nonequilibrium diffusion coefficient. For higher frequencies, there occurs a minimum as the $\omega^{-\beta}$ decay turns into a ω^{α} increase. The position of the minimum is approximately at $\omega \sim \omega_c$ where the crossover between nonequlibrium low-frequency and equilibrium high-frequency behavior occurs. The subsequent maximum, on the other hand, is approximately at $\omega \sim 1/t_{over}$ and thus at the transition from overdamped to underdamped behavior, which is related to the size of the friction coefficient γ. From the high-frequency falloff, the equilibrium exponent α can be extracted. Consequently, the velocity spectral density is well suited to represent both the equilibrium and nonequilibrium dynamics of the system.

Determining the properties of the system from the position spectral density, on the other hand, is not as straightforward. For the equilibrium part, we have instead of Eq. (4.12),

$$\tilde{C}_x(s_2, s_1) = \frac{k_B T}{m s_2 s_1 (s_2 + s_1)} \left[\frac{1}{s_2 + \gamma \tilde{k}(s_2)} + \frac{1}{s_1 + \gamma \tilde{k}(s_1)} \right]. \tag{4.29}$$

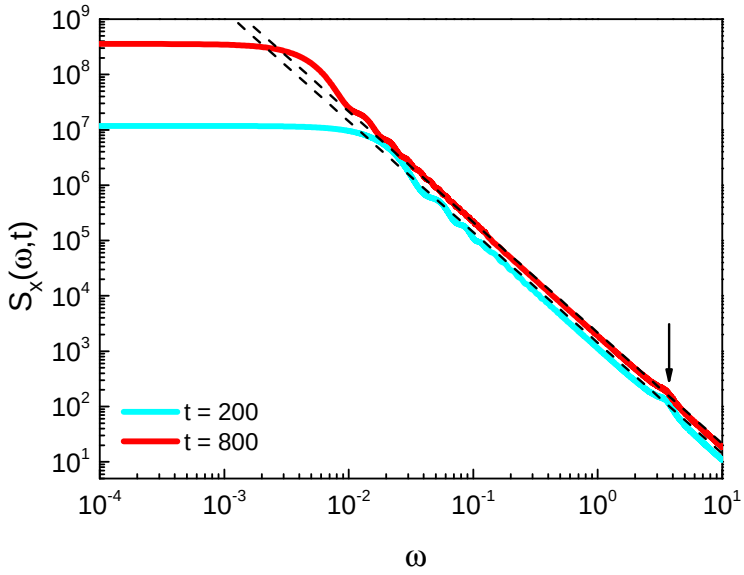

Figure 4.5: Position spectral density for $\alpha = 0.8$ and $\beta = 0.6$ as a function of frequency obtained from Langevin simulations (colored lines). The model used for the nonequlibrium motion is the stationary Lévy walk. Asymptotically, the spectral density decays as ω^{-2}, with a magnitude that increases weakly with time. The dashed lines are the analyitcal result Eq. (3.160). The equilibrium part of the spectral density only appears as a small peak (indicated by the arrow) in the dominant nonequilibrium contribution.

The dominant poles in the Laplace inversion in Eq. (4.10) are still the ones at $s_2 = i\omega$, $s_1 = -i\omega$, so we find the simple relation for $\omega t \gg 1$,

$$S_x(\omega, eq) = \omega^{-2} S_v(\omega, eq). \tag{4.30}$$

Thus the position spectral density decays as $\omega^{\alpha-4}$ for $\omega \ll 1/t_{over}$ (see Fig. 4.5) and as $\omega^{\alpha-4}$ for $\omega \gg 1/t_{over}$. For the nonequilibrium contribution, we saw in Section 3.4 that this relation does not hold due to the superdiffusive nature of the process. The nonequilibrium contribution to the position spectral density behaves as $S_x(\omega, t) \sim t^{\beta}\omega^{-2}$, see Eqs. (3.148) and (3.160) for details. Determining the nonequilibrium exponent β from the position spectral density thus requires measuring the latter over different times and then obtaining β from the observed increase in magnitude at low frequencies. In particular, as noted before, there exists no simple relation like Eq. (4.30) between nonequilibrium contribution to the velocity respectively position spectral density.

Similar considerations hold for the spectral density of the nonequilibrium noise $S_\xi(\omega, t)$, discussed in Section 3.4.3. For the typical value of the exponents $\alpha \sim 0.8$ and $\beta \sim 0.6$, the nonequlibrium noise is nonstationary, see Eqs. (2.62), (2.65) and (2.69). For $t \gg \tau$, the magnitude of the noise correlations increases as $\langle \xi^2(t) \rangle \sim t^{2\alpha+\beta-1} = t^{1.2}$. The external noise process itself is thus superdiffusive and its long-time spectral density is given by $S_\xi(\omega, t) \sim t^{2\alpha+\beta-2}\omega^{-2}$, i.e. depends on frequency as ω^{-2} and increases with time as $t^{0.2}$. At first glance this may seem peculiar, since a noise force that is nonstationary in time, no less with a magnitude that increases superdiffusively, is not a common occurrence. This peculiarity

however stems form the fact, that $\xi(t)$ as defined in Eq. (2.35) is an effective noise force, that describes the viscoelastic coupling to a moving medium. The properties of $\xi(t)$ are more easily understood by imagining applying an external force $-\xi(t)$ to the particle, which exactly cancels out the nonequilibrium motion of the tracer. Since the entire system (i.e. the portion of the cytoskeleton the tracer is attached to) is moving at a velocity $v_m(t)$ and the tracer is viscoelastically coupled to the system, it tends to get displaced further and further from its starting point. Consequently, we need to apply an increasing force to keep the particle in place against the viscoelastic force. Note that the nonstationarity and an increasing magnitude of the nonequilibrium noise is actually a necessity in order to find agreement with the experimentally observed values for the exponents α and β within the fractional Langevin formalism. The most strongly correlated stationary noise possible – although the term noise is not really appropriate – is one that is constant in time $\xi(t) = \xi_0$ with ξ_0 random. This corresponds precisely to the situation with an applied constant external force discussed in Section 2.3.3. There we saw that under these circumstances, the displacement of the particle increases for long times as $x(t) \sim \xi_0 t^{1-\alpha}$. This implies that the mean-square displacement behaves as $\langle \Delta x^2(t) \rangle \sim \langle {\xi_0}^2 \rangle t^{2-2\alpha}$. For $\alpha \sim 0.8$, the mean-square displacement due to a fully correlated noise thus increases as $t^{0.4}$, which is subdiffusive and far from the $t^{1.6}$ behavior found in experiment. Consequently, if we want to describe both sub- and superdiffusion within the framework of the fractional Langevin equation, we require an effective nonequilibrium noise whose magnitude increases with time. The ω^{-2} behavior for the nonequilibrium force spectral density was measured by Lau et al. [Lau 03] for intracellular stress fluctuations using two-point microrheology, which supports our finding for the nonequilibrium noise. If the noise spectrum were time-independent, then this would imply that the scaling exponent for the nonequilibrium noise, Eq. (3.162), is $2\alpha + \beta - 1 = 1$, i.e. that $\beta = 2 - 2\alpha$ [Lau 03]. In this case, we would have found a direct relation between the equilibrium and the nonequilibrium exponent. However, as we discussed above, a ω^{-2} dependence of the nonequilibrium noise spectrum also applies to $2\alpha - \beta - 1 > 1$, i.e. this only tells us that $\beta > 2 - 2\alpha$, which agrees with the typical values extracted from the diffusion exponents. A direct measurement of a time-dependent ω^{-2} nonequilibrium noise spectral density would thus confirm our results and show that, while the equilibrium and nonequilibrium exponents are generally not independent of each other, there is more flexibility in the properties of living cells than the simple equality implies.

For different values of α and β, we find a threshold for stationarity of the nonequilibrium noise at $2\alpha + \beta = 1$, or equivalently at $\nu_{super} - 2\nu_{sub} = 0$, where ν_{sub} and ν_{super} are the diffusion exponents for the sub- and superdiffusive behavior, respectively. For $2\alpha + \beta < 1$, the nonequilibrium noise is stationary. In this regime, we refer to the nonequilibrium dynamics of the tracer particle as "force-like", since we can imagine canceling out the nonequilibrium contribution to the particle's motion by applying a force $-\xi(t)$, whose average magnitude is constant in time. Conversely, we can treat $\xi(t)$ as an actual force acting on the particle embedded in the equilibrium viscoelastic medium. This changes for $2\alpha + \beta > 1$. Here, the nonequilibrium noise is nonstationary and we would have to apply an ever

increasing force to cancel out the nonequilibrium motion. We call the dynamics in this regime "velocity-like", since the particle is being pulled along by the moving viscoelastic medium rather than being displaced relative to the latter by a the nonequilibrium noise. In the situation discussed above, where the tracer is bound to the cytoskeleton itself, we typically have slow subdiffusion ($\alpha \sim 0.8$) and fast superdiffusion ($\beta \sim 0.6$) and the nonequilbrium motion is velocity-like [Trep 08]. For small tracers endogenous to the cell and not bound to the cytoskeleton, the subdiffusion exponent is generally much larger, while the superdiffusion exponent is reduced (see e.g. Ref. [Brun 09], where $\alpha \sim 0.03$ and $\beta \sim 0.36$). This leads to force-like nonequilibrium motion. This distinction points to a fundamental difference between the two situations: The tracer bound to the cytoskeleton is forced to follow the latter's active and rather directed motions, leading to velocity-like dynamics. The tracer dynamics thus directly mirrors the one of the cytoskeleton; a dense network, which is more elastic than viscous (large α) and moves in a very correlated manner (large β) due to the action of molecular motors. For a small tracer not bound to the cytoskeleton, on the other hand, the subdiffusive motion mirrors the mechanical properties of the cytoplasm rather than the cytoskeleton, which are viscous rather than elastic (small α). Moreover, the tracer only experiences the active motion of the cytoskeleton as mediated through the cytoplasm, resulting in less correlated long-time motion (smaller β). This indirect action of the cytoskeletal motion on the tracer also warrants a description in terms of an actual non-equilibrium noise and thus force-like dynamics, as was done in Ref. [Brun 09].

Finally, let us make a few general remark about spectral densities and the associated random processes. For a stationary process, the situation is relatively straightforward: The stationary correlation function and the spectral density are related via a Fourier transform by the Wiener-Khinchine theorem Eq. (3.86). For the particular case of a power-law correlation function, this means that a $\omega^{-\mu}$ decay of the spectral density with $0 < \mu < 1$ corresponds to a $\tau^{\mu-1}$ decay of the correlation function. This is also the result we obtained from our scaling correlation function in Section 3.3.3. There we saw that this result also extends to subdiffusive processes, whose correlation function is nonstationary, but whose spectral density nevertheless exhibits a time-independent $\omega^{-\mu}$ decay with $1 < \mu < 2$. This provides an appealing unification of stationary and subdiffusive processes in terms of their spectral density. However, for subdiffusive processes, the spectral density is not related to the stationary correlation function via a Fourier transform, as the latter does not exists. It would thus be wrong to conclude that a $\omega^{-\mu}$ spectral density with $1 < \mu < 2$ corresponds to a stationary power-law correlation function that increases as $\tau^{\mu-1}$. As we noted in Section 3.4.2, such a $\omega^{-\mu}$ behavior, albeit time dependent, also occurs for the ballistic Lévy walk whose velocity process is not subdiffusive by asymptotically constant. This underlines the fact that the one-to-one correspondence between the power-law exponent of the spectral density and the velocity correlation function breaks down for $\mu > 1$. For superdiffusive systems, we saw in Section 3.3.3 that the spectral density generally exhibits a ω^{-2} decay, which is time-dependent. Here, there is no more relation between the exponent of the frequency dependence of the spectral density and the characteristic exponent of the superdiffusive process. This relation now enters the time dependence of the

spectral density, as a time-independent ω^{-2} behavior corresponds to normal diffusive (Brownian-like) motion, whereas an increasing magnitude of the spectral density is related to superdiffusion. The bottom line is, that one should be aware that the relation between frequency-dependent and time-dependent quantities is not always just a matter of adding exponents. An at first glance simple spectral density may just be hiding the complexities of the dynamics.

4.4 NON-GAUSSIAN STATISTICS AND CONFINEMENT

While the mean-square displacement is a useful measure to describe the diffusive properties of the system, it does not yield much information about the statistics of the involved processes. A notable exception is when the underlying system is Gaussian, then the entire probability distribution of the particle displacement is uniquely determined by the mean and mean-square displacement. There is, however, strong experimental evidence that, while the short-time equilibrium dynamics is indeed Gaussian, the long-time nonequilibrium dynamics in living cells is non-Gaussian [Burs 05, Toyo 11, Gal 13]. It is thus necessary to consider the influence of non-Gaussian statistics. A quantity which expresses the degree to which the statistics differ from Gaussian statistics is the so-called non-Gaussian parameter [Rahm 64],

$$\mathrm{NGP}(t) = \frac{\langle \Delta x^4(t) \rangle}{3\langle \Delta x^2(t) \rangle^2} - 1. \tag{4.31}$$

For a Gaussian process, we have from the Gaussian moment theorem Eq. (3.139), $\langle \Delta x^4(t) \rangle = 3\langle \Delta x^2(t) \rangle^2$ and thus the non-Gaussian parameter is zero. For non-Gaussian processes, $\mathrm{NGP}(t) > 0$ indicates that the fourth moment is bigger compared to a Gaussian process and more weight is given to the tails of the displacement distribution, i.e. that the probability to have unusually large displacements is enhanced. By contrast, $\mathrm{NGP}(t) < 0$ tells us that more weight is given to the center of the distribution; this is typically the case in confined geometries, where there is an upper limit to the maximal displacement that can occur. In experiments [Burs 05] on living cells, this non-Gaussian parameter is initially zero for times much shorter than the crossover time t_c between subdiffusion and superdiffusion, indicating that the equilibrium subdiffusion is indeed Gaussian. It then increases until it reaches its maximum value at roughly the transition time, whereupon it decreases again and finally even becomes negative. The increase of the non-Gaussian parameter as the dynamics are more and more dominated by the nonequilibrium motion of the cytoskeleton indicates that the latter is a non-Gaussian process. In Section 3.4, we discussed the Lévy walk as a possible process to model the velocity of the moving viscoelastic medium. For the Lévy walk, the non-Gaussian parameter increases as [Rebe 13],

$$\mathrm{NGP}(t) \simeq \frac{\beta^2(\beta+1)^2(2-\beta)}{3(1-\beta)(\beta+2)(\beta+3)} \left(\frac{t}{t_\beta}\right)^{1-\beta} - 1. \tag{4.32}$$

However, the above only holds for long times, if the displacement of the tracer particle is allowed to increase arbitrarily. In actual experiments, the maximal displacement is limited by the size of the cell, providing a cutoff on the displacement

distribution. Such a cutoff affects the fourth moment of the displacement – which depends strongly on the tails of the distribution – more strongly than the second moment, reducing the non-Gaussian parameter. Since large displacements occur for long times, the impact of confinement due to the finite extension of the cell increases with time. Thus the non-Gaussian parameter will typically reach a maximum value, where the particles' behavior is dominated by the nonequilibrium dynamics but not yet by the confinement. For longer times, confinement effects become important and the non-Gaussian parameter decreases again and may even become negative, which indicates that large displacements are suppressed compared to a Gaussian distribution. For a confined geometry, the particles will eventually be uniformly distributed over the volume, which leads to $\mathrm{NGP} = -2/5$ in one dimension or $-1/10$ in a circular two-dimensional confinement. Qualitatively, this mirrors the experimentally observed behavior of the non-Gaussian parameter [Burs 05, Toyo 11, Gal 13]. Confinement is also expected to lead to a reduction in the mean-square displacement, which coincides with the experimental observations [Burs 05] on time scales of several tens of seconds, where the superdiffusive behavior is diminished.

In our numerical simulations, we include confinement by placing the particle in a potential $U(x) \sim (x/x_c)^{12}$, where the large exponent is chosen to approximate a hard-wall potential. We choose the length scale x_c of the confinement such that the mean-square displacement deviates from the superdiffusive behavior at around 40 s, akin to what is observed in experiments. The mean-square displacement and non-Gaussian parameter for the parameters in Eq. (4.2) are shown in Figs. 4.6 and 4.7. Compared to the experimental results in Fig. 4.8, we note that, in the experiment the maximum value for the non-Gaussian parameter occurs at roughly the transition time from sub- to superdiffusion. By contrast, the numerical simulations exhibit a maximum at a later time, roughly where the mean-square displacement starts to deviate from the superdiffusive behavior due to confinement. The latter behavior is what we intuitively expect: Since both the anomalous diffusion and the non-Gaussian behavior are due to long periods of ballistic motion, which the confinement effectively truncates, the effect of confinement on the mean-square displacement and the non-Gaussian parameter should be noticeable at roughly the same time. Why then is the experimentally observed behavior different? A clue to this may be found by noting that all curves for the non-Gaussian parameter in Fig. 4.8 tend towards the same negative value at about 10 s. This in itself might be explained with the displacement distribution becoming uniform. However, at the same time, the mean-square displacement continues to grow significantly for even longer times, which contradicts an almost uniform distribution. Further, the gray curve in the figure represents a control bead, which was glued to the coverslip. Here, the non-Gaussian parameter is almost zero (as expected, since it should only experience Gaussian thermal fluctuations) before reaching the same negative value at long times. But a bead glued to the coverslip is not subject to the enhanced active diffusion of those bound to the cytoskeleton and should not feel a possible confinement in the same manner. Since the non-Gaussian parameter nevertheless tends to the same negative value at precisely the same time, we speculate that the sharp decrease of the non-Gaussian parameter observed in this experiment

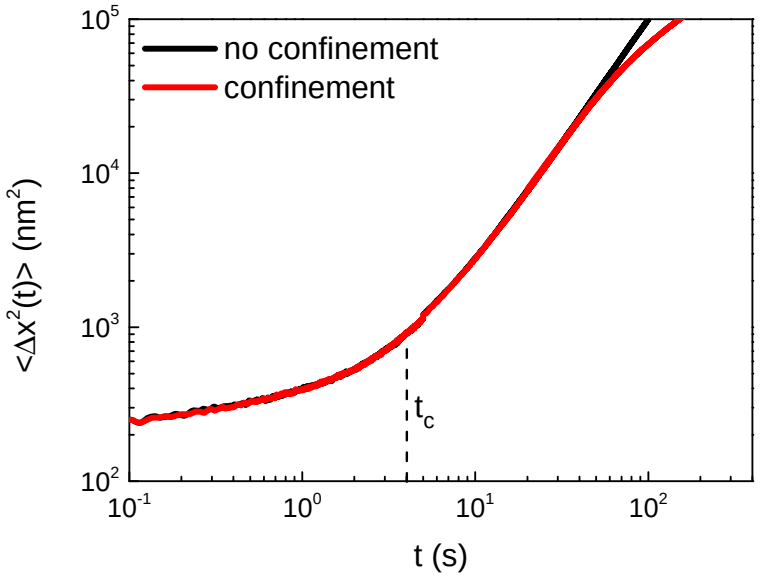

Figure 4.6: Mean-square displacement Eq. (4.1) as a function of time, numerical Langevin simulations for the parameters of Eq. (4.2). Confinement (red line) leads to a reduction of the mean-square displacement compared to the unconfined superdiffusive motion (black line) for long times.

may be an artifact of the data analysis procedure. If true, this would imply that the maximum in the non-Gaussian parameter might actually occur at a later time. This conclusion is supported by the findings of Ref. [Gal 12], where the maximum of the non-Gaussian parameter was indeed found to occur at the same time as deviations from the superdiffusive behavior, although not for beads bound to the cytoskeleton but for tracers in the cytoplasm. Finally, we note that the long-time reduction of the mean-square displacement and the decrease of the non-Gaussian parameter could also be attributed to binding and unbinding of molecular motors from the actin filaments, and thus a cutoff on the maximal duration of ballistic motion [Kuli 08, Gal 12]. We included such a cutoff on the waiting time distribution of the Lévy walk in our simulations, however, the result is qualitatively the same as for confinement: The maximum in the non-Gaussian parameter occurs at the same time as the deviations from superdiffusion. To conclude, while our model is able to include non-Gaussian effects in general, whether these agree quantitatively with what is found in experiments is yet inconclusive.

The fact that the process is non-Gaussian leads to direct consequences for the measurement: In Section 3.4.2, we saw that the non-Gaussian nature of the Lévy walk leads to enhanced variation in time-averaged square displacement between individual trajectories. This enhanced variation compared to a Gaussian process is of course not only present in time averages but also in the instantaneous displacement. While this does not change the values of ensemble averaged quantities like the mean-square displacement, it does necessitate better statistics, i.e. a larger number of trajectories, to reliably reproduce those ensemble averages. The occurrence of unusually large displacements is more likely and leads to greater variation

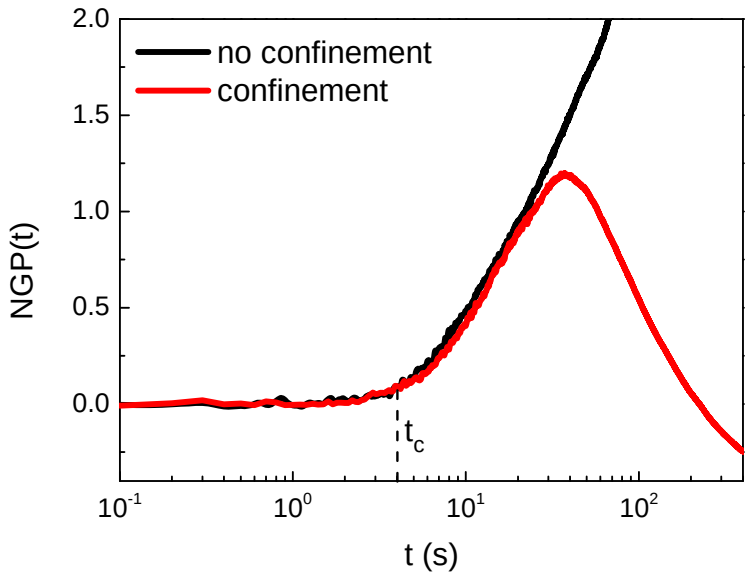

Figure 4.7: Non-Gaussian parameter Eq. (4.31) as a function of time, numerical Langevin simulations for the parameters of Eq. (4.2). For short-time equilibrium subdiffusion, the non-Gaussian parameter is zero and the process is Gaussian. At the transition from sub- to superdiffusion, the non-Gaussian parameter starts to grow, indicating the increasingly non-Gaussian properties of the process. For unconfined motion, the non-Gaussian parameter for the Lévy walk grows indefinitely (black line). However, once confinement effects become important, the non-Gaussian parameter decreases and eventually becomes negative as the distribution approaches a uniform distribution (red line). Note that the maximal value of the non-Gaussian parameter occurs at roughly the same time, where the mean-square displacement noticeably deviates from superdiffusion (see Fig. 4.6).

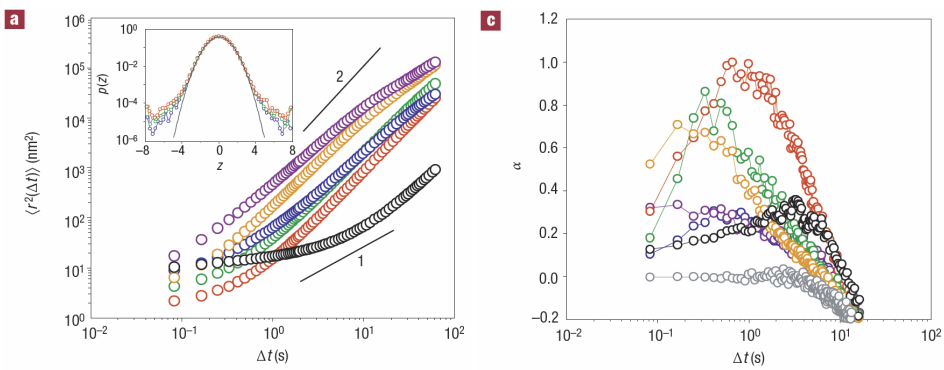

Figure 4.8: Experimentally observed mean-square displacement (left) and non-Gaussian parameter (right) of tracer beads bound to the cytoskeleton. The transition from sub- to superdiffusion in the mean-square displacement occurs at roughly the same time as the maximum of the non-Gaussian parameter. For long times, the mean-square displacement deviates slightly from the superdiffusive behavior, which may be due to confinement or a maximum time for which directed motion occurs. Image taken from [Burs 05].

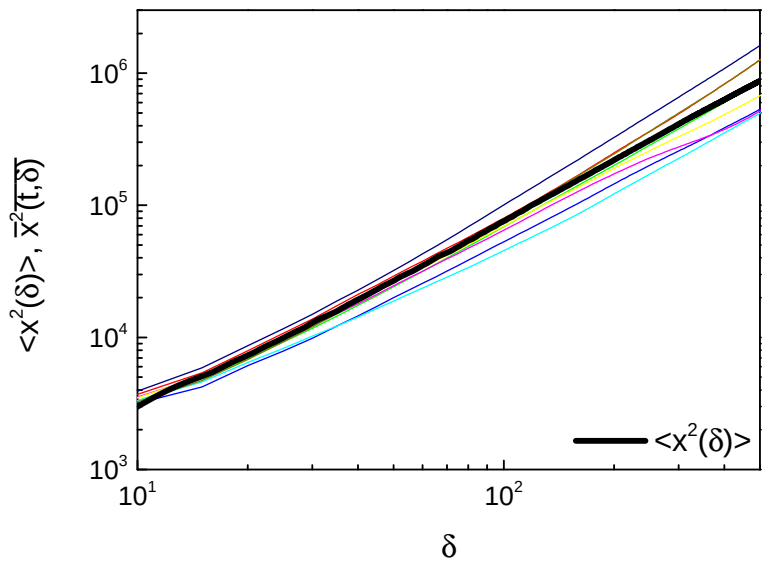

Figure 4.9: Mean-square displacement (thick black line) and several realizations (thin colored lines) for the time-averaged square displacement, Langevin simulations for stationary fractional Brownian motion with $\beta = 0.6$ and averaging time $t = 5000$. While due to the finite averaging time, there are variations between individual trajectories, the ensemble average is reproduced rather accurately by the time average.

between individual trajectories and in particular to a larger number of trajectories that deviate strongly from the average behavior. These unusually large displacements can even be seen on the level of individual trajectories, see Fig. 4.11, and are caused by long ballistic flights during which the velocity of the particle does not change. Even if the system is in principle ergodic (see the discussion in Section 3.4), this causes a considerable distribution of diffusion coefficients obtained from the time-averaged square displacement [Froe 13], see Fig. 4.10, compared to the Gaussian case shown in Fig. 4.9.

4.5 LINEAR RESPONSE

So far, we mostly considered the diffusive dynamics of the system and only referred to the response to an external force insofar as it is related to the former by the Stokes-Einstein relation. However, due to the long-range temporal memory in the system, the response itself exhibits some interesting and nonintuitive properties. In particular, similar to the diffusive dynamics, initial conditions play an important role and the response may exhibit aging.

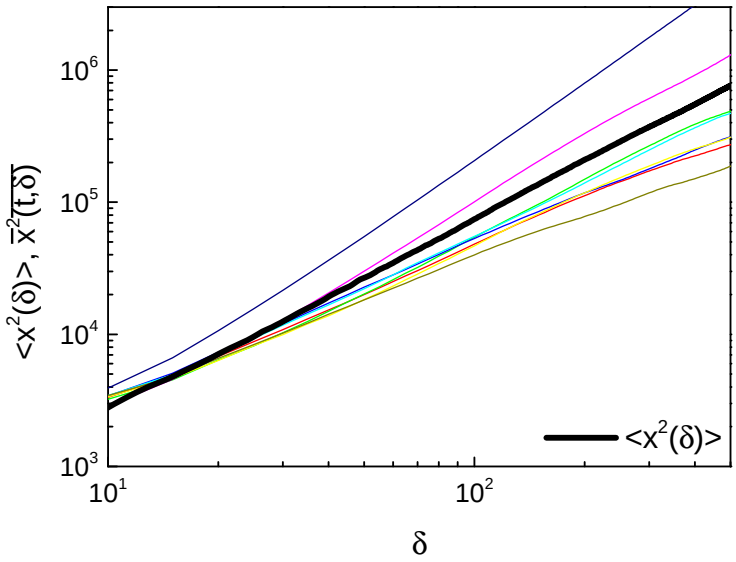

Figure 4.10: Mean-square displacement (thick black line) and several realizations (thin colored lines) for the time-averaged square displacement, Langevin simulations for the stationary Lévy walk $\beta = 0.6$ and averaging time $t = 5000$. Compared to the Gaussian case, the variations between individual trajectories are greatly enhanced, even though the system is in principle ergodic. Accurately determining the diffusion exponent and coefficient from a single trajectory thus requires exceedingly long averaging times.

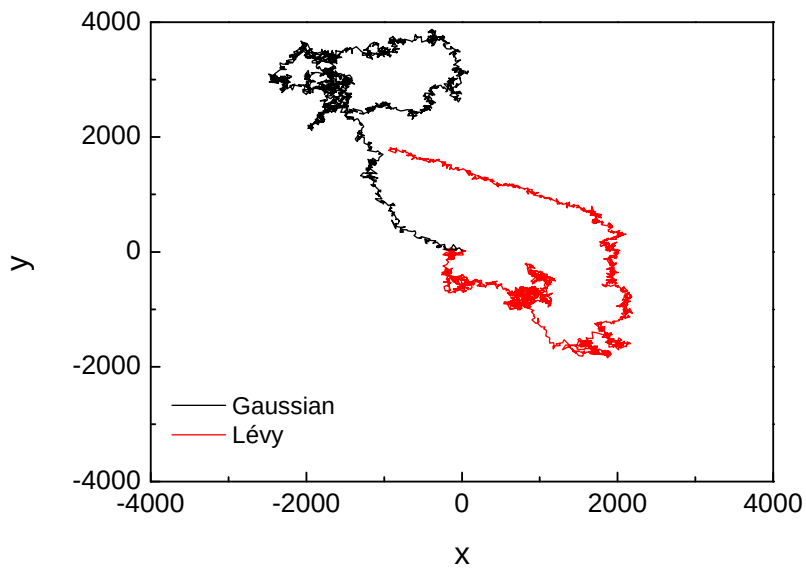

Figure 4.11: Typical trajectories from Langevin simulations for fractional Brownian motion (black) and the Lévy walk (red) for $\alpha = 0.8$, $\beta = 0.6$ and parameters that lead to the same mean-square displacement. In the Gaussian case, while the motion is highly correlated on long time scales, it is more or less homogeneous in time. For the Lévy walk, on the other hand, periods of inactivity alternate with long ballistic flights.

4.5.1 *Creep function, initial conditions and diffusion*

The creep function for the viscoelastic medium described by the fractional Langevin equation was obtained in Eq. (2.101)

$$J(t) = \frac{1}{m} t^2 E_{\alpha+1,3}\left(-\gamma t_\alpha \left(\frac{t}{t_\alpha}\right)^{\alpha+1}\right)., \tag{4.33}$$

and the response of the particle is given by,

$$\langle x(t)\rangle = \langle x_0\rangle + \int_0^t dt'\, J(t-t')\frac{\partial F_p(t')}{\partial t'} + J(t)F_p(0) + m\langle v_0\rangle \frac{\partial J(t)}{\partial t}. \tag{4.34}$$

For now, we will stick to the case of a constant force $F_p(t) = F_0$, and thus,

$$\langle x(t)\rangle = F_0 J(t) + m\langle v_0\rangle \frac{\partial J(t)}{\partial t}. \tag{4.35}$$

Where we assumed that we measure the displacement of the particle relative to its initial position and set $x_0 = 0$. For long times, the creep function asymptotically behaves as Eq. (2.105) and we have for the long-time displacement,

$$\langle x(t)\rangle = \frac{{t_\alpha}^\alpha}{\Gamma(2-\alpha)m\gamma}\left(F_0 t^{1-\alpha} + (1-\alpha)m\langle v_0\rangle t^{-\alpha}\right). \tag{4.36}$$

The displacement thus slowly increases as a power-law in time, in contrast to the purely viscous normal diffusive case $\alpha \to 0$, where the displacement is linear in time. As discussed in Section 2.3.3, this slow sublinear growth leads to a velocity that tends to zero despite a constant applied force. This "death of response" [Rice 12] is due to the elastic component of the medium, however, in contrast to the fully elastic case $\alpha \to 1$, the displacement continues to grow and does not saturate at a constant value. Another important difference to the normal case is that the effect of the initial velocity on the displacement decays a power-law decay, whereas in a viscous medium it leads to a constant contribution. This effect is also caused by the elastic-like behavior, which causes the particle to slowly return to its initial position. In both cases, the initial velocity can only be neglected for long times, $t \gg (1-\alpha)m\langle v_0\rangle/F_0$.

While the random nonequilibrium motion of the tracer does not impact the ensemble average of the displacement, it may have a substantial effect on individual trajectories. We saw in Section 4.1.1 that the mean-square displacement for long times grows as $\langle \Delta x^2(t)\rangle \sim t^{\beta+1}$. The average displacement, on the other hand, grows as $\langle x(t)\rangle \sim t^{1-\alpha}$ according to Eq. (4.36). The total squared displacement is composed of the mean-square displacement plus the square of the average displacement,

$$\begin{aligned}\langle x^2(t)\rangle &= \langle \Delta x^2(t)\rangle + \langle x(t)\rangle^2 \\ &\simeq 2D_\nu t^{\beta+1} + \frac{{t_\alpha}^{2\alpha}{F_0}^2}{\Gamma^2(2-\alpha)m^2\gamma^2} t^{2-2\alpha}.\end{aligned} \tag{4.37}$$

For the typical values of $\alpha \sim 0.8$ and $\beta \sim 1.6$, the term due to the mean-square displacement increases much faster than the contribution from the average displacement. This means that for long times, the standard deviation of the particle displacement grows faster than its average, making the result from a single trajectory less and less reliable. For finite times, this can be circumvented using a large enough probe force, however, at some point the nonequilibrium diffusive motion will win over. The experimental relevance of this issue of course depends on the relative values of the diffusion coefficient D_ν and the applied force, especially since the extension of the cell is finite and confinement effects may become important even prior to that. In principle, however, this means that it is not possible to measure the response of the tracer to an arbitrarily small force. This is in contrast to the equilibrium case, where the mean-square displacement grows as $\langle \Delta x^2(t)\rangle_{eq} \sim t^{1-\alpha}$ and any small force will eventually lead to a discernible effect on the particle's displacement for sufficiently long times.

4.5.2 *Aging and history dependence of the response*

While the added displacement due to the initial velocity is negligible for long times, there can be substantial aging effects in the response of the particle to an external force. In the following we consider a simple protocol for the applied probe force: First a constant force F_i is applied for a time t_i, then we let the system relax in the absence of an external force for a time t_w and finally we apply a constant force F_m and measure the displacement of the particle for a time t_m,

$$F_p(t) = \begin{cases} 0 & \text{for } t < 0 \\ F_i & \text{for } 0 < t < t_i \\ 0 & \text{for } t_i < t < t_i + t_w \\ F_m & \text{for } t_i + t_w < t. \end{cases} \tag{4.38}$$

The corresponding displacement we write in terms of the response function $R(t)$, Eq. (2.98) instead of the creep function to avoid having to deal with the derivatives at the discontinuities of the force,

$$\langle x(t)\rangle = \frac{1}{m}\int_0^t dt'\, R(t-t')F_p(t'), \tag{4.39}$$

where we assume that the particle is initially at rest at the origin. We want to evaluate the displacement $\langle \Delta x(t_m)\rangle$, relative to the displacement a time $t = t_i + t_w$ as a function of the measurement time $t_m = t - t_i - t_w$. t_m is the time that has elapsed after applying the force F_i, which we term prestress, and waiting for a time t_w. Then we have,

$$\begin{aligned} \langle \Delta x(t_m)\rangle &= \langle x(t)\rangle - \langle x(t_i + t_w)\rangle \\ &= \frac{1}{m}\Bigg[\int_0^{t_i+t_w+t_m} dt'\, R(t_i + t_w + t_m - t')F_p(t') \\ &\quad - \int_0^{t_i+t_w} dt'\, R(t_i + t_w - t')F_p(t')\Bigg]. \end{aligned} \tag{4.40}$$

The response function in time space is given by,

$$R(t) = tE_{\alpha+1,2}(-\gamma {t_\alpha}^{-\alpha} t^{\alpha+1}). \tag{4.41}$$

Then we have for Eq. (4.40), using the force protocol Eq. (4.38),

$$\begin{aligned}\langle \Delta x(t_m)\rangle = \frac{1}{m}\Bigg[& F_i \int_{t_w+t_m}^{t_i+t_w+t_m} dt'\, t' E_{\alpha+1,2}(-\gamma {t_\alpha}^{\alpha} {t'}^{\alpha+1}) \\ & + F_m \int_0^{t_m} dt'\, t' E_{\alpha+1,2}(-\gamma {t_\alpha}^{\alpha} {t'}^{\alpha+1}) \\ & - F_i \int_{t_w}^{t_i+t_w} dt'\, t' E_{\alpha+1,2}(-\gamma {t_\alpha}^{\alpha} {t'}^{\alpha+1})\Bigg]\end{aligned} \tag{4.42}$$

To evaluate the integrals we use the integral identity for the Mittag-Leffler function,

$$\int dt\, t^{b-1} E_{a,b}(ct^a) = t^b E_{a,b+1}(ct^a), \tag{4.43}$$

which is straightforward to prove using the definition of the Mittag-Leffler function Eq. (2.19). With the expression Eq. (4.33) for the creep function, we get,

$$\langle \Delta x(t_m)\rangle = F_m J(t_m) - F_i\Big[J(t_i+t_w) + J(t_w+t_m) - J(t_i+t_w+t_m) - J(t_w)\Big]. \tag{4.44}$$

For $F_i = 0$ or $t_i = 0$, i.e. no prestress, this reduces to,

$$\langle \Delta x(t_m)\rangle = F_m J(t_m), \tag{4.45}$$

precisely the expression for the creep in the presence of a constant force we obtained previously, Eq. (2.103). Otherwise, the behavior of the displacement depends strongly on the relative size of the involved time scales. If there is no waiting time between applying the prestress and the measurement $t_w = 0$, and we assume that the involved time scales t_m, t_i are long compared to the transition time $t_{over} = t_\alpha(\gamma t_\alpha)^{-1/(\alpha+1)}$, then we can use the large argument expansion of the Mittag-Leffler function Eq. (2.23) and find,

$$\begin{aligned}\langle \Delta x(t_m)\rangle \simeq & \frac{{t_\alpha}^{\alpha}}{\gamma m \Gamma(2-\alpha)} F_m {t_m}^{1-\alpha} \\ & \times \left[1 - \frac{F_i}{F_m}\left[1 + \left(\frac{t_i}{t_m}\right)^{1-\alpha} - \left(1+\frac{t_i}{t_m}\right)^{1-\alpha}\right]\right].\end{aligned} \tag{4.46}$$

The expression within the inner square brackets is always positive, so that the response is reduced compared to the case of no prestress if F_i and F_m have the same sign and enhanced otherwise. This describes the expected elastic-like behavior of the viscoelastic medium: If a spring is already extended before extending it further, the relative response is diminished, while if it was compressed before, the response is enhanced. This means that the displacement of the particle ages as a function of the system's history. For $t_i \gg t_m$, this further simplifies to,

$$\langle \Delta x(t_m)\rangle \simeq \frac{{t_\alpha}^{\alpha}}{m\gamma\Gamma(2-\alpha)}(F_m - F_i){t_m}^{1-\alpha}. \tag{4.47}$$

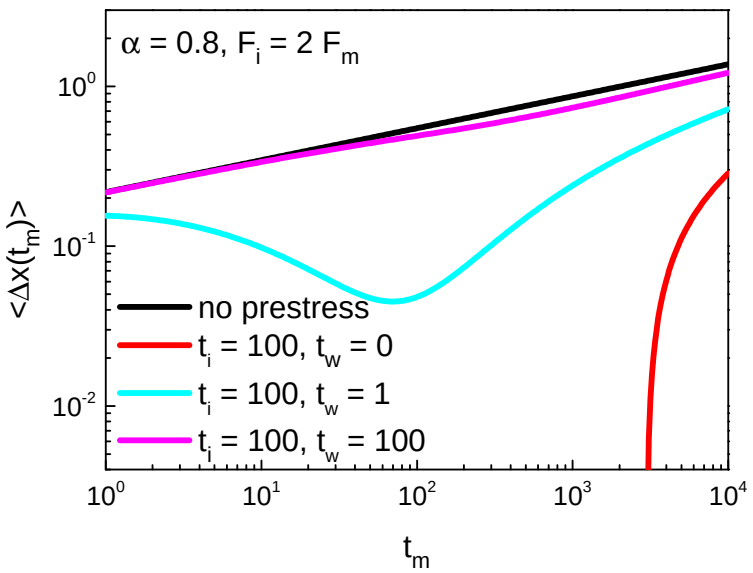

Figure 4.12: Response to an applied external force as a function of time and prestress for $\alpha = 0.8$ and $F_i = 2F_m$. If no force is applied to the system before the start of the measurement, the response follows a power-law with exponent $1-\alpha$ (black). If a prestress is applied that exceeds the measurement force, the particle will initially move in the opposite direction and only follow the applied force for times much longer than the applied prestress (red). If the system is allowed to relax between the application of the prestress and the measurement, then the response is unaffected by the prestress (magenta). This turnover is a consequence of the interplay of viscous and elastic behavior and thus characteristic for viscoelastic systems. For a short waiting time, the system may exhibt a turnover between first following the measurement force for up to $t \sim t_w$ when the delayed response to the prestress forces it to reverse before it again follows the applied force for long times (cyan).

Here, while the displacement also behaves as ${t_m}^{1-\alpha}$ as in the case of no prestress, the prefactor now depends on the difference of the measurement force and the prestress. If $F_m > F_i$, the measurement force is strong enough to displace the particle further against the restoring force, otherwise, the particle slowly relaxes towards its initial position against the measurement force. On the other hand, if $t_m \gg t_i$, then we have,

$$\langle \Delta x(t_m) \rangle \simeq \frac{{t_\alpha}^\alpha}{m\gamma\Gamma(2-\alpha)} \left[F_m {t_m}^{1-\alpha} - F_i {t_i}^{1-\alpha} \right]. \tag{4.48}$$

In this case, the behavior depends in a sensitive manner on the relative sizes of both the involved time scales and forces. If $F_m {t_m}^{1-\alpha} \gg F_i {t_i}^{1-\alpha}$, then the measurement is almost unaffected by the prestress, however if $F_m {t_m}^{1-\alpha} \ll F_i {t_i}^{1-\alpha}$, then the relaxation out of the prestressed configuration dominates the behavior. If we allow for a finite waiting time t_w before starting the measurement, then, if $t_w \ll t_i$, we reobtain the results above, since the waiting time is too short for the system to relax from the prestress. On the other hand, if $t_w \gg t_i$, then the prestress is almost gone at the beginning of the measurement and the system behaves as if no prestress was applied.

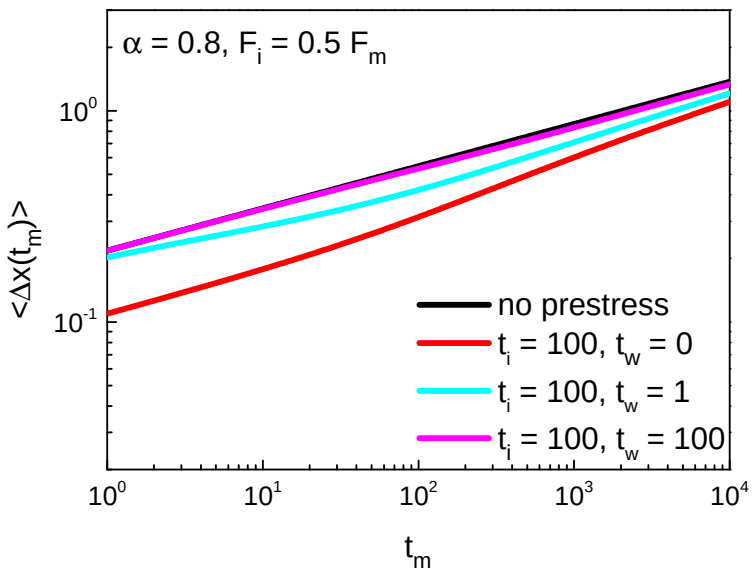

Figure 4.13: Response to an applied external force as a function of time and prestress for $\alpha = 0.8$ and $F_i = 0.5F_m$. If the magnitude of the prestress is smaller than the measurement force, the particle will always move in the direction of the latter. For long waiting times, the effect of the prestress on the displacement becomes negligible (magenta), whereas if the measurement starts immediately after applying the prestress the response may be reduced significantly (red).

These limiting cases highlight that the response of the system depends in a intricate manner on its previous history, see also Figs. 4.12 and 4.13. Note that in these examples, all involved time scales are much longer than the overdamped transition time $t_{over} \sim 10^{-3}$. A peculiarity, which represents the scale-free long-time dynamics of the system, is that there is no intrinsic relaxation time for the system to lose its history dependence. The waiting time necessary for the prestress to no longer affect the measurement depends directly on the duration of the prestress. This is very different from the viscous case $\alpha \to 0$, where we have from Eq. (4.44),

$$\langle \Delta x(t_m) \rangle \simeq \frac{F_m}{m\gamma} t, \tag{4.49}$$

which apart from exponentially small short-time corrections is entirely independent of the history. This shows that the aging of the response described above is characteristic for the long-time memory present in the system. Aging and history dependence in the response to an external force is known from colloidal glasses [Vias 02, Dere 03]. However, there the aging effects are of a different nature. The microscopic structure of these systems possesses metastable states in which they may get stuck after applying an external stress and only slowly relax to their equilibrium configuration. A characteristic feature of this kind of dynamics is the so-called rejuvenation: Applying a large oscillatory stress provides the necessary energy for the system to overcome its internal energetic barriers and relax out of a metastable state. Such an oscillatory stress thus greatly reduces the effect of aging and rejuvenates the system. This effect is absent in our case, since the aging here is due to the viscoelastic behavior of the medium and not due to the microscopic ener-

getics. The aging effects in living cells observed in [Burs 05] are of the energetic type. There, a measurable reduction in the response was observed even for waiting times much longer than the initially applied prestress, and the response was significantly enhanced by a rejuvenation protocol. By contrast, the viscoelastic type of aging described above displays a characteristic dependence of the waiting time on the duration of the prestress and the relative magnitude of the latter and the measurement force, which allows to distinguish it from the energetic kind of aging. Observing this history dependence of the response in cells would provide a strong indication that the equilibrium dynamics are indeed described by the fractional Langevin type of motion.

5 DISCUSSION AND OUTLOOK

Analogous to the title of this thesis, we can divide its main results into two distinct but related groups: Those concerning the model for nonequilibrium dynamics in living cells and its application to experiments; and those relevant to superdiffusive scaling systems in a more general context. We start by discussing the latter, since these results also have implications for the dynamics in cells.

Scale invariant superdiffusive systems

In Section 3.1, we introduced a general scaling form for a velocity correlation function, which describes correlated, scale-invariant velocity dynamics. It includes stationary power-law correlations and typical aging correlation functions as special cases. Despite this generality, we were able to derive a number of important physical quantities and relations from the existence of this scaling correlation function. These relations will hold for any system described asymptotically by such a scaling correlation function.

The first central result is a generalization of the Green-Kubo formula, termed scaling Green-Kubo relation, derived in Section 3.1.2. The long-time correlations implied by the scaling behavior of the correlation function lead to superdiffusion, $\langle \Delta x^2(t) \rangle = 2D_\nu t^\nu$. The anomalous diffusion coefficient is determined by an integral over a scaling function, which captures the aging properties of the system. In this regard, the scaling Green-Kubo relation is similar to the original Green-Kubo formula, which expresses the normal diffusion coefficient as an integral over the stationary velocity correlation function. Aside from providing a universal relation between the scaling correlation function and the anomalous diffusion coefficient and exponent, the scaling Green-Kubo relation also reveals a substantial difference between the normal diffusive and superdiffusive case (Section 3.1.3). For normal diffusion, the initial state of the system has no influence on the asymptotic diffusive behavior, i.e. the diffusion coefficient. The long-range correlations present in superdiffusive systems, on the other hand, leads to the peculiar situation that the diffusive behavior depends on the initial state of the system even for long times.

The second central result is that for scale-invariant systems, ergodicity and stationarity are intimately related. As our explicit calculation of the time-averaged square displacement in Section 3.2 shows, for superdiffusive scale-invariant dynamics, ergodicity requires the system to be initially stationary. If the system is nonstationary, the time- and ensemble-averaged square displacements are not equivalent and the system is not ergodic with respect to the mean-square displacement. On the one hand, this generally prevents substituting time averages for ensemble averages, as one is used to from ergodic systems. On the other hand, it can serve to probe the stationarity of the system by comparing time and ensemble averages.

The third central result is a scaling from for the spectral density, which generalizes the Wiener-Khinchine theorem to nonstationary scale-invariant processes. This generalization derived in Section 3.3 relates the asymptotic behavior of the spectral density to the properties of the scaling correlation function of the respective process in a straightforward manner. Contrary to the usual stationary processes, the nonstationarity introduces a time-dependence in the spectral density. However, if the process is at most subdiffusive, as is the case for the velocity, the spectral density becomes time-independent in the long-time limit, even though the process itself is nonstationary. For superdiffusive processes like the position, the time-dependence of the spectral density persists in the long-time limit. In both cases, there exists a time-dependent low frequency cutoff.

All these results are fundamentally related to the scale-invariance of the underlying dynamics. Scale-invariance means that there are no intrinsic time scales that govern the dynamics. In the scaling velocity correlation function, this absence of intrinsic time scales manifests itself in two ways. The first is an algebraic dependence on time, the second is the occurrence of a scaling function which depends on the ratio of the time lag τ and the age t of the system. The scaling function reveals an important consequence of the scale-invariance: In the absence of any characteristic intrinsic time scales, it is the age of the system that sets the time scale for the decay of the velocity correlations. This importance of relative time scales carries through to all other results: The relaxation time sets the time scale on which the system can be considered as stationary. Which expression for the diffusion coefficient is appropriate and also whether the system is ergodic thus depends on the relative size of the measurement time and the relaxation time. For the spectral density, it is the measurement time which sets the frequency scale and determines what constitutes a low or high frequency.

Since the above results only depend on the scaling velocity correlation, they can be applied in a straightforward manner to different systems. Both fractional Gaussian processes and the Lévy walk are paradigmatic examples for scale-invariant systems, although the actual dynamics and the associated trajectories are qualitatively very different. Our treatment unifies these processes within a common framework and exposes the common properties due to their scaling behavior (see Section 3.4). In a broader context, it is also applicable to other scale invariant systems, a notable example being diffusion in optical lattices, where the long-range correlations are induced by a nonlinear velocity-dependent dissipation [Dech 14]. Considering the conceptual differences between these processes, the fact that several key quantities, among those the mean square displacement and spectral densities, are determined by the processes' scaling behavior indicates that the latter is a fundamental property rather than a chance occurrence. Both the Green-Kubo formula and the Wiener-Khinchine theorem are central and invaluable results of nonequilibrium statistical mechanics. We generalized them to scale-invariant processes, both stationary and nonstationary, and showed that these generalizations directly lead to a number of insights about this important class of stochastic processes.

Nonequilibrium dynamics in living cells

The stochastic model for superdiffusive nonequilibrium dynamics in living cells, which we introduced in Chapter 2, is based on the fractional Langevin equation. It is mainly aimed at describing the motion of a tracer bead coupled to the cytoskeleton and in particular the transition from subdiffusion to superdiffusion, though it is general and flexible enough to be applied to other experimental situations, e.g. the diffusion of tracers within the cytoplasm. The two main ingredients of our model are the equilibrium fractional Langevin equation for diffusion in a viscoelastic medium and the random medium velocity process $v_m(t)$, which captures the nonequilibrium motion of the viscoelastic medium itself. In the present case, the viscoelastic medium is the cytoskeleton of an eukaryotic cell and its motion is due to molecular motors acting on the fibers making up the cytoskeleton. As above, we summarize our findings as three central results.

Firstly, the moving viscoelastic medium model reproduces the experimentally observed transition from short-time subdiffusion to long-time superdiffusion, see Section 4.1. While the equilibrium fractional Langevin equation results in anticorrelated subdiffusion with diffusion exponent $1-\alpha$, the correlated medium velocity induces superdiffusion with exponent $\beta+1$ on long times. Here α and β are the exponents characterizing the viscoelastic properties of the medium and the medium velocity process $v_m(t)$, respectively. Subdiffusion is thus attributed to the equilibrium mechanical properties of the cytoskeleton and its thermal fluctuations. Superdiffusion, on the other hand, arises from the correlated motion of the cytoskeleton, which is being driven out of equilibrium by the action of molecular motors. The universality of the diffusion exponents [Trep 08] implies that those mechanisms are qualitatively the same for a range of different cells. Beyond the diffusive behavior, our model, like the equilibrium model it is based on, incorporates the anomalous, sublinear response to an external force. Further, we are able to account for the non-Gaussian nature of the nonequilibrium dynamics observed in experiments by using the non-Gaussian Lévy walk as the medium velocity process. In this way, we find good qualitative agreement between the trajectories described by our stochastic model and the intermittent trajectories observed in experiment. Finally, our treatment also provides a unification of two previous models for the transition from sub- to superdiffusion [Metz 07, Brun 09], which emerge as special cases.

Our second central result are the generalized nonequilibrium Stokes-Einstein relation and the effective temperature introduced in Section 4.2. The Stokes-Einstein relation expresses the response of a tracer particle to an external force in terms of the temperature and the mean-square displacement. This connects active and passive measurement, as measuring the response fixes the mean-square displacement and vice versa. However, being a direct consequence of the fluctuation-dissipation theorem, the Stokes-Einstein relation is only valid for equilibrium systems and consequently breaks down for living cells, which are by definition out of equilibrium. By defining a time-dependent effective temperature, we obtain a generalized non-equilibrium Stokes-Einstein relation. In our model, the same effective tempera-

ture also governs the transition between the short-time subdiffusive and long-time superdiffusive behavior, and can be expressed as a function of the diffusion exponents and the transition time. Thus the effective temperature can be obtained solely from the passive measurement of the mean-square displacement, thereby restoring the connection between active and passive measurement for the nonequilibrium case. Physically, the effective temperature measures how far the system, when observed on different time scales, is from equilibrium. When applied to the to our knowledge only experiment where both active and passive measurements were performed on the same samples [Gall 09], we determine the effective temperatures obtained solely from the passive measurement and from comparing the active and passive measurement. Both temperatures indeed agree, supporting the validity of our model.

The third central result is the classification of the nonequilibrium dynamics in terms of the crucial parameters of our model, the exponents α and β, which are related in a straightforward manner to the diffusion exponent and thus readily accessible in experiments. These exponents enter the effective nonequilibrium noise in Section 4.3, which emerges as a result of the active motion of the viscoelastic cytoskeleton. If this nonequilibrium noise can be modeled as a stationary stochastic process, which is the case for $2\alpha + \beta < 1$, we refer to the dynamics as force-like. In this regime, we can view the tracer particle as in contact with an equilibrium viscoleastic environment and additionally subject to forces that are induced by the active motion of the cell and mediated through the environment. This will generally be the case for a small tracer in the relatively viscous cytoplasm, in which the tracer can move rather freely and which smooths out the strongly directional motion generated by molecular motors in the cytoskeleton [Brun 09]. For a more elastic medium and $2\alpha + \beta > 1$, on the other hand, the tracer is dragged along with the medium, which manifests in an effective noise force that increases with time and is thus nonstationary. This nonstationarity expresses the fact that one would need to apply an ever increasing force in order to keep the particle in place against the motion of the surrounding medium, hence we call this type of nonequilibrium dynamics velocity-like. This situation occurs for tracers bound to the cytoskeleton, which is mostly elastic, causing the tracer to experience the directional motion directly [Burs 05, Gall 09].

In summary, our stochastic model of a randomly moving viscoelastic medium is able to reproduce some of the most important observations from microrheological experiments on tracers bound to the cytoskeleton of living cells: The crossover from sub- to superdiffusion, the anomalous response, the non-Gaussian dynamics, the noise spectrum and even the qualitative trajectories. Since these observations can be related in a straightforward manner to the parameters of the model, it promises to be a useful tool for the analysis and classification of the dynamics. It further reconnects passive and active microrheology in the nonequilibrium environment of a living cell, by generalizing the equilibrium Stokes-Einstein relation via the introduction of an effective temperature.

Outlook

From the point of view of our results on general scale invariant systems, an obvious next step would be to look for more models and systems that asymptotically exhibit the desired type of scaling correlation function and to which our theory is thus applicable. This is not necessarily restricted to systems where the scaling occurs in the velocity correlations, one example to the contrary are intensity correlations in blinking quantum dots [Jung 02], which can be described by the Lévy walk and thus treated within this framework [Dech 14]. On a more fundamental level, there is the question of whether our scaling theory can be extended to subdiffusive dynamics. This extension is not straightforward, since subdiffusion requires the normal diffusion coefficient to vanish, which will generally only occur if the velocity correlation function exhibits short-time oscillations. Thus, contrary to the superdiffusive case, where the short-time dynamics are asymptotically unimportant, they will need to be taken into account for subdiffusion.

Our model for nonequilibrium dynamics in living cells certainly should be compared to experimental data in a more thorough fashion than was possible in this thesis. This includes the relatively straightforward analysis of measurements of the mean-square displacement and response function and their connection via the nonequilibrium Stokes-Einstein relation and the effective temperature. Perhaps more intriguing form a theorist's point of view are the non-Gaussian properties of the nonequilibrium motion. Foremost, the apparent disagreement between our theory and one of the experiments concerning the non-Gaussian parameter and its time-dependence (see Section 4.4) needs to be investigated further, in particular as to whether it is an artifact in the data analysis method or has physical meaning. Another observation made in experiment and connected to the non-Gaussian dynamics, is the occurrence of what is called strong anomalous diffusion [Gal 10], where different moments of the displacement distribution exhibit a different scaling behavior. Our model should be able to reproduce this, since a similar behavior is known for the Lévy walk [Rebe 13]. The Lévy walk also directly captures the idea of actin filaments being moved relative to each other by the motor proteins linking them. During one such event, the actin filament to which the tracer bead is bound moves ballistically at a constant velocity, corresponding to the ballistic motion during the waiting times in the Lévy walk. At some point, the motor protein unbinds from the actin filament, ending the ballistic motion, whereupon another protein may move the actin filament in a different direction, corresponding to choosing a new direction and waiting time in the Lévy walk. This similarity between the nonequilibrium dynamics and the Lévy walk, poses the intriguing question of the origin of the power-law waiting time distribution in this case. We speculate that the latter may follow from the cooperative action of multiple molecular motors on a single actin filament, which can lead to greatly enhanced transport distances and thus times [Klum 05].

Apart from the non-Gaussian dynamics, there other quantities that can serve to determine how well our model is able to reproduce the experimental system. One example for this is the directional persistence [Leno 07], which quantifies to

what degree a particle tends to move in the same or opposite direction after a certain time. For short times, the motion has been found to be antipersistent, in agreement with the anticorrelated subdiffusive behavior described by the fractional Langevin equation. For longer times, this reverses into persistent motion, which also is expected for the superdiffusive correlated dynamics. While qualitatively, the results seem to agree with our model, it remains to be seen whether quantitative agreement can also be reached.

A strong prediction of our model is, that for a bead bound to the cytoskeleton, the effective nonequilibrium noise force will be nonstationary, and that, in particular, its power spectrum will depend on frequency as ω^{-2} and will increase with time as $t^{2\alpha+\beta-2}$. While the ω^{-2}-dependence has been postulated before and was obtained indirectly from experimental data [Lau 03], the time dependence of the power spectrum has not yet been observed experimentally. For this, it would be necessary to directly measure the effective nonequilibrium noise force. This might be accomplished by measuring the force necessary to prevent the active motion of the tracer bead. However, this procedure is not straightforward at all, since one would need to exclude effects of a possible center-of-mass motion of the entire cell and also make sure that the applied force is not too big, so as not lead to inelastic deformations of the cytoskeleton or even detachment of the bead. Nevertheless, the time-dependent noise spectrum provides a direct testable prediction of our nonequilibrium model. Observing it in experiment would be compelling evidence in favor of the model.

A

APPENDIX: MATHEMATICAL DETAILS

A.1 MATHEMATICAL IDENTITIES

Frequently, we encounter expressions in the Laplace domain which are of the form,

$$\frac{\tilde{f}(s_2, s_1}{s_2 + s_1}. \tag{A.1}$$

In order to express them via the inverse Laplace transform of the function $\tilde{f}(s_2, s_1)$, we use the identity

$$\frac{1}{s_2 + s_1} = \int_0^\infty dt' \, e^{-(s_2+s_1)t'}, \tag{A.2}$$

to obtain a general Laplace inversion rule,

$$\begin{aligned}
\mathcal{L}^{-2}\left[\frac{\tilde{f}(s_2, s_1)}{s_2 + s_1}\right]_{s_1 \to t_1}^{s_2 \to t_2} &= \int_0^\infty dt' \, \mathcal{L}^{-2}\left[e^{-(s_2+s_1)t'}\tilde{f}(s_2, s_1)\right]_{s_1 \to t_1}^{s_2 \to t_2} \\
&= \int_0^\infty dt' f(t_2 - t', t_1 - t')\theta(t_2 - t')\theta(t_1 - t') \\
&= \int_0^{\min(t_2, t_1)} dt' \, f(t_2 - t', t_1 - t'),
\end{aligned} \tag{A.3}$$

where we used the time shift property of the Laplace transform, $\mathcal{L}[f(t - t')\theta(t - t')]_{t \to s} = e^{-st'}\tilde{f}(s)$, with the Heaviside step function $\theta(t)$. Assuming, without loss of generality, that $t_2 \geqslant t_1$ and defining $t \equiv t_1$, $\tau \equiv t_2 - t_1$, we can write this as,

$$\mathcal{L}^{-2}\left[\frac{\tilde{f}(s_2, s_1)}{s_2 + s_1}\right]_{s_1 \to t}^{s_2 \to t+\tau} = \int_0^t dt' \, f(t + \tau - t', t - t'). \tag{A.4}$$

A more general version of Eq. (A.4) concerns expressions of the type,

$$\tilde{g}(s_2 + s_1)\tilde{f}(s_2, s_1), \tag{A.5}$$

where $g(t)$ is understood to be a function of a single variable whereas $f(t_2, t_1)$ is a function of two variables, and $\tilde{g}(s)$ respectively $\tilde{f}(s_2, s_1)$ are the corresponding one- and two-time Laplace transforms. The time-domain representation of the above expression turns out to be,

$$\begin{aligned}
\mathcal{L}^{-2}\left[\tilde{g}(s_2 + s_1)\tilde{f}(s_2, s_1)\right]_{s_1 \to t_1}^{s_2 \to t_2} &= \int_0^{\min(t_2, t_1)} dt' \, g(t')f(t_2 - t', t_1 - t') \\
&\equiv h(t_2, t_1).
\end{aligned} \tag{A.6}$$

To prove this, we take the two-time Laplace transform of the above to find,

$$\begin{aligned}
\tilde{h}(s_2, s_1) = &\int_0^\infty dt_2 \int_0^{t_2} dt_1 \int_0^{t_1} dt' \, e^{-s_2 t_2 - s_1 t_1} g(t')f(t_2 - t', t_1 - t') \\
&+ \int_0^\infty dt_2 \int_{t_2}^\infty dt_1 \int_0^{t_2} dt' \, e^{-s_2 t_2 - s_1 t_1} g(t')f(t_2 - t', t_1 - t').
\end{aligned} \tag{A.7}$$

In the first integral, we exchange the order of the t_2 and t_1 integration,

$$\tilde{h}(s_2, s_1) = \int_0^\infty dt_1 \int_{t_1}^\infty dt_2 \int_0^{t_1} dt' \, e^{-s_2 t_2 - s_1 t_1} g(t') f(t_2 - t', t_1 - t') + \int_0^\infty dt_2 \int_{t_2}^\infty dt_1 \int_0^{t_2} dt' \, e^{-s_2 t_2 - s_1 t_1} g(t') f(t_2 - t', t_1 - t'), \tag{A.8}$$

and then exchange the order of the t' and t_1 integration in the first, respectively of t' and t_2 in the second term,

$$\tilde{h}(s_2, s_1) = \int_0^\infty dt' \int_{t_1}^\infty dt_2 \int_{t'}^\infty dt_1 \, e^{-s_2 t_2 - s_1 t_1} g(t') f(t_2 - t', t_1 - t') + \int_0^\infty dt' \int_{t_2}^\infty dt_1 \int_{t'}^\infty dt_2 \, e^{-s_2 t_2 - s_1 t_1} g(t') f(t_2 - t', t_1 - t'). \tag{A.9}$$

In the first term, we now change the variable of the t_1-integration to $\tau = t_1 - t'$, in the second term we change from t_2 to $\theta' = t_2 - t'$,

$$\tilde{h}(s_2, s_1) = \int_0^\infty dt' \int_{t'+\tau}^\infty dt_2 \int_0^\infty d\tau \, e^{-s_2 t_2 - s_1 (t'+\tau)} g(t') f(t_2 - t', \tau) + \int_0^\infty dt' \int_{t'+\theta'}^\infty dt_1 \int_0^\infty d\theta' \, e^{-s_2 (t'+\theta') - s_1 t_1} g(t') f(\theta', t_1 - t'). \tag{A.10}$$

Another change of variables from t_2 to $\theta = t_2 - t' - \tau$ and from t_1 to $\tau' = t_1 - t' - \theta'$ brings us to,

$$\tilde{h}(s_2, s_1) = \int_0^\infty dt' \int_0^\infty d\theta \int_0^\infty d\tau \, e^{-s_2 \theta - (s_2+s_1)(t'+\tau)} g(t') f(\theta + \tau, \tau) + \int_0^\infty dt' \int_0^\infty d\tau' \int_0^\infty d\theta' \, e^{-(s_2+s_1)(t'+\theta') - s_1 \tau'} g(t') f(\theta', \theta' + \tau'). \tag{A.11}$$

The t'-integration in both terms yield precisely the Laplace transform of $g(t)$,

$$\tilde{h}(s_2, s_1) = \tilde{g}(s_2 + s_1) \Bigg[\int_0^\infty d\theta \int_0^\infty d\tau \, e^{-s_2 \theta - (s_2+s_1)\tau} f(\theta + \tau, \tau) + \int_0^\infty d\tau' \int_0^\infty d\theta' \, e^{-(s_2+s_1)\theta' - s_1 \tau'} f(\theta', \theta' + \tau') \Bigg]. \tag{A.12}$$

A final change of variables from θ to $t = \theta + \tau$ and from τ' to $t' = \theta' + \tau'$ yields,

$$\tilde{h}(s_2, s_1) = \tilde{g}(s_2 + s_1) \Bigg[\int_0^\infty d\tau \int_\tau^\infty d\theta \, e^{-s_2 t - s_1 \tau} f(t, \tau) + \int_0^\infty d\theta' \int_{\theta'}^\infty dt' \, e^{-s_2 \theta' - s_1 t} f(\theta', t') \Bigg], \tag{A.13}$$

and after exchanging the order of integration in the second term,

$$\tilde{h}(s_2, s_1) = \tilde{g}(s_2 + s_1) \Bigg[\int_0^\infty d\tau \int_\tau^\infty dt \, e^{-s_2 t - s_1 \tau} f(t, \tau) + \int_0^\infty dt' \int_0^{t'} d\theta' \, e^{-s_2 \theta' - s_1 t'} f(\theta', t') \Bigg]. \tag{A.14}$$

Now, all we need to do is rename t' into τ and θ' into t, to get to our desired result,

$$\begin{aligned}\tilde{h}(s_2, s_1) &= \tilde{g}(s_2 + s_1) \int_0^\infty d\tau \int_0^\infty dt\ e^{-s_2 t - s_1 \tau} f(t, \tau) \\ &= \tilde{g}(s_2 + s_1) \tilde{f}(s_2, s_1),\end{aligned} \tag{A.15}$$

which proves Eq. (A.6). Note that this result includes Eq. (A.4) as a special case for $g(t) = 1$.

We generally have two ways of representing the two-time autocorrelation function of some observable $x(t)$. The first one is the symmetric autocorrelation,

$$C_x(t_2, t_1) = C_x(t_1, t_2) = \langle x(t_2) x(t_1) \rangle, \tag{A.16}$$

with $t_2, t_1 > 0$, which is by definition invariant under the exchange of its two time arguments. By ordering the two times and calling the lesser of the two times t (the overall time) and the difference between the greater and the lesser τ (the time lag), we may also define a time-ordered autocorrelation,

$$\vec{C}_x(t, \tau) = \langle x(t + \tau) x(t) \rangle, \tag{A.17}$$

where both t and τ are positive. We can also express the symmetric autocorrlelation in terms of the time-ordered one,

$$C_x(t_2, t_1) = \vec{C}_x(t_1, t_2 - t_1)\theta(t_2 - t_1) + \vec{C}_x(t_2, t_1 - t_2)\theta(t_1 - t_2), \tag{A.18}$$

where $\theta(t)$ is the Heaviside-theta function. Of each of the two representations, we may now take the double Laplace transform,

$$\begin{aligned}\tilde{C}_x(s_2, s_1) &= \mathcal{L}^2 \Big[C_x(t_2, t_1) \Big]_{t_2 \to s_2}^{t_1 \to s_1} \\ \tilde{\vec{C}}_x(s, u) &= \mathcal{L}^2 \Big[\vec{C}_x(t, \tau) \Big]_{t \to s}^{\tau \to u}.\end{aligned} \tag{A.19}$$

Equation (A.18) implies a relation between the two Laplace transforms. To obtain it, we use the definition,

$$\begin{aligned}\tilde{C}_x(s_2, s_1) &= \int_0^\infty dt_2 e^{-s_2 t_2} \int_0^\infty dt_1\ e^{-s_1 t_1} C_x(t_2, t_1) \\ &= \int_0^\infty dt_2 e^{-s_2 t_2} \int_0^{t_2} dt_1\ e^{-s_1 t_1}\ C_x(t_2, t_1) \\ &\quad + \int_0^\infty dt_2\ e^{-s_2 t_2} \int_{t_2}^\infty dt_1\ e^{-s_1 t_1} C_x(t_2, t_1) \\ &= \int_0^\infty dt_2\ e^{-s_2 t_2} \int_0^{t_2} dt_1\ e^{-s_1 t_1} \vec{C}_x(t_1, t_2 - t_1) \\ &\quad + \int_0^\infty dt_2\ e^{-s_2 t_2} \int_{t_2}^\infty dt_1\ e^{-s_1 t_1} \vec{C}_x(t_2, t_1 - t_2) \\ &= \int_0^\infty dt_1\ e^{-s_1 t_1} \int_{t_1}^\infty dt_2\ e^{-s_2 t_2} \vec{C}_x(t_1, t_2 - t_1) \\ &\quad + \int_0^\infty dt_2\ e^{-s_2 t_2} \int_{t_2}^\infty dt_1\ e^{-s_1 t_1} \vec{C}_x(t_2, t_1 - t_2).\end{aligned} \tag{A.20}$$

In the last step, we exchanged the order of integration in the first integral. Now we introduce the new variables $\tau_2 = t_2 - t_1$ in the first and $\tau_1 = t_1 - t_2$ in the second integral to find,

$$\begin{aligned}\tilde{C}_x(s_2, s_1) &= \int_0^\infty dt_1\ e^{-s_1 t_1} \int_0^\infty d\tau_2\ e^{-s_2(t_1+\tau_2)} \vec{C}_x(t_1, \tau_2) \\ &\quad + \int_0^\infty dt_2\ e^{-s_2 t_2} \int_{t_2}^\infty d\tau_1\ e^{-s_1(t_2+\tau_1)} \vec{C}_x(t_2, \tau_1) \\ &= \tilde{\vec{C}}_x(s_2 + s_1, s_2) + \tilde{\vec{C}}_x(s_2 + s_1, s_1),\end{aligned} \tag{A.21}$$

where we used the definition of the Laplace transform of the time-ordered autocorrelation. In the particular case of a stationary autocorrelation function that is independent of the initial time t,

$$\vec{C}_x(t, \tau) = C_s(\tau), \tag{A.22}$$

we have,

$$\tilde{\vec{C}}_x(s, u) = \frac{\tilde{C}_s(u)}{s}, \tag{A.23}$$

where $\tilde{C}_s(u)$ denotes the Laplace transform of $C_s(\tau)$ with respect to τ. Thus Eq. (A.21) implies,

$$\tilde{C}_x(s_2, s_1) = \frac{\tilde{C}_s(s_2) + \tilde{C}_s(s_1)}{s_2 + s_1}. \tag{A.24}$$

A.2 ASYMPTOTIC ANALYSIS OF FRACTIONAL INTEGRALS

In this section, we will examine the asymptotic properties of several integrals that appear in a number of contexts throughout this thesis. The first integral we consider is of the general form,

$$I^1_{a,b}(y) = \int_0^1 dz\ (y + z - \epsilon y z)^a z^b, \tag{A.25}$$

with $b > -1$, $0 \leqslant \epsilon \leqslant 1$ and $y > 0$. At first we also assume a and $a + b$ to be non-integer. This integral may in principle be expressed as a hypergeometric function or incomplete beta function whose asymptotic properties for small and large y are known, however, it is instructive to derive the asymptotic behavior explicitly, in particular as we will employ similar arguments for some of the more complicated integrals. For $y \ll 1$, we note that the value of the integral is finite as $y \to 0$, as long as $a + b > -1$. We will first discuss the case $a + b < -1$, where the integral diverges as $y \to 0$. The latter divergence occurs at the lower boundary, where the integrand is equal to z^{a+b} for $y = 0$. In order to get rid of the divergence, we change variables to $v = z/y$,

$$I^1_{a,b}(y) = y^{a+b+1} \int_0^{\frac{1}{y}} dv\ (1 + v - \epsilon y v)^a v^b. \tag{A.26}$$

Here we note that for $y \ll 1$, we obviously have $\epsilon y v \ll v$. We then expand the first factor,

$$(1+v-\epsilon y v)^a \simeq (1+v)^a - a(1+v)^{a-1}\epsilon y v + \dots, \tag{A.27}$$

and plug this expansion back into our integral,

$$\begin{aligned} I^1_{a,b}(y) \simeq y^{a+b+1} &\int_0^{\frac{1}{y}} dv\ (1+v)^a v^b \\ &- a\epsilon y^{a+b+2} \int_0^{\frac{1}{y}} dv\ (1+v)^{a-1} v^{b+1} + \dots\ . \end{aligned} \tag{A.28}$$

Now, since $a+b<-1$, all the integrals in this expansion are finite as $y \to 0$, where the upper boundary tends to infinity. We then write,

$$\int_0^{\frac{1}{y}} dv\ (1+v)^a v^b = \int_0^{\infty} dv\ (1+v)^a v^b - \int_{\frac{1}{y}}^{\infty} dv\ (1+v)^a v^b. \tag{A.29}$$

The first integral is just a constant, while in the second one, we have $v > 1/y \gg 1$, and can again expand,

$$(1+v)^a \simeq v^a + a v^{a-1} + \dots\ . \tag{A.30}$$

We thus have,

$$\begin{aligned} \int_0^{\frac{1}{y}} dv\ (1+v)^a v^b &\simeq \frac{\Gamma(1+b)\Gamma(-a-b-1)}{\Gamma(-a)} \\ &\quad - \int_{\frac{1}{y}}^{\infty} dv\ \left[v^{a+b} + a v^{a+b-1} + \dots\right] \\ &= \frac{\Gamma(1+b)\Gamma(-a-b-1)}{\Gamma(-a)} \\ &\quad + \frac{1}{a+b+1} y^{-a-b-1} + \frac{a}{a+b} y^{-a-b} + \dots\ . \end{aligned} \tag{A.31}$$

This procedure is the same for any of the terms in the expansion Eq. (A.28) and we find for the asymptotic behavior of our integral in the case $y \ll 1$ and $a+b<-1$,

$$\begin{aligned} I^1_{a,b}(y) \simeq &\frac{\Gamma(1+b)\Gamma(-a-b-1)}{\Gamma(-a)} y^{a+b+1} + \frac{1}{a+b+1} \\ &- \frac{a\epsilon\Gamma(2+b)\Gamma(-a-b-1)}{\Gamma(1-a)} y^{a+b+2} \\ &+ \left(\frac{a}{a+b} - \frac{a\epsilon}{a+b+1}\right) y + \mathcal{O}(y^{a+b+3}), \end{aligned} \tag{A.32}$$

where we assumed $-2 < a+b < -1$ for the ordering of the terms. For $a+b<-2$, the leading order term is the same, but the order of the sub-leading terms changes. In the case $a+b>-1$, it is easy to see that the leading order term (i.e. for $y=0$) is the constant one in the above equation. In fact, the sub-leading terms are also given by the above expressions, which is, however, not straightforward since the integrals, which yielded the Gamma-function coefficients are no longer finite in

this case. To find the sub-leading order, we take the derivative of Eq. (A.25) with respect to y,

$$\frac{\partial}{\partial y} I^1_{a,b}(y) = a \int_0^1 dz\, (y + z - \epsilon y z)^{a-1} \left(z^b - \epsilon z^{b+1}\right). \tag{A.33}$$

For the derivative, we have exactly the same situation as with the original integral, however, the threshold value is now $a + b = 0$ in the first term and $a + b = -1$ in the second one. For $-1 < a + b < 0$, we thus have,

$$\begin{aligned}\frac{\partial}{\partial y} I^1_{a,b}(y) \simeq\ & \frac{a\Gamma(1+b)\Gamma(-a-b)}{\Gamma(1-a)} y^{a+b} + \frac{a}{a+b} - \frac{a\epsilon}{a+b+1} \\ & - \frac{a(a-1)\epsilon\Gamma(2+b)\Gamma(-a-b)}{\Gamma(2-a)} y^{a+b+1} + \frac{a(a-1)}{a+b-1} y \\ & + \mathcal{O}(y^{a+b+2}).\end{aligned} \tag{A.34}$$

Integrating this with respect to y, using the property of the Gamma function $\Gamma(a+1) = a\Gamma(a)$ and taking into account the constant term, we obtain precisely the same as above. For $y \ll 1$ and non-integer a and $a + b$, the asymptotic behavior of the integral is thus given by,

$$\begin{aligned} I^1_{a,b}(y) \simeq\ & \frac{\Gamma(1+b)\Gamma(-a-b-1)}{\Gamma(-a)} y^{a+b+1} + \frac{1}{a+b+1} \\ & + \frac{\epsilon\Gamma(2+b)\Gamma(-a-b-1)}{\Gamma(-a)} y^{a+b+2} \\ & + \left(\frac{a}{a+b} - \frac{a\epsilon}{a+b+1}\right) y + \mathcal{O}(y^{a+b+3}).\end{aligned} \tag{A.35}$$

Now we turn to the case where either a or $a + b$ are integer. If $a = -n$ is a negative integer or $a + b = -m$ is a negative integer with $m > 1$, Eq. (A.35) remains valid. If a is a positive integer, $a = n$, then we can use the binomial formula in Eq. (A.25),

$$(y + z - \epsilon y z)^n = \sum_{k=0}^{n} \frac{n!}{k!(n-k)!} y^k (1 - \epsilon z)^k z^{n-k} \tag{A.36}$$

The leading order is then obviously given by the $k = 0$-term, the sub-leading one by $k = 1$ and so on. We find,

$$\begin{aligned} I^1_{n,b}(y) &\simeq \int_0^1 dz\, z^{n+b} + ny \int_0^1 dz\, (1 - \epsilon z) z^{n+b-1} + \mathcal{O}(y^2) \\ &= \frac{1}{n+b+1} + \left(\frac{n}{n+b} - \frac{n\epsilon}{n+b+1}\right) y + \mathcal{O}(y^2).\end{aligned} \tag{A.37}$$

This is basically Eq. (A.35) without the fractional order terms. The most interesting integer case is $a + b = -1$, where the integral diverges logarithmically in the limit of small y. Here, we again consider the derivative in the case $\epsilon = 0$,

$$\frac{\partial}{\partial y} I^1_{a,-a-1}(y) = a \int_0^1 dz\, (y + z)^{a-1} z^{-a-1}. \tag{A.38}$$

We introduce $v = z/y$,

$$\frac{\partial}{\partial y} I^1_{a,-a-1}(y) = a y^{-1} \int_0^{\frac{1}{y}} dv\, (1+v)^{a-1} v^{-a-1}. \tag{A.39}$$

This integral is finite in the limit $y \to 0$ and we have,

$$\begin{aligned} \frac{\partial}{\partial y} I^1_{a,-a-1}(y) \simeq a y^{-1} \int_0^{\infty} dv\, (1+v)^{a-1} v^{-a-1} - a \\ - \frac{a(a-1)}{2} y + \mathcal{O}(y^2), \end{aligned} \tag{A.40}$$

which, upon integration with respect to y gives us,

$$I^1_{a,-a-1}(y) \simeq -\ln(y) + c - ay - \frac{a(a-1)}{4} y^2 + \mathcal{O}(y^3), \tag{A.41}$$

with some constant c, which turns out to be an Harmonic number, $c = -H_{-a-1}$. If $a + b = n$ is a positive integer, $n \geqslant 0$, then the integral can be brought into the appropriate form by taking derivative with respect to y. The leading order is then constant with a sub-leading term of order $y \ln(y)$ for $n = 0$ or y for $n > 0$. For $y \gg 1$, the asymptotic behavior is comparably straightforward. In Eq. (A.25), we then have $y(1 - \epsilon z) \gg z$ and expand the first factor,

$$\begin{aligned} (y + z - \epsilon y z)^a \simeq y^a (1 - \epsilon z)^a + a y^{a-1} (1 - \epsilon z)^{a-1} z \\ + \frac{a(a-1)}{2} y^{a-2} (1 - \epsilon z)^{a-2} z^2 + \mathcal{O}(\ddagger^{\ni}). \end{aligned} \tag{A.42}$$

The asymptotic behavior of the integral for $y \gg 1$ is then given by,

$$\begin{aligned} I^1_{a,b}(y) \simeq y^a \int_0^1 dz\, (1 - \epsilon z)^a z^b + a y^{a-1} \int_0^1 dz\, (1 - \epsilon z)^{a-1} z^{b+1} \\ + \mathcal{O}(y^{a-2}) \end{aligned} \tag{A.43}$$

In summary, we have for the asymptotic behavior of the integral, apart from the special integer cases,

$$I^1_{a,b}(y) \simeq \begin{cases} y^a \int_0^1 dz\, (1 - \epsilon z)^a z^b + a y^{a-1} \int_0^1 dz\, (1 - \epsilon z)^{a-1} z^{b+1} \\ \quad + \mathcal{O}(y^{a-2}) \\ \qquad \text{for } y \gg 1 \\ \frac{\Gamma(1+b)\Gamma(-a-b-1)}{\Gamma(-a)} y^{a+b+1} + \frac{1}{a+b+1} \\ \quad + \frac{\epsilon \Gamma(2+b)\Gamma(-a-b-1)}{\Gamma(-a)} y^{a+b+2} \\ \quad + \left(\frac{a}{a+b} - \frac{a\epsilon}{a+b+1}\right) y + \mathcal{O}(y^{a+b+3}) \\ \qquad \text{for } y \ll 1. \end{cases} \tag{A.44}$$

The next integral we consider is somewhat more involved,

$$I^2_{a,b}(y) = \int_0^1 dz \int_0^z du\, (1 + y - z)^a (1 - u)^a \big((z - u)^b - z^b\big), \tag{A.45}$$

with $-1 < a, b < 0$. First we change variables to $v = u/z$,

$$I^2_{a,b}(y) = \int_0^1 dz \int_0^1 dv\ (1+y-z)^a (1-vz)^a z^{b+1}\big((1-v)^b - 1\big). \tag{A.46}$$

For $y \gg 1$, we can expand,

$$(1+y-z)^a \simeq y^a + ay^{a-1}(1-z) + \mathcal{O}(y^{a-2}), \tag{A.47}$$

and thus have,

$$\begin{aligned} I^2_{a,b}(y) \simeq y^a \int_0^1 dz \int_0^1 dv\ (1-vz)^a z^{b+1}\big((1-v)^b - 1\big) \\ + ay^{a-1} \int_0^1 dz \int_0^1 dv\ (1-z)(1-vz)^a z^{b+1}\big((1-v)^b - 1\big) \\ + \mathcal{O}(y^{a-2}). \end{aligned} \tag{A.48}$$

For $y \ll 1$, we first change variables from z to $1-z$ and from v to $1-v$ in Eq. (A.46),

$$I^2_{a,b}(y) = \int_0^1 dz \int_0^1 dv\ (y+z)^a (v+z-vz)^a (1-z)^{b+1}(v^b - 1). \tag{A.49}$$

Introducing the functions

$$\begin{aligned} f_1(z) &= \int_0^1 dv\ (v+z-vz)^a v^b \\ f_2(z) &= \int_0^1 dv\ (v+z-vz)^a, \end{aligned} \tag{A.50}$$

the above can be written as,

$$I^2_{a,b}(y) = \int_0^1 dz (y+z)^a (1-z)^{b+1}(f_1(z) - f_2(z)). \tag{A.51}$$

Note that $f_1(z)$ corresponds precisely to the integral Eq. (A.25), whereas $f_2(z)$ is Eq. (A.25) with $b = 0$. All the individual terms in the above expression are regular for $y = 0$ at the upper boundary $z = 1$, so the leading-order asymptotic behavior is dictated by the possibly divergent behavior near $z = 0$. In particular, we have from Eq. (A.44),

$$\begin{aligned} f_1(z) &\simeq \frac{\Gamma(1+b)\Gamma(-a-b-1)}{\Gamma(-a)} z^{a+b+1} + \frac{1}{a+b+1} \\ f_2(z) &\simeq -\frac{1}{a+1} z^{a+1} + \frac{1}{a+1}. \end{aligned} \tag{A.52}$$

From this we see, that the first term in Eq. (A.51) is finite in the limit $y \to 0$ if $2a + b > -2$ whereas the second one is always finite since $a > -1$. We first concentrate on the case $2a + b < -2$, where the first term leads to a divergence at the lower boundary and thus the dominant contribution comes from close to $z = 0$.

In this case, we may replace $f_1(z)$ by its small argument expansion Eq. (A.52) and have,

$$\begin{aligned} I^2_{a,b}(y) \simeq & \frac{\Gamma(1+b)\Gamma(-a-b-1)}{\Gamma(-a)} \int_0^1 dz\, (y+z)^a (1-z)^{b+1} z^{a+b+1} \\ & + \frac{1}{a+b+1} \int_0^1 dz\, (y+z)^a (1-z)^{b+1} \\ & - \int_0^1 dz\, (y+z)^a (1-z)^{b+1} f_2(z). \end{aligned} \tag{A.53}$$

Since in the first term, the dominant contribution comes from small z, we may also expand,

$$(1-z)^{b+1} \simeq 1-(b+1)z+\mathcal{O}(z^2). \tag{A.54}$$

We again find terms which are of the form Eq. (A.25) with varying values for the parameter b. Once again employing the small argument expansion where appropriate, we end up with,

$$I^2_{a,b}(y) \simeq -\frac{\pi\Gamma(1+b)\Gamma(-2a-b-2)}{\Gamma^2(-a)\sin(\pi(a+b+1))} y^{2a+b+2} + \mathcal{O}(y^0). \tag{A.55}$$

The constant term can be identified with some effort, however, since it will not be relevant for our purposes, we skip doing so here. In the case $2a+b > -2$, the leading order is term is the constant $I^2_{a,b}(0)$. The sub-leading term can be found by taking the derivative with respect to y,

$$\frac{\partial}{\partial y} I^2_{a,b}(y) = a \int_0^1 dz\, (y+z)^{a-1} (1-z)^{b+1} (f_1(z) - f_2(z)). \tag{A.56}$$

Since $a < 0$, this expression diverges at $z = 0$ as $y \to 0$. We may thus proceed as above and replace $f_1(z)$ respectively $f_2(z)$ by their small argument expansion. Summarizing the above results, the asymptotic behavior of the integral is given by,

$$I^2_{a,b}(y) \simeq \begin{cases} c_1^2 y^a + c_2^2 y^{a-1} + \mathcal{O}(y^{a-2}) \\ \qquad\qquad \text{for } y \gg 1 \\ c_3^2 y^{2a+b+2} + c_4^2 y^{a+1} + \mathcal{O}(y^0) \\ \qquad\qquad \text{for } y \ll 1 \text{ and } -3 < 2a+b < -2 \\ c_5^2 + c_3^2 y^{2a+b+2} + c_4^2 y^{a+1} + \mathcal{O}(y^{2a+b+3}) \\ \qquad\qquad \text{for } y \ll 1 \text{ and } -2 < 2a+b < -1 \\ c_5^2 + c_4^2 y^{a+1} + c_3^2 y^{2a+b+2} + \mathcal{O}(y^{2a+b+3}) \\ \qquad\qquad \text{for } y \ll 1 \text{ and } -1 < 2a+b < 0, \end{cases} \tag{A.57}$$

where the respective constants are given by,

$$
\begin{aligned}
c_1^2 &= \int_0^1 dz \int_0^1 dv\ (v+z-vz)^a (1-z)^{b+1} (v^b-1),\\
c_2^2 &= a \int_0^1 dz \int_0^1 dv\ z(v+z-vz)^a (1-z)^{b+1} (v^b-1),\\
c_3^2 &= -\frac{\pi\Gamma(1+b)\Gamma(-2a-b-2)}{\Gamma^2(-a)\sin(\pi(a+b+1))},\\
c_4^2 &= -\frac{1}{(a+b+1)(a+1)} + \frac{1}{(a+1)^2}\\
c_5^2 &= \int_0^1 dz \int_0^1 dv\ z^a (v+z-vz)^a (1-z)^{b+1} (v^b-1).
\end{aligned}
\tag{A.58}
$$

These constants can be evaluated numerically. One case, which is not covered by the above is the behavior for $a+b=-1$ and $y \ll 1$. In this case, the leading order of $f_1(z)$ is logarithmic, and we obtain,

$$
I_{a,b}^2(y) \simeq c_5^2 + \frac{1}{a+1} y^{a+1} \ln(y) - \left(\frac{H_{-2-a}}{a+1} + \frac{1}{(a+1)^2} \right) y^{a+1}, \tag{A.59}
$$

where H_a denotes an harmonic number.

Our third integral is rather similar to the previous one, Eq. (A.46)

$$
I_{a,b}^3(y) = \int_0^1 dz \int_0^z du\ (1-z)^a (1+y-u)^a \big((z-u)^b - z^b\big). \tag{A.60}
$$

Again we introduce $v = u/z$,

$$
I_{a,b}^3(y) = \int_0^1 dz \int_0^1 dv\ (1-z)^a (1+y-vz)^a z^{b+1} \big((1-v)^b - 1\big), \tag{A.61}
$$

and then change variables from z to $1-z$ and from v to $1-v$,

$$
I_{a,b}^3(y) = \int_0^1 dz \int_0^1 dv\ z^a (y+v+z-vz)^a (1-z)^{b+1} (v^b-1). \tag{A.62}
$$

The further analysis proceeds along the same lines as with the previous integral. We find,

$$
I_{a,b}^3(y) \simeq \begin{cases}
c_1^3 y^a + c_2^3 y^{a-1} + \mathcal{O}(y^{a-2}) \\
\qquad\qquad \text{for } y \gg 1 \\
c_3^3 y^{2a+b+2} + \mathcal{O}(y^0) \\
\qquad\qquad \text{for } y \ll 1 \text{ and } -3 < 2a+b < -2 \\
c_4^3 + c_3^3 y^{2a+b+2} + \mathcal{O}(y) \\
\qquad\qquad \text{for } y \ll 1 \text{ and } -2 < 2a+b < -1 \\
c_4^3 + c_3^3 y^{2a+b+2} + c_5^3 y + \mathcal{O}(y^{2a+b+3}) \\
\qquad\qquad \text{for } y \ll 1 \text{ and } -1 < 2a+b < 0,
\end{cases} \tag{A.63}
$$

where the respective constants are given by,

$$
\begin{aligned}
c_1^3 &= \int_0^1 dz \int_0^1 dv\, z^a (1-z)^{b+1} (v^b - 1), \\
c_2^3 &= a \int_0^1 dz \int_0^1 dv\, z^a (v + z - vz)(1-z)^{b+1} (v^b - 1), \\
c_3^3 &= \frac{\Gamma(a+1)\Gamma(b+1)\Gamma(-2a-b-2)}{\Gamma(-a)}, \\
c_4^3 &= \int_0^1 dz \int_0^1 dv\, z^a (v + z - vz)^a (1-z)^{b+1} (v^b - 1), \\
c_5^3 &= a \int_0^1 dz \int_0^1 dv\, z^a (v + z - vz)^{a-1} (1-z)^{b+1} (v^b - 1).
\end{aligned} \tag{A.64}
$$

The fourth integral we discuss is,

$$
I_{a,b}^4(y) = \int_1^{1+y} dz \int_0^1 du\, \big((1+y-z)(1-u)\big)^a \big((z-u)^b - z^b\big), \tag{A.65}
$$

where as a first step we change variables from z to $z-1$ and from u to $1-u$,

$$
I_{a,b}^4(y) = \int_0^y dz \int_0^1 du\, \big((y-z)u\big)^a \big((z+u)^b - (1+z)^b\big). \tag{A.66}
$$

To proceed, we first define the function,

$$
\begin{aligned}
f(z) &= \int_0^1 du\, u^a \big((u+z)^b - (1+z)^b\big) \\
&= \int_0^1 du\, u^a (u+z)^b - \frac{1}{a+1}(1+z)^b,
\end{aligned} \tag{A.67}
$$

and examine its behavior for large and small z. The first term is precisely Eq. (A.25) with a and b interchanged. Using Eq. (A.44) and expanding the second term accordingly, we find,

$$
f(z) \simeq \begin{cases}
b\left(\frac{1}{a+2} - \frac{1}{a+1}\right) z^{b-1} + \frac{b(b-1)}{2}\left(\frac{1}{a+3} - \frac{1}{a+1}\right) z^{b-2} \\
\qquad \text{for } z \gg 1 \\
\frac{\Gamma(a+1)\Gamma(-a-b-1)}{\Gamma(-b)} z^{a+b+1} - \frac{b}{(a+b+1)(a+1)} \\
\qquad - \frac{b(b-1)}{(a+b)(a+1)} z \\
\qquad \text{for } z \ll 1.
\end{cases} \tag{A.68}
$$

In terms of $f(z)$, our original integral Eq. (A.66) reads,

$$
I_{a,b}^4(y) = \int_0^y dz\, (y-z)^a f(z) = y^{a+1} \int_0^1 dv\, (1-v)^a f(yv), \tag{A.69}
$$

where in the last step we introduced $v = z/y$. For $y \ll 1$, we can now just use the small argument expansion of $f(z)$, Eq. (A.68),

$$\begin{aligned} I^4_{a,b}(y) \simeq & \frac{\Gamma^2(a+1)\Gamma(b+1)\sin(\pi(1-b))}{\Gamma(2a+b+3)\sin(\pi(a+b+1)} y^{2a+b+2} \\ & - \frac{b}{(a+1)^2(a+b+1)} y^{a+1} \\ & - \frac{b(b-1)}{(a+1)^2(a+2)(a+b)} y^{a+2}. \end{aligned} \tag{A.70}$$

For $y \gg 1$, we cannot simply use the large argument expansion of $f(z)$, Eq. (A.68), since the latter diverges at the lower boundary. Instead, we write,

$$I^4_{a,b}(y) = y^a \int_0^y dz \left(1 - \frac{z}{y}\right)^a f(z), \tag{A.71}$$

and expand,

$$\left(1 - \frac{z}{y}\right)^a \simeq 1 - a\frac{z}{y}. \tag{A.72}$$

This gives us,

$$I^4_{a,b}(y) \simeq y^a \left[\int_0^\infty dz\, f(z) - \int_y^\infty dz\, f(z)\right] - a y^{a-1} \int_0^y dz\, z f(z), \tag{A.73}$$

where we used the fact that the integral over $f(z)$ is finite as the upper limit tends to infinity. The integral over $zf(z)$ on the other hand is not, and this thus dominated by the behavior of $f(z)$ at large arguments, allowing us to use Eq. (A.68) in the third term. We may also use this large argument expansion in the second term, since there we have $z > y \gg 1$. We then find for $y \gg 1$,

$$I^4_{a,b}(y) \simeq y^a \int_0^\infty dz\, f(z) + \frac{1}{(a+1)(a+2)} \left(\frac{ab}{b+1} - 1\right) y^{a+b}. \tag{A.74}$$

Summarizing all of the above results, the fourth integral Eq. (A.66) behaves asymptotically as,

$$I^4_{a,b}(y) \simeq \begin{cases} c^4_1 y^a + c^4_2 y^{a+b} + \mathcal{O}(y^{a+b-1}) \\ \qquad\qquad \text{for } y \gg 1, \\ c^4_3 y^{2a+b+2} + c^4_4 y^{a+1} + c^4_5 y^{a+2} + \mathcal{O}(y^{a+3}) \\ \qquad\qquad \text{for } y \ll 1, \end{cases} \tag{A.75}$$

with coefficients given by,

$$
\begin{aligned}
c_1^4 &= \int_0^\infty dz \int_0^1 du\, u^a \big((u+z)^b - (1+z)^b\big) \\
c_2^4 &= \frac{1}{(a+1)(a+2)} \left(\frac{ab}{b+1} - 1 \right) \\
c_3^4 &= \frac{\Gamma^2(a+1)\Gamma(b+1)\sin(\pi(1-b))}{\Gamma(2a+b+3)\sin(\pi(a+b+1)} \\
c_4^4 &= -\frac{b}{(a+1)^2(a+b+1)} \\
c_5^4 &= -\frac{b(b-1)}{(a+1)^2(a+2)(a+b)}.
\end{aligned} \tag{A.76}
$$

The fifth integral reads,

$$
I^5_{\nu,a,b}(y) = \int_0^\infty dz\, (y+z)^{-\nu} \phi(z), \tag{A.77}
$$

with a function $\phi(z)$, that behaves asymptotically as,

$$
\phi(z) \simeq \begin{cases} c_a z^a & \text{with } \mu > -1 \quad \text{for } z \ll 1 \\ \\ c_b z^b & \text{with } \lambda < \nu - 1 \quad \text{for } z \gg 1. \end{cases} \tag{A.78}
$$

For $y \ll 1$, the behavior of $\phi(z)$ for small z is pivotal. For $a < \nu - 1$, the integral diverges at the lower boundary as $y \to 0$ and is thus dominated by the small-z behavior of $\phi(z)$. We have,

$$
\begin{aligned}
I^5_{\nu,a,b}(y) &\simeq c_a \int_0^\infty dz\, (y+z)^{-\nu} z^a \\
&= c_a y^{a-\nu+1} \int_0^\infty du\, (1+u)^{-\nu} u^a \\
&= \frac{c_a \Gamma(a+1)\Gamma(\nu-a-1)}{\Gamma(\nu)} y^{a-\nu+1}.
\end{aligned} \tag{A.79}
$$

On the other hand, if $a > \nu - 1$, the integral is finite as $y \to 0$, the sub-leading order is then found by taking the derivative with respect to y,

$$
\frac{\partial}{\partial y} I^5_{\nu,a,b}(y) = -\nu \int_0^\infty dz\, (y+z)^{-\nu-1} \phi(z), \tag{A.80}
$$

which similarly diverges at the lower boundary if $a < \nu$ and thus,

$$
\begin{aligned}
\frac{\partial}{\partial y} I^5_{\nu,a,b}(y) &\simeq -\nu c_a \int_0^\infty dz\, (y+z)^{-\nu-1} z^a \\
&= -\frac{c_a \Gamma(a+1)\Gamma(\nu-a)}{\Gamma(\nu)} y^{a-\nu}.
\end{aligned} \tag{A.81}
$$

The asymptotic behavior of the integral for $y \ll 1$ is then given by,

$$I^5_{\nu,a,b}(y) \simeq \begin{cases} \frac{c_a\Gamma(a+1)\Gamma(\nu-a-1)}{\Gamma(\nu)} y^{a-\nu+1} \\ \qquad\qquad \text{for } a < \nu - 1 \\ \int_0^\infty dz\, z^{-\nu}\phi(z) + \frac{c_a\Gamma(a+1)\Gamma(\nu-a-1)}{\Gamma(\nu)} y^{a-\nu+1} \\ \qquad\qquad \text{for } \nu - 1 < a < \nu \\ \int_0^\infty dz\, z^{-\nu}\phi(z) - \nu y \int_0^\infty dz\, z^{-\nu-1}\phi(z) \\ \quad + \frac{c_a\Gamma(a+1)\Gamma(\nu-a-1)}{\Gamma(\nu)} y^{a-\nu+1} \\ \qquad\qquad \text{for } \nu < a < \nu + 1, \end{cases} \tag{A.82}$$

where the final case requires taking the second derivative with respect to y. In the limit $y \gg 1$, we see that the integral diverges at the upper boundary as $y \to \infty$ (i.e. if we replace $y + z$ by y) if $b > -1$. In this case, we can replace $\phi(z)$ by its asymptotic behavior for large z and find,

$$\begin{aligned} I^5_{\nu,a,b}(y) &\simeq c_b \int_0^\infty dz\, (y+z)^{-\nu} z^b \\ &= \frac{c_b\Gamma(b+1)\Gamma(\nu-b-1)}{\Gamma(\nu)} y^{b-\nu+1}. \end{aligned} \tag{A.83}$$

For $b < -1$, contributions to the integral stemming from large z are suppressed and we can replace $y + z$ by y to find the leading order behavior. In order to find the sub-leading contribution, we introduce the auxiliary function,

$$\xi(z) = \int_z^\infty dz'\, \phi(z'), \tag{A.84}$$

which is well defined since $\phi(z)$ is integrable for large arguments. The function $\xi(z)$ is the an antiderivative of $\phi(z)$, $(d/dz)\xi(z) = -\phi(z)$, and behaves for large z as,

$$\xi(z) \simeq -\frac{c_b}{b+1} z^{b+1}. \tag{A.85}$$

With this function, we can then integrate Eq. (A.77) by parts to find,

$$\begin{aligned} I^5_{\nu,a,b}(y) &= \left[-(y+z)^{-\nu}\xi(z)\right]_0^\infty - \nu \int_0^\infty dz\, (y+z)^{-\nu-1}\xi(z) \\ &= \xi(0) y^{-\nu} - \nu \int_0^\infty dz\, (y+z)^{-\nu-1}\xi(z). \end{aligned} \tag{A.86}$$

For $b > -2$, the remaining integral again diverges at the upper boundary as $y \to \infty$ and we may replace $\xi(z)$ by its large argument expansion,

$$\begin{aligned} I^5_{\nu,a,b}(y) &\simeq \xi(0) y^{-\nu} + \frac{\nu c_b}{b+1} \int_0^\infty dz\, (y+z)^{-\nu-1} z^{b+1} \\ &= y^{-\nu} \int_0^\infty dz\, \phi(z) + \frac{c_b\Gamma(b+1)\Gamma(\nu-b-1)}{\Gamma(\nu)} y^{b-\nu+1}. \end{aligned} \tag{A.87}$$

Summarizing, the asymptotic behavior of the integral is given by,

$$
I^5_{\nu,a,b}(y) \simeq \begin{cases}
\frac{c_a\Gamma(a+1)\Gamma(\nu-a-1)}{\Gamma(\nu)} y^{a-\nu+1} \\
\qquad\qquad \text{for } y \ll 1 \quad \text{and } a < \nu - 1 \\
\int_0^\infty dz\, z^{-\nu}\phi(z) + \frac{c_a\Gamma(a+1)\Gamma(\nu-a-1)}{\Gamma(\nu)} y^{a-\nu+1} \\
\qquad\qquad \text{for } y \ll 1 \quad \text{and } \nu - 1 < a < \nu \\
\int_0^\infty dz\, z^{-\nu}\phi(z) - \nu y \int_0^\infty dz\, z^{-\nu-1}\phi(z) \\
\qquad + \frac{c_a\Gamma(a+1)\Gamma(\nu-a-1)}{\Gamma(\nu)} y^{a-\nu+1} \\
\qquad\qquad \text{for } y \ll 1 \quad \text{and } \nu < a < \nu + 1 \\
\frac{c_b\Gamma(b+1)\Gamma(\nu-b-1)}{\Gamma(\nu)} y^{b-\nu+1} \\
\qquad\qquad \text{for } y \gg 1 \quad \text{and } -1 < b \\
y^{-\nu} \int_0^\infty dz\, \phi(z) + \frac{c_b\Gamma(b+1)\Gamma(\nu-b-1)}{\Gamma(\nu)} y^{b-\nu+1} \\
\qquad\qquad \text{for } y \gg 1 \quad \text{and } -2 < b < -1 \\
y^{-\nu} \int_0^\infty dz\, \phi(z) - \nu y^{-\nu-1} \int_0^\infty dz \int_z^\infty dz'\, \phi(z') \\
\qquad + \frac{c_b\Gamma(b+1)\Gamma(\nu-b-1)}{\Gamma(\nu)} y^{b-\nu+1} \\
\qquad\qquad \text{for } y \gg 1 \quad \text{and } -3 < b < -2,
\end{cases}
\tag{A.88}
$$

where the expression in the last line requires another integration by parts.

A.3 ASYMPTOTIC BEHAVIOR UNDER LAPLACE INVERSION

A function $f(t)$ and its Laplace transform $\tilde{f}(s)$ are related by,

$$
\begin{aligned}
\tilde{f}(s) &= \int_0^\infty dt\, e^{-st} f(t) \\
f(t) &= \frac{1}{2\pi i} \int_{-i\infty+\epsilon}^{i\infty+\epsilon} ds\, e^{st} \tilde{f}(s),
\end{aligned}
\tag{A.89}
$$

where ϵ is a real number such that $\Re(s_k) < \epsilon$ for all nonanalytic points s_k of $\tilde{f}(s)$. For all the cases we consider, we have $\Re(s_k) \leqslant 0$ and can thus choose ϵ to be a positive infinitesimal. The contour in the inverse Laplace transform, also called the Bromwich path, is a line parallel to the imaginary axis at $\Re(s) = \epsilon$. In practice, we perform the Laplace inversion by closing the contour in the left half-plane $\Re(s) < \epsilon$ via an infinitely extended semicircle. If $\tilde{f}(s)$ has no branch cuts, then $f(t)$ can be obtained via the residue theorem: The integral around the contour is given by the sum of the residues inside the contour. Since the contribution from the semicircle is exponentially suppressed, this sum of residues is also equal to the initial line integral. The situation is a bit more complicated if $\tilde{f}(s)$ has branch cuts, which we choose to be parallel to the negative real axis. Since the integration contour cannot intersect the branch cuts, we have to deform the semicircle in the left half plane to go around the branch cuts. Still, the integral along the closed contour is given

by the sum of residues, however, the former now has contributions from both the initial line integral and the contours around the branch cuts. Thus we need to evaluate the latter to obtain the value of the line integral. Let us consider $\tilde{f}(s)$ having a single branch point at $s = s_k$ and the corresponding branch cut extending from s_k parallel to the negative real line. We parameterize the contour around the branch cut by a line integral running to the right an infinitesimal distance δ above the branch cut, then a circle of a small radius R around the branch point and finally a line integral running to the left infinitesimally below (again distance δ) the branch point. To simplify the calculation, we shift the origin of the complex plane to $s = s_k$, moving the branch point to $s = 0$ and incurring a factor $e^{s_k t}$ from the exponential in inverse Laplace transform in doing so. The contour integral around the branch cut is then given by,

$$\begin{aligned} I_{\text{cut}}(t) = \frac{1}{2\pi i} e^{s_k t} \Big[& \underbrace{\int_{-\infty+i\delta}^{-R+i\delta} ds\ e^{st} \tilde{f}(s)}_{\text{above branch cut}} \\ & + \underbrace{iR \int_{\pi-\frac{\delta}{R}}^{-\pi+\frac{\delta}{R}} d\phi\ e^{Re^{i\phi}t} \tilde{f}(Re^{i\phi}) e^{i\phi}}_{\text{around branch point}} \\ & + \underbrace{\int_{-R-i\delta}^{-\infty-i\delta} ds\ e^{st} \tilde{f}(s)}_{\text{below branch cut}} \Big]. \end{aligned} \tag{A.90}$$

In order to get rid of the infinitesimal δ, we substitute $z = re^{i\pi}$ above the branch cut and $z = re^{-i\pi}$ below the branch cut, which takes care of the discontinuity and allows us to set $\delta = 0$,

$$\begin{aligned} I_{\text{cut}}(t) = \frac{1}{2\pi i} e^{s_k t} \Big[& \int_R^\infty dr\ e^{-rt} \left[\tilde{f}(re^{i\pi}) - \tilde{f}(re^{-i\pi}) \right] \\ & - iR \int_{-\pi}^{\pi} d\phi\ e^{Re^{i\phi}t} \tilde{f}(Re^{i\phi}) e^{i\phi} \Big], \end{aligned} \tag{A.91}$$

where we used the fact that the exponential is analytic. Let us assume that, in the vicinity of the branch point, $\tilde{f}(s)$ behaves as a power law,

$$\tilde{f}(s) \simeq a_\mu s^\mu + a_{\mu+1} s^{\mu+1} + \dots\ . \tag{A.92}$$

Since R is assumed to be small, we can directly substitute this expansion in the part of the contour around the branch point,

$$\begin{aligned} -iR \int_{-\pi}^{\pi} d\phi\ e^{Re^{i\phi}t} \tilde{f}(Re^{i\phi}) \simeq & -ia_\mu R^{\mu+1} \int_{-\pi}^{\pi} d\phi\ e^{Re^{i\phi}t} e^{i(\mu+1)\phi} \\ & - ia_{\mu+1} R^{\mu+2} \int_{-\pi}^{\pi} d\phi\ e^{Re^{i\phi}t} e^{i(\mu+2)\phi}. \end{aligned} \tag{A.93}$$

If $-1 < \mu$, then we can contract the contour and send $R \to 0$, in this case the entire integral tends to zero. If $-2 < \mu < -1$, then we integrate by parts in the first term,

$$\begin{aligned}-iR\int_{-\pi}^{\pi} d\phi\, e^{Re^{i\phi}t}\tilde{f}(Re^{i\phi}) \simeq &-\frac{a_\mu}{\mu+1}R^{\mu+1}e^{-Rt}\left[e^{i(\mu+1)\pi}-e^{-i(\mu+1)\pi}\right]\\ &+i\frac{a_\mu}{\mu+1}R^{\mu+2}t\int_{-\pi}^{\pi} d\phi\, e^{Re^{i\phi}t}e^{i(\mu+2)\phi}\\ &+a_{\mu+1}R^{\mu+2}\int_{-\pi}^{\pi} d\phi\, e^{Re^{i\phi}t}e^{i(\mu+2)\phi}. \end{aligned} \tag{A.94}$$

Now, we can take the limit $R \to 0$ in the second and third terms,

$$-iR\int_{-\pi}^{\pi} d\phi\, e^{Re^{i\phi}t}\tilde{f}(Re^{i\phi}) \simeq 2i\frac{a_\mu}{\mu+1}R^{\mu+1}e^{-Rt}\sin(\pi\mu). \tag{A.95}$$

For $\mu < -2$, this procedure has to be repeated several times, we shall, however, not consider this here. In the contribution from above and below the branch cut, we note that for large t, contributions from further away from the branch point are exponentially suppressed. We may thus also apply the expansion of $\tilde{f}(s)$ in the vicinity of the branch point,

$$\begin{aligned}\int_R^\infty dr\, e^{-rt}\left[\tilde{f}(re^{i\pi})-\tilde{f}(re^{-i\pi})\right] \simeq a_\mu\int_R^\infty dr\, e^{-rt}r^\mu\left[e^{i\mu\pi}-e^{-i\mu\pi}\right]\\ +a_{\mu+1}\int_R^\infty dr\, e^{-rt}r^{\mu+1}\left[e^{i(\mu+1)\pi}-e^{-i(\mu+1)\pi}\right]. \end{aligned} \tag{A.96}$$

For $-1 < \mu$, we can take the limit $R \to 0$ and obtain,

$$\begin{aligned}\int_R^\infty dr\, e^{-rt}\left[\tilde{f}(re^{i\pi})-\tilde{f}(re^{-i\pi})\right] \simeq 2ia_\mu\Gamma(\mu+1)\sin(\pi\mu)t^{-\mu-1}\\ -2ia_{\mu+1}\Gamma(\mu+2)\sin(\pi\mu)t^{-\mu-2}. \end{aligned} \tag{A.97}$$

For $-2 < \mu < -1$, on the other hand, we have to integrate by parts in the first term,

$$\begin{aligned}a_\mu\int_R^\infty dr\, e^{-rt}r^\mu\left[e^{i\mu\pi}-e^{-i\mu\pi}\right] = 2i\frac{a_\mu}{\mu+1}\sin(\pi\mu)\Big[e^{-rt}r^{\mu+1}\Big|_R^\infty\\ +t\int_R^\infty dr\, e^{-rt}r^{\mu+1}\Big]. \end{aligned} \tag{A.98}$$

Taking the limit $R \to 0$ in the second term, we find,

$$\begin{aligned}a_\mu\int_R^\infty dr\, e^{-rt}r^\mu\left[e^{i\mu\pi}-e^{-i\mu\pi}\right] \simeq -2i\frac{a_\mu}{\mu+1}\sin(\pi\mu)e^{-Rt}R^{\mu+1}\\ +2ia_\mu\sin(\pi\mu)\Gamma(\mu+1)t^{-\mu-1}. \end{aligned} \tag{A.99}$$

The contribution from the boundary term exactly cancels the one from the integral around the branch point, Eq. (A.95). Summing up, we find for large t,

$$I_{cut}(t) \simeq \frac{\sin(\pi\mu)}{\pi}e^{s_k t}\left[a_\mu\Gamma(\mu+1)t^{-\mu-1}-a_{\mu+1}\Gamma(\mu+2)t^{-\mu-2}\right]. \tag{A.100}$$

The same can be done for every branch cut. This means that, because of the exponential prefactor, the leading order asymptotic behavior of the inverse Laplace

transform for long times is given by the rightmost nonanalytic point of $\tilde{f}(s)$. If the function $\tilde{f}(s)$ has integer order poles at points $s = s_m$ and branch points at $s = s_k$, then the asymptotic inverse Laplace transform $f(t)$ is given by,

$$f(t) \simeq \sum_m \mathrm{Res}_{s=s_m} \left[e^{st} \tilde{f}(s) \right] - \frac{1}{\pi} \sum_k a_{\mu_k} \Gamma(\mu_k + 1) \sin(\pi \mu_k) t^{-\mu_k - 1} e^{s_k t}, \tag{A.101}$$

where $\mathrm{Res}_{s=s_m}$ denotes the residue at s_m and μ_k are the exponents of the leading order expansion around s_k.

B

APPENDIX: NUMERICAL SIMULATIONS

B.1 LANGEVIN TRAJECTORY SIMULATIONS

In order to verify and support our analytic asymptotic results, we perform numerical simulations of trajectories obeying the corresponding Langevin equation. These simulations are based on a discretized version of the Langevin equation, which is then evaluated on a step-by-step basis. We divide the total time t into small intervals of length Δt and define the discrete times $t_n = n\,\Delta t$, with $n = 0, 1, 2, \ldots$. The velocity v_{n+1} at time t_{n+1} can then be approximated based on its value v_n at t_n via [Kloe 92],

$$v_{n+1} - v_n = -\gamma v_n \Delta t + \sqrt{2D_v \Delta t} W_n, \tag{B.1}$$

where W_n is a random number drawn from a normal distribution with zero mean and unit variance. While in the continuous-time Langevin equation, the white noise $\eta(t)$ is an idealized random process with infinitely short ranged correlations, the latter can only be realized approximately in the discrete time formalism, since the shortest possible correlation time is given by the time step Δt. Equation (B.1) replicates the Langevin equation in the limit $\Delta t \to 0$. For practical purposes, a good approximation of Langevin dynamics requires $\gamma \Delta t \ll 1$, since then the time step is small enough to resolve the correlations in the system, Eq. (2.5). Better time resolution of course requires yet smaller time steps but the aforementioned condition is the minimal requirement to accurately reproduce the dynamics.

For simulation of the fractional Langevin equation, we need to make two changes to Eq. (B.1). First, we need to include the power-law memory kernel, and second, we need to be able to generate power-law correlated noise. For the memory kernel, we can explicitly write down its discrete-time equivalent,

$$k_n = k(t_n) = \frac{1}{\Gamma(\alpha)} {t_n}^{\alpha-1} = \frac{1}{\Gamma(\alpha)} n^{\alpha-1} \Delta t^{\alpha-1}. \tag{B.2}$$

With this, the discrete version of the fractional Langevin equation reads,

$$v_{n+1} - v_n = -\frac{\gamma}{\Gamma(\alpha)} \sum_{i=0}^{n} (n-i)^{\alpha-1} v_i \Delta t^{\alpha+1} + G_n^{\alpha}, \tag{B.3}$$

where we replaced the integral by a sum and G_n^{α} the yet to be specified discrete version of the Gaussian power-law correlated noise. However, there is an issue with the above expression: At the upper bound of the sum, the short-time divergence of the memory kernel leads to an infinite term in the sum. This problem does not occur in the continuous-time version of the equation since the divergence is integrable. The short-time divergence is actually unphysical, as the memory kernel – which also specifies the correlations of the noise – should be finite for all times.

We can remedy this by including a short-time cutoff t^* on the memory kernel, e.g by writing,

$$k(t) = \frac{1}{\Gamma(\alpha)}(t+t^*)^{\alpha-1}. \tag{B.4}$$

Since the asymptotic dynamics are governed by the asymptotic behavior of the memory kernel, this short-time cutoff does not change the former. Generally the short-time cutoff will correspond to some physical time-scale in the system under consideration. However, in order to stay as close to the continuous description as possible, we use the shortest cutoff possible, namely the time step Δt. Equation (B.3) then reads,

$$v_{n+1} - v_n = -\frac{\gamma \Delta t^{\alpha+1}}{\Gamma(\alpha)} \sum_{i=0}^{n} (n-i+1)^{\alpha-1} v_i + G_n^\alpha. \tag{B.5}$$

Computationally, evaluating the power law is expensive, for this reason, we use the recursively defined coefficients [Kasd 95],

$$\begin{aligned} a_0^\alpha &= 1 \\ a_{n+1}^\alpha &= \frac{\alpha+n}{n+1} a_n^\alpha \\ \Rightarrow a_n^\alpha &= \frac{\Gamma(\alpha+n)}{n!\Gamma(\alpha)}, \end{aligned} \tag{B.6}$$

which asymptotically reproduce the power law $n^{\alpha-1}/\mathrm{Gamma}(\alpha)$. In terms of these coefficients, we have,

$$v_{n+1} - v_n = -\gamma \Delta t^{\alpha+1} \sum_{i=0}^{n} a_{n-i}^\alpha v_i + G_n^\alpha. \tag{B.7}$$

Now we have taken care of the memory kernel, we still require a representation for the power-law correlated noise. For this, we make use of the results obtained in Section 2.2.2, in particular Eq. (2.40). There we saw, that a process defined via Gaussian white noise $\xi(t)$ by,

$$\eta(t) = \frac{\sqrt{D_\alpha}}{\Gamma\left(\frac{\alpha}{2}\right)} \int_0^t dt' \, (t-t')^{\frac{\alpha}{2}-1} \xi(t'), \tag{B.8}$$

results in a correlation function,

$$\langle \eta(t+\tau)\eta(t)\rangle = \frac{D_\alpha (-1)^{-\frac{\alpha}{2}}}{\Gamma^2\left(\frac{\alpha}{2}\right)} \tau^{\alpha-1} B\left(-\frac{t}{\tau}; \frac{\alpha}{2}, \frac{\alpha}{2}\right). \tag{B.9}$$

The process $\eta(t)$ is a linear functional of Gaussian white noise and thus Gaussian itself. In the long-time limit $t \gg \tau$, the correlation function is asymptotically stationary,

$$\langle \eta(t+\tau)\eta(t)\rangle \simeq \frac{D_\alpha \Gamma(1-\alpha) \sin\left(\frac{\pi\alpha}{2}\right)}{\pi} \tau^{\alpha-1}. \tag{B.10}$$

Comparing this to the desired noise correlation, Eq. (2.11), the two expressions agree for,

$$D_\alpha = 2m\gamma k_B T \cos\left(\frac{\pi\alpha}{2}\right). \tag{B.11}$$

However, using the coefficients in Eq. (B.6), we can write down a discrete version of $\eta(t)$,

$$H_n^\alpha = \sqrt{D_\alpha}\Delta t^{\frac{\alpha}{2}+\frac{1}{2}} \sum_{i=0}^{n} a_{n-i}^{\alpha/2} W_i. \tag{B.12}$$

In the limit $n \to \infty$, which corresponds to the long-time limit above, the processes H_n^α and G_n^α are equivalent. We can express this as,

$$G_n^\alpha = \lim_{j\to\infty} H_{j+n}^\alpha. \tag{B.13}$$

Since an infinite number of steps cannot be realized in practice, we can only realize the stationary process G_n^α in an approximate manner for $j \gg n$. This means that, if we want to have a process G_n^α, that is approximately stationary for n steps, then we first have to "equilibrate" it for a number of steps j that is much bigger than n. We also can quantify "much bigger", by examining the sub-leading order of the correlation function, which is proportional to $t^{\alpha-1}$. More precisely, if we want the nonstationary contribution to be small in relation to the stationary one, we have to demand that,

$$j^{1-\alpha} \gg n^{1-\alpha} \frac{\Gamma(2-\alpha)\sin\left(\frac{\pi\alpha}{2}\right)\Gamma^2\left(\frac{\alpha}{2}\right)}{\pi}. \tag{B.14}$$

For values of α close to 1, stationarity may thus require an excessively large number of equilibration steps. We note that these equilibration steps necessarily have to be taken before simulating the actual process, even though the noise continues to approach stationarity during the evolution. However, this will lead to discrepancies in the dynamics even at long times, similar to the ones discussed in Section 3.1.3. For the equilibrium fractional Langevin equation, we thus have the discrete approximation,

$$v_{n+1} - v_n = -\gamma\Delta t^{\alpha+1} \sum_{i=0}^{n} a_{n-i}^{\alpha} v_i + \sqrt{D_\alpha}\Delta t^{\frac{\alpha}{2}+\frac{1}{2}} \sum_{i=0}^{j+n} a_{j+n-i}^{\alpha/2} W_i. \tag{B.15}$$

The generation of the power-law noise described above also applies to the stationary and nonstationary Gaussian medium velocity processes discussed in Section 2.2.2,

$$v_{m,n} = \begin{cases} v_{\text{typ}} \sum_{i=0}^{n} a_{n-i}^{\beta/2} W_i & \text{nonstationary} \\ v_{\text{typ}} \sum_{i=0}^{j+n} a_{j+n-i}^{\beta/2} W_i & \text{stationary,} \end{cases} \tag{B.16}$$

where again we require $j \gg n$ in order to guarantee approximate stationarity. For the Lévy walk, the procedure is different, as here, the correlations do not stem from an explicit memory but from the power-law waiting time distribution. We

generate the latter from a uniform distribution U_n, i.e. random numbers drawn from the interval $(0,1)$. Specifically, we determine the random waiting times T_n via [Weis],

$$T_n = t_0 \left[1 + U_n \left(\left(\frac{t_1}{t_0} \right)^{\beta-2} - 1 \right) \right]^{\frac{1}{\beta-2}}, \tag{B.17}$$

which produces a waiting time distribution,

$$P_w(t_w) = \begin{cases} 0 & \text{for } t_w < t_0 \\ \frac{2-\beta}{{t_0}^{\beta-2} - {t_1}^{\beta-2}} {t_w}^{\beta-3} & \text{for } t_0 < t_w < t_1 \\ 0 & \text{for } t_1 < t_w. \end{cases} \tag{B.18}$$

In particular for $t_0 = 1$ and $t_1 = \infty$, we find for $\beta < 2$,

$$P_w(t_w) = \begin{cases} 0 & \text{for } t_w < 1 \\ \frac{2-\beta}{{t_0}^{\beta-2}} {t_w}^{\beta-3} & \text{for } t_0 < t_w. \end{cases} \tag{B.19}$$

This is precisely the type of power-law waiting time distribution required for the Lévy walk. From here, the procedure is straightforward: We draw a random waiting time T_0 according to the above prescription and a random velocity v_m from a Gaussian distribution with variance ${v_{typ}}^2$. As soon as the current time t_n exceeds this waiting time, we draw a new waiting time T_1 and a new velocity, and repeat this process every time t_n exceeds $T_0 + T_1$, $T_0 + T_1 + T_2$ and so on until we reach the end of the specified evolution time. Including the medium velocity, the final discrete-time version of the nonequilibrium fractional Langevin equation takes the form,

$$v_{n+1} - v_n = -\gamma \Delta t^{\alpha+1} \sum_{i=0}^{n} a_{n-i}^{\alpha} (v_i v_{m,i}) + \sqrt{D_\alpha} \Delta t^{\frac{\alpha}{2}+\frac{1}{2}} \sum_{i=0}^{j+n} a_{j+n-i}^{\alpha/2} W_i. \tag{B.20}$$

B.2 OVERVIEW OF SIMULATION PROGRAM

Our numerical simulation program is built around Eq. (B.20). It is written in Fortran and is designed to simulate a large number of stochastic trajectories and analyze the resulting data. In the following we give a short overview over the simulation program and some of its main components.

Since we want to simulate a stochastic system, a central requirement for our program is generating pseudo-random numbers. In order to optimize performance, we designed the program to be able to heavily utilize parallel processing, both for generation of the trajectories and data analysis. However, this prohibits usage of the random number generators built into Fortran, since the latter are not designed with parallel processing in mind. We therefore use a multi-threaded variant of the Mersenne twister [Ishi 11], which is able to generate uniformly distributed

pseudo-random numbers in parallel. From these uniform random numbers, we can generate the normal distributed ones using a Box-Muller algorithm [Vett 89] and the power-law distributed ones according to the prescription given in Eq. (B.17).

The program itself is organized into a main program, which handles data input and output, and several subroutines for generating the trajectories and analyzing the resulting data. The principle mode of operation is the following: The main program reads the input parameters, e.g. the number of trajectories and integration steps, the parameters of the underlying mathematical model, and what types of data analysis to perform, from an input file. It then passes these parameters to the trajectory subroutine which generates the prescribed number of trajectories using these parameters. After the trajectories have been generated, the main program calls the data analysis subroutines to extract the required quantities from the data array. Finally it outputs these quantities in the form of several files, which can then be further processed using e.g. a graphing software. There are a number of both trajectory and data analysis subroutines available. In terms of trajectories, the moving viscoelastic medium model, both with the Gaussian and the Lévy walk medium velocity processes, as well as ordinary Brownian motion, a pure Lévy walk and a semiclassical model for diffusion in optical lattices can be selected. The data analysis subroutines include the determination of arbitrary moments, autocorrelations, distributions, time averages and spectral densities, all for both the velocity and the displacement. Since we want to examine scale-invariant processes, we explicitly use the full power-law memory kernel instead of much faster approximate methods [Sieg 10]. Because the memory kernel has to be recalculated after every step, the computation time scales as the number of steps squared. This turns out to be the main limit for generating long time series; in practice on the order of 10^4 time steps for 10^4 trajectories requires about half an hour of computation time on a fast six-core CPU, increasing the number of steps by a factor of 10 already requires about two days.

We forego more detailed description of or instructions for the program at this point, since for this work, it merely serves as a consistency check for our analytic results. Both the code and documentation are available upon request and will be made public at a later time.

BIBLIOGRAPHY

[Abra 12] M. Abramowitz and I. A. Stegun. *Handbook of Mathematical Functions: with Formulas, Graphs, and Mathematical Tables*. Courier Dover Publications, Apr. 2012.

[Albe 02] B. Alberts, A. Johnson, J. Lewis, P. Walter, M. Raff, and K. Roberts. *Molecular Biology of the Cell 4th Edition: International Student Edition*. Routledge, May 2002.

[Ambl 96] F. Amblard, A. C. Maggs, B. Yurke, A. N. Pargellis, and S. Leibler. "Subdiffusion and Anomalous Local Viscoelasticity in Actin Networks". *Physical Review Letters*, Vol. 77, No. 21, pp. 4470–4473, Nov. 1996.

[Ashk 97] A. Ashkin. "Optical trapping and manipulation of neutral particles using lasers". *Proceedings of the National Academy of Sciences*, Vol. 94, No. 10, pp. 4853–4860, May 1997. PMID: 9144154.

[Ball 06] M. Balland, N. Desprat, D. Icard, S. Féréol, A. Asnacios, J. Browaeys, S. Hénon, and F. Gallet. "Power laws in microrheology experiments on living cells: Comparative analysis and modeling". *Physical Review E*, Vol. 74, No. 2, p. 021911, Aug. 2006.

[Banc 99] A. J. Banchio, G. Nägele, and J. Bergenholtz. "Viscoelasticity and generalized Stokes–Einstein relations of colloidal dispersions". *The Journal of Chemical Physics*, Vol. 111, No. 18, pp. 8721–8740, Nov. 1999.

[Bark 03] E. Barkai. "Aging in Subdiffusion Generated by a Deterministic Dynamical System". *Physical Review Letters*, Vol. 90, No. 10, p. 104101, March 2003.

[Bate 55] H. Bateman and A. Erdelyi. *Higher Transcendental Functions, Vol. 3: Elliptic and Automorphic Functions, Lamé and Mathieu Functions*. McGraw Hill, New York, 1955.

[Baus 98] A. R. Bausch, F. Ziemann, A. A. Boulbitch, K. Jacobson, and E. Sackmann. "Local Measurements of Viscoelastic Parameters of Adherent Cell Surfaces by Magnetic Bead Microrheometry". *Biophysical Journal*, Vol. 75, No. 4, pp. 2038–2049, Oct. 1998.

[Baus 99] A. R. Bausch, W. Möller, and E. Sackmann. "Measurement of Local Viscoelasticity and Forces in Living Cells by Magnetic Tweezers". *Biophysical Journal*, Vol. 76, No. 1, pp. 573–579, Jan. 1999.

[Beil 03] M. Beil, A. Micoulet, G. von Wichert, S. Paschke, P. Walther, M. B. Omary, P. P. Van Veldhoven, U. Gern, E. Wolff-Hieber, J. Eggermann, J. Waltenberger, G. Adler, J. Spatz, and T. Seufferlein. "Sphingosylphosphorylcholine regulates keratin network architecture and visco-elastic

properties of human cancer cells". *Nature Cell Biology*, Vol. 5, No. 9, pp. 803–811, Sep. 2003.

[Bel 05] G. Bel and E. Barkai. "Weak Ergodicity Breaking in the Continuous-Time Random Walk". *Physical Review Letters*, Vol. 94, No. 24, p. 240602, June 2005.

[Bert 12a] O. J. N. Bertrand, D. K. Fygenson, and O. A. Saleh. "Active, motor-driven mechanics in a DNA gel". *Proceedings of the National Academy of Sciences*, Vol. 109, No. 43, pp. 17342–17347, Oct. 2012. PMID: 23045635.

[Bert 12b] E. Bertseva, D. Grebenkov, P. Schmidhauser, S. Gribkova, S. Jeney, and L. Forró. "Optical trapping microrheology in cultured human cells". *The European Physical Journal E*, Vol. 35, No. 7, pp. 1–8, July 2012.

[Bohe 13] P. Bohec, F. Gallet, C. Maes, S. Safaverdi, P. Visco, and F. v. Wijland. "Probing active forces via a fluctuation-dissipation relation: Application to living cells". *EPL (Europhysics Letters)*, Vol. 102, No. 5, p. 50005, June 2013.

[Bonn 03] D. Bonn and W. K. Kegel. "Stokes–Einstein relations and the fluctuation-dissipation theorem in a supercooled colloidal fluid". *The Journal of Chemical Physics*, Vol. 118, No. 4, pp. 2005–2009, Jan. 2003.

[Bouc 92] J. P. Bouchaud. "Weak ergodicity breaking and aging in disordered systems". *Journal de Physique I*, Vol. 2, No. 9, pp. 1705–1713, Sep. 1992.

[Bran 08] C. P. Brangwynne, G. H. Koenderink, F. C. MacKintosh, and D. A. Weitz. "Cytoplasmic diffusion: molecular motors mix it up". *The Journal of Cell Biology*, Vol. 183, No. 4, pp. 583–587, Nov. 2008. PMID: 19001127.

[Bran 09] C. P. Brangwynne, G. H. Koenderink, F. C. MacKintosh, and D. A. Weitz. "Intracellular transport by active diffusion". *Trends in Cell Biology*, Vol. 19, No. 9, pp. 423–427, Sep. 2009.

[Brau 07] R. R. Brau, J. M. Ferrer, H. Lee, C. E. Castro, B. K. Tam, P. B. Tarsa, P. Matsudaira, M. C. Boyce, R. D. Kamm, and M. J. Lang. "Passive and active microrheology with optical tweezers". *Journal of Optics A: Pure and Applied Optics*, Vol. 9, No. 8, p. S103, Aug. 2007.

[Brow 28] R. Brown. "XXVII. A brief account of microscopical observations made in the months of June, July and August 1827, on the particles contained in the pollen of plants; and on the general existence of active molecules in organic and inorganic bodies". *The Philosophical Magazine, or Annals of Chemistry, Mathematics, Astronomy, Natural History and General Science*, Vol. 4, No. 21, p. 161–173, 1828.

[Brun 09] L. Bruno, V. Levi, M. Brunstein, and M. A. Despósito. "Transition to superdiffusive behavior in intracellular actin-based transport mediated by molecular motors". *Physical Review E*, Vol. 80, No. 1, p. 011912, July 2009.

[Buda 06] V. P. Budaev, S. Takamura, N. Ohno, and S. Masuzaki. "Superdiffusion and multifractal statistics of edge plasma turbulence in fusion devices". *Nuclear Fusion*, Vol. 46, No. 4, p. S181, Apr. 2006.

[Burs 05] P. Bursac, G. Lenormand, B. Fabry, M. Oliver, D. A. Weitz, V. Viasnoff, J. P. Butler, and J. J. Fredberg. "Cytoskeletal remodelling and slow dynamics in the living cell". *Nature Materials*, Vol. 4, No. 7, pp. 557–561, July 2005.

[Burs 07] P. Bursac, B. Fabry, X. Trepat, G. Lenormand, J. P. Butler, N. Wang, J. J. Fredberg, and S. S. An. "Cytoskeleton dynamics: Fluctuations within the network". *Biochemical and Biophysical Research Communications*, Vol. 355, No. 2, pp. 324–330, Apr. 2007.

[Call 51] H. B. Callen and T. A. Welton. "Irreversibility and Generalized Noise". *Physical Review*, Vol. 83, No. 1, pp. 34–40, July 1951.

[Casp 02] A. Caspi, R. Granek, and M. Elbaum. "Diffusion and directed motion in cellular transport". *Physical Review E*, Vol. 66, No. 1, p. 011916, July 2002.

[Cast 91] Y. Castin, J. Dalibard, and C. Cohen-Tannoudji. "The limits of Sisyphus cooling". *Light Induced Kinetic Effects on Atoms, Ions, and Molecules*, p. 5, 1991.

[Chen 03] D. T. Chen, E. R. Weeks, J. C. Crocker, M. F. Islam, R. Verma, J. Gruber, A. J. Levine, T. C. Lubensky, and A. G. Yodh. "Rheological Microscopy: Local Mechanical Properties from Microrheology". *Physical Review Letters*, Vol. 90, No. 10, p. 108301, March 2003.

[Chen 07] D. T. N. Chen, A. W. C. Lau, L. A. Hough, M. F. Islam, M. Goulian, T. C. Lubensky, and A. G. Yodh. "Fluctuations and Rheology in Active Bacterial Suspensions". *Physical Review Letters*, Vol. 99, No. 14, p. 148302, Oct. 2007.

[Coff 04] W. Coffey, Y. P. Kalmykov, and J. T. Waldron. *The Langevin equation: with applications to stochastic problems in physics, chemistry, and electrical engineering*. Vol. 14, World Scientific, 2004.

[Cohe 06] M. H. Cohen and P. Venkatesh. "Evidence for Superdiffusion and "Momentum" in Stock Price Changes". In: H. Takayasu, Ed., *Practical Fruits of Econophysics*, pp. 147–151, Springer Tokyo, Jan. 2006.

[Croc 07] J. C. Crocker and B. D. Hoffman. "Multiple-Particle Tracking and Two-Point Microrheology in Cells". In: Yu-Li Wang and Dennis E. Discher, Ed., *Methods in Cell Biology*, pp. 141–178, Academic Press, 2007.

[Cugl 11] L. F. Cugliandolo. "The effective temperature". *Journal of Physics A: Mathematical and Theoretical*, Vol. 44, No. 48, p. 483001, Dec. 2011.

[Cugl 94] L. F. Cugliandolo, J. Kurchan, and G. Parisi. "Off equilibrium dynamics and aging in unfrustrated systems". *Journal de Physique I*, Vol. 4, No. 11, pp. 1641–1656, Nov. 1994.

[Cugl 95] L. F. Cugliandolo and J. Kurchan. "Weak ergodicity breaking in mean-field spin-glass models". *Philosophical Magazine Part B*, Vol. 71, No. 4, pp. 501–514, 1995.

[Cugl 97] L. F. Cugliandolo, J. Kurchan, and L. Peliti. "Energy flow, partial equilibration, and effective temperatures in systems with slow dynamics". *Physical Review E*, Vol. 55, No. 4, pp. 3898–3914, Apr. 1997.

[Dech 12] A. Dechant and E. Lutz. "Anomalous Spatial Diffusion and Multifractality in Optical Lattices". *Physical Review Letters*, Vol. 108, No. 23, p. 230601, June 2012.

[Dech 13] A. Dechant and E. Lutz. "Connecting active and passive microrheology in living cells". *arXiv:1307.6466 [cond-mat]*, July 2013.

[Dech 14] A. Dechant, E. Lutz, D. A. Kessler, and E. Barkai. "Scaling Green-Kubo Relation and Application to Three Aging Systems". *Physical Review X*, Vol. 4, No. 1, p. 011022, Feb. 2014.

[Deng 09] W. Deng and E. Barkai. "Ergodic properties of fractional Brownian-Langevin motion". *Physical Review E*, Vol. 79, No. 1, p. 011112, Jan. 2009.

[Dere 03] C. Derec, G. Ducouret, A. Ajdari, and F. Lequeux. "Aging and nonlinear rheology in suspensions of polyethylene oxide–protected silica particles". *Physical Review E*, Vol. 67, No. 6, p. 061403, June 2003.

[Desp 05] N. Desprat, A. Richert, J. Simeon, and A. Asnacios. "Creep Function of a Single Living Cell". *Biophysical Journal*, Vol. 88, No. 3, pp. 2224–2233, March 2005.

[Desp 11] M. A. Despósito. "Superdiffusion induced by a long-correlated external random force". *Physical Review E*, Vol. 84, No. 6, p. 061114, Dec. 2011.

[Dix 08] J. A. Dix and A. S. Verkman. "Crowding effects on diffusion in solutions and cells". *Annual review of biophysics*, Vol. 37, pp. 247–263, 2008. PMID: 18573081.

[Doet 74] G. Doetsch. *Introduction to the Theory and Application of the Laplace Transformation*. Springer-Verlag, Jan. 1974.

[Doob 90] J. L. Doob. *Stochastic processes*. Wiley, 1990.

[Eins 05] A. Einstein. "Über die von der molekularkinetischen Theorie der Wärme geforderte Bewegung von in ruhenden Flüssigkeiten suspendierten Teilchen". *Annalen der Physik*, Vol. 322, No. 8, p. 549–560, 1905.

[Elli 03] R. J. Ellis and A. P. Minton. "Cell biology: Join the crowd". *Nature*, Vol. 425, No. 6953, pp. 27–28, Sep. 2003.

[Evan 95] E. Evans, K. Ritchie, and R. Merkel. "Sensitive force technique to probe molecular adhesion and structural linkages at biological interfaces". *Biophysical Journal*, Vol. 68, No. 6, pp. 2580–2587, June 1995.

[Fabr 01] B. Fabry, G. N. Maksym, J. P. Butler, M. Glogauer, D. Navajas, and J. J. Fredberg. "Scaling the Microrheology of Living Cells". *Physical Review Letters*, Vol. 87, No. 14, p. 148102, Sep. 2001.

[Fabr 11] B. Fabry, A. H. Klemm, S. Kienle, T. E. Schäffer, and W. H. Goldmann. "Focal Adhesion Kinase Stabilizes the Cytoskeleton". *Biophysical Journal*, Vol. 101, No. 9, pp. 2131–2138, Nov. 2011.

[Fene 01] W. Feneberg, M. Westphal, and E. Sackmann. "Dictyostelium cells' cytoplasm as an active viscoplastic body". *European Biophysics Journal*, Vol. 30, No. 4, pp. 284–294, Aug. 2001.

[Find 13] W. N. Findley and F. A. Davis. *Creep and relaxation of nonlinear viscoelastic materials*. Courier Dover Publications, 2013.

[Flan 89] P. Flandrin. "On the spectrum of fractional Brownian motions". *IEEE Transactions on Information Theory*, Vol. 35, No. 1, pp. 197–199, Jan. 1989.

[Foge 07] H. C. Fogedby and R. Metzler. "DNA Bubble Dynamics as a Quantum Coulomb Problem". *Physical Review Letters*, Vol. 98, No. 7, p. 070601, Feb. 2007.

[Froe 13] D. Froemberg and E. Barkai. "Random time averaged diffusivities for Lévy walks". *The European Physical Journal B*, Vol. 86, No. 7, pp. 1–13, July 2013.

[Gal 10] N. Gal and D. Weihs. "Experimental evidence of strong anomalous diffusion in living cells". *Physical Review E*, Vol. 81, No. 2, p. 020903, Feb. 2010.

[Gal 12] N. Gal and D. Weihs. "Intracellular Mechanics and Activity of Breast Cancer Cells Correlate with Metastatic Potential". *Cell Biochemistry and Biophysics*, Vol. 63, No. 3, pp. 199–209, July 2012.

[Gal 13] N. Gal, D. Lechtman-Goldstein, and D. Weihs. "Particle tracking in living cells: a review of the mean square displacement method and beyond". *Rheologica Acta*, Vol. 52, No. 5, pp. 425–443, May 2013.

[Gall 09] F. Gallet, D. Arcizet, P. Bohec, and A. Richert. "Power spectrum of out-of-equilibrium forces in living cells: amplitude and frequency dependence". *Soft Matter*, Vol. 5, No. 15, pp. 2947–2953, July 2009.

[Gira 04] K. D. Girard, C. Chaney, M. Delannoy, S. C. Kuo, and D. N. Robinson. "Dynacortin contributes to cortical viscoelasticity and helps define the shape changes of cytokinesis". *The EMBO Journal*, Vol. 23, No. 7, pp. 1536–1546, July 2004.

[Godr 01] C. Godrèche and J. M. Luck. "Statistics of the Occupation Time of Renewal Processes". *Journal of Statistical Physics*, Vol. 104, No. 3-4, pp. 489–524, Aug. 2001.

[Gold 06] I. Golding and E. C. Cox. "Physical Nature of Bacterial Cytoplasm". *Physical Review Letters*, Vol. 96, No. 9, p. 098102, March 2006.

[Gree 53] M. S. Green. "Markoff Random Processes and the Statistical Mechanics of Time-Dependent Phenomena. II. Irreversible Processes in Fluids". *The Journal of Chemical Physics*, Vol. 22, No. 3, pp. 398–413, March 1953.

[Guig 08] G. Guigas and M. Weiss. "Sampling the Cell with Anomalous Diffusion—The Discovery of Slowness". *Biophysical Journal*, Vol. 94, No. 1, pp. 90–94, Jan. 2008.

[Haub 11] H. J. Haubold, A. M. Mathai, and R. K. Saxena. "Mittag-Leffler Functions and Their Applications". *Journal of Applied Mathematics*, Vol. 2011, May 2011.

[Hoff 09] B. D. Hoffman and J. C. Crocker. "Cell Mechanics: Dissecting the Physical Responses of Cells to Force". *Annual Review of Biomedical Engineering*, Vol. 11, No. 1, pp. 259–288, 2009.

[Hofl 06] F. Höfling, T. Franosch, and E. Frey. "Localization Transition of the Three-Dimensional Lorentz Model and Continuum Percolation". *Physical Review Letters*, Vol. 96, No. 16, p. 165901, Apr. 2006.

[Hofl 13] F. Höfling and T. Franosch. "Anomalous transport in the crowded world of biological cells". *Reports on Progress in Physics*, Vol. 76, No. 4, p. 046602, Apr. 2013.

[Hull 00] J. Hull. *Options, Futures, & Other Derivatives, Fourth Edition: Instructor's Manual*. Prentice Hall, 2000.

[Hurs 51] H. Hurst. "Long-term storage capacity of reservoirs". *Trans. Amer. Soc. Civil Eng.*, Vol. 116, pp. 770–808, 1951.

[Indr 94] A. V. Indrani and S. Ramaswamy. "Universal self-diffusion and subdiffusion in colloids at freezing". *Physical Review Letters*, Vol. 73, No. 2, pp. 360–363, July 1994.

[Iosi 12] M. Iosifescu and P. Tautu. *Stochastic Processes and Applications in Biology and Medicine I: Theory*. Springer London, Limited, Jan. 2012.

[Ishi 11] K.-I. Ishikawa. "Multiple stream Mersenne Twister PRNG". March 2011.

[Isse 16] L. Isserlis. "On Certain Probable Errors and Correlation Coefficients of Multiple Frequency Distributions with Skew Regression". *Biometrika*, Vol. 11, No. 3, p. 185, May 1916.

[Jeon 11] J.-H. Jeon, V. Tejedor, S. Burov, E. Barkai, C. Selhuber-Unkel, K. Berg-Sørensen, L. Oddershede, and R. Metzler. "In Vivo Anomalous Diffusion and Weak Ergodicity Breaking of Lipid Granules". *Physical Review Letters*, Vol. 106, No. 4, p. 048103, Jan. 2011.

[Jung 02] Y. Jung, E. Barkai, and R. J. Silbey. "Lineshape theory and photon counting statistics for blinking quantum dots: a Lévy walk process". *Chemical Physics*, Vol. 284, No. 1–2, pp. 181–194, Nov. 2002.

[Kamp 81] N. G. v. Kampen. "Itô versus Stratonovich". *Journal of Statistical Physics*, Vol. 24, No. 1, pp. 175–187, Jan. 1981.

[Kamp 92] N. G. V. Kampen. *Stochastic Processes in Physics and Chemistry*. Elsevier, Nov. 1992.

[Kasd 95] N. Kasdin. "Discrete simulation of colored noise and stochastic processes and 1/f alpha; power law noise generation". *Proceedings of the IEEE*, Vol. 83, No. 5, pp. 802–827, May 1995.

[Kasz 07] K. E. Kasza, A. C. Rowat, J. Liu, T. E. Angelini, C. P. Brangwynne, G. H. Koenderink, and D. A. Weitz. "The cell as a material". *Current Opinion in Cell Biology*, Vol. 19, No. 1, pp. 101–107, Feb. 2007.

[Kess 12] D. A. Kessler and E. Barkai. "Theory of Fractional Lévy Kinetics for Cold Atoms Diffusing in Optical Lattices". *Physical Review Letters*, Vol. 108, No. 23, p. 230602, June 2012.

[Khol 95] A. L. Kholodenko and J. F. Douglas. "Generalized Stokes-Einstein equation for spherical particle suspensions". *Physical Review E*, Vol. 51, No. 2, pp. 1081–1090, Feb. 1995.

[Klaf 05] J. Klafter and I. M. Sokolov. "Anomalous diffusion spreads its wings". *Physics world*, Vol. 18, No. 8, pp. 29–32, 2005.

[Klaf 87] J. Klafter, A. Blumen, and M. F. Shlesinger. "Stochastic pathway to anomalous diffusion". *Physical Review A*, Vol. 35, No. 7, pp. 3081–3085, Apr. 1987.

[Klaf 90] J. Klafter, A. Blumen, G. Zumofen, and M. F. Shlesinger. "Lévy walk approach to anomalous diffusion". *Physica A: Statistical Mechanics and its Applications*, Vol. 168, No. 1, pp. 637–645, Sep. 1990.

[Kloe 92] P. E. Kloeden and E. Platen. *Numerical Solution of Stochastic Differential Equations*. Springer, Jan. 1992.

[Klum 05] S. Klumpp and R. Lipowsky. "Cooperative cargo transport by several molecular motors". *Proceedings of the National Academy of Sciences of the United States of America*, Vol. 102, No. 48, pp. 17284–17289, Nov. 2005. PMID: 16287974.

[Koll 11] P. Kollmannsberger and B. Fabry. "Linear and Nonlinear Rheology of Living Cells". *Annual Review of Materials Research*, Vol. 41, No. 1, pp. 75–97, 2011.

[Kolo 07] A. B. Kolomeisky and M. E. Fisher. "Molecular Motors: A Theorist's Perspective". *Annual Review of Physical Chemistry*, Vol. 58, No. 1, pp. 675–695, 2007. PMID: 17163836.

[Kou 04] S. C. Kou and X. S. Xie. "Generalized Langevin Equation with Fractional Gaussian Noise: Subdiffusion within a Single Protein Molecule". *Physical Review Letters*, Vol. 93, No. 18, p. 180603, Oct. 2004.

[Kubo 57] R. Kubo. "Statistical-Mechanical Theory of Irreversible Processes. I. General Theory and Simple Applications to Magnetic and Conduction Problems". *Journal of the Physical Society of Japan*, Vol. 12, No. 6, pp. 570–586, June 1957.

[Kubo 65] R. Kubo. *Tokyo Summer Lectures in Theoretical Physics, Part I: Many-body Theory*. Benjamin, New York, 1965.

[Kubo 66] R. Kubo. "The fluctuation-dissipation theorem". *Reports on Progress in Physics*, Vol. 29, No. 1, p. 255, Jan. 1966.

[Kuli 08] I. M. Kulić, A. E. X. Brown, H. Kim, C. Kural, B. Blehm, P. R. Selvin, P. C. Nelson, and V. I. Gelfand. "The role of microtubule movement in bidirectional organelle transport". *Proceedings of the National Academy of Sciences*, Vol. 105, No. 29, pp. 10011–10016, July 2008. PMID: 18626022.

[Lang 08] P. Langevin. "Sur la théorie du mouvement brownien". *CR Acad. Sci. Paris*, Vol. 146, No. 530-533, 1908.

[Lapa 07] L. C. Lapas, I. V. L. Costa, M. H. Vainstein, and F. A. Oliveira. "Entropy, non-ergodicity and non-Gaussian behaviour in ballistic transport". *EPL (Europhysics Letters)*, Vol. 77, No. 3, p. 37004, Feb. 2007.

[Lau 03] A. W. C. Lau, B. D. Hoffman, A. Davies, J. C. Crocker, and T. C. Lubensky. "Microrheology, Stress Fluctuations, and Active Behavior of Living Cells". *Physical Review Letters*, Vol. 91, No. 19, p. 198101, Nov. 2003.

[Lee 07] S.-H. Lee, Y. Roichman, G.-R. Yi, S.-H. Kim, S.-M. Yang, A. van Blaaderen, P. van Oostrum, and D. G. Grier. "Characterizing and tracking single colloidal particles with video holographic microscopy". *Optics Express*, Vol. 15, No. 26, pp. 18275–18282, Dec. 2007.

[Lee 10] H. Lee, J. M. Ferrer, F. Nakamura, M. J. Lang, and R. D. Kamm. "Passive and active microrheology for cross-linked F-actin networks in vitro". *Acta Biomaterialia*, Vol. 6, No. 4, pp. 1207–1218, Apr. 2010.

[Leib 13] N. Leibovich and E. Barkai. "Everlasting effect of initial conditions on single-file diffusion". *Physical Review E*, Vol. 88, No. 3, p. 032107, Sep. 2013.

[Leno 07] G. Lenormand, J. Chopin, P. Bursac, J. J. Fredberg, and J. P. Butler. "Directional memory and caged dynamics in cytoskeletal remodelling". *Biochemical and Biophysical Research Communications*, Vol. 360, No. 4, pp. 797–801, Sep. 2007.

[Levi 09] A. J. Levine and F. C. MacKintosh. "The Mechanics and Fluctuation Spectrum of Active Gels†". *The Journal of Physical Chemistry B*, Vol. 113, No. 12, pp. 3820–3830, March 2009.

[Lim 02] S. C. Lim and S. V. Muniandy. "Self-similar Gaussian processes for modeling anomalous diffusion". *Physical Review E*, Vol. 66, No. 2, p. 021114, Aug. 2002.

[Liu 08] B. Liu and J. Goree. "Superdiffusion and Non-Gaussian Statistics in a Driven-Dissipative 2D Dusty Plasma". *Physical Review Letters*, Vol. 100, No. 5, p. 055003, Feb. 2008.

[Lutz 01] E. Lutz. "Fractional Langevin equation". *Physical Review E*, Vol. 64, No. 5, p. 051106, Oct. 2001.

[MacK 08] F. C. MacKintosh and A. J. Levine. "Nonequilibrium Mechanics and Dynamics of Motor-Activated Gels". *Physical Review Letters*, Vol. 100, No. 1, p. 018104, Jan. 2008.

[Magd 09] M. Magdziarz, A. Weron, K. Burnecki, and J. Klafter. "Fractional Brownian Motion Versus the Continuous-Time Random Walk: A Simple Test for Subdiffusive Dynamics". *Physical Review Letters*, Vol. 103, No. 18, p. 180602, Oct. 2009.

[Mand 68] B. B. Mandelbrot and J. W. Van Ness. "Fractional Brownian Motions, Fractional Noises and Applications". *SIAM Review*, Vol. 10, No. 4, pp. 422–437, Oct. 1968.

[Maso 00] T. G. Mason. "Estimating the viscoelastic moduli of complex fluids using the generalized Stokes–Einstein equation". *Rheologica Acta*, Vol. 39, No. 4, pp. 371–378, Aug. 2000.

[Maso 95] T. G. Mason and D. A. Weitz. "Optical Measurements of Frequency-Dependent Linear Viscoelastic Moduli of Complex Fluids". *Physical Review Letters*, Vol. 74, No. 7, pp. 1250–1253, Feb. 1995.

[Maso 97] T. G. Mason, K. Ganesan, J. H. van Zanten, D. Wirtz, and S. C. Kuo. "Particle Tracking Microrheology of Complex Fluids". *Physical Review Letters*, Vol. 79, No. 17, pp. 3282–3285, Oct. 1997.

[Mass 07] G. Massiera, K. M. Van Citters, P. L. Biancaniello, and J. C. Crocker. "Mechanics of Single Cells: Rheology, Time Dependence, and Fluctuations". *Biophysical Journal*, Vol. 93, No. 10, pp. 3703–3713, Nov. 2007.

[Metz 07] C. Metzner, C. Raupach, D. Paranhos Zitterbart, and B. Fabry. "Simple model of cytoskeletal fluctuations". *Physical Review E*, Vol. 76, No. 2, p. 021925, Aug. 2007.

[Metz 10] C. Metzner, C. Raupach, C. T. Mierke, and B. Fabry. "Fluctuations of cytoskeleton-bound microbeads—the effect of bead–receptor binding dynamics". *Journal of Physics: Condensed Matter*, Vol. 22, No. 19, p. 194105, May 2010.

[Mill 04] S. Miller and D. Childers. *Probability and random processes: With applications to signal processing and communications*. Academic Press, 2004.

[Mill 93] K. Miller and B. Ross. *An Introduction to the Fractional Calculus and Fractional Differential Equations*. John Wiley & Sons, May 1993.

[Milo 02] E. Milotti. "1/f noise: a pedagogical review". *arXiv:physics/0204033*, Apr. 2002.

[Mizu 07] D. Mizuno, C. Tardin, C. F. Schmidt, and F. C. MacKintosh. "Nonequilibrium Mechanics of Active Cytoskeletal Networks". *Science*, Vol. 315, No. 5810, pp. 370–373, Jan. 2007. PMID: 17234946.

[Mizu 08] D. Mizuno, D. A. Head, F. C. MacKintosh, and C. F. Schmidt. "Active and Passive Microrheology in Equilibrium and Nonequilibrium Systems". *Macromolecules*, Vol. 41, No. 19, pp. 7194–7202, Oct. 2008.

[Morg 02] R. Morgado, F. A. Oliveira, G. G. Batrouni, and A. Hansen. "Relation between Anomalous and Normal Diffusion in Systems with Memory". *Physical Review Letters*, Vol. 89, No. 10, p. 100601, Aug. 2002.

[Mori 65] H. Mori. "Transport, Collective Motion, and Brownian Motion". *Progress of Theoretical Physics*, Vol. 33, No. 3, pp. 423–455, Jan. 1965.

[Niem 13] M. Niemann, H. Kantz, and E. Barkai. "Fluctuations of 1/f Noise and the Low-Frequency Cutoff Paradox". *Physical Review Letters*, Vol. 110, No. 14, p. 140603, Apr. 2013.

[Nyqu 28] H. Nyquist. "Thermal Agitation of Electric Charge in Conductors". *Physical Review*, Vol. 32, No. 1, pp. 110–113, July 1928.

[Papo 02] A. Papoulis and S. U. Pillai. *Probability, random variables, and stochastic processes*. Tata McGraw-Hill Education, 2002.

[Pott 03] N. Pottier. "Aging properties of an anomalously diffusing particule". *Physica A: Statistical Mechanics and its Applications*, Vol. 317, No. 3–4, pp. 371–382, Jan. 2003.

[Pott 05] N. Pottier. "Out of equilibrium generalized Stokes–Einstein relation: determination of the effective temperature of an aging medium". *Physica A: Statistical Mechanics and its Applications*, Vol. 345, No. 3–4, pp. 472–484, Jan. 2005.

[Rahm 64] A. Rahman. "Correlations in the Motion of Atoms in Liquid Argon". *Physical Review*, Vol. 136, No. 2A, pp. A405–A411, Oct. 1964.

[Rebe 13] A. Rebenshtok, S. Denisov, P. Hanggi, and E. Barkai. "Nonnormalizable densities in strong anomalous diffusion: beyond the central limit theorem". *arXiv:1312.3831 [cond-mat, physics:nlin]*, Dec. 2013.

[Reif 09] F. Reif. *Fundamentals of statistical and thermal physics*. Waveland Press, 2009.

[Rice 12] S. A. Rice. *Advances in Chemical Physics*. John Wiley & Sons, Feb. 2012.

[Robe 10] D. Robert, T.-H. Nguyen, F. Gallet, and C. Wilhelm. "In Vivo Determination of Fluctuating Forces during Endosome Trafficking Using a Combination of Active and Passive Microrheology". *PLoS ONE*, Vol. 5, No. 4, p. e10046, Apr. 2010.

[Sade 13] S. Sadegh, E. Barkai, and D. Krapf. "Five critical exponents describing 1/f noise for intermittent quantum dots". *arXiv:1312.3561 [cond-mat]*, Dec. 2013.

[Sagi 12] Y. Sagi, M. Brook, I. Almog, and N. Davidson. "Observation of Anomalous Diffusion and Fractional Self-Similarity in One Dimension". *Physical Review Letters*, Vol. 108, No. 9, p. 093002, March 2012.

[Saxt 97] M. J. Saxton. "Single-particle tracking: the distribution of diffusion coefficients". *Biophysical Journal*, Vol. 72, No. 4, pp. 1744–1753, Apr. 1997.

[Sche 73] H. Scher and M. Lax. "Stochastic Transport in a Disordered Solid. I. Theory". *Physical Review B*, Vol. 7, No. 10, pp. 4491–4502, May 1973.

[Schl 06] M. Schliwa. "Molecular Motors". In: *Encyclopedic Reference of Genomics and Proteomics in Molecular Medicine*, pp. 1160–1174, Springer Berlin Heidelberg, Jan. 2006.

[Schn 97] B. Schnurr, F. Gittes, F. C. MacKintosh, and C. F. Schmidt. "Determining Microscopic Viscoelasticity in Flexible and Semiflexible Polymer Networks from Thermal Fluctuations". *Macromolecules*, Vol. 30, No. 25, pp. 7781–7792, Dec. 1997.

[Sere 12] L. E. Sereshki, M. A. Lomholt, and R. Metzler. "A solution to the subdiffusion-efficiency paradox: Inactive states enhance reaction efficiency at subdiffusion conditions in living cells". *EPL (Europhysics Letters)*, Vol. 97, No. 2, p. 20008, Jan. 2012.

[Shal 05] A. Shalchi. "Time-dependent transport and subdiffusion of cosmic rays". *Journal of Geophysical Research: Space Physics*, Vol. 110, No. A9, p. n/a–n/a, 2005.

[Shle 86] M. F. Shlesinger and J. Klafter. "Lévy Walks Versus Lévy Flights". In: H. E. Stanley and N. Ostrowsky, Eds., *On Growth and Form*, pp. 279–283, Springer Netherlands, Jan. 1986.

[Shle 87] M. F. Shlesinger, B. J. West, and J. Klafter. "Lévy dynamics of enhanced diffusion: Application to turbulence". *Physical Review Letters*, Vol. 58, No. 11, pp. 1100–1103, March 1987.

[Sieg 10] P. Siegle, I. Goychuk, P. Talkner, and P. Hänggi. "Markovian embedding of non-Markovian superdiffusion". *Physical Review E*, Vol. 81, No. 1, p. 011136, Jan. 2010.

[Smol 06] M. von Smoluchowski. "Zur kinetischen Theorie der Brownschen Molekularbewegung und der Suspensionen". *Annalen der Physik*, Vol. 326, No. 14, p. 756–780, 1906.

[Soko 08] I. M. Sokolov. "Statistics and the single molecule". *Physics*, Vol. 1, p. 8, July 2008.

[Soko 12] I. M. Sokolov. "Models of anomalous diffusion in crowded environments". *Soft Matter*, Vol. 8, No. 35, pp. 9043–9052, Aug. 2012.

[Stal 03] K. Staliunas. "Anticorrelations and subdiffusion in financial systems". *Advances in Complex Systems*, Vol. 6, No. 02, p. 251–262, 2003.

[Stuh 12] B. Stuhrmann, M. Soares e Silva, M. Depken, F. C. MacKintosh, and G. H. Koenderink. "Nonequilibrium fluctuations of a remodeling in vitro cytoskeleton". *Physical Review E*, Vol. 86, No. 2, p. 020901, Aug. 2012.

[Szym 09] J. Szymanski and M. Weiss. "Elucidating the Origin of Anomalous Diffusion in Crowded Fluids". *Physical Review Letters*, Vol. 103, No. 3, p. 038102, July 2009.

[Tayl 21] G. Taylor. "Diffusion by continuous movements". *Proceedings of the London Mathematical Society*, Vol. 20, pp. 196–211, 1921.

[Thou 97] O. Thoumine and A. Ott. "Time scale dependent viscoelastic and contractile regimes in fibroblasts probed by microplate manipulation". *Journal of Cell Science*, Vol. 110, No. 17, pp. 2109–2116, Jan. 1997. PMID: 9378761.

[Toli 04] I. M. Tolić-Nørrelykke, E.-L. Munteanu, G. Thon, L. Oddershede, and K. Berg-Sørensen. "Anomalous Diffusion in Living Yeast Cells". *Physical Review Letters*, Vol. 93, No. 7, p. 078102, Aug. 2004.

[Toyo 11] T. Toyota, D. A. Head, C. F. Schmidt, and D. Mizuno. "Non-Gaussian athermal fluctuations in active gels". *Soft Matter*, Vol. 7, No. 7, pp. 3234–3239, March 2011.

[Trep 08] X. Trepat, G. Lenormand, and J. J. Fredberg. "Universality in cell mechanics". *Soft Matter*, Vol. 4, No. 9, pp. 1750–1759, Aug. 2008.

[Tsen 02] Y. Tseng, T. P. Kole, and D. Wirtz. "Micromechanical Mapping of Live Cells by Multiple-Particle-Tracking Microrheology". *Biophysical Journal*, Vol. 83, No. 6, pp. 3162–3176, Dec. 2002.

[Vale 00] R. D. Vale and R. A. Milligan. "The Way Things Move: Looking Under the Hood of Molecular Motor Proteins". *Science*, Vol. 288, No. 5463, pp. 88–95, July 2000. PMID: 10753125.

[Verd 09] C. Verdier, J. Etienne, A. Duperray, and L. Preziosi. "Review: Rheological properties of biological materials". *Comptes Rendus Physique*, Vol. 10, No. 8, pp. 790–811, Nov. 2009.

[Vett 89] W. T. Vetterling, B. P. Flannery, W. H. Press, and S. A. Teukolski. *Numerical Recipes in FORTRAN - The Art of Scientific Computing - Second Edition*. University Press, Camebridge, 1989.

[Vian 99] M. B. Viani, T. E. Schäffer, A. Chand, M. Rief, H. E. Gaub, and P. K. Hansma. "Small cantilevers for force spectroscopy of single molecules". *Journal of Applied Physics*, Vol. 86, No. 4, pp. 2258–2262, Aug. 1999.

[Vias 02] V. Viasnoff and F. Lequeux. "Rejuvenation and Overaging in a Colloidal Glass under Shear". *Physical Review Letters*, Vol. 89, No. 6, p. 065701, July 2002.

[Visw 08] G. M. Viswanathan, E. P. Raposo, and M. G. E. da Luz. "Lévy flights and superdiffusion in the context of biological encounters and random searches". *Physics of Life Reviews*, Vol. 5, No. 3, pp. 133–150, Sep. 2008.

[Webe 10] S. C. Weber, A. J. Spakowitz, and J. A. Theriot. "Bacterial Chromosomal Loci Move Subdiffusively through a Viscoelastic Cytoplasm". *Physical Review Letters*, Vol. 104, No. 23, p. 238102, June 2010.

[Webe 12] S. C. Weber, A. J. Spakowitz, and J. A. Theriot. "Nonthermal ATP-dependent fluctuations contribute to the in vivo motion of chromosomal loci". *Proceedings of the National Academy of Sciences*, Vol. 109, No. 19, pp. 7338–7343, Aug. 2012. PMID: 22517744.

[Week 02] E. R. Weeks and D. A. Weitz. "Subdiffusion and the cage effect studied near the colloidal glass transition". *Chemical Physics*, Vol. 284, No. 1–2, pp. 361–367, Nov. 2002.

[Weih 06] D. Weihs, T. G. Mason, and M. A. Teitell. "Bio-Microrheology: A Frontier in Microrheology". *Biophysical Journal*, Vol. 91, No. 11, pp. 4296–4305, Dec. 2006.

[Weis] E. W. Weisstein. "Random Number – from Wolfram MathWorld". A random number is a number chosen as if by chance from some specified distribution such that selection of a large set of these numbers reproduces the underlying distribution. Almost always, such numbers are also required to be independent, so that there are no correlations between successive numbers. Computer-generated random numbers are sometimes called pseudorandom numbers, while the term "random" is reserved for the output of unpredictable physical processes. When used without...

[Weis 04] M. Weiss, M. Elsner, F. Kartberg, and T. Nilsson. "Anomalous Subdiffusion Is a Measure for Cytoplasmic Crowding in Living Cells". *Biophysical Journal*, Vol. 87, No. 5, pp. 3518–3524, Nov. 2004.

[Weis 13] M. Weiss. "Single-particle tracking data reveal anticorrelated fractional Brownian motion in crowded fluids". *Physical Review E*, Vol. 88, No. 1, p. 010101, July 2013.

[Wien 30] N. Wiener. "Generalized harmonic analysis". *Acta Mathematica*, Vol. 55, No. 1, pp. 117–258, Dec. 1930.

[Wien 32] N. Wiener. "Tauberian Theorems". *Annals of Mathematics*, Vol. 33, No. 1, pp. 1–100, Jan. 1932.

[Wilh 08] C. Wilhelm. "Out-of-Equilibrium Microrheology inside Living Cells". *Physical Review Letters*, Vol. 101, No. 2, p. 028101, July 2008.

[Wirt 09] D. Wirtz. "Particle-Tracking Microrheology of Living Cells: Principles and Applications". *Annual Review of Biophysics*, Vol. 38, No. 1, pp. 301–326, 2009. PMID: 19416071.

[Xu 98] J. Xu, V. Viasnoff, and D. Wirtz. "Compliance of actin filament networks measured by particle-tracking microrheology and diffusing wave spectroscopy". *Rheologica Acta*, Vol. 37, No. 4, pp. 387–398, Aug. 1998.

[Yama 00] S. Yamada, D. Wirtz, and S. C. Kuo. "Mechanics of Living Cells Measured by Laser Tracking Microrheology". *Biophysical Journal*, Vol. 78, No. 4, pp. 1736–1747, Apr. 2000.

[Yild 03] A. Yildiz, J. N. Forkey, S. A. McKinney, T. Ha, Y. E. Goldman, and P. R. Selvin. "Myosin V Walks Hand-Over-Hand: Single Fluorophore Imaging with 1.5-nm Localization". *Science*, Vol. 300, No. 5628, pp. 2061–2065, June 2003. PMID: 12791999.

[Zasl 08] G. M. Zaslavsky and M. Edelman. "Superdiffusion in the dissipative standard map". *Chaos: An Interdisciplinary Journal of Nonlinear Science*, Vol. 18, No. 3, p. 033116, Aug. 2008.

[Zumo 93] G. Zumofen and J. Klafter. "Power spectra and random walks in intermittent chaotic systems". *Physica D: Nonlinear Phenomena*, Vol. 69, No. 3–4, pp. 436–446, Dec. 1993.

[Zwan 80] R. Zwanzig. "Problems in nonlinear transport theory". In: L. Garrido, Ed., *Systems Far from Equilibrium*, pp. 198–225, Springer Berlin Heidelberg, Jan. 1980.

COLOPHON

This document was typeset using the typographical look-and-feel `classicthesis` developed by André Miede. The style was inspired by Robert Bringhurst's seminal book on typography "*The Elements of Typographic Style*". `classicthesis` is available for both LaTeX and LyX:

http://code.google.com/p/classicthesis/

Happy users of `classicthesis` usually send a real postcard to the author, a collection of postcards received so far is featured here:

http://postcards.miede.de/

Final Version as of July 18, 2014 (`classicthesis` version 1.0).

CURRICULUM VITAE

The curriculum vitae has been omitted from the electronic version of this document for privacy reasons.

List of publications:

A. Dechant, E. Lutz, E. Barkai, D. A. Kessler
Solution of the Fokker-Planck equation with a logarithmic potential
J. Stat. Phys. **145**, 1524 (2011)

A. Dechant, E. Lutz, D. A. Kessler, E. Barkai
Fluctuations of time averages for Langevin dynamics in a binding force field
Phys. Rev. Lett. **107**, 240603 (2011)

A. Dechant, E. Lutz, D. A. Kessler, E. Barkai
Superaging correlation function and ergodicity breaking for Brownian motion in logarithmic potentials
Phys. Rev. E **85**, 051124 (2012)

A. Dechant, E. Lutz
Anomalous Spatial Diffusion and Multifractality in Optical Lattices
Phys. Rev. Lett. **108**, 230601 (2012)

A. Dechant, E. Lutz
Connecting active and passive microrheology in living cells
arXiv:1307.6466

P. C. Holz, A. Dechant, E. Lutz
Infinite density for cold atoms in shallow optical lattices
arXiv:1310.3425

A. Dechant, E. Lutz, D. A. Kessler, E. Barkai
Scaling Green-Kubo relation and application to three aging systems
Phys. Rev. X **4**, 011022 (2014)

EIGENSTÄNDIGKEITSERKLÄRUNG

Hiermit erkläre ich, daß ich die vorliegende Dissertation mit dem Thema "Nonequilibrium dynamics in living cells and scale-invariant superdiffusive processes" selbstständig und ohne unerlaubte fremde Hilfe angefertigt habe. Es wurden von mir ausschließlich die angegebenen Quellen und Hilfen in Anspruch genommen. Eine Promotionsarbeit über dieses Thema liegt noch nicht vor.

Berlin, April 2014

Andreas Dechant